Systematic Analysis of Bivalent Configurations and Chiasma Localisation at Metaphase I in Different Varieties and Ploidy Levels of Wheats.

By

Uthman Balgith Algopishi

A thesis submitted to

the University of Birmingham

for the degree of

DOCTOR OF PHILOSOPHY

School of Biosciences

College of Life and Environmental Science

University of Birmingham

March 2023

Abstract

Meiosis is a specialized cell division in eukaryotes which consists of one round of DNA replication followed by two rounds of cell division. During meiosis crossovers (COs) occur which are the genetic exchange that take place between paternal and maternal homologous chromosomes. COs are very important for genetic variation, and they ensure proper chromosome segregation during the first meiotic division (reductional division) by holding the homologous chromosomes (bivalents) by the chiasmata. Depending on where COs have occurred along the homologues different bivalent configurations can be observed at metaphase I. In cereals, specifically in wheat, COs seemed to preferentially occur around telomeric (distal) regions rather than close to the centromeric (proximal) regions. As a result, it restricts the genetic variation that could be available to plant breeders. Thus, analysing the different factors underlining the distal localisation of COs in wheat might provide new insights and tools to plant breeders to manipulate CO localisation and unrestrain the genetic variation available in natural varieties.

In this study, we have systematically analysed the different bivalent configurations observed at metaphase I in a selection of wheat varieties in hexaploid (6X-AABBDD), tetraploid (4X-AABB) and diploid wild relatives of wheat. We have classified the different bivalent configurations in rods and rings and defined the different localizations where the chiasmata are more likely present along the chromosome arm length: distal (d), interstitial 1 (i^1), interstitial 2 (i^2), interstitial 3 (i^3), and proximal (p) regions. This analysis has allowed us to compare the mean chiasma frequency per bivalent in different varieties and different ploidy level species including hexaploid wheat (AABBDD) varieties (Chinese spring, Cadenza, Paragon and Fielder), tetraploid wheat (AABB) varieties (Kronos, Cappelli and Langdon) and three diploid ancestral relatives of wheat (*Trititicum monoccocum* (AA), *Aegilops speltoides* (BB) and *Aegilops tauschii* (DD)). Furthermore, Fluorescence in situ hybridisation (FISH) using 45S and 5S rDNA probes allowed us to differentiate

specific chromosomes among these materials: 5A, 1B, 5B, 6B, 1D and 5D. Our results have shown important differences among varieties, among ploidy level and among different chromosomes in chiasma frequency and localisation. Furthermore, the spatio-temporal polarization of the meiotic progress has been analysed and no differences were observed between diploid, tetraploid and hexaploid wheat species. Nevertheless, time course analysis showed that meiosis was completed faster in diploid species (39h) than in tetraploids (41h) and hexaploids (43h).

Wheat *ph1* mutants (*ph1b* and *ph1c*) and a Langdon substitution line 5D(5B) were analysed. The analysis showed a significant reduction on the mean chiasma frequency, a delay in the meiotic progression and even changes in chiasmata localization in specific chromosomes. Finally, chemical treatments including hydroxyurea (HU) and suberoylanilide hydroxamic acid (SAHA) were applied to hexaploid wheat cultivar Cadenza to manipulate chiasma localization in wheat. Our result show that, the mean chiasma frequency of Cadenza-HU and Cadenza-SAHA were significantly lower compared to the untreated material. Nevertheless, immunolocalization of class l COs using Hei10 antibodies showed a significant increase in the number of Hei10 foci in HU treated Cadenza. Furthermore, treatments with HU and SAHA showed new chiasmata localizations that did not exist in untreated Cadenza.

COVID-19 Impact Statement

COVID-19 was defined by World Health Organisation as a Pandemic. Because of that, The University was closed from March 2020 until August 2020. During this period of time the access to the University facility was declined. As a result of this, I lost all my plant material that it was growing at the University facilities before the pandemic. Thus, my lab work has been delayed and this affected my future plan for finishing my PhD on time. For instance, I was planning to analyse mean chiasma frequencies in some winter wheat that required vernalization during that period that could not be achieved. I start to grow this plant material in the beginning of 2020 and these wheats require two-month vernalization to be ready to move to the glasshouse and it need another three months to be ready for anther dissection and cytological analysis but these plants were dead during the compulsory close period of the University and I lost them.

Another plan that was affected by COVID-19 was the analysis of HEI10 protein in Wheat *ph1* mutants and due to the time limitations and plant growth constraints, this work couldn't be done.

Another challenge due to COVID-19 is that even after the University reopen in August 2020, we were only be able to enter the lab for six hour per day as a rotation timetable forced in the lab to accommodate the maximum number of people at a time. The lab had to be share between postdoc researchers and PhD students which also had an impact to my work specifically on immunolocalization analysis and BrdU experiments.

Moreover, during this pandemic I got limited access to the microscope room (3 hour per day). Because all my work is based on cytological analysis which required slide preparation and analysis under the microscope, these access limitations to this room affected my work progress negatively.

Furthermore, COVID-19 has an impact to my personal life. In July 2021, I lost my father due to COVID-19. It was a huge lose and I was really sad but I got a huge support from my Family at my home country and I got a huge support from my supervisor and my lab team to continue my PhD journey.

Acknowledgments

I really would like to thank Dr. Eugenio Sanchez-Moran for giving me this opportunity to pursue my PhD in his lab. He is such a great mentor and supervised me perfectly during this journey. Also, I would like to thank Dr. Kim Osman for helping and advising me through different lab techniques in the lab. She is always patient with me and I have learned a lot from her.

Additionally, I would like to thank Dr. Juliet Coates for being my internal accessor during my PhD. Dr Juliet always provide me a useful feedback during my yearly progress meetings in my PhD.

Thanks to the horticultural team at the University, Karen Staples and Andy Breckles for taking care and watering my plants during my PhD.

Thanks to Stefan Heckmann for providing us Hei10 antibody (IPK, Gatersleben, Germany).

Moreover, I would like to thank my parents; my mom and my dad (who passed away due to COVID-19) for their support and advice during my journey. Being far from them for almost four years was not easy but I hope that by the end of my journey I will make them proud of me. Of course, I would not be the person who I am today without them.

Big thanks to my wife and my two little angels for being patient with me in the last four years. They support me deeply and emotionally during my PhD.

Thanks to my friends inside and outside the lab for their support and advice.

Thanks to my sponsor King Khalid University who has offered me this scholarship and payed all my fees during this journey.

Finally, I would like to thank Birmingham Children Hospital for taking care of my daughter due to her Sickle Cell Anaemia disease and make her life and our life better by mentoring her health situation while she was here with me in Birmingham.

Table of Contents

Tables of Figures

List of Tables

List of Abbreviation

(DNA) Deoxyribonucleic Acid

(HR) Homologous Recombination

(IHR) Inter Homologous Recombination

(DSBs) Double-Strand Breaks

(CO) Crossover

(NCO) Non-Crossover

(SEI) Single End Invasion

(dHj) Double Holliday junction

(GC) Gene Conversion

(SDSA) Synthesis-Dependant Strand Annealing

(AEs) Axial Element

(LEs) Lateral Elements

(CEs) Central Elements

(SC) Synaptonemal Complex

(TFs) Transverse Filaments

(MI) Metaphase I

(Ph1) Pairing homoeologous 1

(Ph2) Pairing homoeologous 2

(FISH) Fluorescence in Situ Hybridisation

(BrdU) 5-Bromo-2-deoxyuridine

(SAHA) Suberoylanilide Hydroxamic Acid

(HU) Hydroxyurea

(DAPI) 4′,6-diamidino-2-phenylindole

(RT) Room Temperature

Chapter 1. Introduction

1.1 Meiosis overview

Meiosis is a specialised reductional cell division conserved in multicellular eukaryotes which consists of one round of DNA replication followed by two rounds of cell division: first and second meiotic divisions (Osman *et al*., 2011). These two rounds of cell division are halving the paternal and maternal chromosome number by the end of the process which will be resulting in the formation of four haploid gametes. Subsequently, the total chromosome number of the individual will be restored again after sexual fertilization in the offspring to maintain the ploidy level of the species. Importantly, the main feature of meiosis is the generation of genetic exchanges between paternal and maternal chromosomes through the process of meiotic recombination which will result in an increase in genetic variation. Meiosis is classified into two divisions: meiosis I and meiosis II (Figure 1.1). Meiosis I is a reductional division and consists of the random separation of homologous chromosomes into different cell products. Whereas, meiosis II is known as an equational division and is based on sister chromatid separation similar to a mitotic division. If during mitotic division the products are genetically identical, all four meiotic haploid products are not. Meiosis I which starts after DNA replication contains different stages: prophase I, metaphase I, anaphase I and telophase I. From meiosis I to meiosis II no DNA replication is carried out. Meiosis II also can be divided in different stages: prophase II, metaphase II, anaphase II and telophase II (also known in plants as tetrad). One important difference between meiosis I and meiosis II is that meiosis I contains a very long and complex prophase I stage which is also sub-divided to other five substages. These include: leptotene, zygotene, pachytene, diplotene and diakinesis. It is worth to highlight that the term meiosis is derivate from the Greek word “maiosis” which means “reduce” and it was firstly used by Farmer and Moore in 1905 (Sanchez-Moran *et al*., 2008). The first hypothesis that identify the importance of meiosis in biology was done by Sutton and Boveri and defended in their independent work on the chromosome theory of inheritance also known as "Sutton-Boveri Theory" around the years 1902-1904 (Crow and Crow,

2002). The authors explained how the chromosome number had to be reduced in the parents by meiosis and how sexual reproduction recovered the chromosome number in the offspring. In plants, meiosis obviously appears in both male and female organs. In flowering plant, male meiosis takes place in the anthers (parts in the stamen) and produces four gametes also known as pollen grains. Female meiosis takes place in the ovary (a part of the pistil) and although it generates four megaspores, only one megaspore is able to produce an embryo sac (Alabdullah *et al*., 2021).

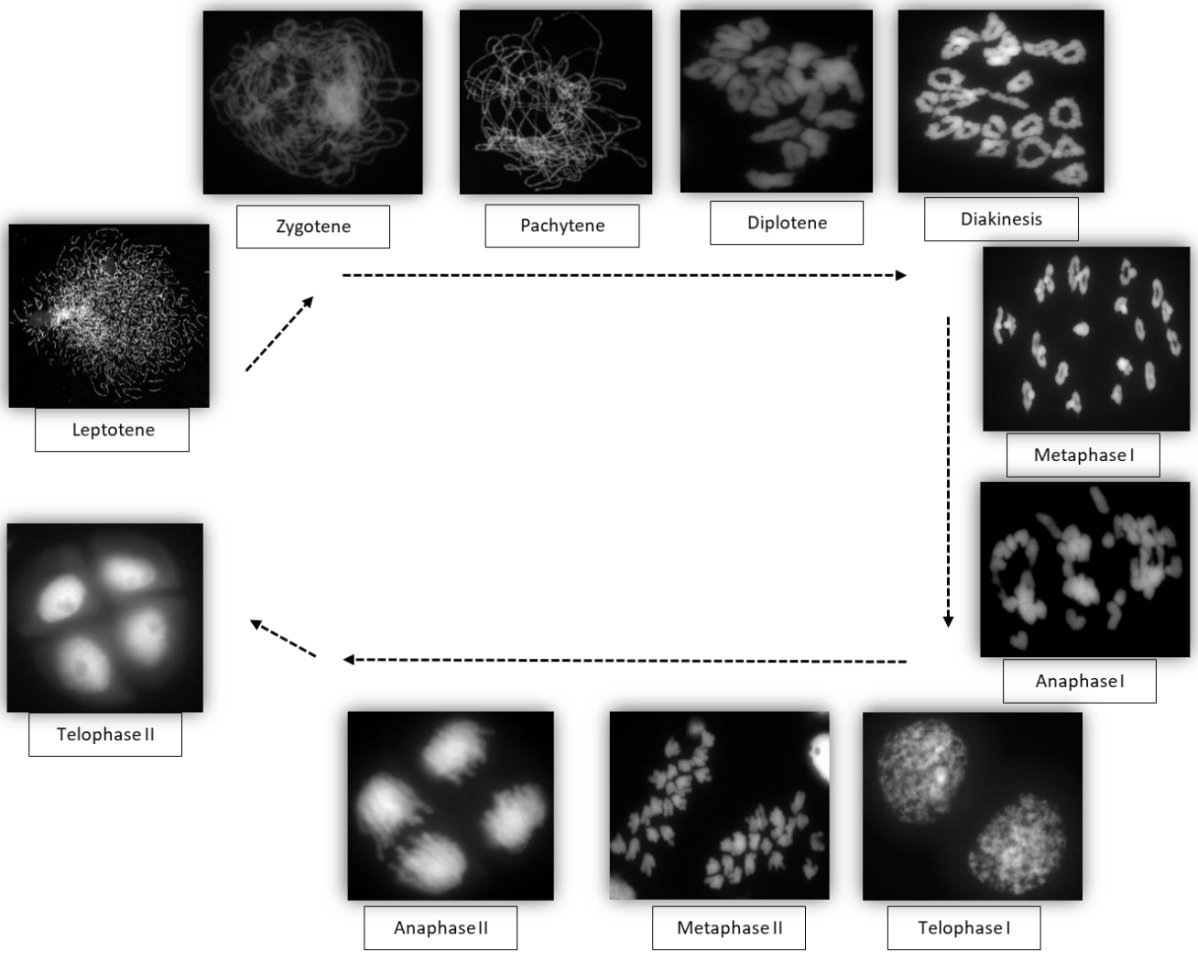

Figure 1.1: Microphotographs of different stages of meiotic division I of pollen mother cells of *Triticum aestivum*. It includes meiosis I: Prophase I (Leptotene, Zygotene, Pachytene, Diplotene and Diakinesis), Metaphase I, Anaphase I and Telophase I, and meiosis II: Prophase II, Metaphase II, Anaphase II and Telophase II).

1.2 Meiotic Stages

Prior to entering meiosis I, specifically in the pre-meiotic S-phase the DNA is fully replicated and as a result each chromosome comprises two sister chromatids held by sister chromatid cohesins. This sister chromatid cohesion complex will be maintained along the whole chromosomes length until anaphase I and from anaphase I till anaphase II only will be kept in the centromere regions, after anaphase II all cohesion will be lost (Nasmyth and Haering, 2005). Following this step, the cell now is ready to enter meiosis I.

1.2.1 Meiosis I – Reductional division

- **Prophase I:** In plants like in other multicellular eukaryotes this stage is very long and complex compared to other stages of meiosis. For example, prophase I takes approximately 21h of a total of 32h long meiosis in *Arabidopsis thaliana* (Armstrong *et al*., 2003) and about 38h of a total of 43h long meiosis in hexaploid wheat (Osman *et al*., 2021). As previously mentioned prophase I contains five sub-stages: leptotene, zygotene, pachytene, diplotene and diakinesis (Figure 1.2).
    - Leptotene: during this stage, chromosome condensation is one of the main features observed at the microscope. At this stage chromosomes appear as thin threads of chromatin. It has been proposed that these chromatin threads are composed of a linear array of higher order chromatin loops attached to the meiotic chromosome axial elements (AE's) (see section 1.6.3) (Sanchez-Moran *et al*., 2008, Zickler and Kleckner, 1999).

Zygotene: during this stage the different chromosomes will identify their homologous chromosome under the process denominated *chromosome pairing* whose exact mechanism is not yet

fully understood (Albini and Jones, 1988). Furthermore, subsequently to *chromosome pairing* another phenomenon called *chromosome synapsis* takes place between the homologous chromosomes and this is the result of the formation of the synaptonemal complex (SC) (Zickler and Kleckner, 1999, Page and Hawley, 2004) (see section 1.6.4). In addition to *chromosome pairing* and *chromosome synapsis* also *meiotic recombination* between homologous chromosome continues at this stage. During zygotene the progression of *chromosome pairing* and *synapsis* is continuously growing along the homologous chromosomes until it is fully complete at pachytene.

  - Pachytene: at this stage the SC will be present between the entire length of the homologous chromosomes. The main characteristic of the chromosomes at this stage is that they have become thicker under a light microscope.
  - Diplotene: after full synapsis is reached at pachytene the SC begins to disassemble between the homologous chromosomes and this allows them to start separating from each other except in the areas where meiotic recombination has occurred (crossovers [COs] or their physical manifestation, chiasmata). As a result, and together with further compaction of the chromosomes, it is at diplotene when the visualization of independent bivalents (homologous chromosome pairs) is possible.
  - Diakinesis: during this stage the chromosomes keep condensing and the chiasmata (defined as the cytological manifestation of COs) between homologs become clearer at the microscope.

- **Metaphase I:** This is the meiotic stage when bivalents (the homologous chromosomes held by chiasmata) are more visibly identifiable as they are orientated in the equatorial plate of the meiotic spindle (Mercier *et al*., 2015). Additionally, chiasmata appear to be more identifiable and possible to quantify at this stage (Sanchez Moran *et al*., 2001). Bivalents orientated at the equatorial plate of the meiotic spindle have the tubulin spindle fibres attached to the centromeres of both

homologous chromosomes producing equal tension in both directions and trying to separate them to opposite poles. At this stage, the sister chromatid cohesion is still intact and together with the chiasmata between the homologous chromosomes is holding the bivalent together. The spindle tension helps to visualise the shape of this bivalent that is fully dependent of the frequency and localization of chiasmata along the chromosome arms (Sanchez Moran *et al*., 2001).

- **Anaphase I:** This is the stage when the separation of the homologous chromosomes occurs under the dual action of the sister chromatid cohesion degradation along the chromosomes (except the centromeres) and the meiotic spindle pulling and separating them to opposite poles.
- **Telophase I:** This is the meiotic stage when mainly decondensation of the chromosomes occur and in plants the two nuclei produced are kept together inside the same cell (dyad).

1.2.2 Meiosis II – Equatorial Division

- **Prophase II**: Importantly, between meiosis I and meiosis II no DNA replication takes place and at this stage the chromosomes in both meiosis I products are starting to condense.
- **Metaphase II**: full chromosome condensation is achieved and the chromosomes are aligned and orientated in the equatorial pole of the meiotic spindle. The spindle fibres are attached to the kinetochores at centromeres in each sister chromatid of each chromosome. At this stage the centromeric sister chromatid cohesion is still intact.
- **Anaphase II**: The centromeric sister chromatid cohesion is degraded and together with the spindle tension, the sister chromatids of each chromosome are pulled apart and separated to opposite poles.
- **Telophase II**: Finally, the separated sister chromatids will start decondensing and form four haploid nuclei still held together in one cell in plant species (tetrad). After telophase II the four

nuclei (four haploid meiotic products) of male meiosis will separate and develop into four gametes (pollen grains).

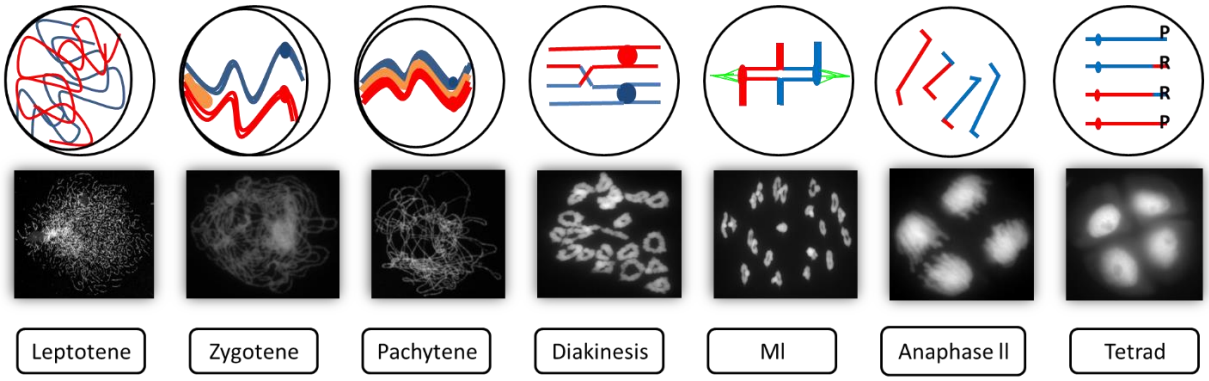

Figure 1.2: Diagram and microphotographs of hexaploid wheat pollen mother cells explaining the different substages of prophase I (Leptotene (chromosome appears as a thin thread), Zygotene (chromosome pairing and synapsis), Pachytene (synapsis completing), Diplotene/Diakinesis (synapsis disassembly and homologous chromosome held by chiasmata), metaphase I(MI) (showing bivalents held by chiasmata), anaphase II (loss of centromere sister chromatid cohesion) and telophase II (tetrad) (four haploid products). Red and Blue colours represent homologous chromosomes. Light brown colour represents SC. Green colour represents spindle.

It is worth to highlight that most of the meiosis process such as homologous recombination (HR), pairing and synapsis appear at early prophase I starting from leptotene until pachytene. HR, also termed inter-homologous recombination (IHR) is proposed to be initiated during leptotene just after the programmed occurrence of meiotic Spo11 dependent DNA double-strand breaks (DSBs). The process of DSBs formation will be explained in detail later on but it is worth to mention that their existence and processing was first suggested by Szostak and his group (Szostak and Orr-Weaver, 1983). These authors suggested that it could be two possible results following the processing/repair of a DSB: a crossover (CO) produced on reciprocal exchange between homologous chromosomes, or a non-crossover (NCO) produced on a non-reciprocal exchange between the homologues.

Moreover, COs that form during early prophase I will be cytologically visible as chiasmata in late prophase I and metaphase I. The first hypothesis, indicating the relationship between COs and

chiasmata, was reported by Janssens in 1909 (reviewed in Koszul *et al*., 2012). This was followed by more explanation to this hypothesis (Wilson and Morgan, 1920) until it finally was scientifically proven using maize chromosomes (Creighton and McClintock, 1935).

1.3 Formation of DNA double-strand breaks (DSBs) during meiosis

Under the action of an evolutionary conserved Spo11 protein, programmed DSBs do generate meiotic homologous recombination producing COs (Keeney *et al*., 1997) (Figure 1.3). The role of this protein in meiosis was first explained by Atcheson and his group in budding yeast (Atcheson et al., 1987). The exact function of this protein was known because it shares identity with DNA topoisomerases characterised in Archaea (Bergerat *et al*., 1997). Basically, these type of DNA topoisomerases are able to modify DNA catenation (between two DNA molecules) through forming DSBs in one DNA molecule pushing the other DNA molecule through the DSB to liberate the catenation and to repair the DSB made in the first step. It was found out that Archaeal Topoisomerase VI generated an heterotetrameric structure comprising of four subunits divided into two A and two B subunits (Bergerat *et al*., 1997). Spo11 seems to share homology with the two A subunits from Topoisomerase VI in Archaea. Spo11 was proposed to be participating in a dimeric structure to generate meiotic DSBs. It is important to mention that SPO11 has been shown to be expressed by single or multiple genes depending on the species (Malik *et al*., 2007). For instance, in budding yeast Spo11 appears to be as a single copy whereas in a plant genome such as *Arabidopsis thaliana* it was found to contain three *SPO11* genes (*AtSpo11-1*, *AtSpo11-2* and *AtSpo11-3*). Nevertheless, only *AtSPO11-1* and AtSpo11-2 were found to be necessary for meiotic DSB formation and homologous recombination. Some authors predicted that they could be working together as an heterodimer during meiosis (Hartung *et al*., 2007b) whereas *AtSPO11-3* seems to be active only in somatic cells (Sugimoto-Shirasu *et al*., 2002).

Furthermore, the characterisation of the two B subunits found in Archaea was subsequently done in *Arabidopsis* (Vrielynck *et al*., 2016). The authors named this subunit the Meiotic Topoisomerase VI B-like (MTOPVIB), whose exact function might be controlling the Spo11-1/Spo11-2 heterodimer to generate meiotic DSB formation.

When analysed at a fine scale, it was very clear that after the DSB has been catalysed by Spo11, it maintains its covalent attachment to the 5'-ends of DNA on both sides of the break site until it is erased through the subsequent processing of the meiotic DSB through homologous recombination.

In *Saccharomyces cerevisiae*, the generation of meiotic DSBs involves at least nine accessory proteins (MRE11, RAD50, XRS2, SKI8, REC102, REC104, REC114, MEI4 and MER2) (de Massy, 2013). Because these proteins are not well conserved among different species, recognizing them in *Arabidopsis* and other plant species has been very challenging. Surprisingly, it was found out that these proteins possess different features even when orthologous sequences have been found. For example, Jolivet and collaborators reported that AtSKI8, was not needed for meiosis at all and that AtMER11 and AtRAD50 were not involved in the formation of meiotic DSBs in Arabidopsis (Jolivet *et al*., 2006). Thus, by traditional genomic screening (revers genetic) another group of genes was identified and found to be necessary for DSB formation in plants (AtPRD1, AtPRD2, AtPRD3/OsPAIR1) (De Muyt *et al*., 2009, De Muyt et al., 2007). Mutation of any of these genes resulted in an identical mutant phenotype during meiosis with full loss of DSB formation, chromosome pairing, synapsis and recombination (chiasmata).

Finally, current studies in eukaryotes have provided insights into the connection between DSB formation complex (SPO11-1, SPO11-2 and MTOPVIB), accessory proteins and axial element proteins (Vrielynck *et al*., 2021). This study demonstrated that unlike Prd3, Prd1 and MTOPVIB do interact with the other accessory proteins. It is thought that MTOPVIB acts as a connector between

the SPO11 and the accessory proteins, however Prd1 appears to be a scaffold for them. According to this study, PRD2 and MTOPVIB interact strongly with meiotic axis formation proteins (Asy1,3). Another interaction was also observed between Prd3 and axis protein Asy1 (Vrielynck *et al*., 2021; Osman *et al*., 2018; Lambing *et al*., 2022).

1.3.1 The processing of DNA DSBs

Following the DSB formation, SPO11 remains covalently attached to the 5' ends of the DNA. Next step consists of the cleavage of the Spo11 from this location and resection of the 5' DNA ends. This step is regulated by the MRE11, RAD50, XRS2/NBs1 (MRX) complex with the functional association of Com1/Sae2 in budding yeast (Mimitou and Symington, 2009). The function of this complex is to release a short stretch of single stranded DNA that still contains Spo11 (AKA Spo11 oligonucleotides/Spo11 oligos) attached to it. Subsequently, Exo1 activity provides the continuous resection at the 5'end which allows the 3'end single strand of DNA to extend and to be involved in the strand invading process (Zakharyevich *et al*., 2010). Following resection, the 3'end ssDNA accumulates the replication protein A (Rpa). These protein works as a protector to the ssDNA and enables the recruitment of the recombinases DMC1 and RAD51 (Soustelle *et al*., 2002). The Rpa function seems to be varied among species. For instance, in plants it was found that one of the five paralogs of *Arabidopsis thaliana* Rpa (AtRpa1a) seems to be fundamental for CO generation (Osman *et al*., 2009) whereas in yeast it is involved in the initiation process of meiotic recombination to exclude additional 5' resection (Soustelle *et al*., 2002). However, it plays an important role in the formation of the nucleoprotein filament where Rpa is replaced by Rad51 and Dmc1 recombinases (Sung *et al*., 2003).

Following the completion of DNA resection, the two homologs of RecA (Rad51 and Dmc1) start to accumulate on the 3'end strand to generate a nucleoprotein filament. This nucleoprotein filament begins to search for homology in the two non-sister chromatids of the homologous chromosome which results in the expanding of the invaded chromatid (Single End Invasion (SEI)) (Hunter and Kleckner, 2001). After the SEI, the 3'end serves as a primer for DNA polymerisation, resulting in the formation of a D-loop structure that extend the invading chromatid. This works as a template to facilitate the 3'end capture on the opposite side of the break (Second End Capture). Following the ligation of the broken DNA strands, the double Holliday junction (dHj) recombination intermediate is formed. In budding yeast the dHjs will be resolved to generate COs (Neale and Keeney, 2006). However, in *Arabidopsis* it has not been fully determined if all dHjs would be able to result in COs or if some are converted into NCOs.

1.4 Stabilisation of dHj intermediates through ZMM proteins.

1.4.1 Class I Crossovers

Following the SEI, the expanding of the D-loop and the Second End Capture, the formation of dHjs takes place through these recombination intermediates (figure 1.3). The dHj intermediates are resolved to form COs, which mainly result in reciprocal exchange between homologous chromosomes. There are two classes of COs that have been identified. Firstly, the class I COs which are interference dependent. Interference is the observed phenomenon when the formation of one CO reduces the ability of another CO to form nearby (more later) (Sturtevant, 1915, Muller, 1916). Secondly, class II COs which are interference independent.

"The ZMMs" group of proteins (an acronym for ZIP1-4, MSH4-5, MER3, SPO16) are responsible for the stabilisation of dHj intermediates and their resolution into class I COs (reviewed in Pyatnitskaya, Borde & De Muyt, 2019). These ZMM proteins were first identified and characterised in yeast and include ZIP1(AtZYP1), ZIP2 (AtSHOC1), ZIP3 (AtHEI10), ZIP4, MER3, MSH4, MSH5 (Lynn *et al*., 2007). These proteins can be categorised into three different sub-groups according to their molecular function. The first group includes proteins which interact directly with DNA as MSH4, MSH5 and MER3. The second group includes proteins which interact with other proteins such as ZIP2, ZIP3 and ZIP4. The third group including proteins involved in the Synaptonemal Complex (SC) formation as ZIP1.

MSH4 and MSH5, are both specifically expressed during meiosis and have been identified to be homologous to MutS Mismatch Repair proteins found in bacteria (MutS4, MutS5) (Ross-Macdonald and Roeder, 1994). The first time MSH4 and MSH5 were identified to have a meiotic function was in budding yeast. Their function was involved in CO formation but without involvement in the process of mismatch repair (Ross-Macdonald and Roeder, 1994). They both seem to act together as a heterodimer which is attached to the strand invasion intermediates and dHjs resulting in their resolution as class I COs formation (Zalevsky *et al*., 1999, Novak *et al*., 2001). This was supported by the analysis of a yeast *msh5* mutant which showed a significant reduction of recombination intermediates like SEIs, dHjs and, as a result, COs (Börner *et al*., 2004). The other protein included in this sub-group is Mre3, which seems to be required to maintain recombination intermediates, catalyse DNA heteroduplexes developing during the strand invasion process and is required for class I COs generation (Börner *et al*., 2004, Mazina *et al*., 2004).

In the second sub-group, ZIP2 is located in the early recombination nodules and seems to play an important role in establishing synapsis (Chua and Roeder, 1998). ZIP3 seems to be essential for CO formation and synapsis. Therefore, mutation of these genes has showed phenotypes with meiotic

defects in synapsis and recombination (Agarwal and Roeder, 2000). In addition to ZIP2 and ZIP3, ZIP4 also plays a fundamental role in CO formation. In fact, it is found that ZIP4 and ZIP2 complex formation is dependent on Zip3 to be loaded onto the chromosome axis, (Perry *et al*., 2005). The main difference between these proteins in yeast is that ZIP2 and ZIP4 are needed for synapsis initiation, whereas ZIP3 is needed for SC elongation (Tsubouchi *et al*., 2006). Finally, ZIP1 is a coiled-coil domain protein with an essential structural function in the generation of the transverse filaments (TFs) in the central region of the SC (Page and Hawley, 2004, Zickler and Kleckner, 1999). ZIP1 forms a dimer that polymerises during synapsis in a zipper-like structure between the full length of the homologous chromosomes forming the central element (CE) part of the SC. This ZIP1 dimer consists of a N-terminal region localised at the CE of the SC and a C-terminal domain localised at the lateral element (LE) of the SC (meiotic axis) (Page and Hawley, 2004, Zickler and Kleckner, 1999).

Identification and characterization of ZMMs orthologs in plants has been reported specifically in the model plant species *Arabidopsis thaliana*. Thus, AtZYP1 (Zip1), AtSHOCH1 (Zip2), AtHEI10 (Zip3), AtZIP4, AtMRE3, AtMSH4 and AtMSH5 have been identified in *A. thaliana* (Chelysheva *et al*., 2007, Chelysheva *et al*., 2012, Higgins *et al*., 2004, Higgins *et al*., 2005, Osman *et al*., 2011, Osman *et al*., 2006). In addition to these orthologues, Parting Dancer (Ptd), with no homolog appearance to this protein in yeast, was also categorised as a ZMMs protein in *A. thaliana* (Wijeratne *et al*., 2006). The functional differences between plant and yeast ZMMs have been reported. For instance, in plants the meiotic recombination was not abolished in the mutation of these protein as seems to be in yeast, it only shows some defects (reduction in COs) (Osman *et al*., 2011). Additionally, in plants these proteins are not essential for the generation of the SC and full synapsis at pachytene except by the structural protein AtZYP1 (Mercier *et al*., 2015). ZYP1 in plants, is an essential component for the SC formation but in its absence (*AtZYP1* mutants) homologous chromosomes are able to pair along their length in absence of SC and CO numbers are not reduced

but increased showing that CO interference and heterochiasmy (different meiotic recombination observed in male and female meiosis) are abolished (Capilla-Pérez *et al*., 2021; France *et al*., 2021). Thus, AtZYP1 might play a crucial role in the regulation of CO interference in class I COs (Capilla-Pérez *et al*., 2021).

Furthermore, although Mlh1 and Mlh3 do not belong to the ZMMs group of proteins, they both are active in the same pathway to regulate dHj intermediates toward class I CO formation (Mercier *et al*., 2015). These two proteins share homology with MutL bacterial mismatch repair protein (Neale and Keeney, 2006, Wang *et al*., 1999). Both, Mlh1 and Mlh3, form a heterodimer that is able to resolve dHjs towards class I COs (Neale and Keeney, 2006, Wang *et al*., 1999, Jackson *et al*., 2006). In plants, both Mlh1 and Mlh3, appear to be involved in crucial roles in meiosis, specifically in CO formation (Osman *et al*., 2011). This was confirmed by mutant analysis which showed class I COs full disappearance.

1.4.2 Class II Crossovers

Analysis of *Atmsh4/Atmsh5* mutants showed an important decrease of chiasmata but with some residual chiasmata still left at MI and no direct effect on non-CO products (Higgins *et al*., 2004, Higgins *et al*., 2008). These residual COs were named class II COs. The main feature of these COs is that they seem to be non-sensitive to CO interference and that they counted for ~15% of the total number of COs in budding yeast (de los Santos *et al*., 2003) and plants (de los Santos *et al*., 2003, Higgins et al., 2004) (figure 1.3). However, there are a few exemptions where class II COs represent almost all COs such as in the case of fission yeast (Hollingsworth and Brill, 2004). The formation of class II COs is regulated under the action of MUS81. In yeast, the endonuclease MUS81 forms a complex with MMS4 whereas in plants the complex involves Eme1 (de los Santos *et al*., 2003, Higgins *et al*., 2008). This complex regulates dHj intermediates towards a CO pathway (Higgins *et*

al., 2008). Interestingly, the antirecombinase AtFancm helicase has been found to act as a suppressor to the generation of the AtMUS81/AtEME1 complex in plants and regulates dHj intermediates toward non-COs pathways (Crismani *et al*., 2012, Knoll *et al*., 2012).

Recently, Class II COs have been seen to have at least two parallel and independent pathways in *Arabidopsis:* one involving AtMUS81 (Berchowitz *et al*., 2007; Higgins *et al*., 2008) and another involving AtFANCD2 (a homolog of Fanconi Anemia Complementation Group D2) (Kurzbauer *et al*., 2018). Both, At MUS81 and At FANCD2 seem to generate independently non-interference COs. The triple mutant *Atmsh4 Atmus81 Atfancd2* shows some residual COs so it is very likely that other factors apart from AtMUS81 and AtFANCD2 could be working in producing class II COs. Thus, it seems that different meiotic recombination intermediates could be processed by a variety of independent proteins similar to AtMus81/AtFancd2 to produce interference-free class II COs (Kurzbauer *et al*., 2018).

1.4.3 Non-Crossovers

Despite CO formation, it has been observed that non-crossover (NCOs) formation, when non-reciprocal exchange occurs between the homologous chromosomes, can occur and result in gene conversion (GC) (Börner *et al*., 2004, Szostak and Orr-Weaver, 1983). It has been suggested that the majority of meiotic NCOs are generated through Synthesis-Dependent Strand Annealing (SDSA) (Allers and Lichten, 2001) (figure 1.3). In plants, SDSA activity might be controlled by the action of the Fancm helicase (Knoll *et al*., 2012). AtFANCM seems to restrict the formation of class II COs and to force recombination intermediates to be directed to the SDSA pathway which will be producing NCOs (Knoll *et al*., 2012, Crismani et al., 2012). Arabidopsis *Atfancm* mutant combined with a ZMMs class I CO mutation showed an increase in COs compared to the ZMMs single mutant (Crismani *et al*., 2012, Knoll *et al*., 2012) and this increase was related to an increase in class II COs.

In contrast to the dHj intermediates that resolve to form COs, some intermediates could be resolved to NCOs. This mechanism is controlled under the action of anti-recombinase factors such as the RTR complex (Hartung *et al*., 2007a, White, 2008). The Arabidopsis RTR complex contains AtRECQ4A/AtRECQ4B, AtTOP3α and AtRMI/AtBLAP75 and its function is to regulate dHj intermediates towards the SDSA NCO pathway (Hartung *et al*., 2007a, White, 2008).

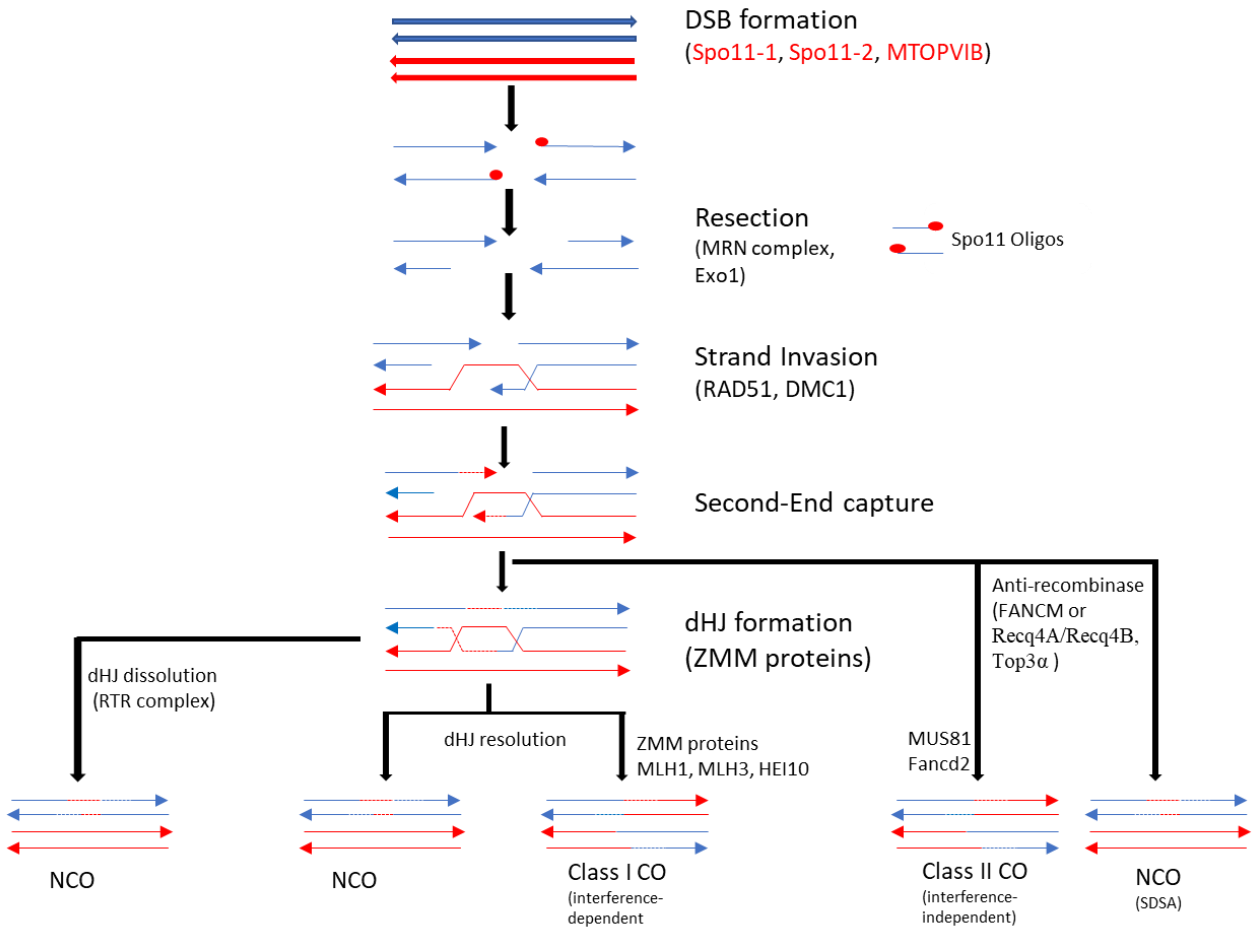

Figure 1.3: Molecular control of meiotic recombination in plants (modified from Osman et al., 2011). Double Strand Break initiate under the action of SPO11 (section 1.3). Following the break, the resection of SPO11 oligonucleotide were proceed by MRX/N complex (section 1.3). This followed by strand invasion by the two recombinases RAD51 and DMC1 (section 1.3.1) which resulted in the formation of dHJ that might resolve to COs (section 1.4.1 and 1.4.2) or NCOs (section 1.4.3).

1.5 Factors controlling CO localisation and distribution

1.5.1 Hotspots

CO frequency and distribution is a very tightly controlled mechanism and there are some different factors which control its formation such as hotspots. COs are restricted to specific regions in the genome and are not randomly distributed (Choi *et al*., 2013, Mancera *et al*., 2008, Tock *et al*., 2021). These specific regions that have more COs are also known as hotspots and they normally accumulate in ~1-2 Kb regions. In budding yeast DSB/CO hotspots seems to be mostly found in regions with less nucleosome occupancy on the genome, normally in promoter regions (rarely happening in exons and gene terminators) (Wu and Lichten, 1994; Fan and Petes, 1996; Pan *et al*., 2011; Lam and Keeney, 2015). Furthermore, in plant species it has been found that hotspots are also localised in nucleosome-depleted regions (Choi *et al*., 2018). In Arabidopsis, the CO hotspots appear to be enriched in nucleosome free regions, non-repetitive sequence regions, low DNA methylation regions and in euchromatin gene rich regions often in proximity to H3K4me3 (trimethylation of lysine 4 of histone 3) marks (Choi *et al*., 2018, Tock *et al*., 2021). There is a connection between hotspots and a specific family of transposons known as the Helitron family (Choi *et al*., 2018). The link association between histone modification H3K4me3 marks and early recombination events was studied also in budding yeast and it was found that Spp1 (Set domain protein) was involved in the interaction with H3K4me3 and MER2 which is proposed to be connecting hotspots to the DSB mechanism (Tock and Henderson, 2018). However, in mammals, hotspots were detected in areas enriched by PRDM9 protein (histone lysine trimethyl transferase) (Baudat *et al*., 2010). This protein is able to detect specific DNA motifs via their zinc finger protein motif which might be catalysing them to become a DSB hotspot (Baudat *et al*., 2010).

1.5.2 CO Interference

The phenomena of CO interference were firstly described independently by A. H. Sturtevant (1915) and H. J. Muller (1916). It was observed that when one CO was formed in one chromosome region there was little chance to get another CO in its proximity. This observation suggests that the formation of one CO reduces the ability of another CO to form nearby. This phenomenon was called *CO interference*. In fact, the exact mechanism controlling this phenomenon is very poorly understood but there are several hypotheses built using different observations in different models trying to explain it.

The first model proposed was by King and Mortimer (1990) and was called "the polymerization model". They suggested that CO formation at a specific site of the chromosome could catalyse a polymerization of a signal and this signal seems to remain active and strong to be able to spread until it reaches another CO polymerization signal that occurs in a different site of the same chromosome. However, this model was not continuously supported as it proposed that the interference signal could become weaker over the distance from the CO (Drouaud *et al*., 2007, Zhang *et al*., 2014).

The second model, proposed by Foss and his group (1993), was called "the counting model" which proposed that some of the early recombination events (DSBs) will be repair as NCOs (Stahl *et al*., 2004). It is predicted from this model that the change by increase or decrease of the number of the DSBs should result in an increase or decrease to the COs events. However, reducing early recombination events (DSBs) by using different *spo11* mutants in budding yeast did not show an effect on CO events and surprisingly the CO number was preserved at the expense of NCOs (Martini *et al*., 2006). This phenomenon was called "CO homeostasis".

The third model by Kleckner and collaborators (2004) was called "the mechanical stress model" and proposed that CO distribution might be controlled by a mechanical stress relief mechanism. Thus, CO interference signal could be generated after cycles of chromatin induced stress and stress relief

during early meiotic prophase I when the meiotic chromosomes chromatin is involved in different processes of expansion and contraction along the chromosome axis producing a high level of stress. The authors used the analogy of a metal beam as the meiotic chromosome axis coated on a film as the chromatin and the flaw on the film as the recombination precursors or DSBs (Kleckner *et al*., 2004). When stress is applied in the beam (chromosome axis expansion and contraction process during prophase I), it will result in beam (chromatin) stress. This stress could form a crack in a flaw area on the beam (a CO designation on a DSB [beam flaw]) and that allows a bidirectional stress release around that crack (CO), being stronger closer to the COs and weaker farther from the CO (like the interference). This stress relieved from around the crack (CO) makes it more unlikely that any other flaw (DSB) around that area would form another crack (CO) nearby. The main feature of this model is that when one CO is formed the interference signal will be spread over the distance resulting in a decreasing possibility of forming another CO around that area (Kleckner *et al*., 2004, Zhang *et al*., 2014, Zickler and Kleckner, 2015). The mechanical model implies that the meiotic chromosome axis is establishing the CO interference. Direct evidence came when analysing a mutant for the chromosome axis protein topoisomerase II in budding yeast that showed loss of interference on Zip3 foci distribution (Zhang *et al*., 2014). Furthermore, in Arabidopsis another meiotic axis protein (ASY1) has been associated in the stabilization of tetraploid *Arabidopsis arenosa* probably by regulating interference (Yant *et al*., 2013).

There is scientific evidence that supports the idea that the SC could be the key factor in the polymerization model of interference. There are several mutations that affect synapsis: *zip1*(Sym & Roeder, 1994), *pch2 (*Zanders & Alani, 2009), *syp1RNAi* (Libuda *et al*., 2013) that seem to result in a CO interference defect. Nevertheless, 2-D gel analysis of recombination products and their quantification showed that *zmm* budding yeast mutants affected in COs numbers had unaltered NCO numbers (Borner *et al*., 2004; Bishop & Zickler, 2004). This supported the idea that CO designation

and therefore interference are set up in early prophase I prior to stable single end invasion (SEI). If CO designation occurs in early prophase I this would mean that at this point interference should have been already set up then and only the maturation of the CO/NCO will be taking part in mid-late prophase I while SC polymerization is finalised (Borner *et al*., 2004). Thus, it seems that SC polymerization is not involved in transducing the interference "signal" to impose the CO/NCO fate.

Surprisingly, current studies in *Arabidopsis thaliana* have shown that the central element component of the SC, ZYP1, seems to play an important role in controlling CO interference (Capilla-Pérez *et al*., 2021). Analysis of null *zyp1* mutants in *Arabidopsis* suggests that a CO interference signal might propagate along the SC polymerization. Furthermore, these authors showed that in the absence of the SC, CO frequencies become identical in both Arabidopsis sexes, suggesting that heterochiasmy is due to variation of CO interference imposed by the SC (Capilla-Perez *et al*., 2021). In addition, loss of the Zyp1 protein results in failure to form an obligatory CO between each homolog pair in Arabidopsis (France *et al*., 2021). Further support has been provided when over expressing Hei10 in a *zyp1* mutant in Arabidopsis (Durand *et al*., 2022). HEI10 seems to be captured at the middle of the SC and coarsens into large pro-CO foci as the SC polymerizes throughout Prophase I. The number of large pro-CO foci coincides with class I COs and is determined by the SC length and HEI10 expression levels (Durand *et al*., 2022). HEI10 overexpression increases CO number, and weakens interference but maintains heterochiasmy in Arabidopsis but in a *zyp1* mutant HEI10 is exchanged directly between the foci and the nucleoplasm abolishing both interference and heterochiasmy and the number of foci depends on Hei10 expression level (Durand *et al*., 2022). This HEI10 coarsening process might explain CO distribution and interference in Arabidopsis (Morgan *et al*., 2021a; 2021b).

Additionally, AE components such as ASY1 and ASY3 have also been suggested to regulate the CO interference mechanism (Morgan *et al*., 2021). Chromosome axis-associated HORMA domain proteins (ASY1/3) are crucial for meiotic recombination (Sanchez-Moran *et al*., 2007; Ferdous *et al*.,

2012). ASY1 is assembled on the axis at early meiotic prophase I and requires ASY3 to be already present on the axis (Ferdous *et al*., 2012). Asy1 seems to be depleted from the chromosomes when the SC polymerises between the homologous chromosomes (Ferdous et al., 2012). Both processes, ASY1 assembly and disassembly, are catalysed by the AAA+ ATPase PCH2 together with its cofactor COMET (Balboni *et al*., 2020; Yang *et al.*, 2020). This Asy1 remodelling complex seems to be temporally and spatially differently assembled: PCH2 and COMET directly interact in the cytoplasm in early meiosis, then PCH2 is recruited by ZYP1 and brought to the ASY1-COMET complex assuring the timely removal of Asy1 during chromosome synapsis (Balboni *et al*., 2020; Yang *et al.*, 2020; 2022). Analysis of a *zyp1* mutant with the PCH2 binding site deleted (Yang *et al*., 2022) showed that ASY1 disassembly from the axis was compromised, maintaining class I COs elevated in numbers and the obligate CO (that was not maintained in a *zyp1* null mutant before; Capilla-Perez *et al*., 2021; France *et al*., 2021). These results indicate that PCH2 mediated eviction of ASY1 from the meiotic axis at zygotene seems to control interference and restrict CO formation in *Arabidopsis* (Yang *et al*., 2022).

1.5.3 Obligate CO and Homeostasis

Obligate CO or CO assurance means that at least one CO (chiasma) between homologous chromosomes is needed to insure correct and proper segregation at anaphase l (Jones and Franklin, 2006). If the obligate CO is not maintained between homologous chromosomes, chromosome mis-segregation at anaphase I might lead to the formation of aneuploid gametes (Jones and Franklin, 2006).

CO homeostasis was firstly observed in budding yeast *spo11* not fully null mutants with different levels of formation of DSBs (Martini *et al*., 2006). When the number of DSBs was reduced, up to a

level, the number of CO events was preserved by reducing the number of NCOs (Martini *et al*., 2006).

1.6 Chromosome Structure in meiosis (meiotic axis structure)

The chromosome axis during meiosis contains an Axial Element (AE) which is formed by a proteinaceous complex between the sister chromatids very early on at the initiation of meiosis at G2-leptotene (Page and Hawley, 2004, Zickler and Kleckner, 1999). It is important to mention that the termed AE is only used when the homologous chromosomes have not started synapsis in that region but once the SC is polymerising then the AEs are called Lateral Elements (LEs). The initial accumulation of axis proteins in the nucleus started just after the S-phase in G2. At leptotene the protein axis rapidly polymerises to form the AEs along the two sister chromatids on each homologous chromosome, these AEs act as anchors for the chromatin loops (Zickler and Kleckner, 1998, Zickler and Kleckner, 1999).Interestingly, the size and position of a chromatin loop appears to be similar within the same species whereas it shows some variation between different species (Zickler and Kleckner, 1999). Subsequently, at zygotene when the synapsis is starting to form between homologous chromosomes, the AEs passed to be LEs of the SC (Kleckner, 2006).

AEs are mainly formed of three types of protein complexes; which are called cohesins, condensins and axis associated proteins (Kleckner, 2006).

1.6.1 Cohesins

The multi-protein complex cohesin is a fundamental component that plays an important role in both meiosis and mitosis such as protecting chromosome architecture and insuring proper segregation (Mainiero and Pawlowski, 2014). The different cohesins will be responsible for ensuring that the sister chromatids in each chromosome will be staying together during S-phase, prophase and metaphase during mitosis; and during S-phase, prophase I and metaphase I during meiosis. The

cohesin complex appears as a ring form structure that binds sister chromatids during mitotic and meiotic divisions. The cohesin proteins are named according to their specific role, and they are part of a protein family called Sister Chromatid Cohesion (SCC). During mitosis, cohesins consist of four different proteins: two Structural Maintenance Chromosome proteins (SMC) that include SMC1 and SMC3, and two non-SMC proteins that include Sister Chromatid Cohesion 1 and 3 (SCC1, SCC3) (Mainiero and Pawlowski, 2014). However, this cohesin structure varies during the meiotic process. For example, in budding yeast SSC1 (α-kleisin) is exchanged during meiosis by the Recombination protein 8 (REC8) (Klein *et al*., 1999). In the model plant *A. thaliana*, the cohesin Rec8 is also known as SYN1 (Cai *et al*., 2003). The roles of SYN1/REC8 in *A. thaliana* have been proposed to include the initiation of SCC at early meiosis, homologous chromosomes pairing and synapsis, and the accumulation of SCC3 (Chelysheva *et al*., 2005). These roles were confirmed by the *syn1/rec8* mutant analysis which showed several chromosome structural defects during prophase I such as a reduction in chromosome pairing and synapsis, chromosome fragmentation at metaphase I and chromatin disruptions during prophase I (Cai *et al*., 2003, Chelysheva *et al*., 2005). The interaction between cohesin proteins and other proteins that play crucial roles in modulating their activities during meiosis have been observed such as SCC4 and ECO1 and WPL1/2 proteins (reviewed in: Mainiero and Pawlowski, 2014).

1.6.2 Condensins

The second structural component of the chromosome axis are the condensins. They play a fundamental role in both meiotic and mitotic cell by controlling the chromosome structure and maintenance during cell division (Yu and Koshland, 2003, Hirano, 2002). There are two different types of condensins based on their ring like structure. The first type includes SMC2, SMC4 and

kleisin CAP-H accompanied by two associated proteins CAP-D2 and CAP-G (Hirano, 2012, Mainiero and Pawlowski, 2014). Its function has been reported to be participating in chromosome compaction. The second type contains SMC2, SMC4 and kleisin CAP-H2 accompanied by two associated proteins CAP-D3 and CAP-D2 (Hirano, 2012, Mainiero and Pawlowski, 2014). Its function appears to be involved in the axis length compaction. Finally, it is important to mention that most of the research and study for condensin proteins have been done in mitotic division with a few observations in meiotic division (Smith *et al*., 2014).

1.6.3 Axis Associated proteins

The third component of the axis structure are the axis associated proteins which are not responsible for chromosome axis structural maintenance but rather being involved in other roles like recombination and synapsis during meiosis (Page and Hawley, 2004) (Figure 1.4). This group contains four major proteins: ASY1, ASY2, ASY3 and ASY4. The first group contains HORMADs proteins (ASY1 and ASY2) (Armstrong *et al*., 2002). The name HORMAD comes from three HORMAD domain proteins in yeast: Hop1, Rev1 and Mad1(Woltering *et al*., 2000). Arabidopsis ASY1 was identified to be a homologue to the yeast Hop1 (Armstrong *et al*., 2002). However, ASY2 does not share any homology with yeast and their paralog has not being characterised in other plants (Armstrong *et al*., 2002). The second group contains two coiled-coil proteins (ASY3 and ASY4). Arabidopsis Asy3 shares homology with Red1 in budding yeast (Ferdous *et al*., 2012). On the other hand, ASY4 doesn't share homology with yeast (Chambon *et al*., 2018).

ASY3 is a coiled-coil domain protein similar to budding yeast Red1 (Thompson & Roeder, 1989; delosSantos & Hollingsworth, 1999), mammalian SCP3/COR1 (Dobson *et al*., 1994), rice OsPair3 (Yuan *et al*., 2009; Wang *et al*., 2011) and maize DSY2 (Lee *et al*., 2015). All these proteins are

components of the AEs and their amino acid sequences not very well conserved. ASY3 appears like small foci in early prophase I and at leptotene starts polymerising into a linear signal along the chromosome axis until pachytene (Ferdous *et al*., 2012). Interestingly, after the SC elongation ASY3 appears to maintain the association with the LEs not like Asy1 that appears to disappear from the LEs as the SC polymerises (see below). Functional analysis of ASY3 has shown that it has an important role in CO and synapsis formation and is also required for the loading of ASY1 to the chromosome axis (Ferdous *et al*., 2012; West *et al*., 2019).

ASY1 (Asynaptic 1); has been widely studied in *Arabidopsis thaliana* as well as other plant species. The genetic analysis of *Asy1* has shown that it is essential for the process of synapsis between homologous chromosomes and is very important for homologous recombination (Armstrong *et al*., 2002). This was confirmed by the analysis of *asy1* mutant that showed meiotic abnormalities such as a big reduction of chiasmata (COs), incomplete synapsis and chromosome mis-segregation (Armstrong *et al*., 2002, Sanchez Moran *et al*., 2001). ASY1 loading at chromosome axes (AEs) requires the presence of ASY3 on the axis (Ferdous *et al*., 2012). The AAA+ ATPase PCH2 seems to have two specific roles in remodelling the chromosome axis by ASY1 (Lambing *et al*., 2015; Balboni *et al*., 2020; Yang *et al*., 2020; 2022). Firstly, PCH2 seems to facilitate the association between ASY1 and the meiotic chromosome axis (AEs) as in *Arabidopsis pch2* mutation, Asy1 signal on the axis appears to be very weak (Lambing *et al*., 2015). This PCH2 function seems to be conserved in multicellular eukaryotes, for instance in budding yeast, PCH2 is essential for the recruitment of Hop1 (ASY1 homologue) to the chromosome axis during early prophase I (Börner *et al*., 2008). Secondly, PCH2 has a role in the removal of ASY1 from the axis when the SC starts elongating during mid prophase I (Lambing *et al*., 2015). This ASY1 remodelling complex mainly involves Pch2 and COMET directly interacting in the cytoplasm in early meiosis, then PCH2 is recruited by ZYP1 and brought to the ASY1-COMET complex assuring the timely removal of ASY1

during chromosome synapsis (Balboni *et al*., 2020; Yang *et al.*, 2020; 2022). As explained before, a *zyp1* mutant with the PCH2 binding site deleted (Yang *et al*., 2022) has showed a compromised ASY1 disassembly from axis, which maintains class I COs elevated in numbers and the obligate CO (Capilla-Perez *et al*., 2021; France *et al*., 2021). Furthermore, as explained before PCH2 mediated eviction of ASY1 from the meiotic axis at zygotene appears to have a role in the control of CO interference and the restriction of CO formation in *Arabidopsis* (Yang *et al*., 2022).

The coiled-coil protein ASY4 appears to also play an important role in the formation of COs and synapsis (Osman *et al*., 2018; Chambon *et al*., 2018). The *asy4* mutants resulted in chromosome abnormalities during early meiosis such as incomplete synapsis and defective CO formation (Chambon *et al*., 2018). ASY4 appears as foci in early meiosis and similar to ASY1/3 polymerises and aligns with chromosome axis (AEs) at leptotene. Interestingly, similar to ASY3, ASY4 remains attached to the LEs following synapsis (Chambon *et al*., 2018).

In multicellular eukaryotes, the meiotic axis formation seems to be initiated after the interaction between coiled coil domain proteins (ASY3/4) and HORMA domain proteins (ASY1/2) (West *et al*., 2019). For instance, in yeast the coiled coil protein Red1 accumulates first in the axis and then the HORMA domain protein Hop1 gets recruited through the so called "closure motif" (West *et al*., 2019). The same mechanism appears to be conserved in plants, the coiled coil protein ASY3 loads first in the axis followed by the recruitment of the HORMA domain protein ASY1 (West *et al*., 2019). It is suggested that the coiled coil domain proteins in yeast, plants and mammals might be self-assembled in the axis via a similar mechanism. For example, in plants the interaction of coiled coil proteins ASY3 and ASY4 at their C-terminal domain results in the formation of an heterotetrametric structure which can oligomerize as filamentous structures and connect to the N-terminal of the HORMA domain protein ASY1 (West *et al*., 2019). Similarly, mammalian SYCP2 and SYCP3 coiled

coil domain proteins would act in the same manner (West *et al*., 2019). This suggests a conserved mechanism of these proteins across different species.

1.6.4 Synaptonemal Complex (SC)

The multicomplex proteinaceous structure called the SC was firstly identified by Moses (1956) in crayfish chromosomes and by Fawcett in pigeon, cat, and human chromosomes (1956) by using electron microscopy to study chromosome structure during gametogenesis (Zickler and Kleckner, 1999) (Figure 1.4). It is defined as a proteinaceous (tripartite zipper-like) structure that consist of AEs that later when synapsis starts will become LEs, and a central region consisting of central elements or filaments (CEs) (Zickler and Kleckner, 1999). Thus, the SC gets assembled between the homologous chromosomes from mid prophase during zygotene and completes its full assembly at pachytene. Following pachytene, at diplotene, the SC disassembles between the homologous chromosomes (Klein *et al*., 1999, Page and Hawley, 2004, Zickler and Kleckner, 1999, Zickler and Kleckner, 2015). As previously explained the main component of the SC are the LEs and CEs (Page and Hawley, 2004). There are two LEs in the SC, each one of them is assembled in each pair of the homologous chromosomes. The LEs component was previously explained to be consisted of cohesins, condensins and axis associated proteins (see before). The CEs consist of transverse filaments proteins (TF) which are orientated in a linear manner and attached to the LEs (Kleckner, 2006, Zickler and Kleckner, 1999). The most important component of the TFs is the coiled coil protein ZIP1 that seems to be conserved in different species such as budding yeast and plants (called Zyp1). ZIP1 in budding yeast seems to be an essential component for the SC formation (Heyting, 1996, Sym *et al*., 1993). At the molecular level, ZIP1 proteins are composed of helical coiled coil region flanked by N-terminal and C-terminal globular domains (Kleckner, 2006). The orientation of

this ZIP1 protein in the TFs appears to be very important and evolutionarily conserved: the C-terminal domain is attached to the LEs whereas the N-terminal domain forms the TF central part (CE) and allows the dimerization of Zip1 (Kleckner, 2006, Page and Hawley, 2004).

The central region length is about 100 nm and its structure appears to be preserved in different species (Zickler and Kleckner, 1999) such as yeast, plant and mammals although the amino acid sequence seems not to be highly conserved among species (Osman et al., 2006).

Arabidopsis ZYP1 (ortholog to Zip1 in budding yeast) has been identified and characterised to be a component of the TF (Capilla-Pérez *et al*., 2021, Higgins *et al*., 2005, Osman *et al*., 2006). Arabidopsis ZYP1 protein is encoded by two genes: *AtZYP1a* and *AtZYP1b* and both are expressed with a redundant function (Higgins *et al*., 2005). Additionally, AtZYP1 seems not to be required for CO formation as its mutation only shows moderate defects in chiasma formation (Higgins *et al*., 2005). Unexpectedly, the rice AtZYP1 ortholog, OsZEP1, appeared to work differently than in Arabidopsis. *Oszep1* mutants showed an increase in chiasma frequency (Wang *et al*., 2010). In cereals, more specifically in Barley, ZYP1 has shown a similar role to Arabidopsis in CO formation at meiosis (Barakate *et al*., 2014).

However, until recent years, all plant ZYP1 mutants analysed were obtained just by RNAi and they were not fully null mutants. Current studies in *Arabidopsis thaliana* using CRISPR-Cas9 to produce null mutants have shown that AtZYP1 is important in controlling CO interference (Capilla-Pérez *et al*., 2021). Null *Atzyp1* mutants have increased CO frequency similarly to that one reported in rice mutants (Wang *et al*., 2010; Capilla-Pérez *et al*., 2021; France *et al*., 2021). This suggests that the CO interference signal might be able to propagate along the SC polymerization via ZYP1. These analysis as discussed before also suggested that heterochiasmy could be due to variation of CO interference

imposed by the SC (Capilla-Perez *et al*., 2021) and the maintenance of the obligatory CO between each homolog pair in Arabidopsis (France *et al*., 2021).

It is worth to highlight that ZYP1 is not involved in the mechanism of pairing. Moreover, pairing still exists even in the mutation of this protein (France *et al*., 2021). In fact, mutation of the DSBs and SEI formation proteins show a great defect in synapsis formation which imply that synapsis initiation depends on early meiotic recombination process (Da Ines *et al*., 2012).

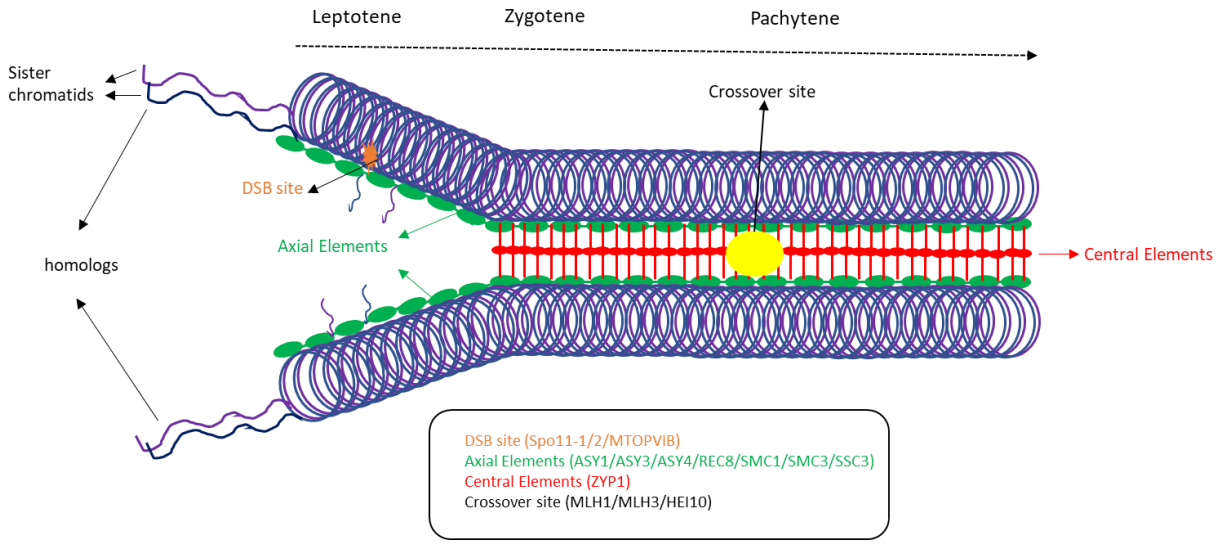

Figure 1.4: Synaptonemal Complex and chromosome axes components. In leptotene, double strand break initiated and homology search started following the chromosome axes formation. In zygotene, after pairing and synapsis initiation, the Axial Elements (ASY1/ASY3 and ASY4)) will be now Lateral Elements (ASY3/ASY4) which will bring the homologous chromosome to be oriented facing each other via Central Elements (ZYP1). In pachytene, the synapsis will be completed and COs (MLH1/MLH3 and HEI10) (yellow bold) will form between homologous chromosomes.

1.6.5 Relationship between chromosome axis, SC and recombination:

Recombination appears to be essential for normal pairing and synapsis in different species such as yeast, plants and mammals. Disruption to pairing and synapsis normally occurs as a result of the mutation of early recombination proteins such as SPO11, DMC1 and RAD51 (Da Ines *et al*., 2012,

Zickler and Kleckner, 2015). On the other hand, recombination is not required for normal pairing and synapsis in some species. For instance, synapsis and pairing take place before recombination in the worm *C. elegans* (Zickler and Kleckner, 2015, Zickler and Kleckner, 2016). Noticeably, the number of COs seems to be higher in organisms with high pairing and synapsis compared to organisms where synapsis is independent of recombination (de Massy, 2013). Highlighted the species that required recombination for pairing and synapsis, it is suggested that the recombination intermediates that are not involved in class I and class II COs generate NCOs (Zickler and Kleckner, 2015). Additionally, DSBs that are not involved in producing COs might play a role in pairing of homologous chromosomes by facilitating homologous recognition (Zickler and Kleckner, 2015).

Moreover, based on the "tethered-loop axis" model in yeast, Spo11 complex accumulates to the chromatin but remains to be inactive until the axis is fully formed/polymerised (Panizza et al., 2011). Following the axis formation, SPO11 complex generates DSBs on the axis resulting in the formation of SEI and therefore the initiation of the homology search (Panizza *et al*., 2011). Subsequently, the two homologues can be reoriented together resulting in the initiation of pairing (Zickler and Kleckner, 2015). In mid prophase, specifically zygotene, in coincidence with continuation of chromosome pairing the protein rich foci visualised on electron microscopy (EM) spreads and called "early recombination nodules" seem to be attached to the AEs. These foci seem to be responsible for the "inter axis bridge" formation which will be also the anchoring structures of the CE of the SC (Albini and Jones, 1988). Following zygotene and in pachytene these foci are replaced by the so called "late recombination nodules" which are mainly located in the centre of the SC (Albini and Jones, 1988). Molecular analysis of these two structures has shown that "early recombination nodules" seem to include early recombination proteins such as DMC1, RAD51 and MER3 (Dubois et al., 2019, Moens *et al*., 2007) whereas the "late recombination nodules" include late recombination proteins such as HEI10 (Dubois *et al*., 2019). Based on these analyses the number of "late recombination nodules"

appears to be similar to the chiasmata frequency observed at Metaphase I indicating a direct association between them.

1.7 The origin of polyploid wheats

One of the earlier studies of wheat genetics involved the discovery of wheats chromosome number (Sakamura, 1918, Sax, 1918). They indicate that wheat species consisted of diploid species (2n = 2X = 14 chromosomes), tetraploid species (2n = 4X = 28 chromosomes) and hexaploid species (2n = 6X = 42 chromosomes). Wheats polyploidization process involved different species, thus wheats are allopolyploid species (Kihara, 1924, Sax, 1922). Allopolyploid species are the result from the hybridization between two or more different species (although evolutionary related) followed by genome duplication. This hybridization process will result in different sub-genomes (homoeologous chromosomes) set in tetraploid and hexaploid wheat (Levy and Feldman, 2022).

Tetraploid wheat was first identified by Aaronson (1906). Tetraploid wheat has been proposed to appear about 800,000 years ago (Levy and Feldman, 2022) (Figure 1.5). Allotetraploid wheat (2n = 4X = AABB) was formed from the hybridization of two grasses species: The A genome donor which is thought to be diverged from *Triticum urartu* that appeared more than 1 million years ago. The B genome which exact donor species is not fully known yet but it must be closely related to one of the Sitopsis family species (*Aegilops bicornis*, *Ae. longissima*, *Ae. searsii*, *Ae. sharonensis* and *Ae. speltoides*). The tetraploid B genome diverged from one of these species about 4 million years ago (Marcussen *et al*., 2014). Recently, a phylogenetic study analysing the whole-genome sequence of different species inside the Sitopsis family revealed that the B donor diverged from an ancestral progenitor lineage related to *Ae. speltoides* and *Ae. mutica* (Li *et al*., 2022). The Fertile Crescent in the Mediterranean western Asia was one of the major centres of plant domestication, including

wheats, mostly originated around 10,000 years ago (reviewed in Preece *et al*., 2017). The emmer wheat (*Triticum turgidum* L. *ssp. dicoccoides*) appeared in this region at that time and it is an ancient two rowed hulled tetraploid wheat with a high protein content that is mainly used for pasta and different flatbreads and pilaf recipes in Ethiopia, India and even in Italy (known as Farro) (Matsuoka, 2011). Domestication of wild emmer started around 10,000 years ago in coincidence with the agricultural evolution in the fertile crescent which resulted in the appearance of cultivated tetraploid wheats *T. turgidum* (*ssp.durum*) and is thought to have originated in present day Turkey (Salamini et al., 2002). Durum wheat is mainly used to make fresh pasta (spaghetti, ravioli, linguini,…), semolina, cookies and puddings.

Triticum aestivum (2n = 6X = AABBDD), also known as bread wheat, is a hexaploid species that appeared just around 9,000-8,500 years ago through the hybridization between a domesticated tetraploid wheat (AABB) and *Aegilops tauschii* (donor of the D genome) (Kihara, 1944; McFadden and Sears, 1946; Levy and Feldman, 2022).

The genus *Triticum* consists of six species divided into three categories (Li et al., 2022, Matsuoka, 2011). The first category includes the diploid species such as *T. monococum* and *T. urartu* (2n = 2X = AA). The second category includes tetraploid species such as *T. turgidum* (2n = 4X = AABB) and *T. timopheevii* (2n = 4X = AAGG). *T. timopheevii* is the domesticated form of its wild relative *T. araraticum* (Li *et al*., 2022, Matsuoka, 2011). The third category includes hexaploid species such as *T. aestivum* (2n = 6X = AABBDD) and *T. zhukovskyi* (2n = 6X = AAAAGG). *T. zhukovskyi* was developed through the hybridization between tetraploid wheat *T. timopheevii* (AAGG) and the diploid wheat *T. monococcum* (AA) (Li *et al*., 2022, Matsuoka, 2011).

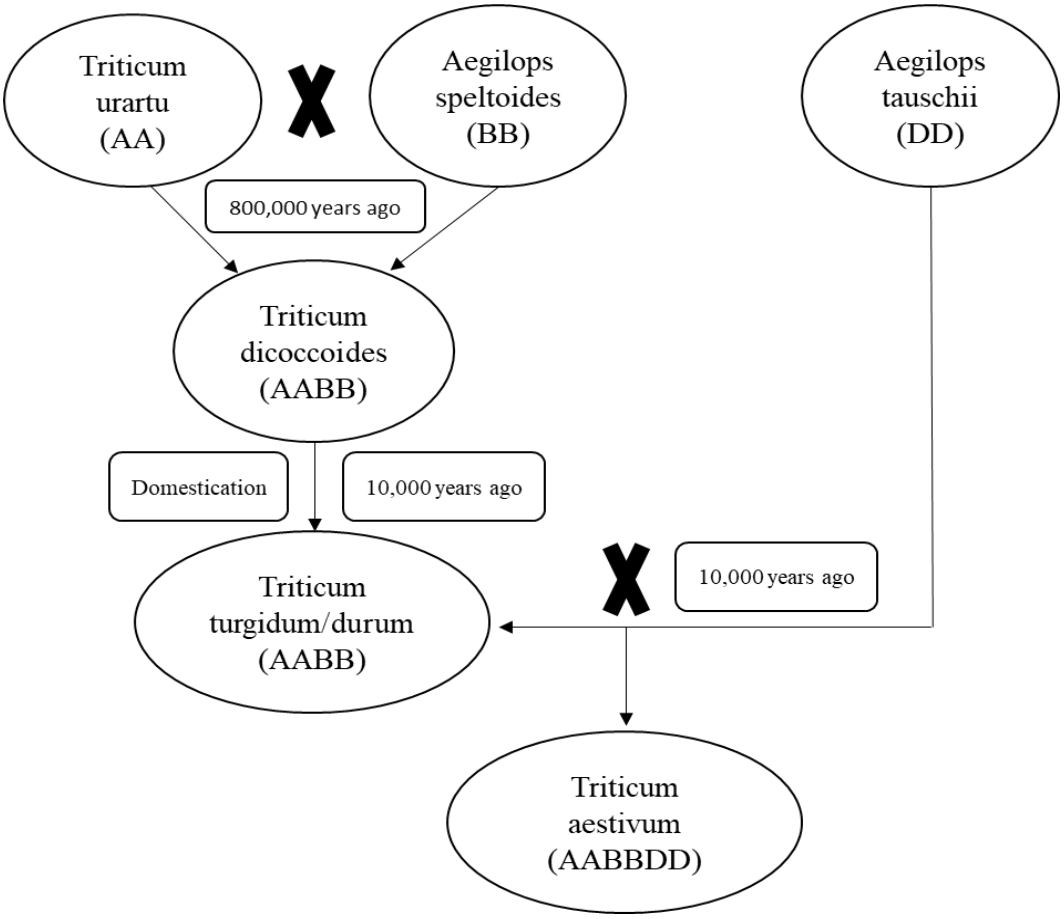

Figure 1.5: Origin of polyploid wheat. The first hybridisation occurred between *T.urartu* (AA) and *A.speltoides* (BB) about half a million years ago which resulted in developing of tetraploid wheat (AABB). This tetraploid wheat was domesticated in the Fertile Crescent about 10.000 years ago. The second hybridisation happened between tetraploid and diploid wheat A.tauschii (DD) about 9000 to 10.000 years ago which resulted in developing of hexaploid wheat (AABBDD) (modified from Desjardins et al., 2020).

1.7.1 Meiosis in polyploid species

The first research in meiosis of polyploid species was done over a century ago in triploid and pentaploid tulips (Newton and Darlington, 1929). Naturally, there are two types of polyploid species. The autopolyploid species which are the result from the whole genome duplication of the original (diploid) genome such as potato (Soares *et al.*, 2021). And the allopolyploid species which are the result from the hybridization between two or more related species such as allopolyploid wheats (Soares *et al.*, 2021). The main difference between these two polyploid species is that autopolyploids

contain two or more homologous chromosomes whereas allopolyploids contain just two homologous chromosomes but two or more homoeologous chromosomes (Soares *et al*., 2021, Svačina *et al*., 2020, Yant *et al*., 2013). These homoeologous chromosomes present in allopolyploids might contain differences in the gene order along the chromosome, differences at DNA sequence level and even in chromosome structure (Soares *et al*., 2021, Svačina *et al*., 2020). In this thesis I will be focusing on allopolyploid wheat species.

The main advantages of being a polyploid species are the duplication of the gene content, the heterosis and reproduction (Comai, 2005). Genetic duplication allows for gene redundancy which might be able to hide deleterious effects of recessive alleles by increasing the chance to present one dominant allele. Heterosis is the phenomenon observed in crosses between species which shows offspring with greater biomass, speed of development, and fertility than both parents. In polyploids this heterosis is also observed.

Despite the advantages of polyploids, there are some disadvantages such as changes in chromosome architecture (e.g. chromosome rearrangements), changes in epigenetic marks (e.g. DNA methylation patterns) and production of aneuploid cells during mitotic and meiotic divisions (Liu *et al*., 2014).

1.7.2 Meiosis in polyploid wheats

The pairing process between wheat homologous chromosomes during meiosis starts early in prophase l through centromere association (Martinez-Perez *et al*., 2003, Martinez-Perez *et al*., 2000). This centromeres association appears as a cluster associated on the nuclear envelope even before the telomere bouquet is observed. Thus, telomere bouquet associated in a side of the nuclear envelope (Rabl configuration) is proposed to play an important role in homologous recognition and pairing (Martinez-Perez *et al*., 2000, Osman *et al*., 2021). Subsequently to the bouquet formation the polymerization of the SC and initiation of synapsis start to form between homologous chromosomes and this synapsis formation initiates from the telomere bouquet region (Osman *et al*., 2021; Sepsi *et al*., 2017).

Triticum timopheevii (2n = 4X = A^tA^tGG) is a tetraploid wheat that has both wild and cultivated forms which seems to have evolved independently from *T. turgidum.* The *T. timopheevii x T. turgidum* hybrids are sterile with different chromosomal aberrations during meiosis (Champman and Kimber, 1992). Interestingly, EM studies of the chromosome behaviour at early meiotic stages in wild *T. timopheevii* have shown a lower frequency of multivalents (more than two homologous/homoeologous chromosome recombine with each other such as trivalent, quadrivalent and hexavalent) at pachytene than at zygotene (Martinez *et al*., 1996). This suggests that there might exist a mechanism to correct non-homologous/homoeologous pairing working during zygotene in polyploid wheats. Furthermore, in wild forms of tetraploid wheats *T. turgidum* and *T. timopheevii* this correction is faster than in cultivated forms (Martinez *et al*., 2001). This might indicate that during the wild wheat domestication some deleterious changes in the control of the homologous pairing occurred (Martinez *et al*., 2001). Thus, due to the presence of homologous and homoeologous pairing during zygotene multivalents can be observed but these multivalent configurations are resolved during zygotene and at metaphase l only bivalents are observed in wild and domesticated tetraploids

(Sybenga, 2012). As described before, strand invasion and recombination intermediates occur between homologous and non-homologous chromosomes at zygotene (Hobolth, 1981). Nevertheless, this does not result in CO formation between non-homologous chromosomes (Jenkins and Rees, 1991). Furthermore, the full synapsis will be only occurring between homologous chromosomes at pachytene without any synapsis between homoeologous chromosomes. As a result, chiasmata are only observed between homologous chromosomes at metaphase I.

1.7.2.1 Diploidization of polyploids in wheat: Bivalent Formation in wheats

As previously explained, chiasmata only occur between homologous chromosome at metaphase I in wheat (Jenczewski and Alix, 2004). Thus, allopolyploid wheat during meiosis is behaving like any diploid species with only chiasmata occur between homologous chromosomes. This meiotic behaviour is very important to allopolyploid wheat to ensure correct segregation of chromosomes during meiosis and full fertility (Jenczewski and Alix, 2004).

The diploid-like behaviour in allopolyploid wheats is not due to random events but genetic control. One of the most important genetic controls in the diploidization of polyploid wheats was identified in 1957 and was called *pairing homoeologous 1* locus (*Ph1*) (Riley and Chapman, 1958, Sears, 1958). This locus was found to be located in the long arm of chromosome 5B and its deletion results in the presence of multivalent configurations at metaphase I as a result of homoeologous recombination in early prophase I (Okamoto, 1957). The length size of the deletion including the *Ph1* locus was estimated to be 70 Mb (Gill *et al*., 1993). Subsequently, other deletions were produced using X-ray irradiation and two mutants were identified: *ph1b* mutant in hexaploid wheat and *ph1c* mutant in tetraploid wheat (Sears 1977; Giorgi 1978; Jauhar *et al*., 1999). The estimated length of the *Ph1b* locus was calculated to be approximately about 59 Mb and it contains around 1,170 genes.

1.7.3 The Role of Telomeres in chiasma localization in wheat

The telomeres become associated in a bouquet at early meiosis and this seems to be important in several events in wheat such as pairing, synapsis and recombination. Cereals in general such as barley and wheat show constraints in meiotic recombination which results in the accumulation of most recombination on distal sub-telomeric regions (Higgins *et al*., 2014, Higgins *et al*., 2012, Mercier *et al*., 2015, Osman *et al*., 2021). However, interstitial and proximal chromosome regions very rarely are involved in genetic exchange during meiosis. Importantly, many genes in these regions are important for wheat breeding (Mayer *et al*., 2011). A further disadvantage of this distal localization of chiasmata in wheat is linkage-drag producing undesirable effects of genes linked together in those regions that seem impossible to separate (Higgins *et al*., 2012). There is more than 30% of gene content located in interstitial and proximal regions which rarely recombine (Mayer *et al*., 2014). Hexaploid wheat contains a genome size of 17 Gb (Bennett and Smith, 1976) with about 5.5 Gb size for each one of the three sub-genomes A, B and D (Mayer *et al*., 2014) and most of the recombination events occur in less than 15% of the genome (Mayer *et al*., 2014). Understanding the molecular and cytological factors that affect these distal chiasmata distribution in wheat would facilitate the possibility of exploiting the gene variability included in these interstitial and proximal regions in the chromosome.

The first description of the telomere bouquet was explained by Fussell (1987) as a telomere clustering to the opposite side of centromere side of nuclear periphery called Rabl configuration. The role of this telomere bouquet during meiosis in cereals such as barley and wheat have been intensively studied (Higgins *et al*., 2012; Osman *et al*., 2021). In wheat the initial chromosome axis and SC formation has been found to be associated with telomeric distal regions before progressing to more

interstitial and proximal regions in each chromosome (Osman *et al*., 2021). This has been confirmed by FISH-analysis using telomere DNA probes, immunolocalization of HORMA domain protein ASY1 and the SC transverse filament ZYP1 (Osman *et al*., 2021). Additionally, early recombination events as DSBs labelled by the phosphorylated histone variant H2AX (γH2AX), were also found to be associated first with telomeric distal regions on wheat (Sanchez-Moran *et al*., 2007; Osman *et al*., 2021). Similarly, the two recombinases DMC1 and RAD51 involved in strand invasion also starts from telomeric distal regions in early prophase l before progressing into more interstitial regions (Osman *et al*., 2021). A meiotic time course using BrdU labelling of DNA replication indicated that early DNA replication events may start in the telomeric regions in early prophase I and progresses through the chromosome interstitial regions until finalising at centromeres in wheat (Osman et al., 2021). All these observations indicate that early meiotic events in wheat from meiotic DNA replication, chromosome axis formation, SC initiation and meiotic recombination events progress from distal telomeric regions, continuing to more interstitial and centromere proximal regions in wheat. Based on this study, it could be stated that the distal telomeric chiasmata observed in wheat might occur as an indirect result of the early DNA replication and recombination events associated with telomeric regions in early prophase I in wheat.

1.7.4 *Pairing Homoeologous 1* (*Ph1*) locus in Wheat

Molecular analysis revealed that the *Ph1* locus contains a cluster of cyclin-dependant like kinases (CDKs) and methyl-transferase genes which are located in the long arm of chromosome 5B (Griffiths *et al*., 2006, Al-Kaff *et al*., 2008). These CDKs seemed to be involved in altering the chromatin structure in early prophase l during meiosis and they were reported to play an important role chromatin condensation, DNA replication and histone phosphorylation (Krasinska et al., 2008, Viera

et al., 2009). There are three copies of CDKs on chromosome 5A, 5B and 5D. However, the deletion of the CDKs on the chromosome 5B leads to the increase of expression of the CDKs in 5A and 5D (Knight *et al*., 2010). This increase of the CDKs expression in 5A and 5D might be regulating chromosome condensation in early meiosis. This was suggested by measuring the length of Asy1 signal in wheat x rye hybrids with and without *Ph1* which showed a significant difference between them with the Asy1 signal expanding more when *Ph1* was absent (Knight *et al*., 2010). In addition, in the absence of *Ph1* histone H1 phosphorylation was increased altering the chromatin structure and resulted in a delay of DNA replication during S-phase (Greer *et al*., 2012). CDKs are serine/threonine kinases and they have been reported to be involved in cell cycle progression (Knight *et al*., 2010). Interestingly, treating hexaploid wheat lacking the *Ph1* locus with okadaic acid, which is known to be an inhibitor of threonine and serine kinases, showed an increase in CO formation in these genome background (Knight *et al*., 2010).

Despite its role in the early process of meiosis, *Ph1* locus has been observed to play a later role in meiosis, specifically at mid-prophase by regulating the mismatch repair protein Mlh1 decision (Martín *et al*., 2014). Surprisingly, the number of MLH1 foci is not significantly different between wheats with or without *Ph1* locus. However, this observation was not consistent with the chiasma frequency observed at metaphase I which was higher when the *Ph1* locus is present (Martín *et al*., 2014). It has been shown that in *Arabidopsis* MLH1 co-localizes with interference-sensitive class I CO sites and that all MLH1 sites seem to resolve as COs, later physically observed as chiasmata at metaphase I (Lhuissier *et al*., 2007). Thus, it seems that the *Ph1* locus might have a role in controlling MLH1 sites between homoeologous chromosomes to become COs/chiasmata in polyploid wheats (Martín *et al*., 2014).

Bhullar and collaborators (2014) reported to have found a single gene identified as *C-Ph1* gene that was responsible for the *Ph1* activity. However, sequence analysis has not found any Arabidopsis

orthologue expressed during meiosis and it was shown previously by other authors that in the absence of this gene the wheat does not exhibit the same phenotype as the *Ph1* deletion phenotype (Al-Kaff et al., 2008). More recently, another group have proposed another gene candidate in this region that could be the *Ph1* locus and that was identified as ZIP4 (Martín *et al*., 2018). ZIP4 is a member of the ZMMs group of recombination proteins that I have previously explained (Chelysheva et al., 2007, Shen *et al*., 2012). ZIP4 is a tetratricopeptide protein which is found to be involved in CO formation specifically in class I COs in *Arabidopsis* and rice (Chelysheva *et al*., 2007, Shen *et al*., 2012).

As I previously mentioned the estimated size of the *ph1* deletion is about 59 Mb and it estimated to contain more the 1100 genes (Martín *et al*., 2018). Within these genes, ZIP4 is contained and it is estimated to be 0.5 Mb in length (Martín *et al*., 2018). In fact, in hexaploid wheat four copies of *Zip4* gene have been identified. Three of them were located in chromosome number 3 group (*TaZip4-A1*, *TaZip4-B1*, *TaZip4-D1*) and the fourth copy located in chromosome 5B (*TaZip4-B2*) (Alabdullah *et al*., 2019). The origin of *TaZip4 5B* arose through the duplication and divergent evolution of a segment of chromosome 3B containing *TaZip4 3B* and some heterochromatin and inserted in the *CDKs* cluster in the *Ph1* locus in 5B (Griffiths *et al*., 2006, Martín *et al*., 2014, Martín *et al*., 2018, Martín *et al*., 2017, Rey *et al*., 2017, Rey *et al*., 2018). The mutation of *TaZip4-B2* results in a *ph1*-like phenotype that shows an increase of homoeologous recombination and a decrease in homologous recombination (Rey *et al*., 2017). Furthermore, *TaZip4-B2* plays an important role in promoting pairing and synapsis between homologous chromosomes in polyploid wheat. Further confirmation of the role of *TaZip4-B2* in promoting homologous recombination was obtained by using a CRISPR-Cas9 mutant for this gene (Rey *et al*., 2017, Rey *et al*., 2018). Additionally, a cross between this mutant with the wild relative species *Ae. variabilis* was done to develop a hybrid and thus identify that homoeologous recombination also occurred in this hybrid background (Rey *et al*., 2017, Rey *et*

al., 2018). In summary, *TaZip4-B2 (Ph1)* promotes pairing and synapsis between homologues in early prophase I and supresses COs between homoeologous chromosomes at late prophase I.

A recent study has revealed a separation-of-function *Tazip4-B2* TILLING mutant: the *zip4-ph1d* is a stable *ph1* mutant which preserves the function of promoting chromosome synapsis between homologues in early prophase I but cannot supress COs between homoeologous chromosomes at late prophase I (Martín *et al*., 2021). Thus, this *zip4-ph1d* mutant does not present multivalents at MI and all recombination occurs among homologous chromosomes, only some univalents are observed in some cells showing the loss of the control of the obligate chiasma (Martín *et al*., 2021). Moreover, plant fertility as number of seeds produced in the mutant had no significant differences from the WT (Martín *et al*., 2021). Nevertheless, haploid wheat plants carrying the *zip4-ph1d* mutation showed homoeologous crossover formation, and makes this mutant line a great recommended option for using in plant breeding programmes for introgression of agronomical traits in cultivated wheats (Martín *et al*., 2021).

1.7.5 *Pairing Homoeologous 2* (*Ph2*)

The *Ph2* locus was first discovered by Mello-Sampayo in 1968-1971 in pentaploid wheat hybrids (Mello-Sampayo, 1971). It is located in the short arm of chromosome 3D and is estimated to be inside a region of 80 Mb in length size (Mello-Sampayo, 1971, Sutton *et al*., 2003). Currently, it has been identified that the *Ph2* locus is located inside a 125 Mb region in the short arm of chromosome 3D (Svačina *et al*., 2020). E. R. Sears (1982) obtained *ph2a* mutant using X-ray mutagenesis. Whereas, *ph2b* mutant was obtained by chemical mutagenesis (Wall *et al*., 1971). The effect of the *Ph2* locus in homoeologous recombination is weaker than that of *Ph1* on wheat hybrids but has no effect in the *ph2a* mutant itself (Sears, 1982). Also, in the hexaploid *ph2b* mutant no homoeologous associations

but a few univalents have been observed at metaphase I (Martinez *et al*., 2001, Sánchez-Morán *et al*., 2001). Also *ph2b* in wheat hybrids have shown an effect on homoeologous recombination at an intermediate level to the one observed in *ph1* mutants (Prieto *et al*., 2005).

Ph2 locus identification has been recently reported as *TaMsh7-3D*, encoding for a DNA mismatch repair protein (Serra *et al*., 2021). Msh7 is a (MutS homolog 7) that shares homology with Msh6 in budding yeast (Dong *et al*., 2002). Msh6 belongs to the mismatch repair group (MMR) and their function is known in plants to be regulating the heteroduplex and strand invasion towards CO formation (Osman *et al*., 2011). A mutant with *Tamsh7-3D* deletion in hexaploid wheat was crossed with *Ae. variabilis* and the hybrids showed a high increase of homoeologous recombination (about 5 times more) than in WT hybrids (Serra *et al*., 2021). This result indicates that *TaMsh7-3D* is a very good candidate gene for the *Ph2* locus.

1.7.6 Exploiting *Ph1* and *Ph2* loci in wheat breeding programmes

Wheat wild relatives such as *Ae. variabilis* and *Secale cereale* have been reported to contain valuable genes that might improve wheat breeding programmes improving different agronomical traits such as disease resistance and abiotic stress (Moore, 2014; Rey *et al*., 2017; Serra *et al*., 2021). Inter species crosses between wheat and wild relatives result in haploid sets of chromosomes with no homoeologous recombination (Rey *et al*., 2017). Nevertheless, the use of wheat *ph1* and *ph2* mutants in hybrids have resulted in exploiting homoeologous recombination to be able to obtain introgression of agronomically interesting traits in wheat (Sears, 1977). Additionally, recently discovered specific mutations of *Ph1* (*zip4-ph1d* and *Ph2 Tamsh7-3D*) should allow plant breeders to further exploit more introgression of desirable traits from wild relatives into wheat (Martín *et al*., 2021, Rey *et al*., 2017, Serra *et al*., 2021).

1.8 The Role of Meiosis and Wheat Research to Food Security

According to the World Food Summit (1996), Food Security is defined as "a condition existing when everyone has physical and economic access to sufficient, safe and nutritious food which meet their dietary needs for healthy life" (World Food Summit, 1996). Food security in the last two and a half decades has been facing many challenges such as increasing population numbers, abiotic stresses (e.g.: temperature, drought), biotic stresses (e.g.: fungi, insects), and other restricted economic factors that affect the availability of food resources (World health organization, 2018). Additionally, in 2050 the world population is expected to be around 9 billion and by 2100 this number could be expected to be around 11 billion (FAO, 2017). On the other hand, crop production is facing many biotic and abiotic stresses that directly could affect their overall production. Based on these data, the goals of Food Security is far from being guarantee specially with such an increase of populations in some low-income countries in Africa and South East Asia (FAO, 2017, Organization, 2018). As a result of this, the Intergovernmental Panel on Climate Change (IPCC) recommended the use of plant breeding tools and availability of natural genetic resources to accelerate and increase the overall crop production in order to face these challenges (Pachauri and Reisinger, 2008).

In the last century, research studying cereal crops such as wheat, rice and maize facilitates their adaptation and distribution worldwide. Wheat is one of the most staple crops with a production of more than 670 million tons in the last decade (Shewry and Hey, 2015). It is classified to be the third highest crop in terms of production behind rice and maize respectively (Shewry and Hey, 2015). Thus, it is being an important source of different nutrients such as proteins, fibres, vitamins and minerals. Most of the wheat production is consumed by humans. For instance, hexaploid wheat *T. aestivum* is known as bread wheat because it is mainly involved in bread production whereas tetraploid wheat *T. durum* is known as pasta wheat because is mainly involved in pasta production (Shewry and Hey, 2015). However, the rest of wheat production is mainly used for feeding livestock.

Shiferaw and collaborators (2011) suggested that exploiting wheat species that contain desirable and valuable traits that could be adopted to mitigate climate change and diseases would be key to facilitate enhancing Food Security.

Using traditional plant breeding methods for crop improvement has been done widely in wheat. These methods are mainly based on crosses between two parental species, one that contains the desirable genetic traits and the other the cultivated species to which these traits are wanted to be transferred. The F1 hybrid progenies of these crosses are supposed to contain the transfer or exchange of some of these traits as a result of meiotic recombination and they should be identified through selection. However, this methodology requires long times involving crossing (mainly manual labour) and selection (with different molecular technologies involved) which reduces the efficiency required to reach Food Security targets in the near future in a timely manner. Thus, the use of new plant breeding molecular techniques such as gene editing would allow to speed the needs of a high crop production in order to achieve Food Security (Borrill *et al*., 2019).

Classical plant breeding methodologies to improve crop production will depend on genetic and allelic exchange occurring during meiotic recombination in meiosis (Blary and Jenczewski, 2019). The meiotic process is tightly regulated in plants and it results in small numbers of COs/chiasmata (one to three) between a pair of homologous chromosomes. In the case of wheat, these chiasmata are mainly distributed or localised in distal chromosome regions. One of the biggest wheat chromosomes, chromosome 3B, has about 80% of all its chiasmata localised at telomeric regions (Consortium *et al*., 2018, Consortium *et al*., 2014). A recent study in our laboratory also have revealed that about 88% of chiasmata appears to be localized at telomeric regions in hexaploid wheat with only 12% occurring at interstitial and proximal regions (Osman *et al*., 2021). Understanding the meiosis process in model plant species such as *Arabidopsis* and wheat (hexa and tetraploid species) and applying this

knowledge to the different crop species would be an important step for improving plant breeding programs and achieving Food Security in the near future.

1.9 Project Objectives

The main general aim of this project has been to be able to manipulate meiotic recombination in cultivated wheats by understanding the meiotic progress dynamics and recombination distribution in different wheat and wild-relative species, cultivars, and mutants. To achieve this aim, several objectives were carried out:

1. Analysis of chiasma frequency and distribution in different wheat and wild-relative species and cultivars.

2. Evaluation of the meiotic process dynamics in different wheat and wild-relative species and cultivars.

3. Investigation of changes in chiasma frequency and distribution in specific wheat chromosomes identified with rDNA probes (5A/1B/5B/6B/1D/5D) in different cultivars and ploidy levels.

4. Study of the meiotic process dynamics and chiasma frequency and distribution in different *ph1* wheat mutants (*ph1b and ph1c*) and in a 5D(5B) substitution line.

5. Exploration of the use of chemicals to change DNA replication timing: suberoylanilide hydroxamic acid (SAHA) and hydroxyurea (HU) to try to alter meiotic recombination in hexaploid wheat.

Chapter 2. Materials and Methods

2.1 Plant Material

The seeds of the plant material used in this thesis were obtained from www.seedstore.ac.uk. The plant material used is listed in table 2.1:

Cultivar Accession	**Species**	**Ploidy level**	**Genome**
T 1020002	*Triticum monococcum*	2X	AA
T 2140005	*Aegilops speltoides*	2X	BB
T 2220053	*Aegilops tauschii*	2X	DD
Kronos	*Triticum durum*	4X	AABB
Capellii	*Triticum durum*	4X	AABB
Langdon	*Triticum durum*	4X	AABB
Langdon (5B)-5D WPGS 5011	*Triticum durum*	4X	AABB
Capellii *ph1c* mutant WPGS 5587	*Triticum durum*	4X	AABB
Chinese Spring (CS)	*Triticum aestivum*	6X	AABBDD
Cadenza	*Triticum aestivum*	6X	AABBDD
Paragon	*Triticum aestivum*	6X	AABBDD
Fielder	*Triticum aestivum*	6X	AABBDD
CS *ph1b* mutant WBCDB 0018	*Triticum aestivum*	6X	AABBDD

Table 2.1: Plant material use in this thesis. The seeds were obtained from www.seedstore.ac.uk.

2.1.1 Plant Growth Conditions

All different wheat species were grown in the glass house at the University of Birmingham under controlled environmental conditions at a constant temperature of 18ºC, a photoperiod of 16h of light and 60% humidity.

Plants were grown in a pot of 17cm of diameter and three wheat plants were grown in each pot. Wheat plants were kept growing until their anthers were ready for meiotic analysis (Figure 2.1). Different wheat species required different times for anthers to be ready for this meiotic analysis (Table 2.2). Additionally, each meiotic stage was found to coincide in specific anthers size and coincide in the different wheat material (Table 2.3).

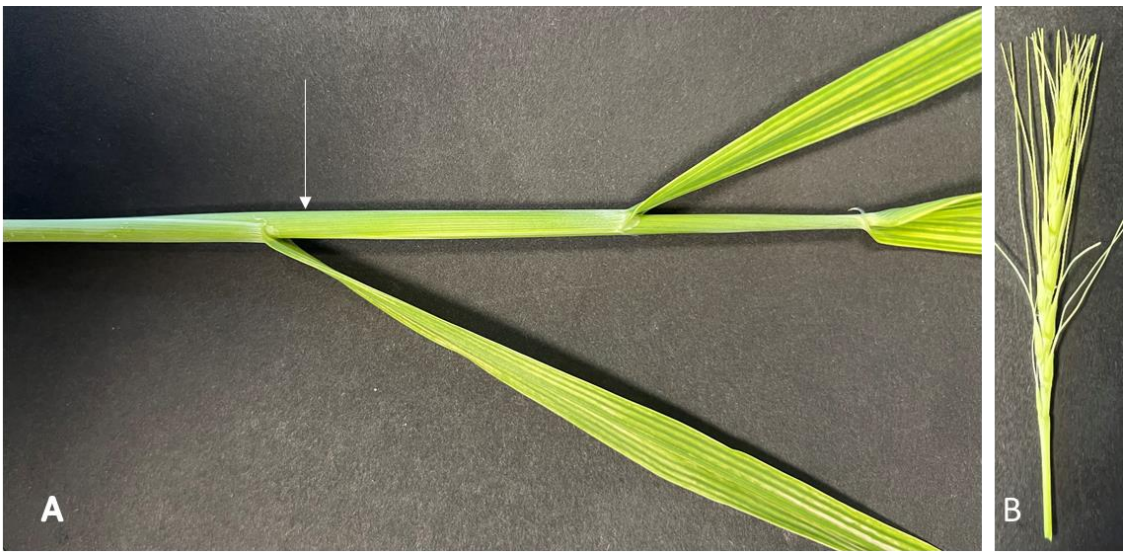

Figure 2.1: Wheat plant ready for meiotic analysis. (A) Developing wheat tiller containing the spike inside that is ready for dissection (arrow point to place where spike is present inside the tiller). (B) The wheat spike containing the florets which contain the anthers for dissection and meiotic analysis.

Wheat species	Dissecting time	Spike size
Chines spring	12 weeks	6-8 cm
Cadenza	11-12 weeks	6-8 cm
Paragon	11 weeks	6-8 cm
Fielder	8 weeks	5 cm
Kronos	6 weeks	4 cm
Capellii	12-13 weeks	6 cm
Langdon	10 weeks	5-6 cm
AA	8 weeks	4-5 cm
BB	4-5 months	6 cm
DD	4-5 months	6 cm
Chinese spring Ph1b	14 weeks	4 cm
Capellii Ph1c	11 weeks	3-4 cm
Langdon (5B)-5D	9 weeks	4 cm

Table 2.2: Appropriate time for spike and anther dissection of different wheat material and their appropriate spike size.

Stages of meiosis	Anther size
Leptotene	0.5 mm
Zygotene	0.6-0.7 mm
Pachytene	0.8 mm
Diplotene	0.9 mm
Diakinesis	1 mm
Metaphase I	1.1-1.2 mm
Telophase I (dyad)	1.3 mm
Telophase II (tetrad)	1.4-1.5 mm

Table 2.3: Identification of different stages of meiosis in different anther sizes.

2.1.2 Sample size (N)

Chiasma frequency is defined as an estimation of meiotic recombination using configuration or bivalents at metaphase I that can be calculated per genome, meiocyte and bivalents.

N is a sample size. In terms of comparing mean chiasma frequency (N=50) refer to the number of meiocyte that counted. In each meiocytes several numbers of bivalents counted. For example, 21 bivalents in hexaploid, 14 bivalents in tetraploid and 7 bivalents in diploid wheats were counted for each meiocyte. Thus, in each hexaploid wheat cultivars a total of (50*21=1050) bivalents counted, in each tetraploid wheat cultivars a total of (50*14=700) bivalents counted and each diploid wild relatives' wheat a number of (50*7=350) bivalents counted.

In terms of FISH analyses, (N=50) refer to the number of single bivalents labelled by FISH probe in each meiocyte. For example, 50 meiocyte were used for counting and the bivalent will only be appearing once a time per meiocyte. That means in 50 meiocyte, 50 bivalents will be counted for each chromosome, 50 5A, 50 1B, 50 5B, 50 1D and 50 5D.

It worth to mention that between 8 to 10 different wheat plants for each cultivar and wild relatives were used for these analyses.

For wheat mutant, only 3 different plants were used in this thesis and this is because of the poor growth and limitation in spike formation.

2.2 Methods

2.2.1 Leaf DNA extraction for genotyping

A 0.5 ml microfuge tube was used to collect a small piece of leaf. Care was taken when collecting samples from several plants to not cross-contaminate them. A total of 50 µl of extraction buffer (100 mM Tris, 10 mM EDTA, 250 mM KCl) was added in each tube. After that, the leaf disc was broken down in the tube by using a sterile micropipet tip and then the tube containing the broken leaf and extraction buffer was heated in a PCR machine at 95^{o}C for 10 minutes (min). After this time, the tube was cooled down in an ice box for at least 2 min. A 50 µl of dilution buffer (3% Bovine Serum Albumin (BSA)) was added to the tube and the content of the tube was mixed using a vortex. The tube was then put in a centrifuge and spun at 13,000 rpm for 2 min. Afterwards, the DNA was ready to use or to store at -20^{o}C.

2.2.2 Anther dissection and fixation

For dissecting anthers, a binocular microscope containing a measuring scale in the oculars was used as well as precission forceps, petri dishes, filter paper and scissors. Following the spike dissection, the anthers were divided in different groups based on their size in a petri dish. After that, anthers were fixed in a fixative solution (containing 3 ml absolute ethanol and 1 ml acetic acid) and kept in a fridge until used for slide preparation.

2.2.3 Meiotic Spreading technique, Slide Preparation and staining with DAPI

For slide preparation of meiotic stages in the different wheat material, three solutions were needed to be prepared in advance: Citrate buffer (10 mM pH4.5) which was prepared adding 445 µl of Sodium Citrate (100 mM) to 556 µl of Citric Acid (100 mM) and to 9 ml of sterile water. 70% acetic acid (10 ml) was freshly prepared in each occasion and kept on ice. Fixative solution (3 ml of absolute ethanol and 1 ml of acetic acid) (Howell and Armstrong, 2013). After that, anthers were taken from the fixative solution and placed in a glass container (preferred to be of dark colour to visualise the fixed anthers better as after fixation they have a white colour). Then, the anthers were washed three times with the Citrate buffer for about 2 min each wash.

Next, the Citrate buffer was changed and digestion enzyme mix applied. To prepare the digestion mix a stock enzyme mix was prepared and consisted of 1% cellulose and 1% pectolyase diluted in 10 mM Citrate buffer). The digestion enzyme mix used on anthers was then prepared by diluting a volume of 333 µl of the enzyme stock in 666 µl of Citrate buffer. This digestion enzyme mix was added to the anthers and incubated at 37^{o}C for 1 hour (h) and 30 min. Following this, the digestion enzyme mix was replaced by cold sterile water to stop the digestion.

At this time a hotplate temperature was adjusted to 45^{o}C. A microscope slide was used to add a drop of ~5 µl of sterile water and 5 to 6 anthers. Then, the anthers were squeezed gently with a brass rod to extract the meiocytes from the inside and then placed on a hotplate (45^{o}C) for 1 min and 15 seconds (sec). During that time, 10 µl of 70% acetic acid were added to the slide and mixed gently with a needle. Finally, 130 µl of fixative solution was added to the slide. The slide preparation was air dried for 5 to 10 min and finally the preparations were stained by adding 15 µl of 4′,6-diamidino-2-phenylindole (DAPI) / Vectashield solution (5 µg DAPI in 1 ml Vectashield solution). The slide was

covered with a coverslip and used for microscope imaging and analysis directly or kept at 4^{o}C until used.

2.2.4 Fluorescence *In Situ* Hybridization (FISH) using 45S and 5S rDNA probes

5S rDNA probe

For preparing 5S rDNA probe the plasmid pTa794 were used which containing the 5S rDNA repeat of *T. aestivum* as a 410 bp cloned insert (Gerlach and Dyer, 1980). This DNA plasmid will be labelled by dUTP-biotin/digoxigenin using nick translation kit according to manufactures' instruction (Cat. No. 11745808910).

45S rDNA probe

For preparing 45S rDNA probe, the plasmid pTa71 were used which containing 18S-25S rDNA genes and spacer region from *T. aestivum* as a 9 kb cloned insert (Gerlach and Bedbrook, 1979). This DNA plasmid will be labelled by dUTP-biotin/digoxigenin using nick translation kit according to manufactures' instruction (Cat. No. 11745808910).

The final mix will be: DNA (45S and/or 5S) + SDW+ nick translation mix. This mix will put at 15C for 90 min. After that, the mix will be moved to RT and 0.5M EDTA will be added. Finally, the mix will be put at 60C for 15 min to degrade the enzyme and now the mix will ready to use in FISH or stored at -20C.

First slides containing a good amount of metaphase I meiocytes were chosen by scanning at a Nikon 90i Epifluorescence microscope (see 2.2.9). These chosen slides were washed in 100% ethanol in a copulin jar for 10 minutes to dismount and remove the coverslips. Then the slides without the coverslips were washed in 4T (4 x Saline-Sodium Citrate Buffer [SSC] and 0.1% Tween20) for 1 h. Afterwards, the slides were washed in 2 x SSC for 10 min.

Then, the slides were washed in a pepsin solution (0.01% pepsin in 0.01M HCl) for 1 min and 30 sec. Following this, the slides were washed in 2 x SSC for 10 min. Another wash was done to fix the slides in 4% formaldehyde for 10 min. After this fixation, the slides were dehydrated by consecutive 2 min washes of 70%, 80% and 100% ethanol. Then, the slides were left to air dry for at least 10 to 15 min before adding the probes.

Following this, 20 µl of hybridization mix containing the DNA probes were added to each slide. The hybridization mix consisted of 1 g dextran sulphate (MW 500,000) diluted in 5 ml deionized formamide (molecular biology grade), 1 ml of 20 x SSC to and made up to 7 ml with sterile deionized water (dissolved at 65 °C). The hybridization mix was cooled to room temperature (RT) and the pH adjusted to 7.0. The hybridization mix was aliquoted and stored at -20°C. For 45S and 5S rDNA FISH analysis, the rDNA probes were added to the hybridization mix in a ratio of 1:20 for each probe (e.g.: 1 µl 5S rDNA probe/ 1 µl 45S rDNA probe/ 18 µl hybridization mix). The hybridization mix containing the DNA probes was denatured by heating the tube in a PCR machine for 10 min at 95ºC before being added to the slides. Then, the denatured DNA probes in the hybridization mix were added to the slides and a coverslip on top. The slides were placed on a hotplate at 75ºC for 4 min. Afterwards, the slides were incubated at 37ºC overnight in a moist chamber.

In the second day, the slides were washed 3 times in 50% formamide/2 x SSC for 5 minutes each, in a preheated water bath at 45ºC. 50% formamide consisting of Amberlite Resin added to formamide

and kept overnight at RT. The formamide was filtered from the resin using filter paper and then it was diluted using 20 x SSC dilute to it to make the 50% formamide/2 x SSC). Afterwards, the slides were washed for 5 min in 2 x SSC followed by another wash for 5 min in 4 x SSC. Both of these washes were in a preheated water bath at 45ºC. The last wash was in 4 x SSC for 5 min at RT. The slides were kept to air dry at RT for 5 min.

The secondary antibodies were added to the slides to detect the probes localization on the chromosomes. To detect digoxigenin-labelled probes, we used a digoxigenin specific antibody conjugated to the fluorophore fluorescein isothiocyanate (FITC, green). Antibodies were diluted to 5 ng/µl in digoxigenin blocking solution just prior to use (e.g.: 1 µl of anti-DIG FITC (green) in 50µl of DIG block solution and 1µl of anti-BioCy3 (red) in 200µl of milk block solution). The blocking solution was prepared by dissolving 0.5% digoxigenin blocking reagent (Roche) in 4T buffer. To detect biotin-labelled probes, we used streptavidin-Cy3 (red) (Roche) made up in biotin blocking solution. The blocking solution was prepared by dissolving 0.5% dried skimmed milk in 4T wash buffer.

Between 50-80 µl of the secondary antibody mix was added to the slide and cover with Parafilm (TM). Then, the slides were incubated for 30 min at 37ºC in a moist chamber.

Following the secondary antibody incubation, the slides were washed 3 times in 4 x SSC for 5 min at RT. Finally, 15 µl of DAPI/Vectashield solution was added to each slide and covered with a coverslip.

2.2.4.1 FISH probes For Telomere and Centromere localization

Centromere probe

The following oligonucleotides were used to produce the centromere probe: 5′-AAGAGGGGGGAATTTCGTGG-3′ and 5′-TTGAAGCCGCCATAAGGAGT-3′. A primary PCR reaction containing these oligonucleotides and leaf DNA was conducted. Followed it by a secondary PCR reaction in which the dTTP nucleotide was substituted by dUTP-biotin or digoxigenin analogues. Both PCR reactions were conducted as following: 1 cycle of 93ºC (3 min); 35 cycles of 93ºC (30 sec)/54ºC (30 sec)/ 72ºC (45 sec); and 1 cycle of 72ºC (10 min).

Telomere probe

The following oligonucleotides were used to produce the telomere probe: 5′-$(TTTAGGG)_5$-3′ and 5′-$(CCCTAAA)_5$-3′. A primary PCR reaction containing these oligonucleotides and leaf DNA was conducted. Followed it by a secondary PCR reaction in which the dTTP nucleotide was substituted by dUTP-biotin or digoxigenin analogues. Both PCR reactions were conducted as following: 1 cycle of 93ºC (3 min); 35 cycles of 93ºC (30 sec)/54ºC (30 sec)/ 72ºC (45 sec); and 1 cycle of 72ºC (10 min).

2.2.4.2 FISH with telomere and centromere probes

The telomere and centromere FISH protocol was carried out in the same way as with the 45S and 5S rDNA FISH (see above section 2.2.4). The only difference was that the hybridisation mix contained the mastermix with telomere and centromere probes instead of 45S and 5S rDNA probes.

2.2.5 Immunolocalization for meiotic proteins (using fresh material)

This technique was first described by Armstrong and collaborators (2002) in Arabidopsis and Brassica plants (Armstrong et al., 2002) and it has been adapted in wheat with some modifications. Firstly, the wheat spike was dissected and the anthers divided to different groups based on their size in a petri dish cover by a wet filter paper. 6 to 9 anthers were placed in a poly-L-lysine coated glass slide with 20µl of digestion enzyme mix (20mg cytohelicase + 75mg sucrose + 50mg polyvinylpyrrolidone diluted in sterile water) and then incubated for 4 minutes in a hotplate at 37ºC. After that, the anthers were squeezed gently using a brass rod to push the meiocytes out of the anther and then the slide was returned to incubate at the hotplate for 3 minutes. After this short incubation, 2µl of the enzyme mix was added to the slide together with 10µl of 1% Lipsol and the solution was spread gently by using a needle. After that, 12µl of 4% paraformaldehyde was added to the slide and left in fume hood to dry for a minimum of 2 hours.

When the slide was dry, a total of 3 washes of Phosphate Buffer Saline-Triton (PBST) (137 mM NaCl, 2.7 mM KCl, 10 mM Na_2HPO_4, 1.8 mM KH_2PO_4, pH 7.4, 0.1% Triton X-100) were carried out (5 min each). Next, 50µl of Block Solution was added to the slide and covered with Parafilm (TM). The Block Solution contained 3% BSA (Bovine Serum Albumen) in PBST. The slides with the Blocking solution were incubated at RT for 30 min. After that, a total of 50µl of the primary antibodies (see Table 2.4), which were diluted in 3%BSA-PBST, were added accordingly to the slide and covered with parafilm. The slides were then incubated with the primary antibodies overnight at 4ºC in a moist chamber.

Antibodies	Dilution	Reference
α-ASY1 Guinea-pig	1:400	Armstrong et al., 2002
α-ASY3 Rabbit	1:400	Ferdous et al., 2012
α-ZYP1 Rabbit	1:400	Osman et al., 2018
α-HEI10 Guinea-pig	1:400	Desjardins et al., 2020

Table 2.4: List of primary antibodies that were used during immunolocalization analysis.

In the second day the slides were washed 3 times on PBST (5 min each). Following this, the secondary antibodies (see Table 2.5) were diluted in 3% BSA-PBST and added to the slides and covered with parafilm. Then, the slides were incubated with the secondary antibodies at 37^{o}C for 30 min. After the incubation, the slides were washed for 3 times in PBST (5 min each). Finally, the slides were left to dry between 3-5 min before adding 15µl DAPI and covering with a coverslip.

Antibodies	Dilution	Reference
α-Guinea-pig (FITC)	1:50	Thermo Fisher Scientific
α-Rabbit (Alexa 594)	1:200	Thermo Fisher Scientific

Table 2.5: List of secondary antibodies that were used during immunolocalization.

2.2.6 Immunolocalization for meiotic proteins (using fixed material)

This type of immunolocalization is also called "*microwave technique*". Instead of using fresh material, in this technique slides obtained from fixed material were used (fixative solution containing 3 parts of absolute ethanol and 1 part of glacial acetic acid). This technique is based in Chelysheva and collaborators (2010) with some key modification. An important note, the material should not be fixed for longer than 3 days or the immunolocalization will not give the best result. For best results,

the material was fixed from 7-9am to get more cells in prophase I and fixed for 3 days, then the slides were prepared as described above (see section 2.2.3). Following this, a citrate buffer (pH=6) was heated in a microwave at full power for 4 minutes (it was preferable to open the microwave after each minute to avoid over heating of solution). The Citrate buffer consisted of 2.50g of tri-sodium citrate (10 mM) diluted in 1L of sterile water (with drops of Citric acid added to adjust the pH). Following the microwave heating, this heated citrate buffer was placed in a coupling jar and the slides placed in its racks. The coupling jar containing the slides with the citrate buffer was placed inside the microwave for 45 second at half power (it was preferable to open the microwave each 10 sec). After that, the slides were washed once in PBST for 10 min. Next, the slides were left to dry at RT for 2 min before adding the Block solution (3%BSA-PBST) to each slide and covered them in parafilm. The next steps were identical to the ones followed in the fresh immunolocalization for meiotic proteins technique using fresh material (see above section 2.2.5).

2.2.7 Time course Immunolocalization for meiotic proteins

5-Bromo-2-deoxyuridine (BrdU) is a nucleotide (T) analog which can be incorporated into the DNA during the S phase (DNA replication). BrdU has been used to measure the different times of the meiotic stages (meiotic time course) (Armstrong, 2013; Osman *et al*., 2021; Osman *et al*., 2022).

Firstly, wheat spikes at the right stage were injected with 500µl of BrdU (10mM of BrdU dissolve in PBS and stored at -20^{o}C) and 1µl of Tween 20 using a hypodermic needle and a syringe (Figure 2.2). The BrdU solution was injected in the tiller's cavity above the developing spike. The time of injection was counted as time zero and the spikes were dissected and the anthers fixed at different time points. After the different time course anthers were fixed, the anthers were used for cytological analysis as described above (see section 2.2.3).

Once the slides were obtained, the microwave technique for immunolocalization was followed (see above section 2.2.6). For primary antibody we used a mouse anti BrdU antibody diluted 1:50 times in 3%BSA-PBST solution. For the secondary antibody, we used an anti-Mouse antibody diluted (1:20) in 3%BSA-PBST.

Figure 2.2: The injection of BrdU solution on the wheat flag cavity using a hypodermic needle and a syringe. The end of the needle will be at the top of spike. When injection started the BrdU will reach the spike from the top and will continue going down to reach all the spike parts. By the end of injection, the spike inside the cavity will be covered by BrdU.

2.2.8 Combination of FISH and Immunolocalization

Meiotic stages slides were prepared following the immunolocalization methodology for fresh material (see above section 2.2.5) with some changes. The primary antibody used (e.g.: anti-Zyp1) was always one raised in rabbit. During the second day, the slides were washed 3 times in PBST (5 min each). Followed by the incubation with the secondary antibody conjugated with biotin (α-rabbit biotin) diluted in 3%BSA-PBST at 37ºC (30 min). This secondary antibody works as a protector and label of the primary antibody against the meiotic protein (ex: rabbit anti-ZYP1) during the FISH stages. Following this incubation, the slides were prepared following the FISH protocol described above (see section 2.2.4). Finally, the slides were analysed using the epi-fluorescence microscope (see section 2.2.11).

2.2.9 Treatment of wheat meiotic S phase with Hydroxyurea

Hydroxyurea (Sigma H8627**)** was diluted in water at a concentration of 10mM (stock solution). A total of 500 µl of hydroxyurea (0.5 mM) solution was injected in the cavity above the wheat spikes as described for BrdU (see figure 2.2). After that the anthers were dissected and fixed at different time points. The slides were prepared using the DAPI spreads technique (see above section 2.2.3).

2.2.10 Treatment of wheat meiotic S phase with SAHA

Suberoylanilide Hydroxyamic Acid (SAHA; Tocris 4652) was diluted in DMSO at 100mM. Once dissolved in DMSO, a 1mM stock solution was made by adding sterile water to the 100mM SAHA solution in DMSO. A total of 500µl of SAHA (0.1mM) solution was injected in the cavity above the wheat spike. After that the spike was dissected and the anthers fixed. The meiotic slides were prepared using the spreading technique (see above section 2.2.3).

2.2.11 Microscope Analysis

All the slides were analysed by using a Nikon 90i Epifluorescence microscope equipped with a Hamamatsu CCD camera (C4742-80-12AG Hamamatsu Photonics K.K.) at the University of Birmingham. This microscope is controlled by NIS-Elements (Advance Research v3.0) software from Nikon. For DAPI spread slides, a single DAPI channel was used with a Z-stack tool (Figure 2.3). For immunolocalization and FISH slide analysis, the multi-channel (DAPI + GFP + mCherry filters) were used together with a Z-stack tool for capture (Figure 2.4). Images were saved in a hard drive and later analysed by using FIJI (ImageJ) software.

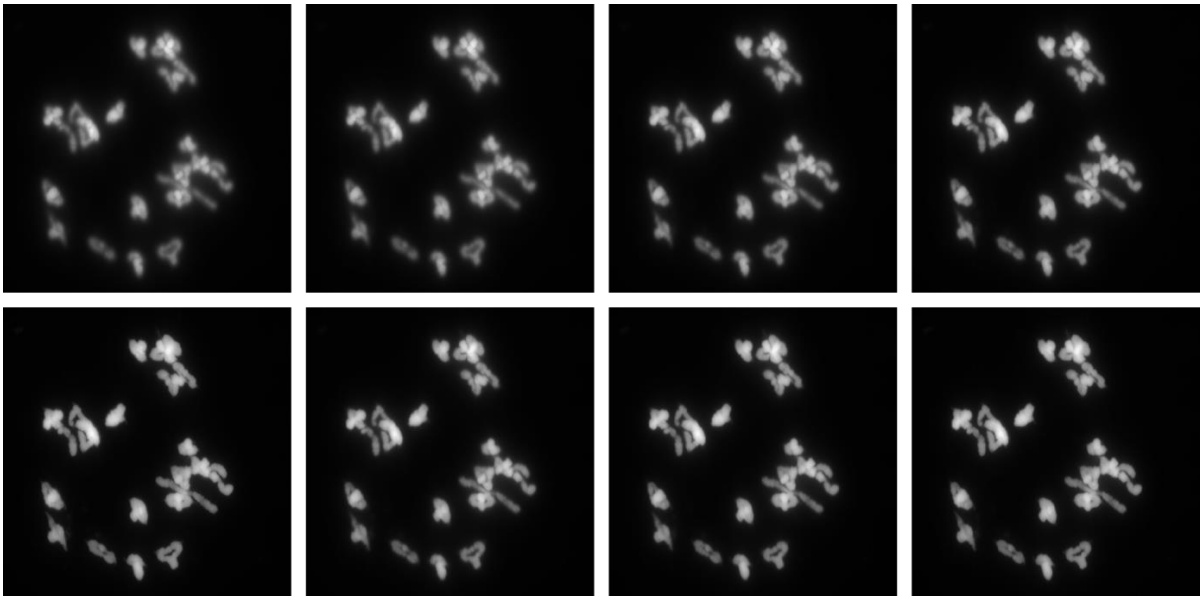

Figure 2.3: An example of using Z-stack tools for capturing imaging with single-channel to facilitate bivalent and chiasmata identification. For instance, when the two or more bivalents alien in the top of each other, it will be difficult to identify them but using Z-stack tools allow the capturing of the images at different focal which make it possible to identify bivalents alien in the top of each other or close to each other.

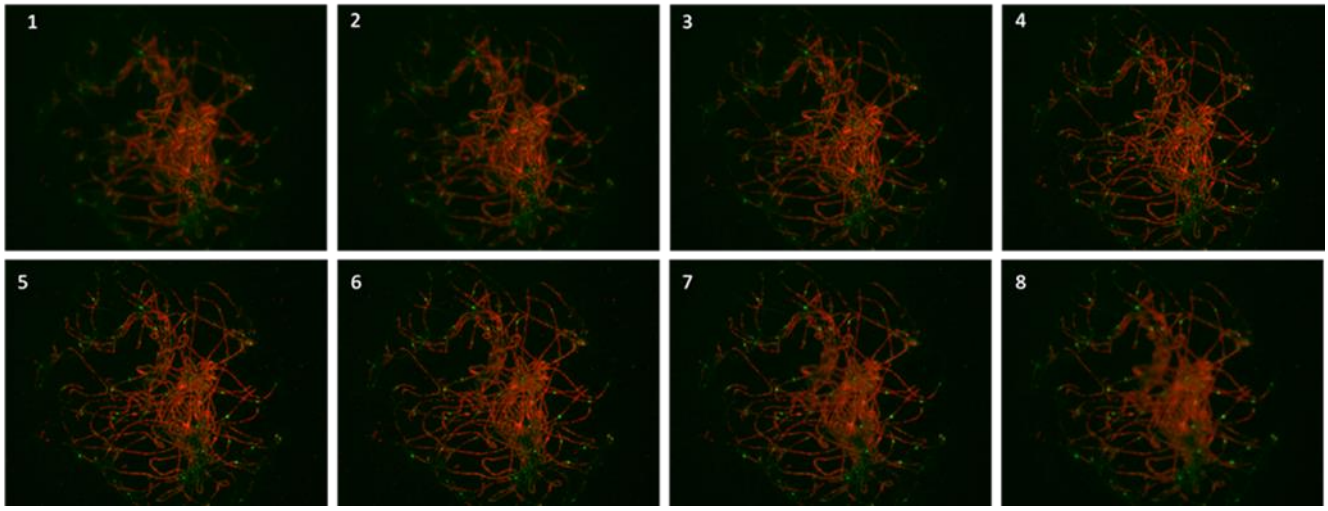

Figure 2.4: An example of using Z-stack tools for capturing imaging with multi-channel. This tool was used for images that contain more than two colours and it facilitate the identification of the different parts of the cell in the slide. For instance, image number 1, the centre of the cell is clear but the border of the cell is not. Thus, in image number 6 and 7 the border of the cell is clear whereas the centre is not.

2.2.12 Statistical Analysis

Statistical analysis was conducted by GraphPad Prism 9 and Microsoft Excel software. Firstly, the test of normality conducted by D'Agostino-Pearson test and Shapiro-Wilk test. When the data pass the normality, the parametric test is conducted. Alternatively, if the data do not pass the normality, non-parametric test is conducted.

In this thesis, to compare the mean chiasma frequency between different wheat cultivars and their wild relatives I use the following tests:

- Welch's One-way ANOVA multiple comparison test were used to compare the mean chiasma frequency between more than two groups. Thus, in terms of comparison between two groups Welch's t Test was conducted.

For non-normal distribution data and this happen normally when comparing the mean chiasma frequency of FISH chromosomes between different wheat cultivars and their wild relatives, Kruskal-Wallis test were conducted.

Chapter 3. Meiotic Bivalent Configurations and Chiasma Frequency and Distribution in Wheat species

3.1 Introduction

One meiotic chiasma is the cytological physical manifestation of one CO at diakinesis and metaphase I stages. Chiasmata (plural) are then the manifestation of COs. Cytologically, chiasmata can be first observed during diplotene after the disassembly of the SC. The homologous chromosomes will separate but stayed together in the places where COs were formed (chiasmata). As chromosomes condense progressively from diakinesis to metaphase I these associations are more visible (Sánchez-Morán *et al*., 2001). Chiasmata were first hypothesized by Janssens in his "Chiasmatype Theory" (reviewd in Koszul *et al*., 2012). This hypothesis supported the chromosomal basis of heredity by connecting cytological observations of meiosis with genetics data and proposed that the physical connections observed between the homologous chromosomes at metaphase I (the chiasmatype or chiasma) could be the regions of genetic crossing over (COs). The cytological observations came from the independent analysis of meiosis made by different authors: A. Weismann (1885), E. Strasburger (1888), T. Boveri (1889; 1904), T.H. Montgomery (1901), W.S. Sutton (1902; 1903) and V. Grégoire (1904). This Janssens' chiasmatype theory could explain different observations: the role of chromosome segregation during anaphase I (to produce haploid cells with the correct chromosome constitution), the physical links between the homologous chromosomes at metaphase I as the physical manifestation of COs, that the meiotic process consists of two meiotic divisions and that the meiotic second division was a simple division of chromatids (similar to mitosis), the different changes in chromosome pairing and synapsis during prophase I (from zygotene to diplotene), that the outcome of male meiosis produces tetraspores or four haploid cells; and provided a broader view of mendelian genetics (Janssens, 1909). In subsequent years, work carried out in *Drosophila* showed how this chiasmatype theory coincide with the COs observed along different markers on different chromosomes (Sturtevant, 1913; Bridges 1914). Several observations supported the point of this hypothesis that meiotic recombination occurred in 2 of the 4 chromatids between the homologous

chromosomes (Wilson and Morgan, 1920) but this was not fully confirmed until scientists did isotope-labelling studies (Taylor, 1965; Peacock, 1970; Jones, 1971). The direct scientific evidence of chiasmata being the points of crossing over came decades later by analysis of the meiosis in maize using chromosome rearrangements material (Creighton and McClintock, 1931) and *Drosophila* (Stern, 1931). This was supported by the proof that there was chiasma interference in beans (Maeda, 1930; Haldane, 1931) and further cytogenetic studies have fully demonstrated that chiasmata are the physical manifestation of COs (Whitehouse, 1967; Jones, 1971; Sybenga, 1975; Tease, 1978; Tease & Jones, 1978; Jones, 1984).

Chiasma location has been classified into two main categories: distal (close to telomeres) and proximal (close to centromeres) (Darlington, 1935; Darlington and La Cour; 1941). A third category has also been described to be intermediate to these two; interstitial chiasma (Darlington and Ammal, 1932). The observation of these three categories and how high numbers of distal chiasmata seem to be accumulated at metaphase I implied the hypothesis of chiasmata terminalization (Darlington, 1932). C.D. Darlington (1929) defined the terminalization of chiasmata as the displacement of chiasmata from proximal/interstitial regions towards distal regions as a progression of metaphase I to anaphase I producing the effect that most of chiasmata are localized distally. Nevertheless, G.H. Jones (1977) and other authors (Tease, 1978; Tease & Jones, 1978; Kanda & Kato, 1980; Jones 1984) demonstrated that terminalization of chiasmata didn't exist by analysing differential chromatid BrdU labelling patterns in different species. Thus, the chiasma localization observed at metaphase I corresponds with the physical location where the CO formed earlier on during prophase I.

Chiasmata localization and frequency can be used as a tool to identify the distribution of genetic exchanges between homologous chromosomes. Chiasmata number are widely studied in plants and it has been identified to be widely spaced and following a Poisson distribution along the chromosome length with normally between 1 to 3 chiasmata occurring between two homologous chromosomes

(Higgins *et al*., 2014, Mercier *et al*., 2015). Chiasma interference influences the distribution of chiasmata along the chromosome arms and limits their number per bivalent (Haldane, 1931; Jones, 1984; Jones & Franklin, 2006). Furthermore, the fact that all pairs of homologous chromosomes have at least one chiasma to form a bivalent at metaphase I shows that there is another control during meiosis that makes sure that there are not univalents miss-segregating at anaphase I; this is known as the obligate chiasma (Mather, 1937; Jones, 1984).

Chiasma localization on the bivalents tends to be confined in specific regions depending on the species and even on the chromosomes involved (reviewed in Jones, 1984). Some species have the chiasmata localized close to the centromeres (proximal distribution) like *Stethophyma grossum* males or *Allium fistulosum* (Jones, 1971; Albini & Jones, 1988). Other species the localization is confined in regions closer to the telomeres (distal distribution) like rye (Jones, 1967). In cereals, specifically in barley and wheat, despite the low number of chiasmata, their localization seems to be biased to distal regions (close to telomeric regions) restricting the amount of genetic exchanges localised in interstitial or proximal (closer to centromeres) regions. Several studies have revealed that more than 82% of chiasmata occurs at distal regions in hexaploid wheat (Lukaszewski *et al*., 1992; Osman *et al*., 2021). Thus, these results indicate that chiasma localization in wheat is not randomly distributed along the homologous chromosomes and that they would rather occur at specific distal regions rather than other more interstitial or proximal ones.

In this chapter, the analysis was conducted for chiasma frequency and localization by analysing the different bivalent configurations observed at metaphase I. To analyse chiasmata position on chromosomes, Z-stack clear epifluorescence microphotographs of metaphase I pollen mother cells were obtained (figure 3.1). In this thesis we have been able to differentiate several chiasma localizations in wheat species: distal (d), interstitial 1 (i^1), interstitial 2 (i^2), interstitial 3 (i^3), and proximal (p).

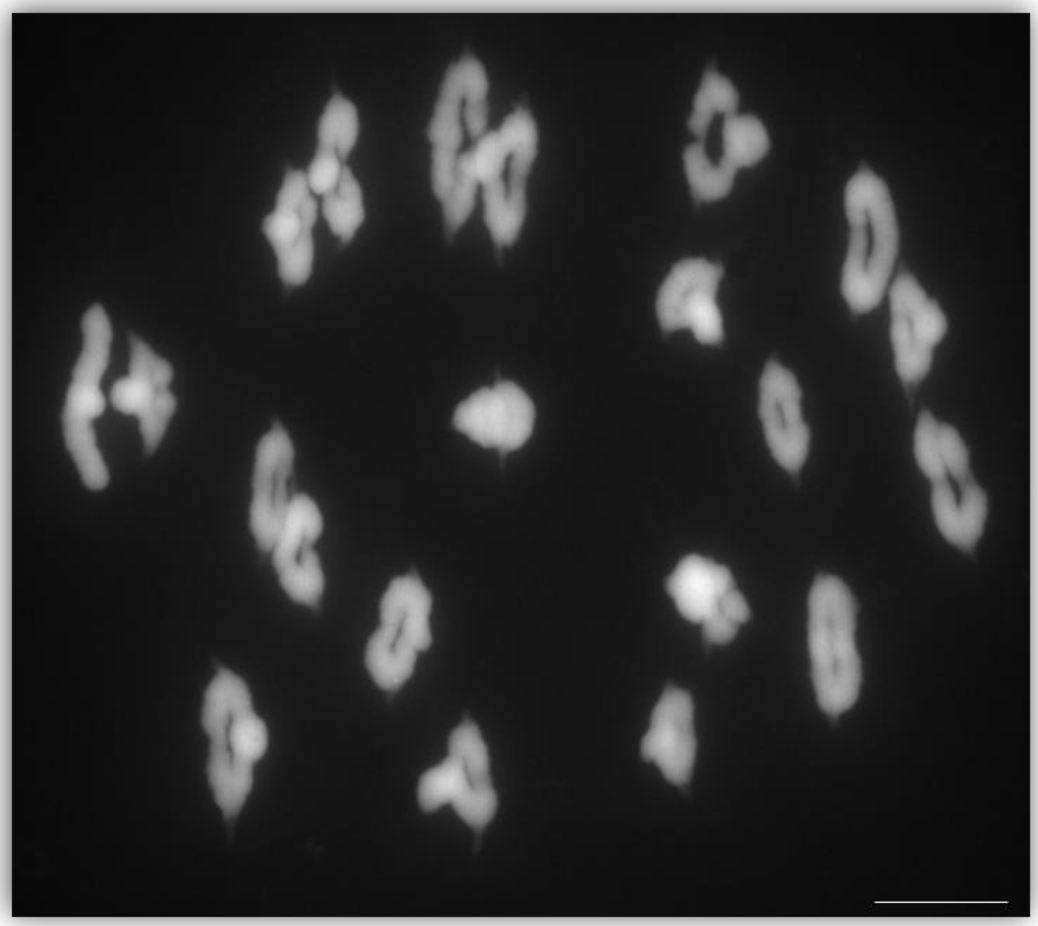

Figure 3.1: An example of a microphotograph of a pollen mother cell at metaphase I of hexaploid wheat (cultivar CS). It shows a perfect separation of bivalents to allow the identification and characterization of chiasma frequency and localization. Scale bar = 10 μm.

3.2 Results

3.2.1 Wheat meiotic configurations at metaphase l:

In order to quantify and characterize the localization of chiasmata on each bivalent at metaphase I, several points must be considered:

- During the pre-meiotic S phase the DNA is replicated and immediately the Cohesion complex would hold the two sister chromatids together by the loading of cohesins (Sister Chromatids Cohesion-SCC). This SCC is maintained during prophase I along the whole chromosome length including the regions where meiotic recombination occurs (COs/chiasmata). This SCC is maintained during metaphase I but the SCC will be dismantled from the chromosome arms by the proteolytic degradation of cohesins by a separase at anaphase I and the SCC will only be maintained at centromeric regions due to their proteolysis protection provided by Shugoshin (Clift and Marston, 2011). Only at anaphase II the centromeric SCC will be dismantled to allow the sister chromatids to divide to different poles.
- The first division meiotic spindle is formed by the polymerization of microtubules (α/β tubulin) at metaphase I. This polymerization is related to the nuclear membrane break down at this stage. Some microtubules will attach to the chromosome kinetochore (the two sister chromatids kinetochores act as one single kinetochore at metaphase I). This allows the microtubules to attach to the kinetochores of both homologous chromosomes involved in a bivalent and the spindle tension would translate into the bivalent bi-orientation at the equatorial plate of the cell at metaphase I.
- The position of the chiasma is the place where meiotic recombination (CO) has occurred.

Bearing in mind these facts, at metaphase I the meiotic configurations observed of the bivalents have to preserve all these characteristics: SSC is preserved along all the chromosome arms and centromeres, bi-orientated tension by the meiotic spindle of the bivalents and the position of the chiasma is the exact position where the CO was formed (figure 3.2).

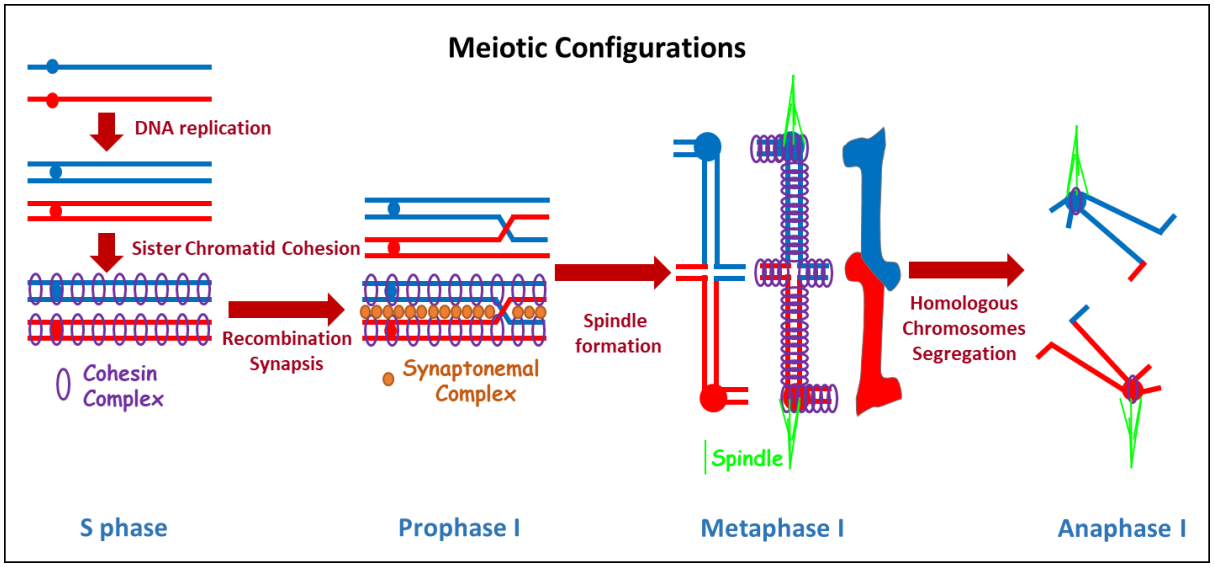

Figure 3.2: Meiotic configurations. After DNA replication the sister chromatids will be held together by cohesins at S phase (SCC). During prophase I recombination, pairing and synapsis will occur, producing COs and the polymerization of the SC. At metaphase I, the meiotic spindle will be formed and the nuclear membrane broken. Already the SC has been depolymerized at diakinesis (end of prophase I). The microtubules will attach to the centromeres of each bivalent and bi-orientate the bivalents at the equator of the cell. The meiotic configurations of bivalents observed depend on the spindle tension, the SCC and the chiasmata (COs).

In wheat, like in other species, there are two type of bivalent configurations that can be observed at metaphase l. Rod and ring bivalents which they form based on the chiasma number and localisation at the chromosome arms. Rod bivalents are formed when one or more chiasmata occur only in one chromosome arm (figures 3.3 and 3.4). In contrast, ring bivalents are formed when at least one or two chiasmata occur at both chromosome arms (figures 3.5 to 3.9).

3.2.1.1 Sub-classification of Rod Bivalents in wheat species

In a rod bivalent, only one chromosome arm is involved in recombination between the homologous chromosomes. One or even more COs/chiasmata can occur along this chromosome arm between homologous chromosomes and where these COs occurred would dictate the shape of the bivalent. For this thesis, a sub-classified of rod bivalents in wheat species according to the chiasmata number and their localization along the chromosome arm (figures 3.3 and 3.4). Distal rods (d): one chiasma forms at a distal region (close to telomeres) of the chromosome arm. Interstitial rods class 1 (i^1): one chiasma forms at a interstitial region of the chromosome not too far from the telomere region. Interstitial rods class 2 (i^2): one chiasma forms at a interstitial region of the chromosome further away from telomeres than i^1. Interstitial rods class 3 (i^3): one chiasma forms at a interstitial region close to the centromeres. Proximal rods (p): one chiasma forms close to the centromeric region. In addition to these categories with only one chiasma (d, i^1, i^2, i^3, p), rods with two chiasmata were classified in other subcategories (figure 3.4): Rod bivalents with a distal (d) and an interstitial class 3 (i^3) chiasmata ($d+i^3$). Rod bivalents with a distal (d) and a proximal (p) chiasmata (d+p).

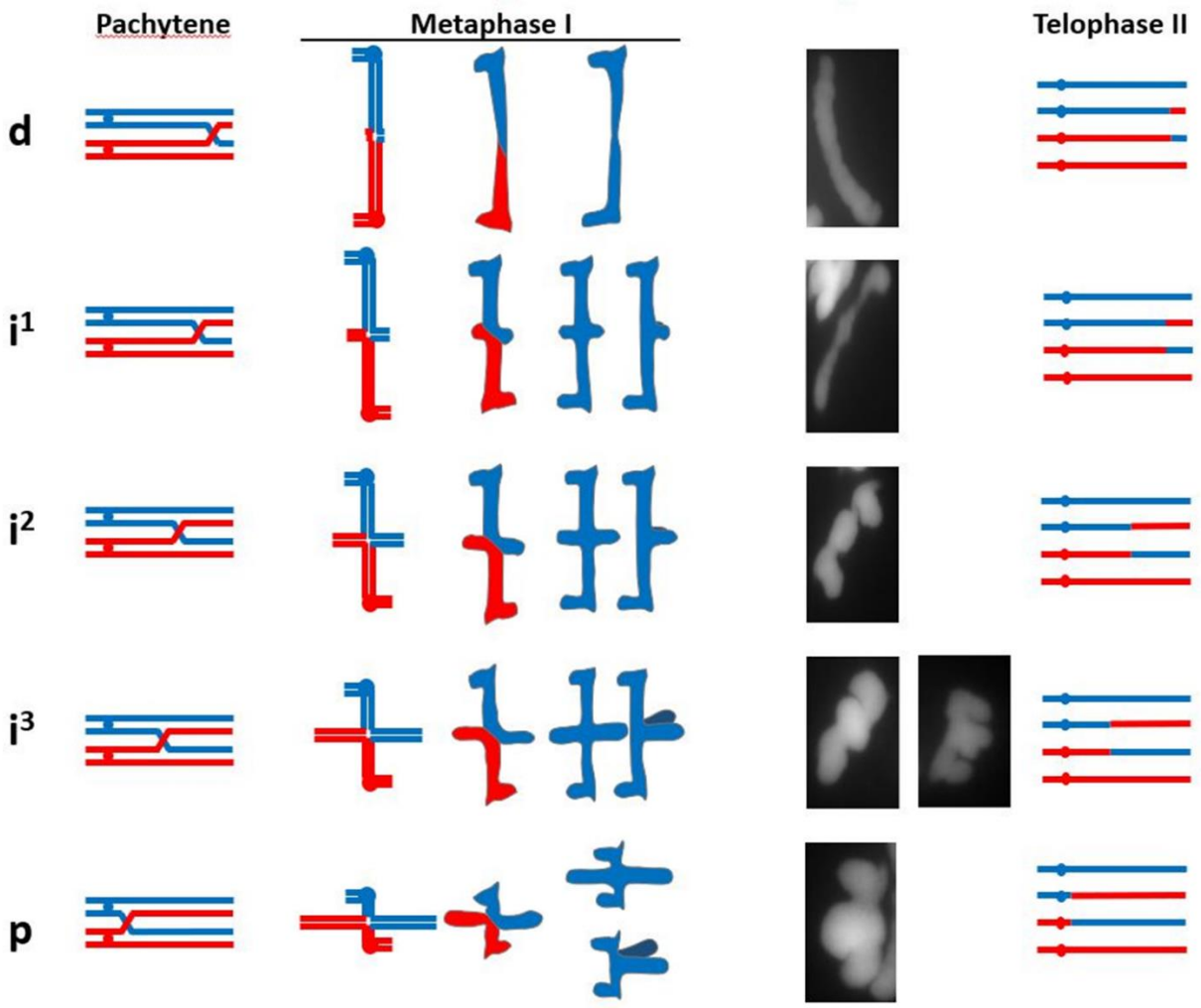

Figure 3.3: Sub-classification of rod bivalent configurations with only one chiasma in wheat species. The diagrams show how the localization of the CO will change the shape of the rod configuration at metaphase I. Different examples of DAPI stained wheat bivalents observed at the fluorescence microscope are provided for each sub-class.

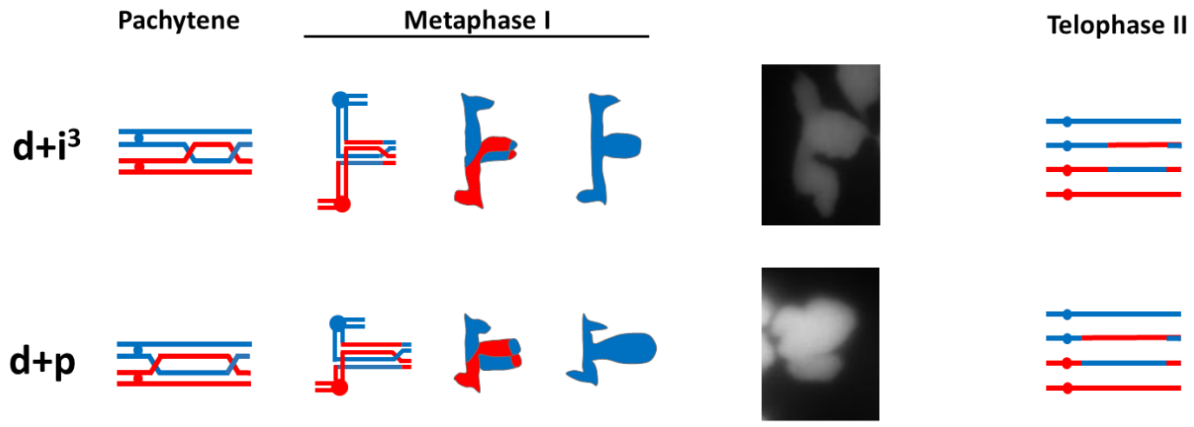

Figure 3.4: Sub-classification of rod bivalent configurations with two chiasmata in wheat species. The diagrams show how the localization of the COs changes the shape of the rod configurations at metaphase I. Different examples of DAPI stained wheat bivalents observed at the fluorescence microscope are provided for each sub-class.

3.2.1.2 Sub-classification of Ring Bivalents in wheat species

In ring bivalents, both chromosome arms are involved in recombination between the homologous chromosomes. One or even more COs/chiasmata can occur along each chromosome arm between homologous chromosomes and where these COs occurred would dictate the shape of the ring bivalent. For this thesis, ring bivalents were classified according to the chiasmata number and their localization along the chromosome arms (figures 3.5 - 3.9). Distal-distal rings (d+d): one chiasma forms at a distal region (close to telomeres) in each chromosome arm. Distal-Interstitial class 1 ring (d-i^1): one chiasma forms at a distal region (close to telomeres) in one chromosome arm and another chiasma forms at an interstitial region of the chromosome not too far from the telomere region in the other arm. Distal-Interstitial class 2 ring (d-i^2): one chiasma forms at a distal region (close to telomeres) in one chromosome arm and another chiasma forms at an interstitial region of the chromosome further away from telomeres than i^1. Distal-Interstitial class 3 ring (d-i^3): one chiasma forms at a distal region (close to telomeres) in one chromosome arm and another chiasma forms at an interstitial region close to the

centromeres. Distal-proximal (d-p): one chiasma forms at a distal region (close to telomeres) in one chromosome arm and another chiasma forms close to the centromeric region.

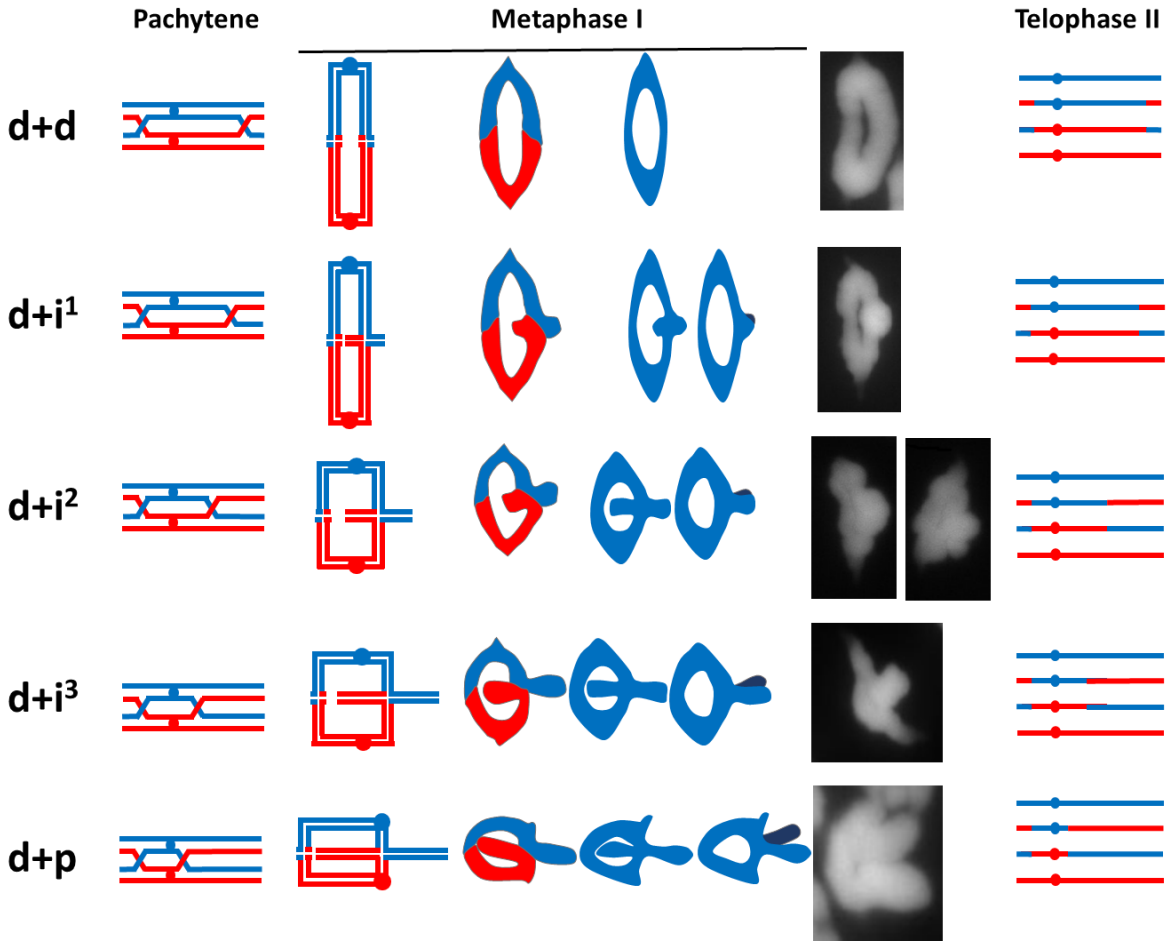

Figure 3.5: Sub-classification of ring bivalent configurations with at least one distal chiasma in one chromosome arm in wheat species. The diagrams show how the localization of the chiasmata/COs changes the shape of the ring configurations at metaphase I. Different examples of DAPI stained wheat bivalents observed at the fluorescence microscope are provided for each sub-class.

In addition to these categories with always one chiasma at a distal location in one arm (d-d, d-i^1, d-i^2, d-i^3, d-p), rings in other subcategories depending on the number of chiasmata in each arm and their localization were classified (figure 3.6-3.9). Ring bivalents with a total of two chiasmata but without any distal (d) but different arrangements of interstitial chiasmata (i^1, i^2, i^3) (figure 3.6). Ring bivalents with two interstitial class 1 (i^1) chiasmata (i^1+ i^1). Ring bivalents with an interstitial class 1 (i^1) and

an interstitial class 2 (i^2) chiasmata (i^1+i^2). Ring bivalents with two interstitial class 2 (i^2) chiasmata (i^2+ i^2).

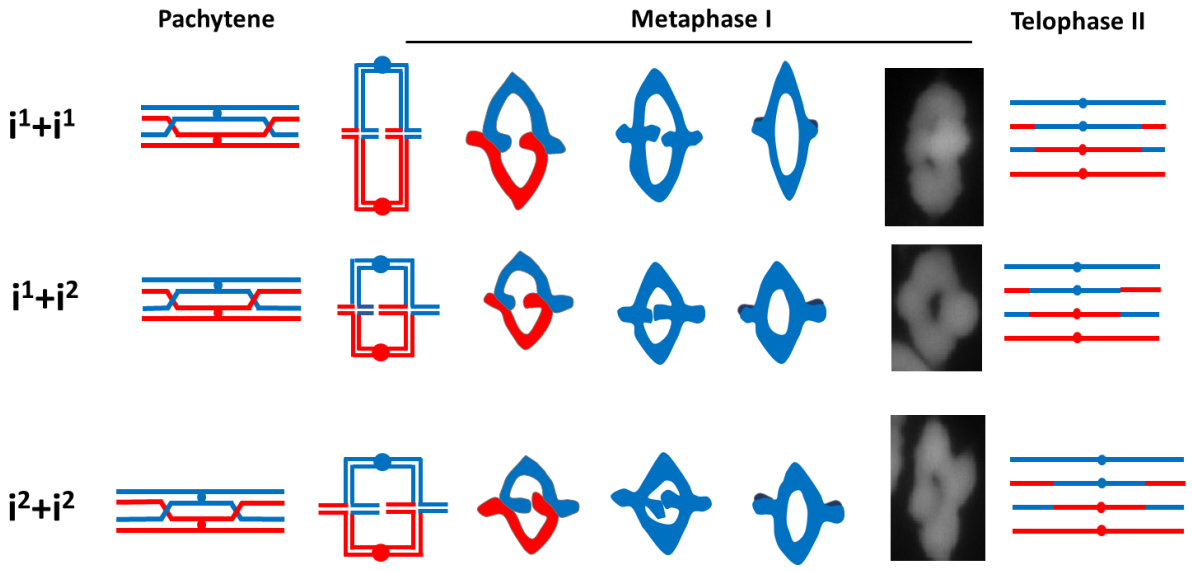

Figure 3.6: Sub-classification of ring bivalent configurations with interstitial chiasmata in wheat species. The diagrams show how the localization of the chiasmata/COs changes the shape of the ring configurations at metaphase I. Different examples of DAPI stained wheat bivalents observed at the fluorescence microscope are provided for each sub-class.

Furthermore, ring bivalents with 3 chiasmata (one chiasma in one arm and two chiasmata in the other chromosome arm) were observed in wheat species (figures 3.7-3.8). Ring bivalents with a distal chiasma in one arm (d) and a distal (d) and interstitial class 3 (i^3) chiasmata (d+i^3+d). Ring bivalents with a distal chiasma in one arm (d) and a distal (d) and proximal (p) chiasmata (d+p+d) (figure 3.7).

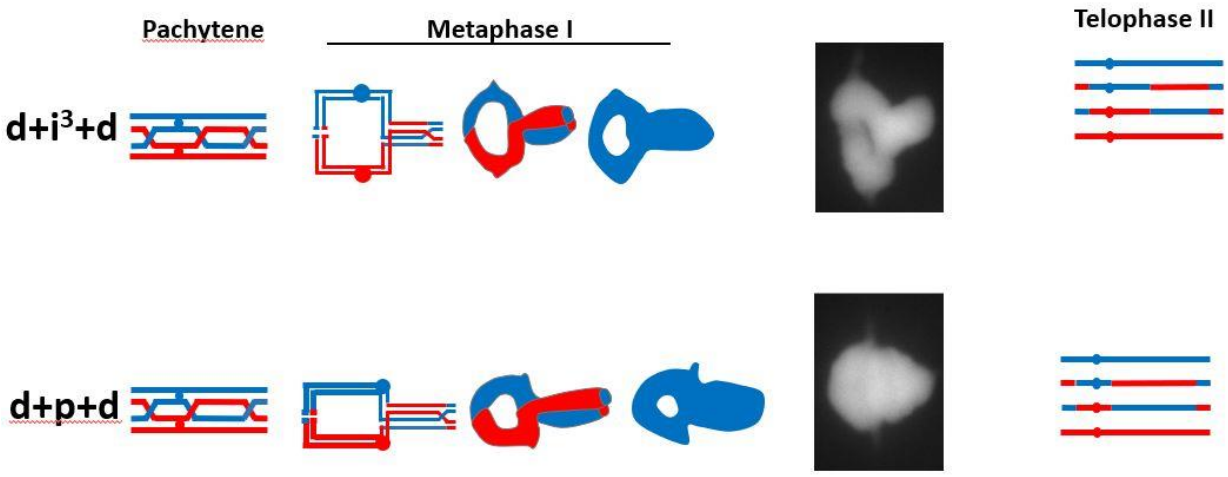

Figure 3.7: Sub-classification of ring bivalent configurations with three chiasmata per bivalent (one in one arm and two in the other arm) in wheat species. The diagrams show how the localization of the chiasmata/COs changes the shape of the ring configurations at metaphase I. Different examples of DAPI stained wheat bivalents observed at the fluorescence microscope are provided for each sub-class.

In addition, other ring bivalent configurations with 3 chiasmata were observed (figure 3.8). Ring bivalents with an interstitial class 1 chiasma in one arm (i^1) and a distal (d) and interstitial class 3 (i^3) chiasmata in the other (i^1+i^3+d). Ring bivalents with an interstitial class 2 chiasma in one arm (i^2) and a distal (d) and interstitial class 3 (i^3) chiasmata in the other (i^2+i^3+d). Ring bivalents with an interstitial class 2 chiasma in one arm (i^2) and a distal (d) and proximal (p) chiasmata in the other arm (i^2+p+d).

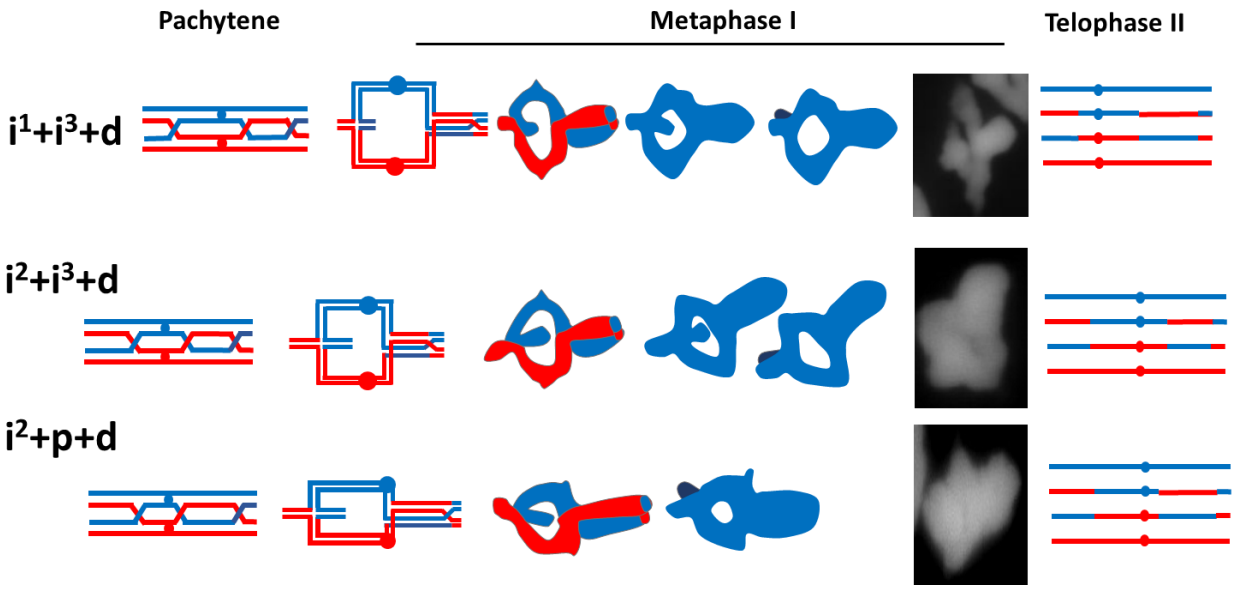

Figure 3.8: Sub-classification of ring bivalent configurations with three chiasmata per bivalent (one in one arm and two in the other arm) in wheat species. The diagrams show how the localization of the chiasmata/COs changes the shape of the ring configurations at metaphase I. Different examples of DAPI stained wheat bivalents observed at the fluorescence microscope are provided for each sub-class.

Finally, a ring bivalent configuration with two chiasmata in each arm also has been observed in wheat species (figure 3.9). Ring bivalents with a distal (d) and an interstitial class 3 (i^3) chiasma in one arm ($d+i^3$) and a distal (d) and a proximal (p) chiasmata in the other chromosome arm (d+p) ($d+i^3+p+d$).

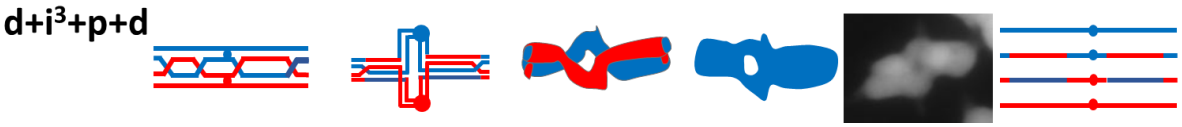

Figure 3.9: Sub-classification of ring bivalent configurations with four chiasmata per bivalent (two in each chromosome arm) in wheat species. The diagrams show how the localization of the chiasmata/COs changes the shape of the ring configurations at metaphase I. Different examples of DAPI stained wheat bivalents observed at the fluorescence microscope are provided for each sub-class.

3.2.2 Validation of the chiasmata analysis in hexaploid Wheat (Chinese Spring variety):

To analyse chiasma frequency and localisation in great detail on Chinese Spring (CS) variety of hexaploid wheat, different molecular cytogenetic techniques were used such as (FISH; Immunolocalization) to validate or to support our interpretation of the bivalent configurations.

3.2.2.1 Total number of Ring vs Rod Bivalents

The bivalent configuration analysis performed in CS (n=50 male meiocytes at metaphase I) showed that out of 1,034 bivalents, 940 were ring bivalents whereas only 94 of rod bivalents. This number indicated that more than 90% of bivalents in CS are ring bivalents with less than 10% as rod bivalents.

3.2.2.2 Chiasma frequency in CS

The total number of chiasmata in CS (n=50) was calculated by identifying the different configurations of bivalents at metaphase I and identifying the number of chiasmata in both rod and ring bivalents. The total number of chiasmata was 2,311 in 50 pollen mother cells at metaphase I. From these ones, 2,206 (95%) chiasmata in ring bivalents whereas 105 (5%) chiasmata in rod bivalents.

3.2.2.3 Chiasma Localization in Rod Bivalents

The chiasmata localization in rod bivalents were analysed in pollen mother cells (n=50). The analysis was done in a total of 94 rod bivalents, from these 45 were localized towards the telomeres (47% distal); 20 were interstitial class 1 (21% i^1); 26 were interstitial class 2 (27% i^2); 11 were interstitial class 3 (11% i^3) and 4 were close to the centromeres or proximal (4% p).

3.2.2.4 Chiasma Localization in Ring Bivalents

The chiasmata localization in ring bivalents were analysed in pollen mother cells (n=50). The analysis was done in a total of 743 ring bivalents, from these 475 were localized towards the telomeres (63% distal); 77 were interstitial class 1 (10% i^1); 85 were interstitial class 2 (11% i^2); 66 were interstitial class 3 (0.08% i^3) and 38 were close to the centromeres or proximal (0.05% p).

All in all, chiasma localization analysis in both rod and ring bivalents in CS revealed that the majority of the chiasmata are localized in chromosome distal regions (58%). These are followed by interstitial chiasmata (~30%) and the number of proximal chiasmata (10%) is very reduced.

3.2.2.5 Telomere and Centromere FISH analysis of bivalents in CS

FISH analysis using DNA probes with telomere and centromere sequences was carried out on metaphase I cells in CS (figure 3.10 and 3.11). The purpose of this analysis was to validate and support the identification of the localization of chiasmata along the chromosome arms. This analysis supported our observations on the metaphase I configurations, the majority of the chiasmata appeared to be localized at telomeric regions (green) with a minority appearing at interstitial and proximal regions close to the centromeres (red).

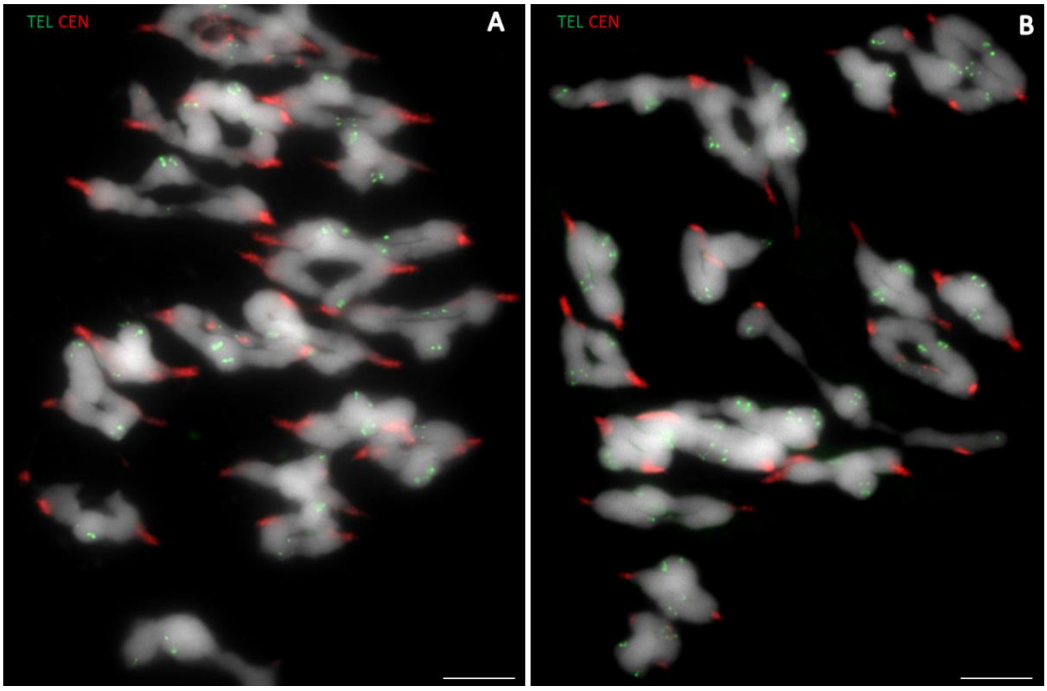

Figure 3.10: FISH using telomere (green) and centromere (red) at metaphase I. Scale bar = 10 µm. A and B images show the Chinese Spring MI labelled by centromere probe (red) and telomere probe (green). It can be observed that centromeric region (red) always lacking chiasmata whereas telomeric region (green) contain more chiasmata. This observation validates that, chiasmata in wheat are more common at telomeric distal region in the chromosome.

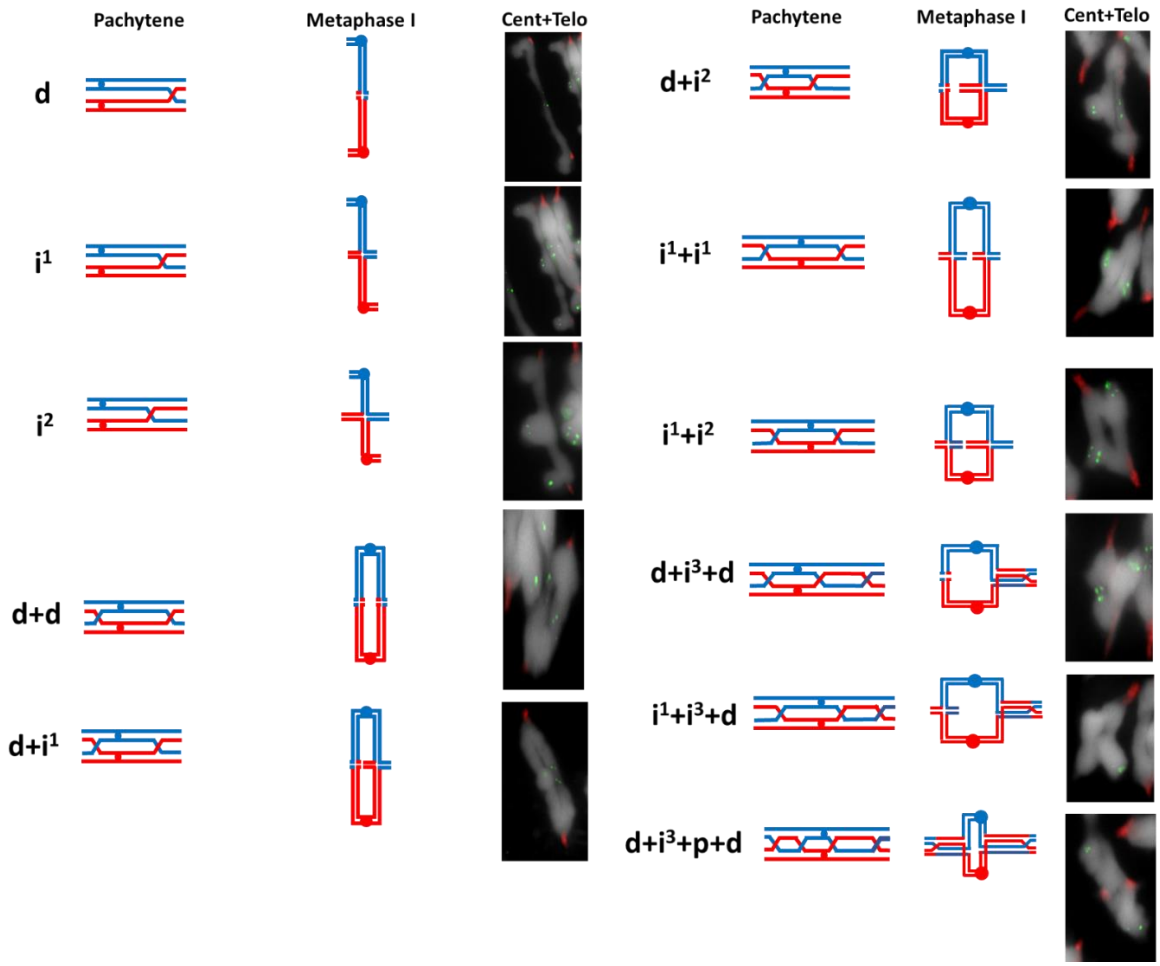

Figure 3.11: Centromere (red) and telomere (green) FISH for specific bivalents at metaphase I. This is to validate that chiasmata in wheat commonly occurs in telomeric region with a few chiasmata observe in interstitial and proximal region.

3.2.2.6 Immunolocalization of HEI10 in CS

In order to detect COs at pachytene and diplotene an immunolocalization of HEI10 protein in pollen mother cells was carried out. Hei10 is a class I COs that regulate recombination intermediate toward COs pathways (Chelysheva *et al*., 2012). In Cadenza HEI10 showing a high number of small foci (~2100) at late leptotene and these foci linearized on the chromosome axis in coincidence with elongation of the synapsis during mid-zygotene until at pachytene (after the synapsis completion) a stable big foci number was visualized (Osman *et al*., 2021). During diplotene and diakinesis HEI10 foci becomes brighter and bigger.

Furthermore, the immunocytological co-localization of HEI10 (Class I COs) with ZYP1 (SC) was carried out in Chinese Spring in order to clarify the timing of the meiocytes mostly from late zygotene-pachytene to late diplotene-early diakinesis (figure 3.12).

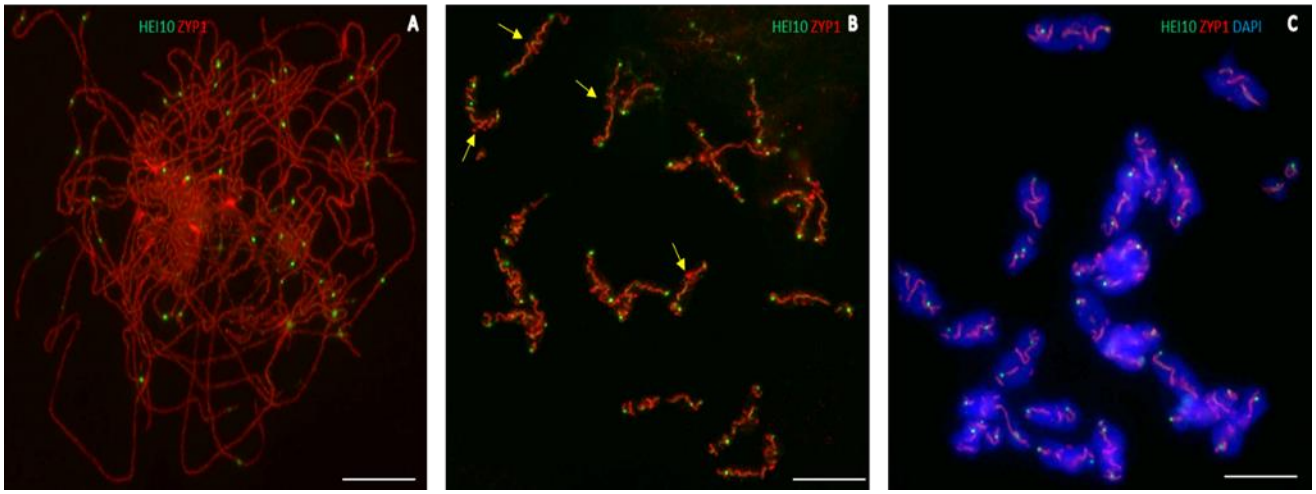

Figure 3.12: Co-immunolocalization of HEI10 (green) and Zyp1 (red) in CS. (A) Late zygotene-pachytene (fresh material) shows that Hei10 foci appear at that stage but their localisation could not be detected due to SC complexity. (B) Late diplotene-early diakinesis (fixed material) shows Hei10 foci at that stage and their localisation can be easily detected. All in all, co-immunolocalization of Hei10 with fixed material show a better localisation of this protein compare to co-immunolocalization with fresh material. (C) Late diplotene-early diakinesis DAPI staining (blue). Scale bar = 10 μm. Yellow arrows highlight the centromeres.

Hei10 foci during late prophase I (diplotene-diakinesis) reveals that this protein accumulates mostly at distal regions of the chromosomes in hexaploid CS (figure 3.12). It was observed that there were clearly 2 to 3 Hei10 foci per bivalent (figure 3.13) which was consistent with the expected number bearing in mind the chiasmata number per bivalent observed at metaphase I. Moreover, to test if all HEI10 foci at pachytene will become a CO/chiasmata at metaphase l, the mean of HEI10 foci compare to the mean of chiasma frequency in hexaploid wheat (Chinese spring). As expected, the mean of HEI10 foci was relatively close to the mean of chiasma frequency with (44.4 ± 0.8) and (46.1 ± 0.4) respectively (figure 3.14). A slight increase in the mean of chiasma frequency compare to the mean of HEI10 is expected because the mean of chiasma frequency represents both class I and class II CO's whereas the mean of HEI10 foci represent only class l CO's.

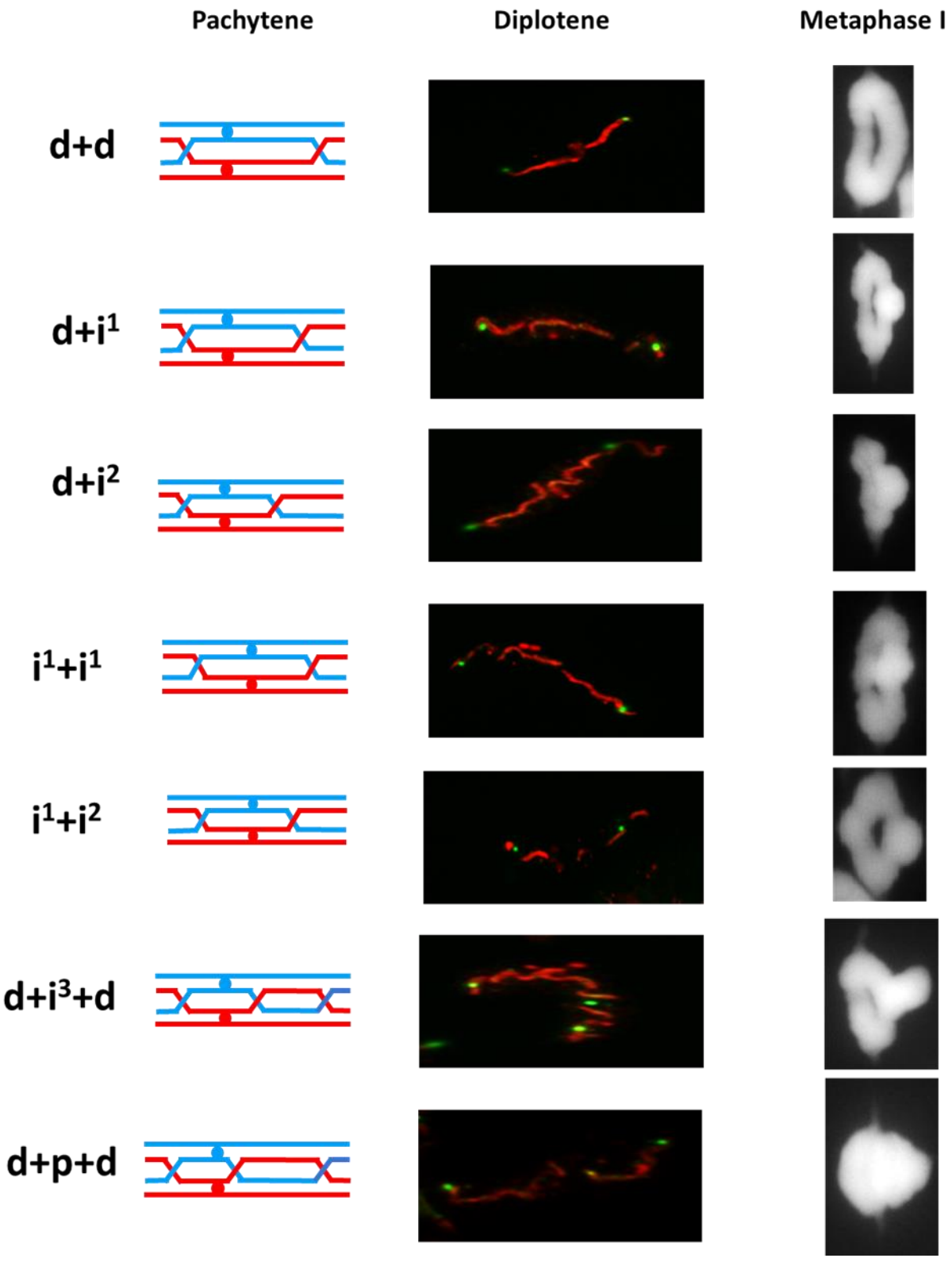

Figure 3.13: Co-immunolocalization of HEI10 (green) and Zyp1 (red) in CS. Localization of HEI10 foci at diplotene almost represent similar localization of chiasmata at metaphase I.

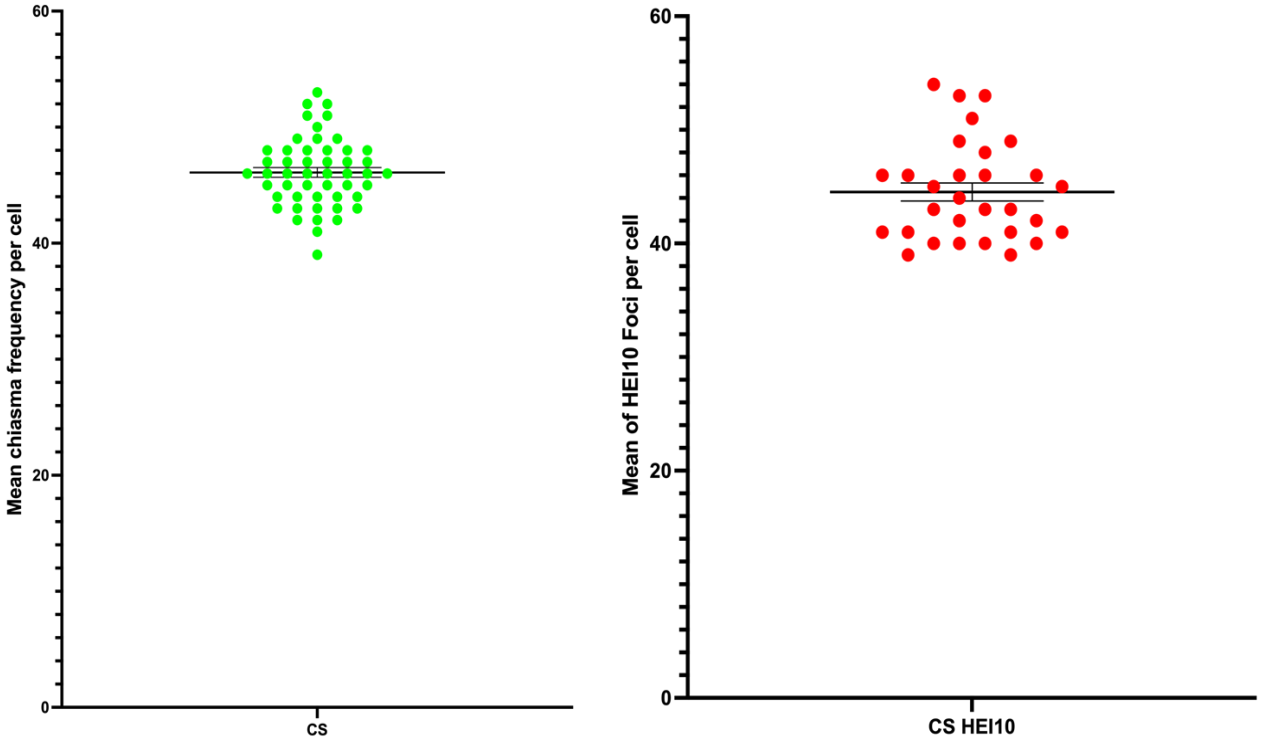

Figure 3.14: Mean of HEI10 foci per cell (44.4±0.8) (N=30) and mean of chiasma frequency per cell (46.1±0.4) was almost identical in hexaploid wheat (CS) (N=50). (±) represent stander error of the mean.

3.2.2.7 HEI10 foci localization in CS

The localization of Hei10 foci per chromosome (21) was analysed in CS (n=15). Our result show that, (~60%) of Hei10 foci appears in distal region of the chromosome. About (~30%) of HEI10 occurs at interstitial region and a low percentage (~9%) of HEI10 foci occurs at proximal region.

3.2.3 Comparisons of chiasma frequency, bivalent configurations and meiotic progression in wheats

3.2.3.1 Bivalent configurations and chiasma frequency in Cadenza and Chinese Spring

As previously published (Osman *et al*., 2021), it has been seen that the bivalent configurations in hexaploid wheat cultivar Cadenza were divided between rods and rings. The localization and number of chiasmata in each arm allows the formation of different ring configurations (see 3.21). Interestingly, in nearly every ring bivalent observed in metaphase I in Cadenza one chromosome arm always showed only one distal chiasma whereas the other arm could have one or two chiasmata and one of these two chiasmata localized in an interstitial/proximal region (figures 3.15). Nevertheless, this was not the case in hexaploid cultivar Chinese Spring where ring bivalents had more complex configurations, including rings with more interstitial/proximal chiasmata in both arms.

The mean chiasma frequency in Chinese Spring was 46.10 $\pm$ 0.42 was statistically higher compared to Cadenza with a mean of 43.7 $\pm$ 0.23 (Welch's t test, p value <0.0001)) (figure 3.16). Additionally, chiasma localization in Chinese Spring also tended to be more frequently located in interstitial and proximal regions compared to Cadenza. Moreover, bivalents in Chinese Spring contained more interstitial and proximal chiasmata in both chromosome arms compared to Cadenza.

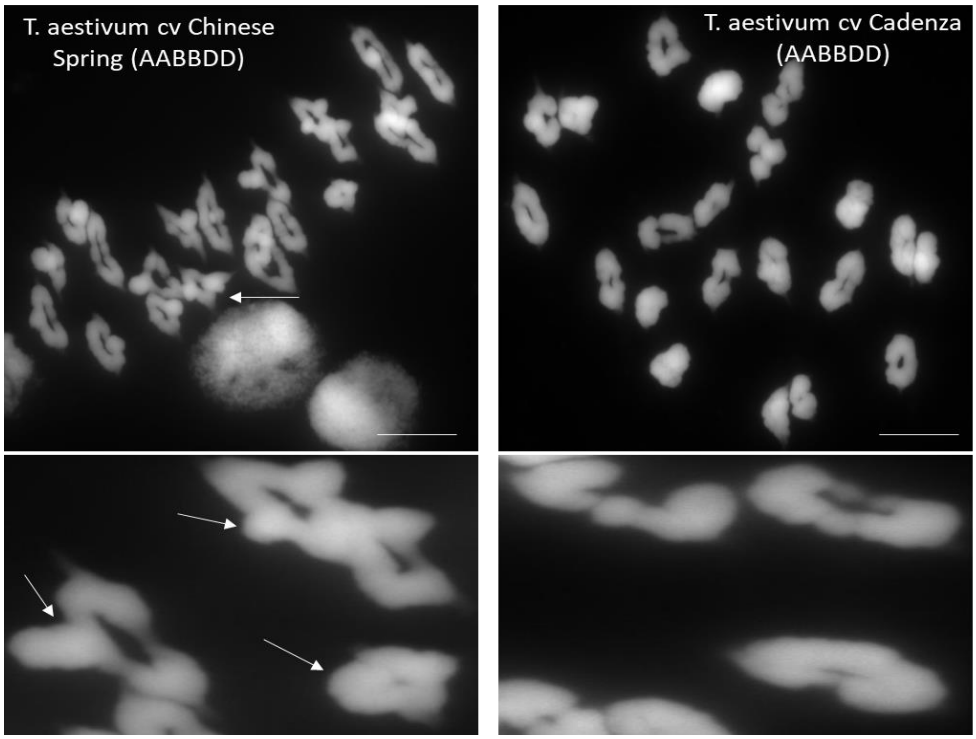

Figure 3.15: Chinese Spring contains more interstitial and proximal chiasmata compare to Cadenza (arrows points to interstitial and proximal chiasmata). Scale bar=10 µm.

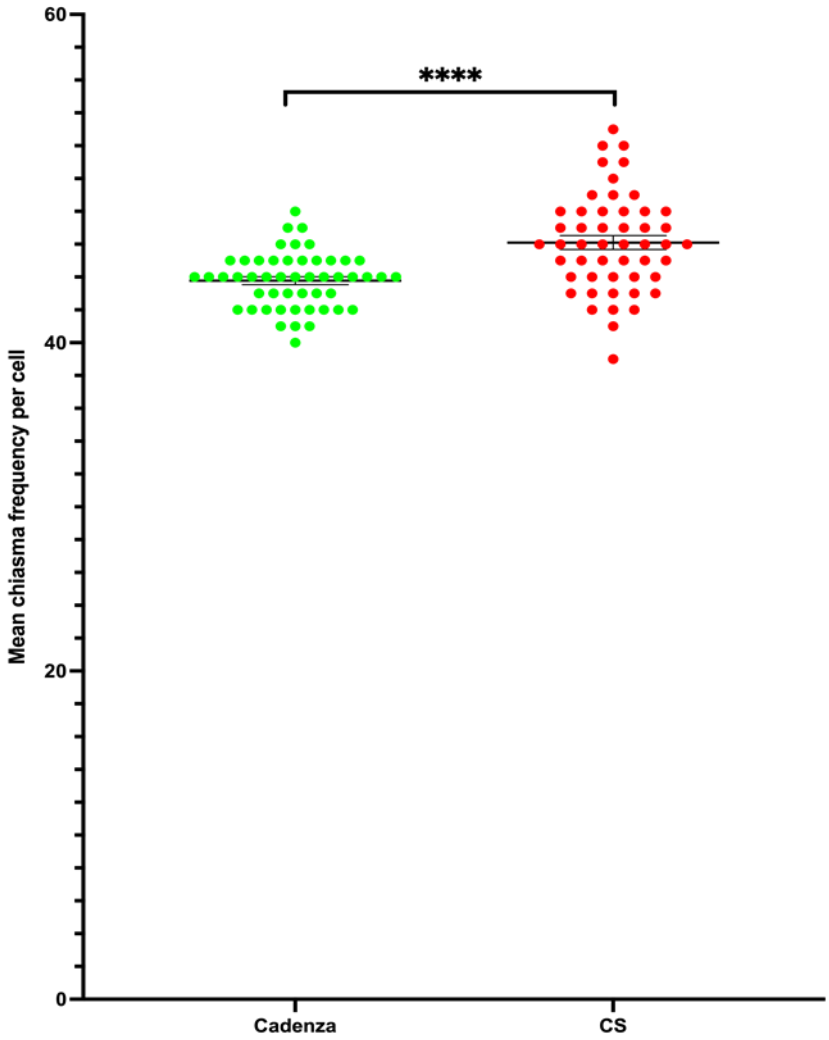

Figure 3.16: Comparison of the mean chiasma frequency between Chinese Spring and Cadenza (Welch's t test p<0.0001, N=50). Mean chiasma frequency of Chinese Spring was significantly higher compare to Cadenza with. The analysis was done in 50 meiocyte in each of them. Each meiocyte contain 21 bivalents, so a total of 2100 bivalents were analysed in Chinese Spring and Cadenza.

3.2.3.2 Meiotic progression in Cadenza and Chinese Spring

In order to identify changes that could cause the significant differences in chiasma frequency and distribution observe between Chinese Spring and Cadenza an immunocytological analysis of chromosome axis and the SC progression was produced. To examine the meiotic chromosome axis, an antibodies against the HORMA domain axis associated protein ASY1 were used and to analyze the SC an antibodies against the central element protein ZYP1 were used. Thus, following the

progression of these two proteins during prophase I, from leptotene to pachytene, we are expecting to be able to identify any differences between Chinese Spring and Cadenza which could explain their differences in chiasma frequency and distribution. These two proteins have been studied widely in different plant species such as Arabidopsis and wheat (Armstrong et al., 2002, Higgins et al., 2012, Higgins et al., 2005, Osman et al., 2021, Osman et al., 2006, Sanchez-Moran et al., 2008, Sepsi et al., 2017).

In hexaploid wheat Cadenza, during leptotene, the ASY1 foci start linearizing in a cluster associated with the telomeric region and this confirmed by immunocytological analysis by using telomer probe in a compensation with axis associated protein Asy1 (Osman *et al*., 2021). ZYP1 appears as discrete foci at this stage all over the nucleus (figure 3.17). In early zygotene, ASY1 is fully linearized and initial polymerization of ZYP1 (synapsis) between homologous chromosomes is initiated also at the telomeric regions. Telomere DNA probes were utilized in FISH in combination with immunolocalization of ZYP1 and validated the observation that the synapsis initiation started from telomeric regions at zygotene (figure 3.18). In mid zygotene, the synapsis (ZYP1 polymerization) continues between homologous chromosomes and the ASY1 signal starts to get weaker and disappear from the axis, at this stage. At pachytene, the synapsis is fully completed between homologous chromosomes and the ZYP1 signal is fully polymerized.

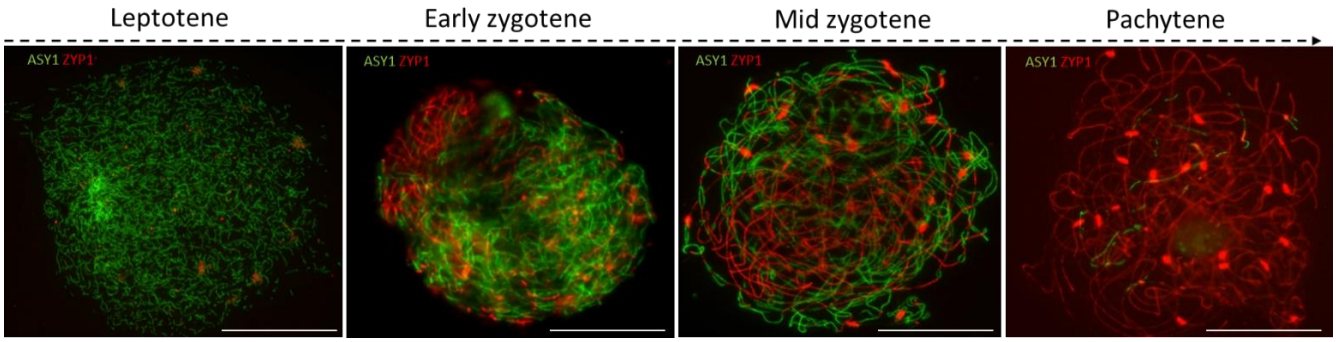

Figure 3.17: Immunolocalization of ASY1(green) and ZYP1 (red) during prophase I in wheat (Chinese Spring). Scale bar=10 µm. In leptotene, the ASY1 foci start linearizing in a cluster associated with the telomeric region while

ZYP1 appears as discrete foci at this stage all over the nucleus. In early zygotene, ASY1 is fully linearized and initial polymerization of ZYP1 (synapsis) between homologous chromosomes is initiated also at the telomeric regions. In mid zygotene, the synapsis (ZYP1 polymerization) continues between homologous chromosomes and the ASY1 signal starts to get weaker and disappear from the axis. At pachytene, the synapsis is fully completed between homologous chromosomes and the ZYP1 signal is fully polymerized.

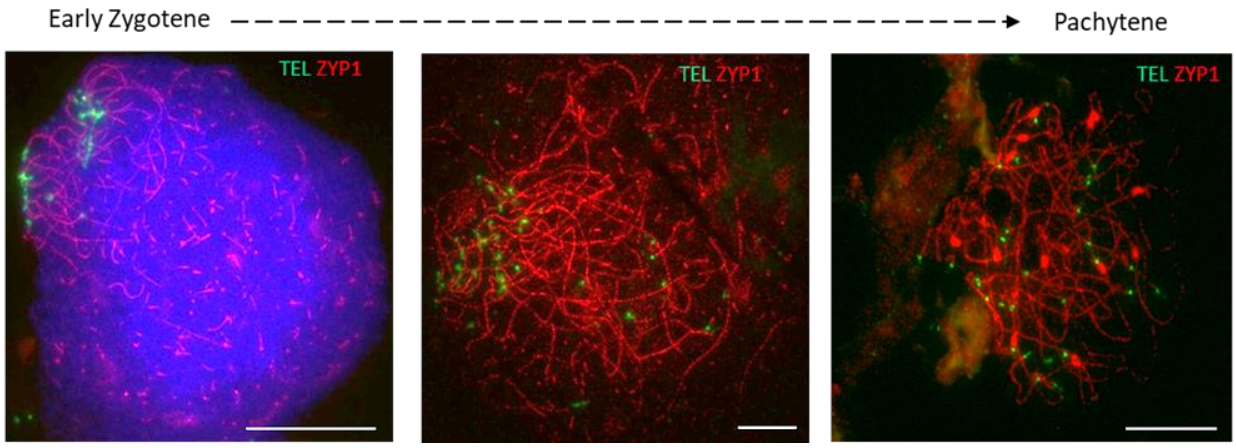

Figure 3.18: FISH analysis of telomeres (green) together with the immunolocalization of SC protein ZYP1 (red) during zygotene and pachytene in wheat (cultivar CS). Scale bar=10 µm. In early zygotene, telomere DNA probes were utilized in FISH in combination with immunolocalization of ZYP1 and validated the observation that the synapsis initiation started from telomeric regions at zygotene. The synapsis will continue during mid zygotene until it is fully completed at pachytene.

In both hexaploid cultivars, Chinese Spring and Cadenza, the spatio-temporal polarization of the meiotic progression from telomeres to centromeres of chromosome axis and SC formation was analyzed by using ASY1 and ZYP1 immunolocalization (figure 3.19). In both cultivars, the chromosome axis protein (ASY1) and the SC central element (ZYP1) appeared to be polarized to the telomeric regions during prophase I. No differences were observed in terms of polarization initiation between them. This is indicating that the spatio-temporal progress of meiotic events is present and similar in both cultivars.

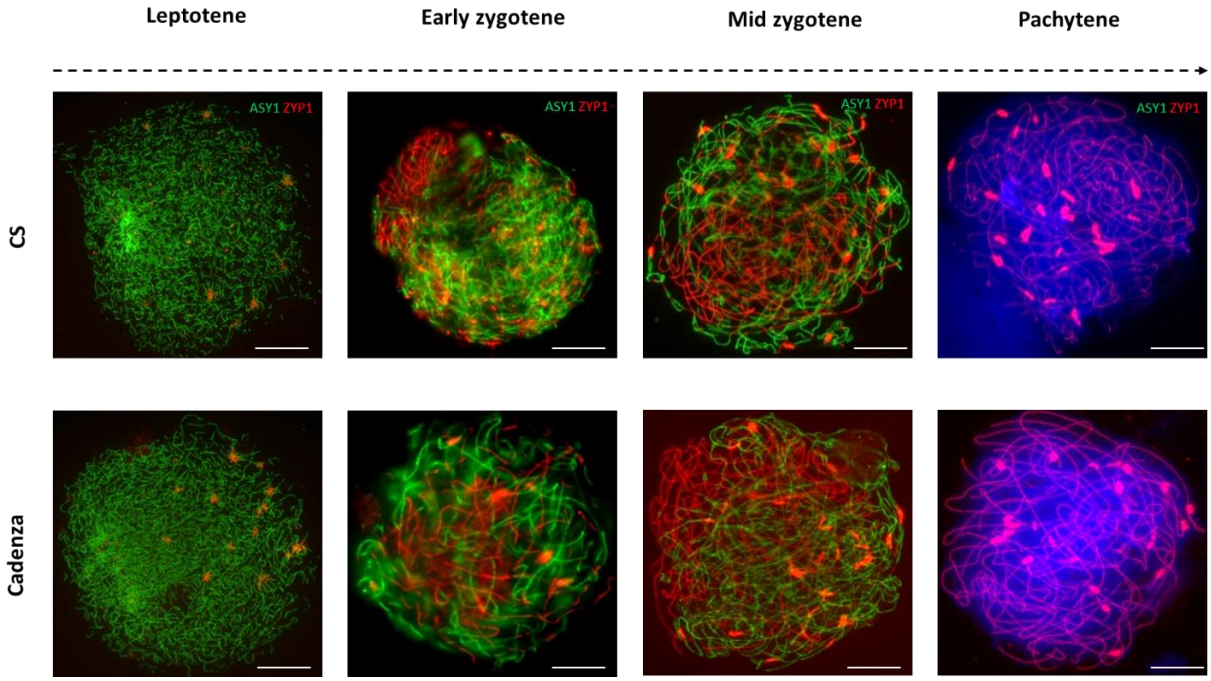

Figure 3.19: Immunolocalization of ASY1 (green) and ZYP1 (red) during prophase I in Chinese Spring and Cadenza hexaploid cultivars. DAPI staining (blue). Scale bar=10 µm. In both hexaploid cultivars, Chinese Spring and Cadenza, the spatio-temporal polarization of the meiotic progression from telomeres to centromeres of chromosome axis and SC formation was analyzed by using ASY1 (green) and ZYP1 (red) immunolocalization. In both cultivars, the chromosome axis protein (ASY1) and the SC central element (ZYP1) appeared to be polarized to the telomeric regions during early prophase I. This polarization was continuing during mid prophase I specially zygotene which ASY1 start to disassemble whereas ZYP1 continuing their polymerization. At pachytene ZYP1 is fully polymerized in the entire length between the homologous chromosomes. All in all, the polarization process in Chinese Spring and Cadenza appear to be conserved between them.

3.2.3.3 Quantification of Class I COs (HEI10 immunolocalization at late diplotene)

Immunolocalization of Class I COs protein HEI10 was conducted in fixed material of both Chinese Spring and Cadenza cultivars at late diplotene (figure 3.26). The purpose of this analysis is to identify if the differences in the mean chiasma frequency observed at metaphase I could be correlated to the Class I COs observed at diplotene. The mean number of HEI10 foci at diplotene was (44.53 ± 0.796) in Chinese Spring and (43 ± 0.636) in Cadenza (figure 3.20). Remarkably, no significant differences were observed between these hexaploid cultivars in Hei10 foci numbers at diplotene (Welch's t test, p value = 0.138).

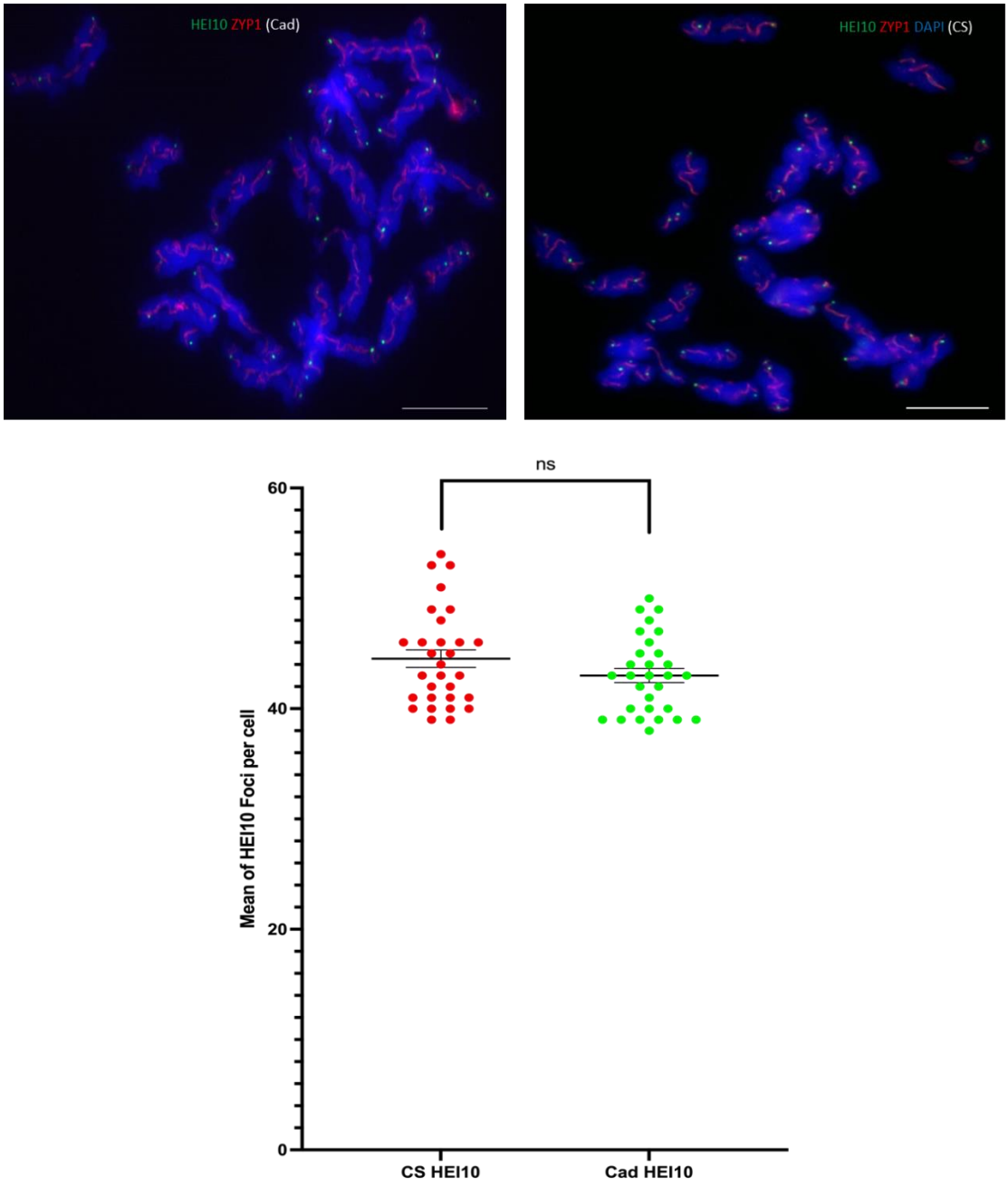

Figure 3.20: Immunolocalizationm of HEI10 in hexaploid cultivars Cadenza and Chinese Spring. DAPI staining (blue). Mean number of Hei10 foci in Chinese Spring and Cadenza does not reflect any significant differences between them (Welch's t test, $p>0.05$) (N=30). Scale bar = 10 µm.

3.2.3.4 Meiotic progression in hexaploid, tetraploid and diploid wheats

An immunocytological analysis of ASY1 and ZYP1 was conducted on different ploidy level wheats: hexaploid wheat (AABBDD) cultivars (Chinese Spring, Cadenza), tetraploid wheat (AABB) cultivar (Cappelli) and diploid (AA) *T. monococcum* to anaylse the satio-tempolar mechanism between them if is it conserved or not. As a result, chromosome axis and the SC progression was analyzed at different stages of prophase I, found that the spatio-tempolar polarization progress from telomere to centromere regions appears to be conserved in these species independently of the ploidy level (figure 3.21).

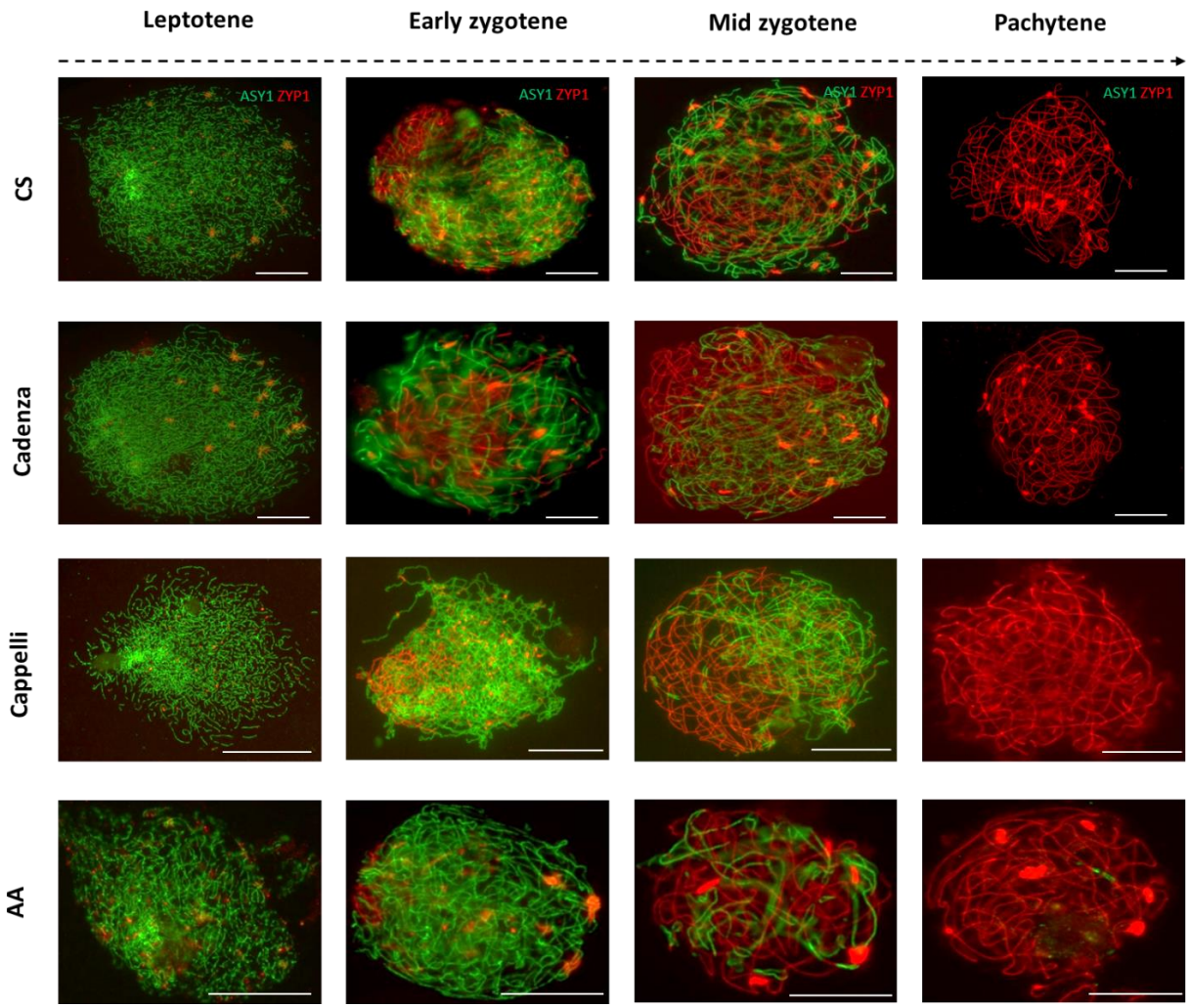

Figure 3.21: Immunolocalization of ASY1 (green) and ZYP1 (red) in different wheat species and cultivars. Scale bar =10 µm. Analysis of chromosome axis and SC progression and polymerization in hexaploid wheat (Chinese Spring and Cadenza), tetraploid wheat (Cappelli) and diploid wheat (*T. monococcum*) shows that polarization mechanism is conserved between them.

3.2.3.5 Chronology of the Meiotic progression in wheats (BrdU Time Course)

The BrdU technique to calculate the meiotic time course was applied in hexaploid cultivars Chinese Spring and Cadenza, as well as in tetraploid cultivar Cappelli and diploid *T. monococcum*. BrdU was injected in the cavity above the spike for different time points (see Material and Methods). The time when BrdU was injected was counted as 0h and the different time points of placing anthers in the fix material included 24h, 30h, 33h, 36h, 39h, 41h and 43h (figure 3.28). These time points were based in our laboratory experience with Cadenza meiotic time course (Osman *et al*., 2021). BrdU staining was combined with the immunolocalization of ZYP1 during early prophase I (24h, 33h) to check the synapsis progression time course. Anti-ASY1 with BrdU was not used because the role of this protein in early meiosis stages in wheat (leptotene) is already published (Osman et al., 2021). The first time point was 24h because it was already published that synapsis in wheat start between 21 and 24h in Cadenza (Osman *et al.*, 2021). The second time point was 30-33h to check the synapsis progression. The third injection time point was 39h to check synapsis disassembly. The fourth and final time point was 41-43h to check the presence of labelled dyads or tetrads as a target of meiosis completion (figure 3.28). All BrdU analysis were done on five different replicates of each meiotic stage and a minimum of 15 cells to a highest of 70 cells were counted in each. For example, five Chinese Spring plants and five Cadenza plants were required to study the time course of early zygotene and similar numbers were used in the other meiotic stages and materials.

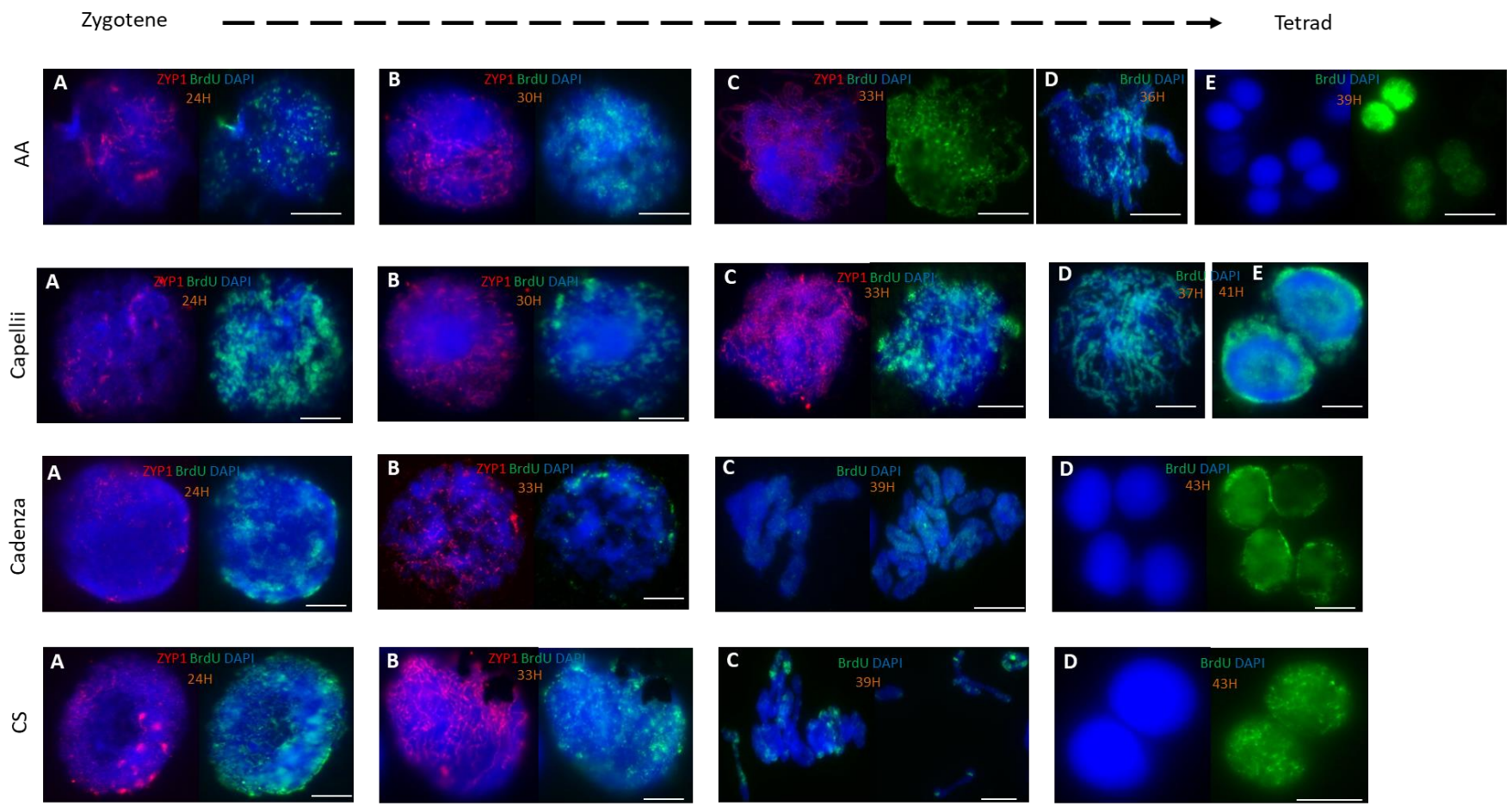

Figure 3.22: Meiotic time course for different wheat species from different ploidy level. In AA, (A) early zygotene, (B) mid-zygotene, (C) pachytene, (D) diakinesis and (E) tetrad. In Cappelli, (A) early zygotene, (B) mid-zygotene, (C) pachytene, (D) diakinesis and (E) tetrad. In Chinese Spring and Cadenza, (A) early zygotene, (B) mid-zygotene, (C) metaphase l and (D) tetrad. Scale bar = 10 µm. In 24h, the synapsis initiation started in all wheats from different ploidy level (hexaploidy CS and Cadenza), tetraploid (Capelli) and diploid *T. monococcum* (figure 3.28. A). In 33h, Capellii (figure 3.28. C) and *T. monococcum* (figure 3.28. C) reach pachytene whereas both hexaploid cultivars still at mid zygotene at this time (figure 3.27.C in CS and Cadenza). In 36h diakinesis observe in *T. monococcum* (figure 3.28. D). In Cappellii diakinesis observe at 37h (figure 3.28. C). In both CS and Cadenza MI observe at 39h (figure 3.28. C). Tetrad and/or dyad observe at 39h in *T. monococcum* (figure3.28. E), at 41h in Cappelli (figure 3.28. E) and 43h in CS and Cadenza (figure 3.28. E). An extra two hours reported between diploid, tetraploid and hexaploid in order to complete meiosis whereas no differences observe in meiosis timing between wheat from the same ploidy level (CS and Cadenza).

BrdU time points revealed that at 24h synapsis was initiated in all material analysed. ZYP1 polymerization in both hexaploid cultivars Chinese Spring and Cadenza were similar with no differences observed. At time point 33h, the labelled meiocytes were almost at mid-zygotene with ZYP1 signal polymerization at levels of being spread up to half of the cell in both Chinese Spring and Cadenza cultivars.

Interestingly, in tetraploid cultivar Cappelli and *T. monococcum* (AA) the synapsis initiation started at 24h similarly to what observed in hexaploid cultivars. However, the synapsis polymerization appeared to be faster as both reached the mid-zygotene at 30h, 3h faster than the hexaploid cultivars (33h). In Cappelli and *T. monococcum* (AA) full synapsis at pachytene was achieved at 33h (figure 3.22). Remarkably, diakinesis appeared earlier in *T. monococcum* (36h) and in tetraploid cultivar Cappelli (37h). At 39h metaphase I cells started to be labelled in both Chinese Spring and Cadenza. Tetrads (telophase II) started to be observed at 43h in both Chinese Spring and Cadenza.

It is worth mentioning that some meiocytes in Chinese Spring at 33h showed a strong signal of ZYP1 compared to Cadenza which could indicate a faster SC progression to full synapsis, thus reaching pachytene earlier. This observation might be due to differences in the cell progression during meiosis in which some cells seem to be faster compared to others. However, all in all, no significant differences were observed in the time to complete meiosis between Chinese Spring and Cadenza and both spend 43h to complete meiosis. Nevertheless, *T. monococcum* (AA) and tetraploid cultivar Cappelli completed meiosis at 39h and 41h respectively, which is faster compared to the hexaploid cultivars. The total time of meiosis completion in hexaploid cultivars was 43h, in tetraploid Cappellii was 41h and *T. monococcum* was 39h. It seems that completion of meiosis increases 2h in each ploidy level, from diploid to tetraploid (39h to 41h) and from tetraploid to hexaploid (41h to 43h).

3.3 Discussion

3.3.1 Wheat meiotic bivalent configurations at metaphase l can be accurately classified and the chiasma frequency and distribution correctly inferred

Cytological analysis has been extensively used to analyse meiotic chromosome behaviour and meiotic recombination in plants (Darlington, 1932; Whitehouse, 1967; Jones, 1971; Sybenga, 1975). Cytogenetics is a powerful tool to quantify chiasma frequency and localization on plant chromosomes and historically was utilized in species with large size chromosomes like cereals (e.g. wheat). The direct relationship between COs and chiasmata has been clearly established in wheat (Fu & Sears, 1973; Riley, 1974; Driscoll *et al*., 1979; Jauhar *et al.*, 1991; Benavente & Sybenga, 1994; Naranjo *et al.*, 2010) as well as the evidence of a genetic control regulating its frequency (Sears, 1976). In this chapter, a preliminary analysis to establish the different bivalent configurations that we could distinguish on Chinese Spring hexaploid wheat at metaphase I and how these correlated to different numbers and positions of the COs along the chromosome arms following similar analysis done in the literature were carried out (Fu & Sears, 1973; Sybenga, 1975). Importantly, good metaphase I slides were required to have a proper separation of bivalents (21 on *T. aestivum*) and thus a proper opportunity to analyse the different configurations. Furthermore, even in our best slides not all the bivalents at metaphase I were in only one plane of focus, thus acquired different numbers of images using the Z-stack capability of our epifluorescence microscope were required (see Material and Methods). The availability of these Z-stacks allowed us to analyse the different focal points of the bivalents at metaphase I. These meiotic configurations (figures 3.3-9) were identified on the basis of key points during the meiotic process: i) after DNA replication the sister chromatids will be held together by the cohesin complex (SCC). ii) during prophase I recombination, pairing and synapsis will occur, producing COs and the polymerisation of the SC. iii) one CO only occur between 2

chromatids of the homologous chromosomes. iv) the meiotic spindle forms at metaphase I breaking the nuclear membrane and attaching the microtubules to the centromeres of each bivalent and bi-orientate the bivalents at the equator of the cell (producing tension between the homologous chromosomes held by COs and SSC). v) the meiotic bivalent configurations observed would be shaped by the spindle tension, the SCC and the chiasmata (COs) and they will be dependent of the number of COs (chiasmata) and their localization (Sybenga, 1975).

In the plant model species Arabidopsis; different techniques have been used to identify and quantify the meiotic COs (reviewed by Kim & Choi, 2022). From cytological analysis using DAPI staining of metaphase I cells (Ross *et al*., 1997; Armstrong & Jones, 2003; Sanchez-Moran *et al*., 2001; 2002), to immunolocalisation of class I COs using MLH1 (Sanchez-Moran *et al.,* 2004), Mlh3 (Jackson *et al.,* 2006) or HEI10 (Chelysheva *et al*., 2012) antibodies, as well as using fluorescent reporters FTLs in seeds (van Tol *et al*. 2018; Kbiri *et al*., 2022), pollen (Yelina *et al.,* 2013) or in tetrads on the *qrt* mutant background (Preuss *et al*., 1994; Copenhaver *et al*., 2000; Francis *et al.,* 2007; Roy *et al*., 2011), and of course, genome-wide CO mapping using crosses between different ecotypes (Drouaud *et al*., 2007; Giraut *et al*., 2011) and even using DNA extracted from pollen grains (Drouaud & Mézard, 2011; Choit *et al*., 2017). Both, immunolocalization of late recombination proteins, sequencing and chiasma frequency analysis allow the studying of recombination in bivalents whereas the FTLs techniques just measure recombination in a specific region. Nevertheless, immunolocalization only can measure one Class at a time (Jackson *et al*., 2006; Chelysheva *et al*., 2012) and the dynamic nature of the foci appearing in great numbers and disappearing as they process the DSBs at different times in the nucleus provides some discrepancies depending on the person who is counting. Sequencing also allows to quantify genome NCOs (Khademian *et al*., 2013) and the FTLs to measure gene conversion (GC) events between specific loci (Berchowitz & Copenhaver, 2009). From all these methodologies, cytogenetic analysis of metaphase I configurations is the cheapest and

simplest option of all and allows a good general estimation of the chiasma frequency and localization of both Class I and Class II COs along the chromosomes (review in Kim & Choi, 2022).

Historically, cereal species like wheats have been ideal to analyse meiotic recombination cytogenetically as they have large chromosomes (Fu & Sears, 1973; Sybenga, 1975). In this thesis, we have tried to analyse systematically the chiasmata on different species of wheat using fluorescence microscopy. In this chapter, all the different bivalent configurations observed at metaphase I were classified. Furthermore, these configurations have been validated by using FISH analysis and telomere and centromere probes and by co-immunolocalization of SC central element ZYP1 and Class I HEI10 protein.

Our results have shown that in Chinese Spring the bivalent configurations observed showed that more than 90% of bivalents were ring bivalents and the rest, less than 10%, were ring bivalents (figures 3.10 & 11). The chiasmata, in both ring and rod bivalents, appeared to be mostly localized on distal regions of the chromosomes in Chinese Spring (figures 3.12- 3.14). A moderate number of chiasmata occur at interstitial regions and very low at proximal regions. These results are consistent to others in the literature in different hexaploid wheat varieties (Choulet et al., 2014, Higgins et al., 2014, Lukaszewski et al., 2012, Osman et al., 2021). Recently, whole-genome sequencing has nicely confirmed this distal bias of COs (Choulet *et al.*, 2014; Darrier *et al.*, 2017; Jordan *et al.*, 2018; Balfourier *et al.*, 2019; Gardiner *et al.*, 2019).

The mean chiasma frequency per cell in Chinese Spring (n=50) observed in this thesis was 46.3 ± 0.41 (figure 3.11). A very similar frequency to the ones observed in previous studies by Riley (1966) [47.15], by Sallee and Kimber (1979) [48.3] and Miller and Reader (1985) [47.73]. This indicates that our classification of bivalent configurations seems to be similar to those historical studies of chiasmata frequency in Chinese Spring. This chiasmata frequency per cell seems to be higher than

the one previously observed in the lab for Cadenza [41.8 ± 0.28] (Osman *et al*., 2021) and significantly higher than Cadenza [44.2 ± 0.25] (see Chapter 4) (ANOVA p = 1.47542E-05). Interestingly, in Chinese Spring there was less distal bias for chiasmata localization than in Cadenza, with 57% and 88% distal chiasmata frequency respectively (Osman *et al*., 2021).

The mean number of HEI10 foci observed at late diplotene is very similar to the mean chiasma frequency observed at metaphase I. It has been proposed that HEI10 colocalise with early recombination intermediates in early prophase I showing hundreds of foci in Arabidopsis but these foci reduce in numbers and increase in size towards the end of prophase I labelling Class I COs (Chelysheva *et al*., 2012). In both, Arabidopsis and wheat, HEI10 foci initially appear as a large number of foci that co-localise with ZYP1 foci in leptotene, then along the SC (ZYP1 polymerised) at zygotene and finally the foci number decreases into brighter and bigger foci at pachytene and diplotene (Chelysheva et al., 2012, Morgan et al., 2021, Osman et al., 2021). The *Hei10* gene encodes for an E3 ubiquitin ligase that shares functional and structural homology with ZIP3 protein a member of ZMM group proteins in budding yeast (Chelysheva *et al.*, 2012). The contribution of this protein in CO formation has been broadly studied in mammals and it has been found to be involved in the formation of Class I COs in mice (Ward *et al*., 2007). In plants a similar role of HEI10 in CO formation has been described in Arabidopsis (Chelysheva *et al.*, 2012). It was found that this protein plays a fundamental role in the formation of Class I COs and lack of this protein results in a reduction of COs (abolition of Class I COs) as univalents can be observed at metaphase I (Chelysheva *et al*., 2012). Interestingly, our HEI10 immunolocalization at diplotene has shown an elevated number of foci (44.4 ± 0.8) (N=30). In Cadenza, we also reported that HEI10 foci appeared elevated at diplotene showing 41.2 ± 1.1 (N=20) foci (Osman et al., 2021). Interestingly, this lower number in Cadenza compared to Chinese Spring coincides with lower chiasma frequency in Cadenza *vs* Chinese Spring. These values would mean that in Chinese Spring (~96%) and Cadenza (~98%) the percentage of

Class I COs are very elevated compared to Arabidopsis (~85%) (Higgins *et al*., 2004;2008; Osman *et al*., 2021). Furthermore, this ~85% Class I COs ratio observed in Arabidopsis has also been found in other plant species like *Oryza sativa*, *Solanum lycopersicum*, *Brassica napus* and *Triticum turgidum subsp. durum* (Higgins *et al*., 2004, 2008b; Luo *et al*., 2013; Anderson *et al*., 2014; Wang *et al*., 2016; Gonzalo *et al*., 2019; Desjardins *et al*., 2020). Nevertheless, it has been shown in Cadenza (Osman *et al*., 2021) that by immunolocalizing Mlh3 at late pachytenes the ratio gets reduced to ~87% of Class I COs. MLH1 and MLH3 are good markers of Class I COs at pachytene in plants (Jackson *et al*., 2006; Chelysheva *et al*., 2010; Phillips *et al*., 2013). This could indicate that HEI10 might be involved in processing other structures not just Class I COs but also, we should consider that chiasma frequency might be underestimating the number of COs in hexaploid wheat. Interestingly, *zmm* mutants for *Msh4* and *Msh5* genes in tetraploid wheat variety Kronos (Desjardin *et al*., 2020) showed that the residual chiasmata (Class II COs) in these mutants was about 15% of the WT with similar values than in Arabidopsis and other plant species (Higgins *et al*., 2004, 2008b; Luo *et al*., 2013; Anderson *et al*., 2014; Wang *et al*., 2016; Gonzalo *et al*., 2019; Desjardin *et al*., 2020). Furthermore, these authors observed that in Kronos the mean number of HEI10 foci per cell was 28.9 ± 0.64 (Desjardin *et al*., 2020). A value higher than the chiasma frequency observed (26.22 ± 0.24) in the same article. This observation could lead to think that indeed it might be underestimating COs numbers by quantifying chiasma frequency. Nevertheless, the authors also did immunolocalization of HEI10 foci in *msh4/msh5* mutants in Kronos and surprisingly they found residual signals on the chromosomes (~3 foci/cell) and although most of them look smaller and fainter, but 17.6% looked similar to those observed in the WT (Desjardin *et al*., 2020). This is point out that perhaps, HEI10 in wheat is not a very good Class I marker as it could be labelling other structures.

3.3.2 The time of meiotic progression seems to be related to the ploidy level in wheats

The chronology of meiosis, or the meiotic time course, has been analyzed in different wheat species to test if time differences might explain the differences in chiasma frequency and/or distribution. In *Arabidopsis*, it has been reported that the meiotic time course last about 33h from S-phase to telophase II (Armstrong et al., 2003). In barley it was established that meiosis last about 38h (Higgins *et al.*, 2012). A historical study in Chinese Spring characterized that meiosis last 24h in this hexaploid cultivar (Bennett, 1972). More recently, a study in our laboratory in the cultivar Cadenza showed meiosis last up to 43h (Osman et al., 2021). It is worth mentioning that two different methodologies were used in these studies. In the first study, tritiated thymidine was used to label the DNA during meiosis (Bennett, 1972) whereas in the most recent study the nucleotide analogue BrdU (Kee *et al*., 2002) was used to label the DNA during meiosis (Osman *et al.*, 2021). Furthermore, differences could have been due to environmental conditions and even genotypic factors. A later study by Bennet (1977) established that meiotic progression in Chinese Spring actually lasted 43h when the temperature was reduced and maintained at 15^{o}C (Bennett, 1977). Recently, the use of BrdU to label the DNA and study the time of meiosis has been widely used because of the availability of anti-BrdU antibody with different labelling tags (fluorescence). BrdU labelling is more efficient, precise and involves less time consuming to do time courses (Armstrong *et al*., 2003).

The chronology of meiosis in Chinese Spring and Cadenza was analyzed to investigate if the timing of the meiosis might directly or indirectly effect the extra chiasmata observed in Chinese Spring. In an old study by (Bennett, 1972) it was reported that meiosis in Chinese Spring takes 24h. However, in a more recent a study by (Osman *et al*., 2021) it has been reported that meiosis in Cadenza takes 43h. Based on these two studies it could have been concluded that Chinese Spring is able to finish meiosis in half the time than Cadenza and this might result in extra chiasma frequency. However, Bennett (1977) also reported that meiosis in Chinese Spring took 43h when the temperature was

reduced from 20ºC to 15ºC. Based on these results it could be concluded that altering environmental condition (temperature or light duration) or using different methodologies (tritiated thymidine in Bennett studies/ BrdU in Osman et al (2021) study) could affect the meiosis time course analysis. To avoid environmental and methodological differences, both Chinese Spring and Cadenza were grown under the same environmental conditions and only BrdU was used to investigate the time course of meiosis. As a result, only the cell that on S-phase would have incorporated the BrdU would be labelled whereas any other cell that already pass the S-phase would not incorporated it and thus not being labelled. BrdU in association with immunolocalization of ZYP1 was applied to Chinese Spring and Cadenza hexaploid cultivars. In both Chinese Spring and Cadenza, the meiotic process was completed in 43h. In Cadenza, early zygotene meiocytes were observed at 24h, mid to late zygotene at 33h, metaphase I cells at 39h and tetrads at 43h. These results are consistent with recent studies carried out by other researchers in our laboratory (Osman *et al*., 2021). It appeared that at 33h some meiocytes in Chinese Spring showed a further polymerization signal of ZYP1 compared to Cadenza which could indicate a faster SC progression. However, these small differences did not affect the final time in meiotic progression between Chinese Spring and Cadenza and both spend 43h to complete meiosis.

Furthermore, we were interested to investigate if the meiosis timing exhibits any change in different ploidy level. BrdU in association with the immunolocalization of ZYP1 was applied to tetraploid cultivar Cappelli and diploid *T. monococcum* (AA). This showed that tetraploid cultivar Cappelli reaches complete meiosis at 41h whereas *T. monococcum* completes meiosis in just 39h which is a similar time to that one reported for the diploid crop barley *(*Higgins *et al*., 2012). Interestingly, both can complete meiosis quicker than the hexaploid cultivars Chinese Spring and Cadenza (43h). It is also interesting that there is an extra 2h period for complete meiosis at each ploidy level (tetraploids 2h more than diploids, and hexaploids 2h more than tetraploids). This increase in the time it takes meiosis to complete might be related to the extra complexity of having an extra genome could have

in different events during meiosis like DNA replication, initiation of recombination (homologous chromosome search), pairing and even synapsis.

3.3.3 The spatio-temporal polarization progress of meiotic processes is conserved among the different ploidy levels in wheat species

In recent years, our laboratory has published some results on hexaploid wheat Cadenza showing that the high frequency of distal chiasmata could be related to the spatio-temporal asymmetry of the meiotic progression (Osman *et al*., 2021). In this chapter, the analysis of early chromosome axis formation and early synapsis initiation in Chinese Spring and Cadenza might have indicated to be a plausible reason to explain the different mean chiasma frequency and distribution between both cultivars. To do so, the chromosome axis and SC polymerization was followed it up by immunolocalization of ASY1 and ZYP1. In both hexaploid cultivars (AABBDD), Chinese Spring and Cadenza, the Asy1 signal started to linearize at leptotene. This Asy1 polymerization occurred first in regions close to the telomeres and progressed to full axis polymerization up to the centromeres at late leptotene. Also, ZYP1 signal appeared as discrete foci all through the leptotene stage without a polarizing pattern. Nevertheless, at early zygotene, some ZYP1 foci started to polymerize (synapsis initiation) initially at telomeric regions. As the ZYP1 signal continues to polymerize between the homologous chromosomes, the ASY1 signal is removed from the axis and appears as a weaker staining on the chromatin. ZYP1 polymerization progresses throughout zygotene from telomeres to centromeres. At pachytene, the ZYP1 signal appeared through the whole length of the bivalents (homologous chromosomes) as the cell has reached full synapsis completion. All these observations were consistent to what has been previously described in wheats (Osman *et al.*, 2021, Sepsi *et al*., 2017) and other cereals like barley (Higgins *et al*., 2012). Our observations on Asy1 and Zyp1 progression through prophase I showed no differences in the hexaploid cultivars Chinese Spring and

Cadenza. Thus, it could be concluded that early polarization of chromosome axis formation and synapsis to the telomeric region is similar in both cultivars and therefore, it could not cause the changes in recombination observed between both (observed as extra chiasma frequency and different bivalent configurations in Chinese Spring at metaphase I).

Moreover, the same cytological analysis was conducted in the tetraploid cultivar Cappelli (AABB) and the diploid species *T. monococcum* (AA) to check if this spatio-temporal polarization process was conserved among different ploidy levels in wheat species. Cappelli and *T. monococcum* showed the same ASY1 and ZYP1 progression polarization observed on the hexaploid cultivars Chinese Spring and Cadenza. From these results it can be concluded that the chromosome axis and synapsis progression seem to be spatio-temporally polarized, starting from telomeric distal regions and finalizing at centromeric regions, in all wheat species studied here with different ploidy levels.

3.3.4 The increase of chiasma frequency in Chinese Spring vs Cadenza does not arise from a Class I CO increase

In this thesis, HEI10 immunolocalization was analysed late diplotene to observe the distribution of COs along the chromosomes arms and to validate what have been observed at metaphase I using chiasma frequency and localization. In both cases, a distal bias preference for COs to occur in Chinese Spring similar to those described in barley were observed (Higgins *et al*., 2012; Phillips *et al*., 2013). Interestingly, we have previously reported by different immunolocalization of meiotic proteins that a spatial-temporal asymmetry occurs on Cadenza hexaploid wheat (Osman *et al.*, 2021). Where the meiotic progression starts on distal regions close to telomeres and progresses finalizing at the centromeres. As the wheat chromosomes have a large size this progression can be visualized on cells where distal regions are more advanced in the meiotic progression than interstitial and proximal regions. This could explain how COs in hexaploid wheats could be biased to these distal regions as

they are the first to progress on homologous recombination and once COs are designated to occur at these regions it would trigger the interference signal to the more interstitial/proximal regions decreasing the chances to COs to occur on those regions.

In this chapter, quantification of HEI10 foci with immunolocalization at late diplotene in both Chinese Spring and Cadenza were conducted to investigate if the significantly increase chiasma frequency in Chinese Spring could be correlated to an increase of Class I COs (HEI10). Although, HEI10 foci in Chinese Spring seems to be higher in number in some cells compared to Cadenza, the mean number of HEI10 foci did not reflect any significant differences between them. Thus, it might be possible that the increased chiasma frequency observed in Chinese Spring could proceed from Class II non-interfering COs. This observation would fit with the different ring bivalent configurations in Chinese Spring with more interstitial and proximal chiasmata.

Chapter 4. Analysis of Meiotic Recombination in allopolyploid wheats and wild relatives

4.1 Introduction

Polyploidy has played an important role in the speciation process in the plant kingdom (Stebbins, 1971). An allopolyploid species contains among its chromosome complement two or more diploid species (Winkler, 1916). During the evolution of *Triticeae* there have been two major processes: A divergent process involving the origin of different species from a common ancestral genome with seven chromosomes (2n = 2X = 14 chromosomes) (AA/BB/DD diploid species) and a convergent process which involved the origin of allotetraploid (2n = 4X = 28 chromosomes; AABB) and allohexaploid (2n = 6X = 42 chromosomes; AABBDD) species. Most tetraploid wheat species the genome A is combined with the genome B, and the hexaploids add to these the D genome (Kihara, 1919). This evolutionary origin from an ancestral genome in common with all the genomes present in wheat allopolyploids allows the presence of chromosomes with similar structure that are called homoeologous chromosomes (e.g.: 1A is homoeologous to 1B and 1D) (Huskins, 1931; Sears, 1952). Interestingly, allopolyploid wheat chromosomes during meiosis behave like diploid species with only meiotic recombination occurring between homologous chromosomes and not between homoeologous. This is known as the diploidization of polyploid wheats (Riley, 1960) and it is also found in different polyploid species (Jenkins and Ress, 1991). The diploid behavior of polyploids seems to be genetically regulated in wheats (Okamoto, 1957; Sears & Okamoto, 1958; Riley & Chapman, 1958; 1964; Riley, 1960; Wall et al., 1971) (further developed in Chapter 5).

The genome A present in polyploid wheats seems to have been originated from *Triticum urartu* (Nishikawa, 1983) or *T. monococcum* (Kerby & Kuspira, 1987). Both *T. urartu* and *T. monococcum* could be considered as the same species (Giorgio & Bozzini, 1969). The genome D donor for hexaploid wheats seems to be *Aegilops tauschii* (synonyms *Ae. squarrosa, T. tauschii*) (Jones *et al*., 1982; Mahjoob *et al*., 2021). The genome B donor seems to proceed from an Aegilops species from the section Sitopsis (*Ae. sharonensis, Ae longissima, Ae. bicornis, Ae, searsii and Ae. speltoides)* (Li

et al., 2022). Molecular, cytological and genetic markers have shown that *Ae. speltoides* might be the closest species to the B ancestor (Gornicki *et al*., 2014; Miki *et al*., 2019; El Baidouri *et al*., 2017).

In chapter 3, the different metaphase I bivalent configurations observed in the hexaploid wheat Chinese Spring (CS) were discussed and classified in great detail. In this chapter, the same tools and classifications to calculate the mean chiasma frequency and assessing the chiasma distribution along the chromosome arms in different cultivars in hexaploid wheat, tetraploid wheat and wild relative species were used. These different wheat species and cultivars included in this analysis were (figure 4.1 and 4.2):

- Hexaploid wheat cultivars (AABBDD) (bread wheat):
    - Chinese spring (CS)
    - Cadenza (Cad)
    - Paragon (Pg, Par)
    - Fielder (Fld)
- Tetraploid wheat cultivars (AABB) (pasta wheat):
    - Kronos (Kr, Kron)
    - Cappelli (Cap, Capp)
    - Langdon (Lnd, Lan)
- Diploid ancestral wild relative species
    - *Trititicum monoccocum* (AA)
    - *Aegilops speltoides* (BB)
    - *Aegilops tauschii* (DD)

		Origin/Breeder/Source
Chinese Spring (CS)	Landrace	Chengdu (Sichuan, China). Famous by E. Sears aneuploid series
Cadenza (Cad)	Cultivar	Breeder CPB Twyford Ltd (pedigree Axona x Tonic) UK 1995
Paragon (Pg)	Cultivar	Balcaskie Estate (Scotland) UK 1999
Fielder (Fld)	Cultivar	University of Idaho USA 1974. Transformation
Kronos (Kr)	Cultivar	Arizona Plant Breeders USA 1992
Cappelli (Cap)	Cultivar	Senatore Cappelli in Foggia Italy 1915 (Nazareno Strampelli)
Langdon (Lnd)	Cultivar	Reference durum cultivar USA. Aneuploid and substitution lines
T. monococcum		AA
Ae. speltoides		BB
Ae. tauschii		DD
Spring Wheat – *T. aestivum* (AABBDD)		Durum Wheat – *T. durum* (AABB)

Figure 4.1: Origin and uses of the different wheat species and cultivars used in this chapter.

These cultivars were chosen because they are elite varieties and widely used by plant breeders in hexaploidy and tetraploid wheats (Cad, Pg, Fld, Kr) and others because they have been historically used in a broad of genetic studies over the years (CS, Cap, Lnd) (McFadden & Sears, 1946; Sears, 1958; Sears, 1977; Giorgi, 1978; Hobolth, 1981; Sears, 1982). Shewry and Hey (2015) indicated that the wheat species that are mostly cultivated around the world are hexaploid (bread wheat) and tetraploid (pasta wheat). The world production of these species is around 35 to 40 million tons per year (Shewry and Hey, 2015).

CS is a landrace hexaploid wheat that was developed in Chengdu (Sichuan, China) and was famously used by E. Sears producing his aneuploid series (Sears, 1954). Cad is a cultivated hexaploid wheat that was first developed by breeders in Tawyford Ltd in the UK in 1995 (pedigree Axona x Tonic). Pg is a cultivated hexaploid wheat that was developed by the Balcaskie Estate in Scotland (UK) in 1999. Fld is another cultivated hexaploid wheat that was developed in the University of Idaho (USA) in 1974. Kr is a cultivated tetraploid wheat that was developed by Arizona plant breeders in 1992 in USA. Cap is a cultivated tetraploid wheat that was developed in Foggia (Italy) in 1915 and its known

by the common name of senator Cappelli. Finally, Lnd is a cultivated tetraploid wheat that was used as reference for durum cultivar in USA and as a source for aneuploid and substitutional lines by E. Sears (1954).

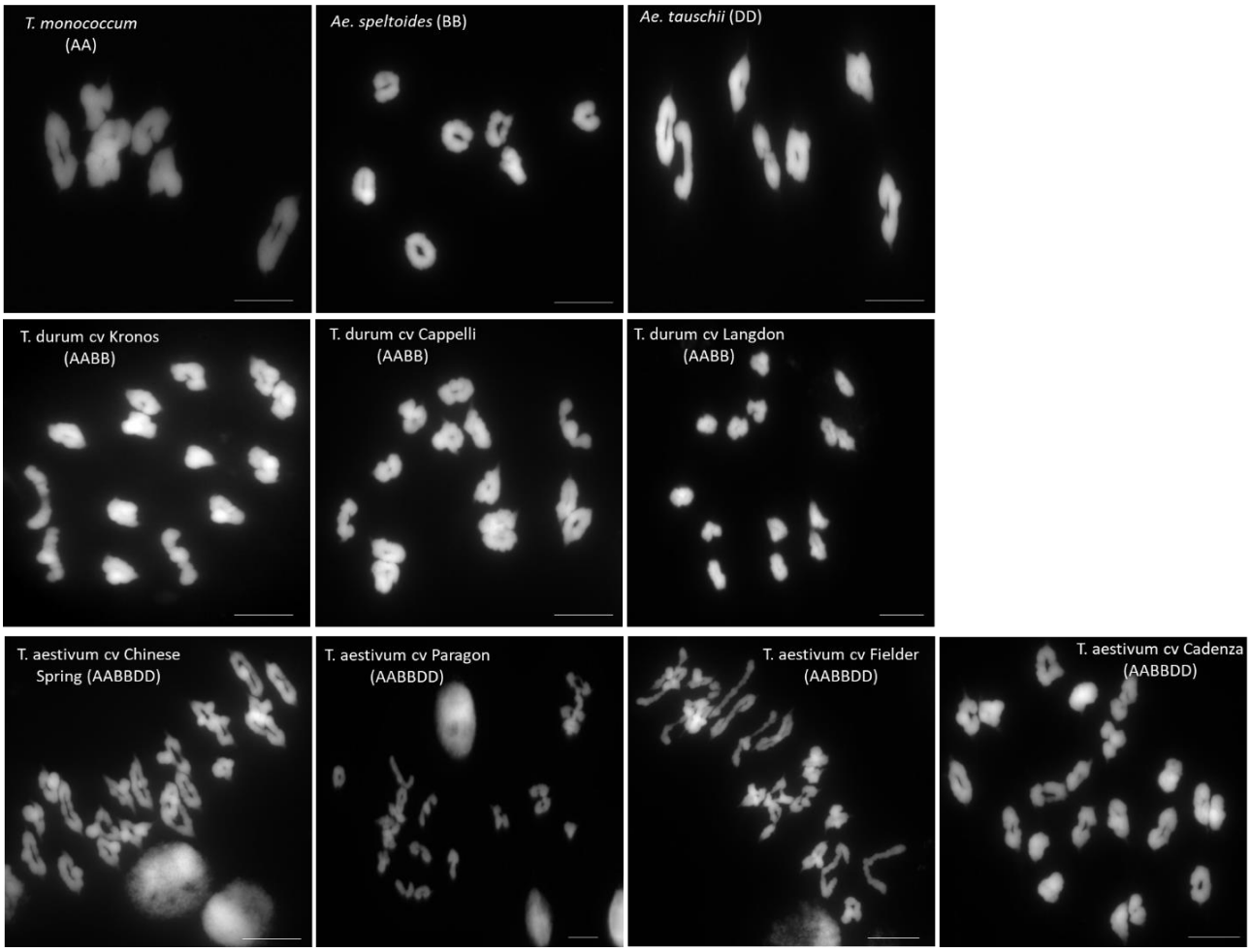

Figure 4.2: DAPI spread images of metaphase I pollen mother cells of different wheat species in this study. Scale Bar = 10 µm. These images show that only a clear MI slides were used for chiasmata count. Unclear images were excluded from being used for analysis in this chapter.

4.2 Results

Comparing the mean chiasma frequencies within wheat species from the same ploidy level was conducted by One-way ANOVA (Welch test multipole comparison) (Table 4.1 see appendix). Before applying ANOVA, a test of normality was conducted by using (D'Agostino-Pearson test) (figures 4.3 and 4.4). The summary of these comparisons is listed in (figure 4.5) and (tables 4.2, 4.3 and 4.4 see appendix). In hexaploid wheats, CS has showed significant differences in the mean chiasma frequency with Cad and Pg, whereas no significant differences were observed when comparing it to Fld. In addition, Cad showed significant differences in chiasma frequency with Fld whereas no significant differences were observed between Cad and Pg. In tetraploid wheats, Kr appeared to be significantly different in mean chiasma frequency to Cap and Lnd. Moreover, Cap and Lnd showed a lower significant difference in the mean chiasma frequency between them. Finally, surprisingly, the three diploid wheat ancestral relative species showed that there were not any significant differences between them.

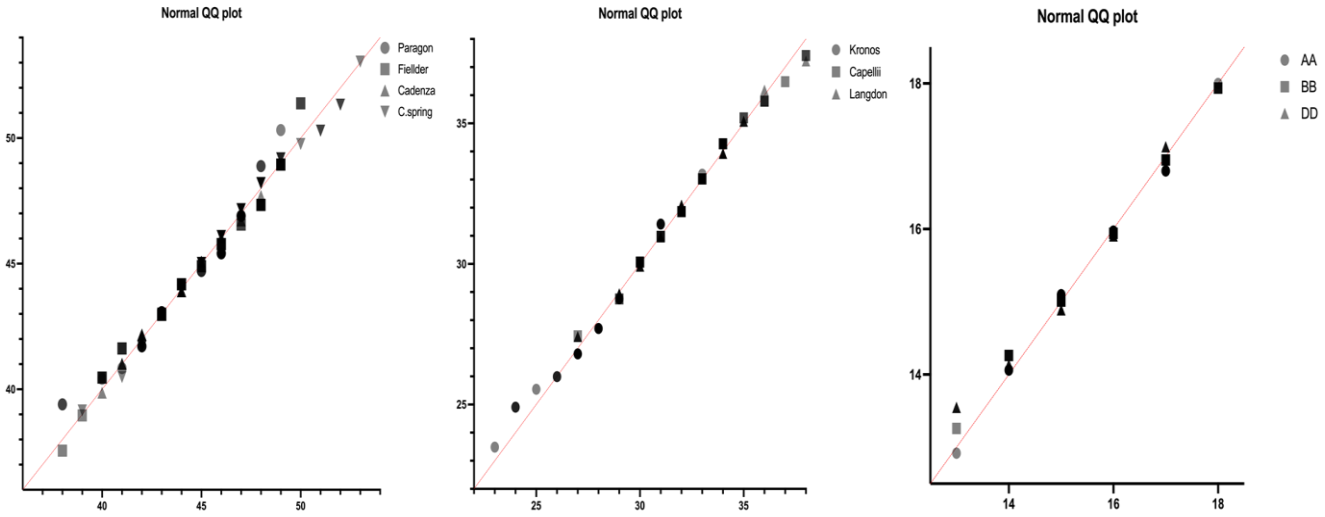

Figure 4.3: Test of normality of different wheat species from different ploidy level (Graph pad).

D'Agostino & Pearson test	Paragon	Fielder	Cad	C.S
K2	3.379	3.393	0.1256	0.4423
P value	0.1846	0.1833	0.9391	0.8016
Passed normality test (alpha=0.05)?	Yes	Yes	Yes	Yes

D'Agostino & Pearson test	Kronos	Cappelli	Langdon
K2	3.566	0.7139	0.3029
P value	0.1681	0.6998	0.8595
Passed normality test (alpha=0.05)?	Yes	Yes	Yes

D'Agostino & Pearson test	AA	BB	DD
K2	0.7653	0.9287	5.120
P value	0.6821	0.6285	0.0773
Passed normality test (alpha=0.05)?	Yes	Yes	Yes

Figure 4.4: Normality test (D'Agostino & Pearson test) (N=50).

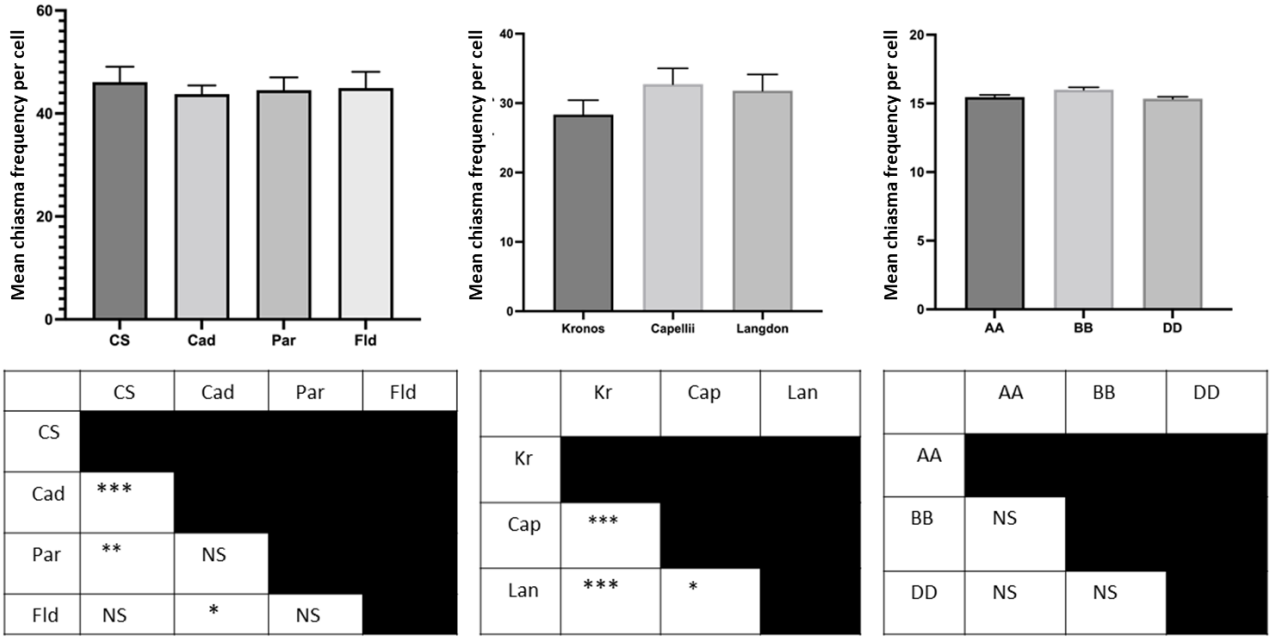

Figure 4.5: Comparison of the mean chiasma frequency per cell between different wheat cultivars and species. In hexaploid wheats, CS has showed significant differences in the mean chiasma frequency with Cad and Pg, whereas no significant differences were observed when comparing it to Fld. In addition, Cad showed significant differences in chiasma frequency with Fld whereas no significant differences were observed between Cad and Pg. In tetraploid wheats, Kr appeared to be significantly different in mean chiasma frequency to Cap and Lnd. Moreover, Cap and Lnd showed a lower significant difference in the mean chiasma frequency between them. Finally, surprisingly, the three diploid wheat ancestral relative species showed that there were not any significant differences between them. One-way ANOVA (NS $p>0.05$/ *$0.05\geq p > 0.005$/ **$0.005> p > 0.0005$/ ***$p < 0.0005$) (N=50).

Comparing the mean chiasma frequency per bivalent of all these cultivars and species facilitated the opportunity to systematically compare them independently of the ploidy level. This analysis was conducted by dividing the total number of chiasmata per cell by the total number of bivalents present in each cell (figure 4.6) (Table 4.1 see appendix). Thus, in diploid species the mean chiasma frequency was divided by 7, in tetraploids by 14 and in hexaploids by 21.

The mean chiasma frequency per bivalent in CS (AABBDD) was significantly different to Cad and Pg in hexaploidy wheats, to Kr and Cap (AABB tetraploid species) and to *Ae. speltoides* (BB diploid

species) but not significant to Fld (AABBDD), Lnd (AABB), *T. monococcum* (AA) and *Ae. tauschii* (DD) (Figure 4.6).

The mean chiasma frequency per bivalent in Cad showed significant differences with CS and Fld whereas non-significant differences to Pg (AABBDD hexaploidy species), significant differences to Kr, Cap and Lnd (AABB tetraploid species) and to *T. monococcum* (AA), *Ae. speltoides* (BB) and *Ae. tauschii* (DD).

Pg showed significant differences in the mean chiasma frequency per bivalent with CS but not with Cad and Fld (AABBDD hexaploidy wheats). Pg showed significant differences in the mean chiasma frequency per bivalent with Kr, Cap and Lnd (AABB) and with *T. monococcum* (AA), *Ae. speltoides* (BB) and *Ae. tauschii* (DD).

Fld was only significantly different in the mean chiasma frequency per bivalent with Cad in hexaploid wheats but not significant with CS or Pg (AABBDD). Fld was also significantly different to tetraploid wheats: Kr, Cap and Lnd (AABB); and to diploid *Ae. speltoides* (BB) but not significant to *T. monococcum* (AA) and *Ae tauschii* (DD).

In tetraploid wheat, Kr showed significant differences in the mean chiasma frequency per bivalent with all wheat species and varieties analysed with different ploidy level.

Cap showed significant differences in the mean chiasma frequency per bivalent with all wheat species and cultivars analysed with the exception of diploid *Ae. speltoides* (BB) that was not significant.

Lnd showed significant differences in the mean chiasma frequency per bivalent with all hexaploid cultivars but with CS (AABBDD), with tetraploid cultivars Kr and Cap (AABB) and with *Ae. tauschii* (DD).

In the diploid species, no significant differences in the mean chiasma frequency per bivalent were observed between *T. monococcum* (AA) and *Ae. speltoides* (BB) and *Ae. tauschii* (DD). Nevertheless, moderate significant differences were observed between *Ae. speltoides* (BB) and *Ae. tauschii* (DD) in mean chiasma frequency per bivalent.

Furthermore, *T. monococcum* (AA) showed significant differences in the mean chiasma frequency per bivalent with hexaploid cultivars Cad and Pg (AABBDD), and with tetraploid cultivars Kr and Cap (AABB). However, no significant differences were observed when comparing to hexaploid cultivars CS and Fld (AABBDD) or tetraploid cultivar Lnd (AABB). In addition, *Ae. speltoides* (BB) showed significant differences in the mean chiasma frequency per bivalent with all hexaploid (AABBDD) wheat cultivars analyzed (CS, Cad, Pg and Fld), with tetraploid cultivar Kr (AABB) and with diploid *Ae. tauschii* (DD) whereas no significant differences were observed when comparing with tetraploid cultivars Cap and Lnd, and diploid species *T. monococcum* (AA). Finally, *Ae. tauschii* (DD) showed significant differences in the mean chiasma frequency per bivalent with hexaploid cultivars Cad and Pg, with tetraploid cultivars Kr, Cap and Lnd, and diploid *Ae. speltoides* (BB); whereas no significant differences were observed when comparing to hexaploid cultivars CS and Fld, and diploid *T. monococcum* (AA).

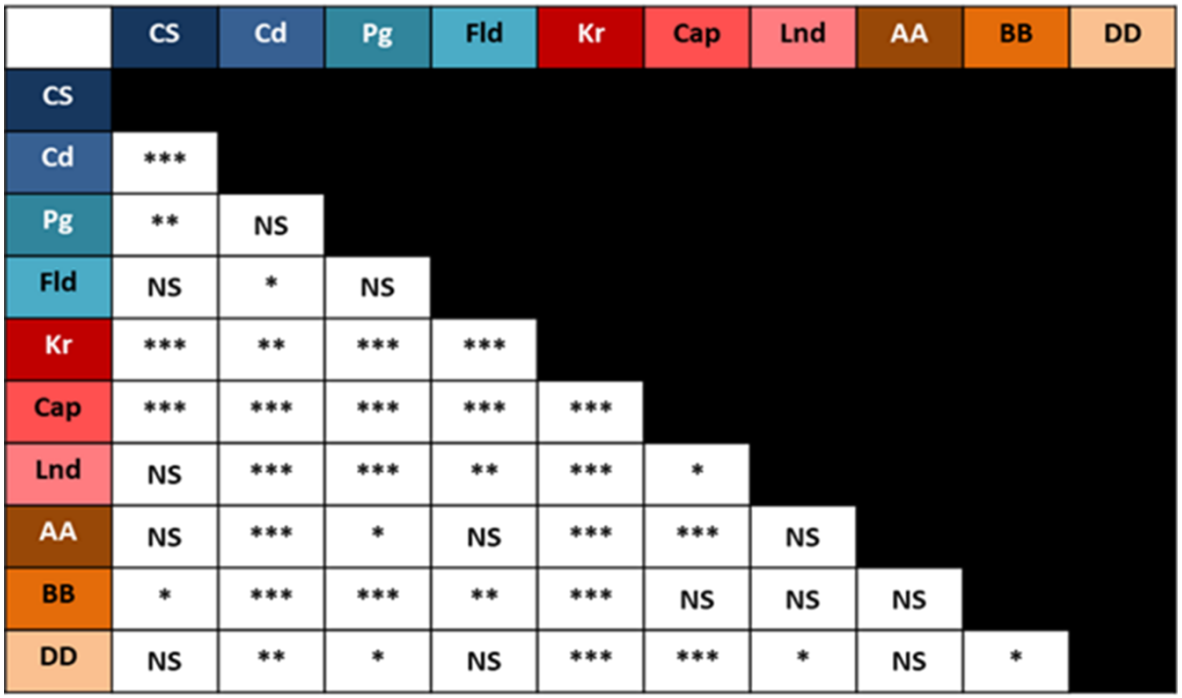

Figure 4.6: Comparison of the mean chiasma frequency per bivalent in wheat species from different ploidy level (N=50). One-way ANOVA (NS p>0.05/ *0.05≥ p > 0.005/ **0.005> p > 0.0005/ ***p < 0.0005) (N=50).

4.2.1 Systematic analysis of mean Chiasma Frequency per Rod and Ring Bivalents

The mean chiasma frequency per rod and ring bivalents were analyzed in all the different species and cultivars (figures 4.7 and 4.8) (Table 4.6 and 4.7 see appendix). The mean chiasma frequency per rod and ring bivalents was calculated (figure 4.7). The mean chiasma frequency in ring bivalents was always higher compared to the mean of rod bivalents with highest values of (2.250±0.0295) chiasmata per ring bivalent (in hexaploid wheat cultivar Cap) and (0.221±0.0178) chiasmata per rod bivalent (in hexaploid wheat cultivar Fld). Interestingly, tetraploid cultivar Cap (AABB) (2.250±0.0295) and diploid *Ae. speltoides* (BB) (2.217±0.0324) showed the highest mean chiasmata per ring bivalent. This was followed by Langdon, *Ae. tauschii*, *T. monococcum* and CS with (2.156±0.0264, 2.137±0.0378 and 2.109±0.0352) chiasmata per bivalent. Following to this,

Cadenza (2.010±0.0185) and Paragon (2±0.0308) showed a low mean of the chiasma frequency in ring bivalents. Finally, Fielder and Kronos showed the lowest mean chiasma frequency per ring bivalents with (1.944±0.0336 and 1.830±0.0345) respectively (Table 4.6 see appendix).

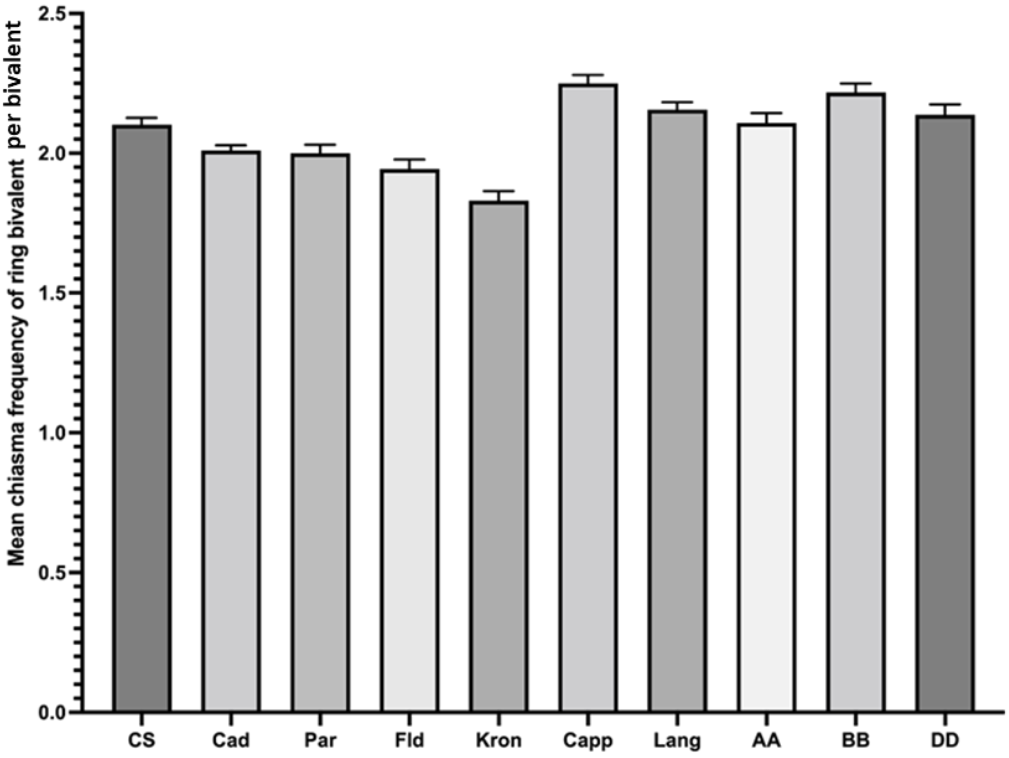

Figure 4.7: Mean chiasma frequency per ring bivalents in different wheat.

For rod bivalents, Fielder and Kronos showed the highest mean chiasma frequency per rod bivalent with (0.221±0.0178 and 0.1986±0.0169) respectively (Figure 4.8; Table 4.7). This was followed by a low mean in Paragon with (0.1333±0.0157) chiasmata. Additionally, CS, Langdon and *T. monococcum* showed a low mean chiasma than paragon with (0.1057±0.009) chiasmata. Finally, Cadenza, Cappelli, *Ae. speltoides* and *Ae. tauschii* showed the lowest mean chiasma (0.0952±0.0135). To investigate significant differences between these values, Kruskal-Wallis test were conducted and the results are summarized in (figure 4.9). Starting with hexaploid wheat, Fld showed significant differences with three hexaploid wheat CS, Cad and Pg with (p value <0.0001,

<0.0001 and 0.01) (Table 4.8 see appendix), and two tetraploid wheat Cap and Lnd with (p value <0.0001) Also, a significant difference was observed when compared to three diploid ancestral wheats *T. monococcum*, *Ae. speltoides* and *Ae. tauschii* (p value <0.0001). Kr was significantly difference compared to the hexaploid wheat CS and Cad (p value = 0.0003), and two tetraploid wheat Cap and Lnd (p value = 0.0001), and all three diploid wheat AA, BB and DD with (p value = 0.0001).

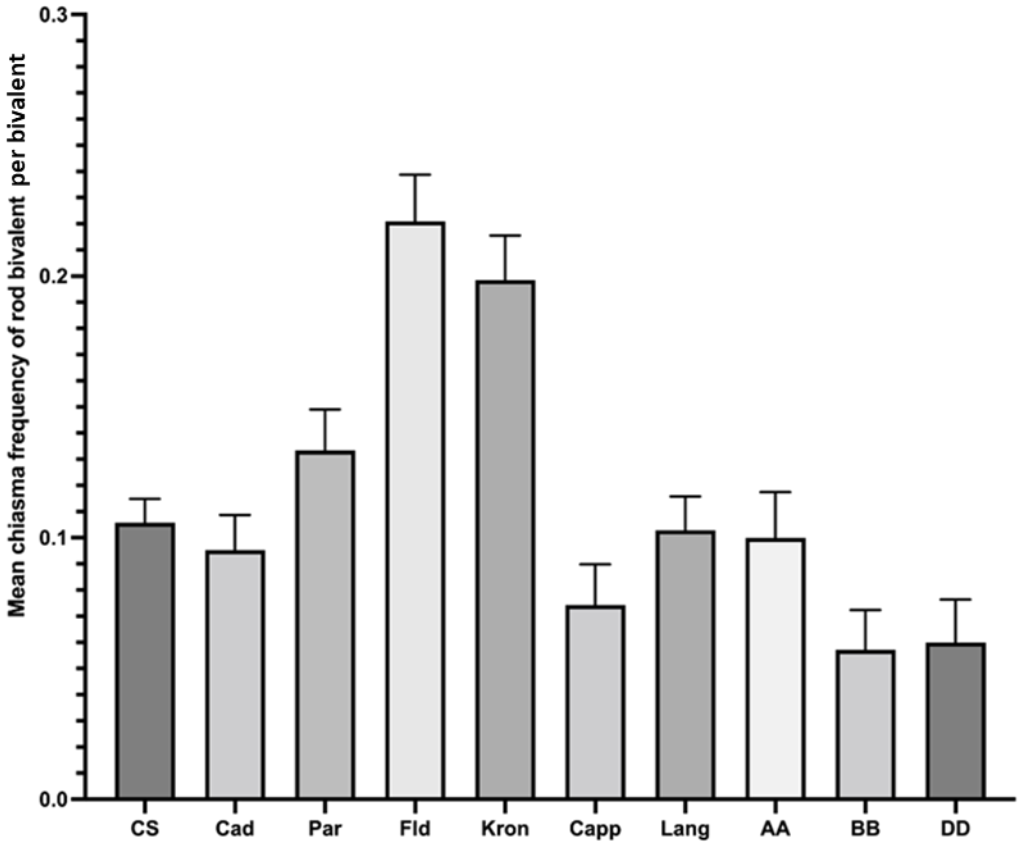

Figure 4.8: Mean chiasma frequency per rod bivalents in different wheat.

	CS	Cad	Pg	Fld	Kr	Cap	Lng	AA	BB	DD
CS										
Cad	ns									
Pg	ns	ns								
Fld	****	****	*							
Kr	***	***	ns	ns						
Cap	ns	ns	ns	****	****					
Lang	ns	ns	ns	****	***	ns				
AA	****	ns	ns	***	**	ns	ns			
BB	ns	ns	*	****	****	ns	ns	ns		
DD	ns	ns	NS	****	****	ns	ns	ns	ns	

Figure 4.9: Comparison of the mean chiasma frequency of rod bivalent in all wheat. Fld showed significant differences with three hexaploid wheat CS, Cad and Pg with (p value <0.0001, <0.0001 and 0.01) and two tetraploid wheat Cap and Lnd with (p value <0.0001) Also, a significant difference was observed when compared to three diploid ancestral wheats *T. monococcum*, *Ae. speltoides* and *Ae. tauschii* (p value <0.0001). Kr was significantly difference compared to the hexaploid wheat CS and Cad (p value = 0.0003), and two tetraploid wheat Cap and Lnd (p value = 0.0001), and all three diploid wheat AA, BB and DD with (p value = 0.0001). Kruskal-Wallis test (NS p>0.05/ *0.05≥ p > 0.005/ **0.005> p > 0.0005/ ***p < 0.0005) (N=50).

Additionally, for ring bivalents Welch's ANOVA test was conducted to investigate the differences observed in the mean chiasma frequency (figure 4.10).

On ring bivalents, Fld (AABBDD) showed significant differences in the mean chiasma frequency per ring bivalent with Cap (AABB) (p value <0.0001) and Lnd (AABB) (p value = 0.0001) (Table 4.9 see appendix). Fld also showed significant differences with all three diploid species analyzed: *T. monococcum* (AA) (p value = 0.04), *Ae. speltoides* (BB) (p value <0.0001) and *Ae tauschii* (DD) (p

value 0.01). Kr (AABB) showed significant differences in the mean chiasma frequency per ring bivalent with the rest of wheat cultivars and species analyzed except for Fld (AABBDD). Finally, Cap (AABB) that showed the highest mean chiasma frequency in ring bivalents (2.250±0.0295), showed significant differences with all hexaploid wheat cultivars (AABBDD) (CS, Cad. Pg, Fld).

	CS	Cad	Par	Fld	Kron	Cap	Lang	AA	BB
CS									
Cad	ns								
Par	ns	ns							
Fld	*	ns	ns						
Kron	****	***	*	ns					
Cap	**	****	****	****	****				
Lang	ns	***	*	***	***	ns			
AA	ns	ns	ns	*	****	ns	ns		
BB	ns	****	****	****	****	ns	ns	ns	
DD	ns	ns	*	*	****	ns	ns	ns	ns

Figure 4.10: Comparison of the mean chiasma frequency of ring bivalent in all wheat. Fld (AABBDD) showed significant differences in the mean chiasma frequency per ring bivalent with Cap (AABB) (p value <0.0001) and Lnd (AABB) (p value = 0.0001). Fld also showed significant differences with all three diploid species analyzed: T. monococcum (AA) (p value = 0.04), Ae. speltoides (BB) (p value <0.0001) and Ae tauschii (DD) (p value 0.01). Kr (AABB) showed significant differences in the mean chiasma frequency per ring bivalent with the rest of wheat cultivars and species analyzed except for Fld (AABBDD). Finally, Cap (AABB) that showed the highest mean chiasma frequency in ring bivalents (2.250±0.0295), showed significant differences with all hexaploid wheat cultivars (AABBDD) (CS, Cad. Pg, Fld). Welch's ANOVA test (NS p>0.05/ *0.05≥ p > 0.005/ **0.005> p > 0.0005/ ***p < 0.0005) (N=50).

4.2.2 Chiasma Distribution along the chromosome arms

The mean chiasma frequency at different chromosome locations were identified and analyzed. To investigate if the differences in mean chiasma frequency in specific localizations along the chromosome length were significantly different between the different wheat cultivars and their wild relative, multiple Welch's ANOVA tests were conducted.

4.2.2.1 Distal chiasmata (d)

The mean of chiasma frequency at distal regions in all wheat cultivars and species were analyzed using Welch's ANOVA to investigate if any significant differences occur between different wheat cultivars and their wild relatives or not (figure 4.11 and 4.12) and (Table 4.10 see appendix).

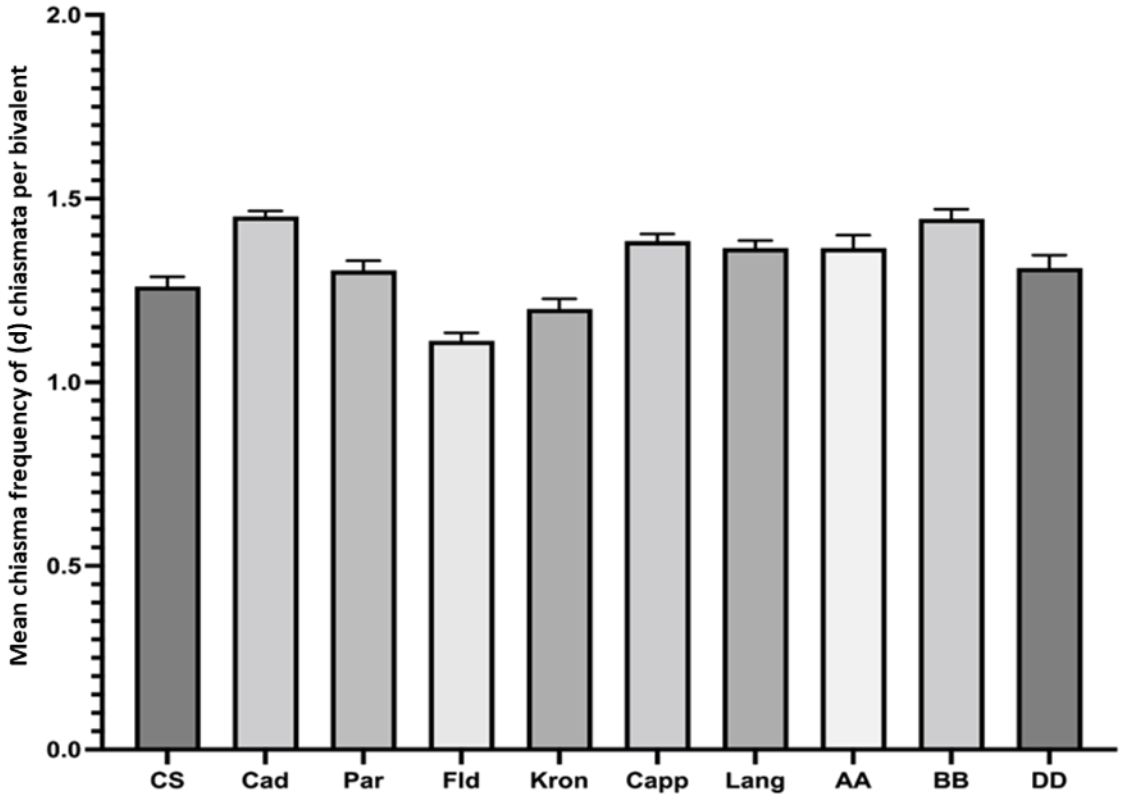

Figure 4.11: Mean chiasma frequency of (d) chiasmata in all wheats.

	CS	Cad	Par	Fld	Kron	Cap	Lang	AA	BB
CS									
Cad	***								
Par	ns	***							
Fld	**	****	****						
Kron	ns	****	ns	ns					
Cap	*	ns	ns	****	****				
Lang	ns	*	ns	****	***	ns			
AA	ns	ns	ns	****	*	ns	ns		
BB	****	ns	**	****	****	ns	ns	ns	
DD	ns	*	ns	***	ns	ns	ns	ns	ns

Figure 4.12: Comparison of the mean chiasma frequency of distal chiasmata in all wheat. Cad (AABBDD) and *Ae. speltoides* (BB) showed the highest mean (1.451±0.0153 and 1.446±0.0253) of distal chiasma frequency compared to the rest of lines. Cad (AABBDD) was significantly different to the other hexaploid wheat cultivars CS, Pg and Fld, also to the tetraploid cultivars Kr and Lnd. However, no significant differences were observed between Cad and tetraploid Cap. *Ae. speltoides* (BB) showed high significant differences compared to the hexaploid CS and Fld, ($p<0.0001$) and to the tetraploid Kr, and moderate significant differences with hexaploid Pg ($p=0.008$). Whereas no significant differences were observed compared to tetraploids Lnd and Cap. Finally, *Ae. speltoides* (BB) did not show any significant differences compared to the diploid species *T. monococcum* (AA) and *Ae. tauschii* (DD). The lowest chiasma frequencies at d localization were observed in Kr (1.2±0.027). Welch's ANOVA test (NS $p>0.05$/ *$0.05\geq p > 0.005$/ **$0.005> p > 0.0005$/ ***$p < 0.0005$) (N=50).

Cad (AABBDD) and *Ae. speltoides* (BB) showed the highest mean (1.451±0.0153 and 1.446±0.0253) of distal chiasma frequency compared to the rest of lines. Cad (AABBDD) was significantly different to the other hexaploid wheat cultivars CS, Pg and Fld, also to the tetraploid cultivars Kr and Lnd. However, no significant differences were observed between Cad and tetraploid Cap.

Ae. speltoides (BB) showed high significant differences compared to the hexaploid CS and Fld, ($p<0.0001$) and to the tetraploid Kr, and moderate significant differences with hexaploid Pg ($p=0.008$) (Table 4.11 see appendix). Whereas no significant differences were observed compared to tetraploids Lnd and Cap. Finally, *Ae. speltoides* (BB) did not show any significant differences compared to the diploid species *T. monococcum* (AA) and *Ae. tauschii* (DD). The lowest chiasma frequencies at d localization were observed in Kr (1.2 ± 0.027).

4.2.2.2 Interstitial region 1 (i^1) chiasmata

The mean of chiasma frequency at interstitial region 1 (i^1) in all wheat cultivars and species were analyzed using Welch's ANOVA to investigate if any significant differences occur between different wheat cultivars and their wild relatives or not (figures 4.13 and 4.14) (Tables 4.12 and 4.13 see appendix).

Ae. tauschii (DD) showed the highest mean of i^1 (0.3657 ± 0.0356) and was significant different to hexaploid Cad (AABBDD), and tetraploids Lnd and Cap (AABB). The second highest mean chiasma frequency in i^1 was observed in hexaploid Fld (AABBDD) (0.3381 ± 0.0158) and it was significantly different to that observed in other hexaploid cultivars Cad and Pg (AABBDD) (Table 4.13), and to tetraploids Cap and Lnd (AABB). Interestingly, *T. monococcum* (AA) did not show any significant difference in the mean chiasma frequency in this i^1 localization (0.2714 ± 0.0235) with any of the material analyzed in this thesis. The lowest chiasma frequencies at i^1 localization were observed in Cad (AABBDD) (0.2114 ± 0.009) and Lnd (AABB) (0.21 ± 0.011).

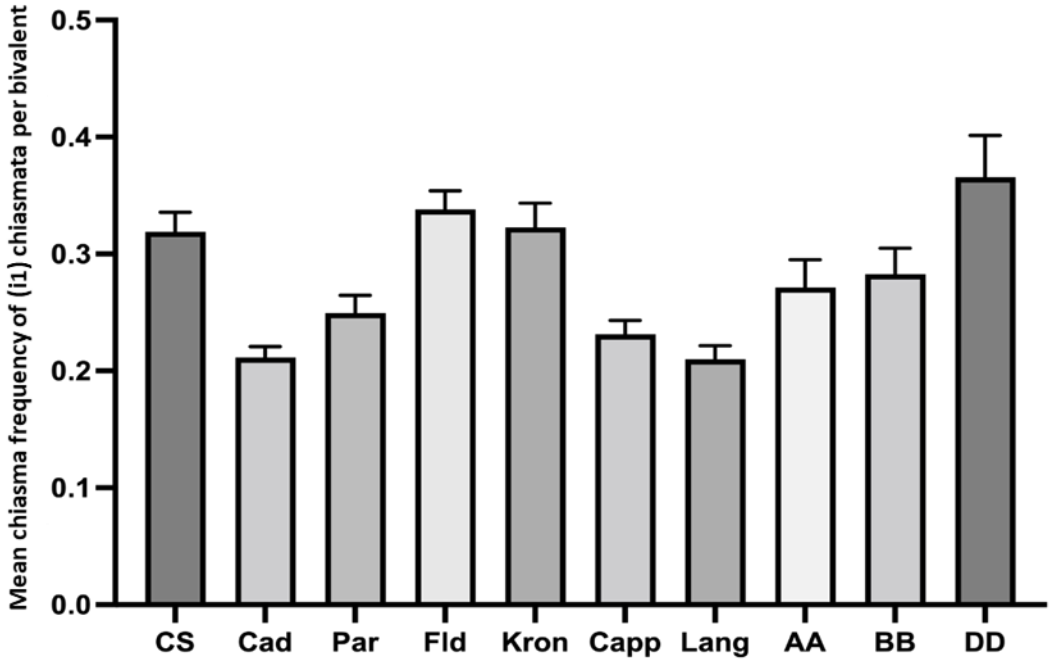

Figure 4.13: Mean chiasma frequency of interstitial region 1 (i^1).

	CS	Cad	Par	Fld	Kron	Cap	Lang	AA	BB
CS									
Cad	****								
Par	ns	***							
Fld	ns	****	**						
Kron	ns	***	ns	ns					
Cap	**	ns	ns	****	*				
Lang	****	ns	ns	****	***	ns			
AA	ns	ns	ns	ns	ns	ns	ns		
BB	ns	ns	**	ns	ns	ns	ns	ns	
DD	ns	**	ns	ns	ns	*	**	ns	ns

Figure 4.14: Comparison of the mean chiasma frequency of interstitial region 1 (i^1). *Ae. tauschii* (DD) showed the highest mean of i1 (0.3657±0.0356) and was significant different to hexaploid Cad (AABBDD), and tetraploids Lnd

and Cap (AABB). The second highest mean chiasma frequency in i1 was observed in hexaploid Fld (AABBDD) (0.3381±0.0158) and it was significantly different to that observed in other hexaploid cultivars Cad and Pg (AABBDD), and to tetraploids Cap and Lnd (AABB). Interestingly, *T. monococcum* (AA) did not show any significant difference in the mean chiasma frequency in this i1 localization (0.2714±0.0235) with any of the material analyzed in this thesis. The lowest chiasma frequencies at i1 localization were observed in Cad (AABBDD) (0.2114±0.009) and Lnd **(AABB) (0.21±0.011).** Welch's ANOVA (N=50).

4.2.2.3 Interstitial region 2 (i^2) chiasmata

The mean of chiasma frequency at interstitial region 2 (i^2) in all wheat cultivars and species were analyzed using Welch's ANOVA to investigate if any significant differences occur between different wheat cultivars and their wild relatives or not (figures 4.15 and 4.16) and (Tables 4.14 and 4.15 see appendix).

Hexaploid cultivar Fld showed the highest mean chiasma frequency in i^2 regions (0.3743±0.0165) and was significantly different to Cad (AABBDD), Kr (AABB), *Ae. speltoides* (BB) and *T. monococcum* (AA). The second highest mean frequency in i^2 was observed in tetraploid cultivar Lnd (AABB) (0.3486±0.0168) and it was significantly different to Cad (AABBDD) and *Ae. speltoides* (BB). Interestingly, *Ae. tauschii* (DD) didn't show any significant difference in the mean chiasma frequency (0.2257±0.0241) in this i^2 localization with any of the material analyzed in this thesis. The lowest chiasma frequencies at i^2 localization were observed in *Ae. speltoides* (BB).

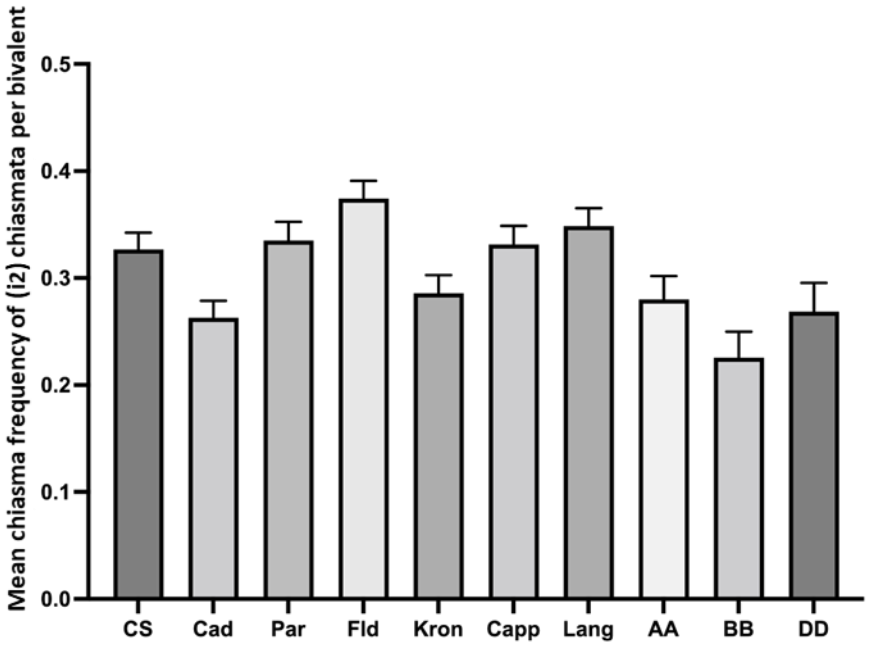

Figure 4.15: Mean chiasma frequency of (i^2) in all wheat.

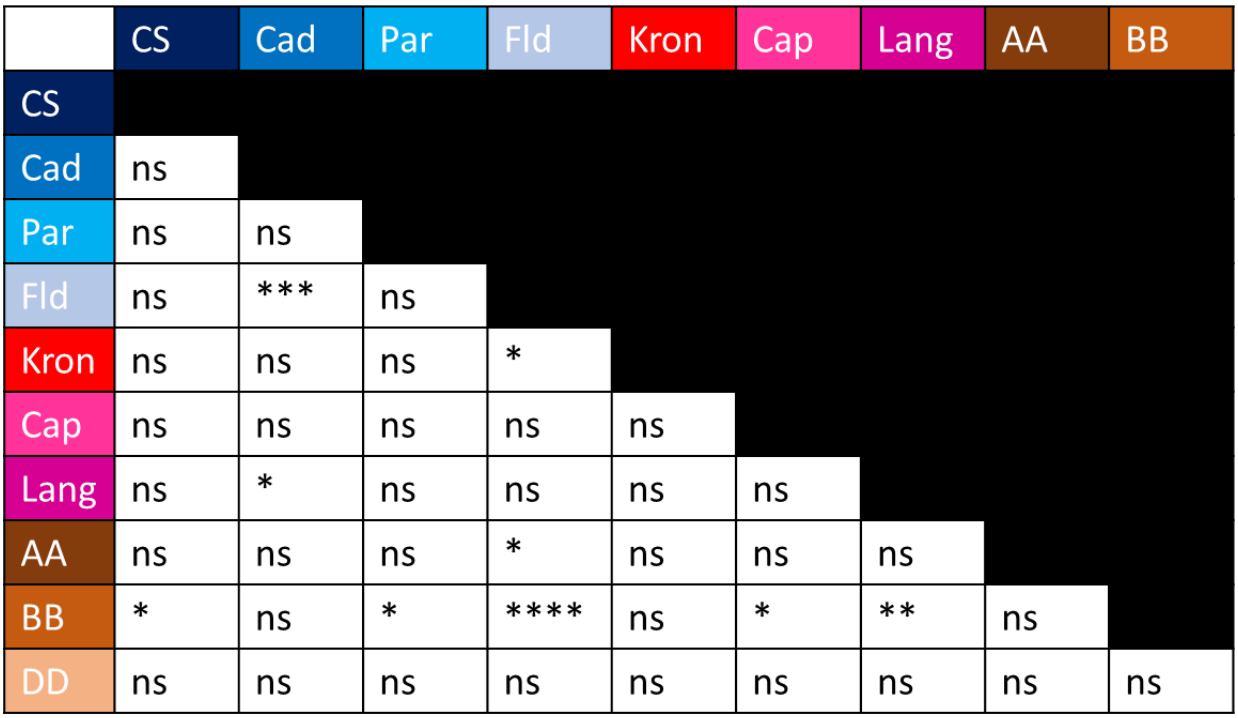

	CS	Cad	Par	Fld	Kron	Cap	Lang	AA	BB
CS									
Cad	ns								
Par	ns	ns							
Fld	ns	***	ns						
Kron	ns	ns	ns	*					
Cap	ns	ns	ns	ns	ns				
Lang	ns	*	ns	ns	ns	ns			
AA	ns	ns	ns	*	ns	ns	ns		
BB	*	ns	*	****	ns	*	**	ns	
DD	ns	ns	ns	ns	ns	ns	ns	ns	ns

Figure 4.16: Comparison of the mean chiasma frequency of (i^2) in all wheats. Hexaploid cultivar Fld showed the highest mean chiasma frequency in i2 regions (0.3743±0.0165) and was significantly different to Cad (AABBDD), Kr (AABB), *Ae. speltoides* (BB) and T. monococcum (AA). The second highest mean frequency in i2 was observed in tetraploid cultivar Lnd (AABB) (0.3486±0.0168) and it was significantly different to Cad (AABBDD) and *Ae. speltoides* (BB). Interestingly, *Ae. tauschii* (DD) didn't show any significant difference in the mean chiasma frequency (0.2257±0.0241) in this i2 localization with any of the material analyzed in this thesis. The lowest chiasma frequencies at i2 localization were observed in *Ae. speltoides* (BB). Welch's ANOVA (N=50).

4.2.2.4 Interstitial region 3 (i^3) chiasmata

The mean of chiasma frequency at interstitial region 3 (i^3) in all wheat cultivars and species were analyzed using Welch's ANOVA to investigate if any significant differences occur between different wheat cultivars and their wild relatives or not (figure 4.17 and 4.18) and (Tables 4.16 and 4.17 see appendix).

Hexaploid cultivar Fld (AABBDD) showed the highest mean chiasma frequency in i^3 (0.2371±0.011) and was significantly different to the hexaploid cultivars Cad and Pg, to the tetraploid cultivar Kr (AABB) and to *Ae. tauschii* (DD) (Table 4.16). Additionally, tetraploid cultivars Lnd

(0.2100±0.0136) and Cap (0.2114±0.0132) (AABB), both showed the second highest mean chiasma frequency in i^3 and both were significantly different to Cad, Pg and *Ae. tauschii* (DD). Interestingly, *Ae. speltoides* (BB) (0.1886±0.0149) didn't show any significant difference in the mean chiasma frequency in this i^3 localization with any of the material analyzed in this thesis. The lowest chiasma frequencies at i^3 localization were observed in hexaploid cultivars Cad (0.0914±0.006) and Pg (0.1352±0.007) (AABBDD), and *Ae. tauschii* (DD) (0.1314±0.0134).

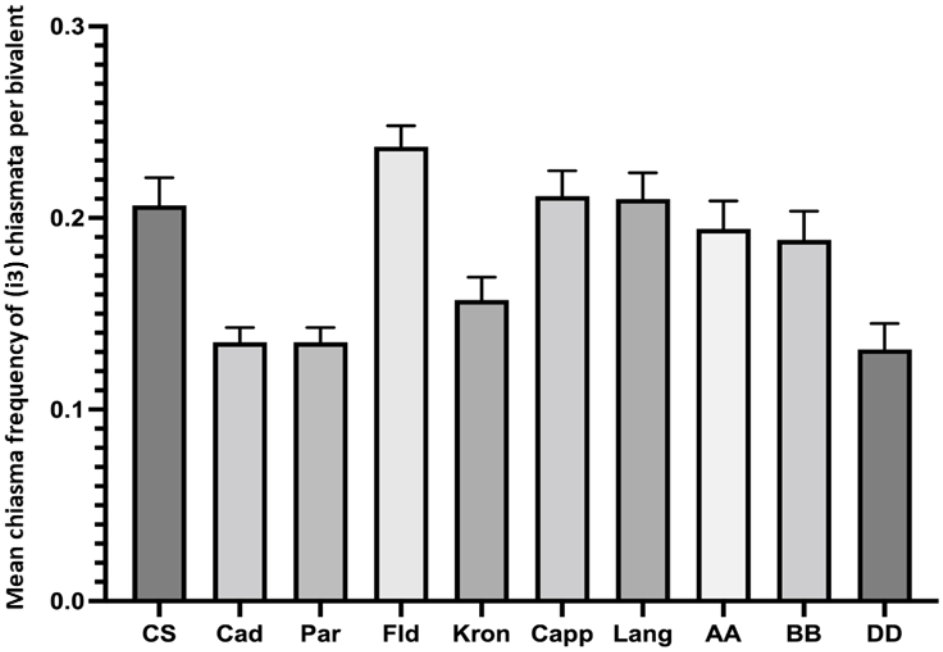

Figure 4.17: Mean chiasma frequency of (i^3) in all wheat.

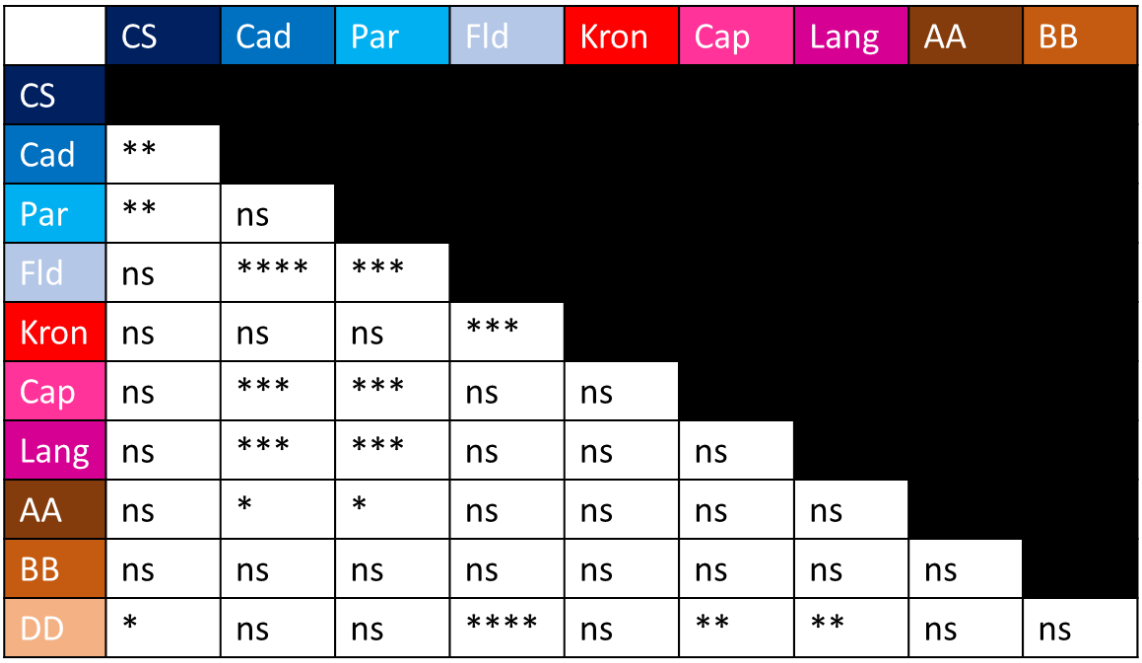

	CS	Cad	Par	Fld	Kron	Cap	Lang	AA	BB
CS									
Cad	**								
Par	**	ns							
Fld	ns	****	***						
Kron	ns	ns	ns	***					
Cap	ns	***	***	ns	ns				
Lang	ns	***	***	ns	ns	ns			
AA	ns	*	*	ns	ns	ns	ns		
BB	ns	ns	ns	ns	ns	ns	ns	ns	
DD	*	ns	ns	****	ns	**	**	ns	ns

Figure 4.18: Comparison of the mean chiasma frequency of (i^3) in all wheats. Hexaploid cultivar Fld (AABBDD) showed the highest mean chiasma frequency in i3 (0.2371±0.011) and was significantly different to the hexaploid cultivars Cad and Pg, to the tetraploid cultivar Kr (AABB) and to *Ae. tauschii* (DD). Additionally, tetraploid cultivars Lnd (0.2100±0.0136) and Cap (0.2114±0.0132) (AABB), both showed the second highest mean chiasma frequency in i3 and both were significantly different to Cad, Pg and *Ae. tauschii* (DD). Interestingly, *Ae. speltoides* (BB) (0.1886±0.0149) didn't show any significant difference in the mean chiasma frequency in this i3 localization with any of the material analyzed in this thesis. The lowest chiasma frequencies at i3 localization were observed in hexaploid cultivars Cad (0.0914±0.006) and Pg (0.1352±0.007) (AABBDD), and *Ae. tauschii* (DD) (0.1314±0.0134). Welch's ANOVA (N=50).

4.2.2.5 Proximal (p) chiasmata

The mean of chiasma frequency at proximal regions (p) in all wheat cultivars and species were analyzed using a Kruskal-Wallis test to investigate if any significant differences occur between different wheat cultivars and their wild relatives or not (figures 4.19 and 4.20) and (Tables 4.18 and 4.19 see appendix). Tetraploid cultivar Cap (AABB) showed the highest mean chiasma frequency in p localization (0.1657±0.012) and was significantly different to all hexaploid cultivars analysed (CS, Cad, Pg, Fld), to tetraploid cultival Kr (AABB) and to *T. monococcum* (AA) (Table 4.19). In contrast, tetraploid cultivar Kr (AABB) (0.0628±0.008) showed the lowest mean chiasma frequency in this

localization and it was significantly different to Cap and Lnd (AABB), and to *Ae. speltoides* (BB) and *Ae. tauschii* (DD).

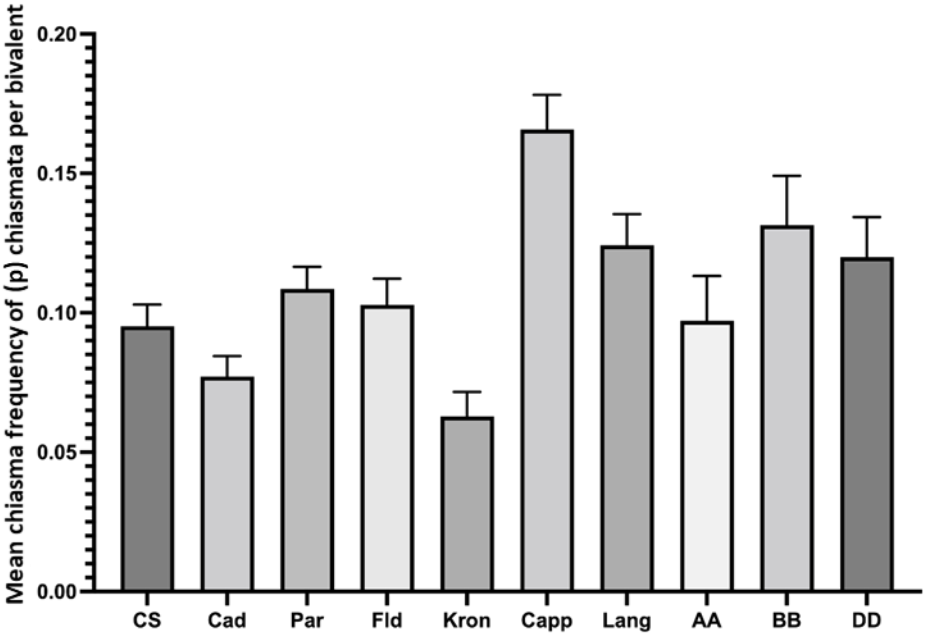

Figure 4.19: Mean chiasma frequency of (p) chiasmata in all wheats.

	CS	Cad	Par	Fld	Kron	Cap	Lang	AA	BB
CS									
Cad	ns								
Par	ns	ns							
Fld	ns	ns	ns						
Kron	ns	ns	**	ns					
Cap	***	****	**	**	****				
Lang	ns	*	ns	ns	**	ns			
AA	ns	ns	ns	ns	ns	*	ns		
BB	ns	ns	ns	ns	*	ns	ns	ns	
DD	ns	ns	ns	****	*	ns	ns	ns	ns

Figure 4.20: Comparison of the mean chiasma frequency of (p) chiasmata in all wheats. Tetraploid cultivar Cap (AABB) showed the highest mean chiasma frequency in p localization (0.1657±0.012) and was significantly different to all hexaploid cultivars analysed (CS, Cad, Pg, Fld), to tetraploid cultival Kr (AABB) and to *T. monococcum* (AA). In contrast, tetraploid cultivar Kr (AABB) (0.0628±0.008) showed the lowest mean chiasma frequency in this localization and it was significantly different to Cap and Lnd (AABB), and to *Ae. speltoides* (BB) and *Ae. tauschii* (DD)**.** Kruskal-Wallis test (N=50).

4.2.3 Chiasma frequency and distribution on specific chromosomes labelled by FISH

4.2.3.1 The use of 45S and 5S rDNA probes to identify wheat chromosomes at different ploidy level

In situ hybridization is a technique that uses specific DNA sequences (probes) to localize where they are distributed along the chromosomes of an organism through a DNA hybridization process (Gall and Pardue, 1969). Early techniques involved the use of radioactive labelling but in 1982 the discovery of non-radioactive labelling allowed to have a broader utilization of this technique (Schwarzacher, 2003).

Fluorescence *in situ* hybridization (FISH) is widely used to identify and distinguish different chromosomes in different plant species such as Arabidopsis, brassicas and wheat. In hexaploid wheat, the first FISH analysis that identified all wheat chromosome was done by (Pedersen and Langridge, 1997) and they used three DNA labelling probes pAs1 (*Aegilops tauschii*), GAA satellite sequence (*Hordeum vulgare*) and pSc119.2 (Rye). Additionally, despite identification of all the chromosomes, FISH was also used in wheat to identify chromosome rearrangements including translocations in hybrids(Guo et al., 2019). Moreover, there are several FISH oligonucleotides probes used in wheat such as pAsl, pSc119.2, pTa713, pTa535, 5s rDNA and 45s rDNA (Tang et al., 2014, Mukai et al., 1993). For this thesis we have used 45s and 5s rDNA (ribosomal DNA) as probes to identify different chromosomes in all wheat cultivars and species analyzed. The 45S rDNA sequence contains the 5.8S, 18S and 26S tandem repeats of rDNA genes (Gerlach and Bedbrook, 1979, Heslop-Harrison, 2000). The 5S rDNA consists of 410 bp of highly conserved tandem repeats in wheat (Gerlach and Dyer, 1980). In both cases, approximately a thousand copies are localized in the genome of eukaryotes with different distribution along the different chromosomes (Heslop-Harrison, 2000, Su *et al*., 2020). Moreover, 45S and 5S rDNA have been used to label different chromosomes in different plant species such as Arabidopsis, brassicas and cereals. For instance, in *Arabidopsis* these two probes were able to identify all the five bivalents during metaphase I (Sanchez-Moran *et al*., 2002). In hexaploid wheat these two probes have allowed us to identify up to six bivalents involving chromosomes 5A, 1B, 5B, 6B, 1D and 5D (Zhang *et al*., 2013). Thus, in tetraploid wheat these two probes allow us to distinguish four bivalents involving chromosomes 5A, 1B, 5B and 6B (Kubaláková *et al.*, 2005).

In this thesis, 45S and 5S rDNA probes have been used to identify these bivalents at metaphase I in hexaploid, tetraploid and diploid species (figure 4.21 and 4.22). This has allowed us to achieve not only the identification of the specific bivalents but also to quantify the mean chiasma frequency and

their localization on the specific chromosomes and compared to the different ploidy levels present in the material analyzed.

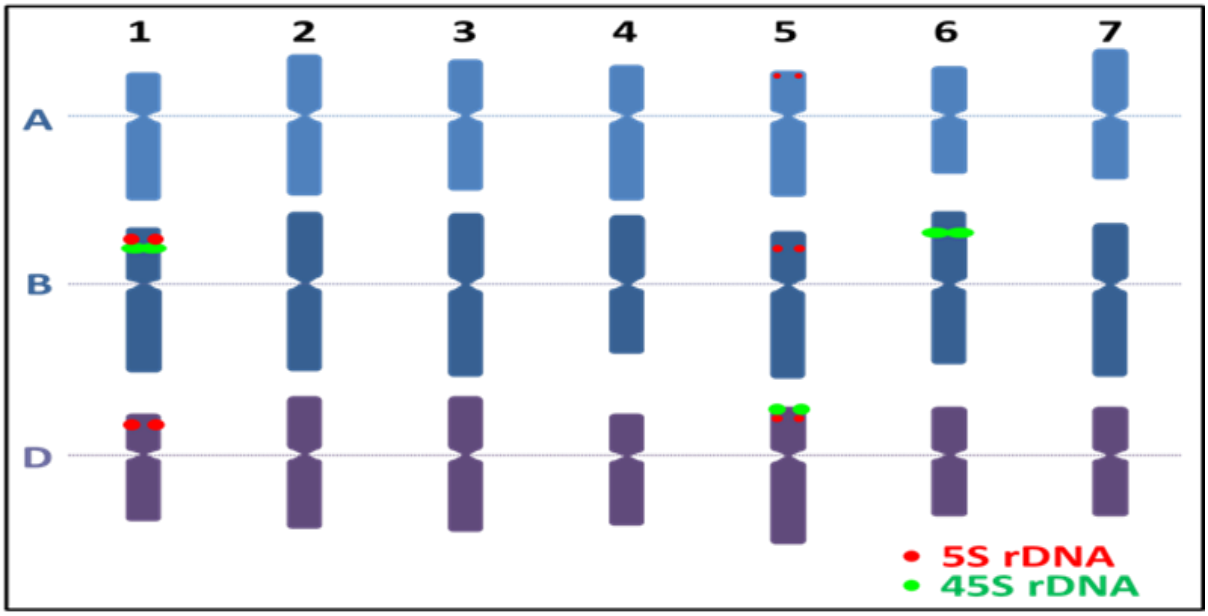

Figure 4.21: Diagram showing a haploid karyotype in hexaploid wheat with the localization of the 45S and 5S rDNA signals annotated. Chromosome 5A labelled by 5S rDNA only, chromosome 1B labelled by both 45S and 5S rDNA, chromosome 5B labelled by 5S rDNA only, chromosome 6B labelled by 45S rDNA only, chromosome 1D labelled by 5S rDNA only and chromosome 5D labelled by both 45S and 5S rDNA.

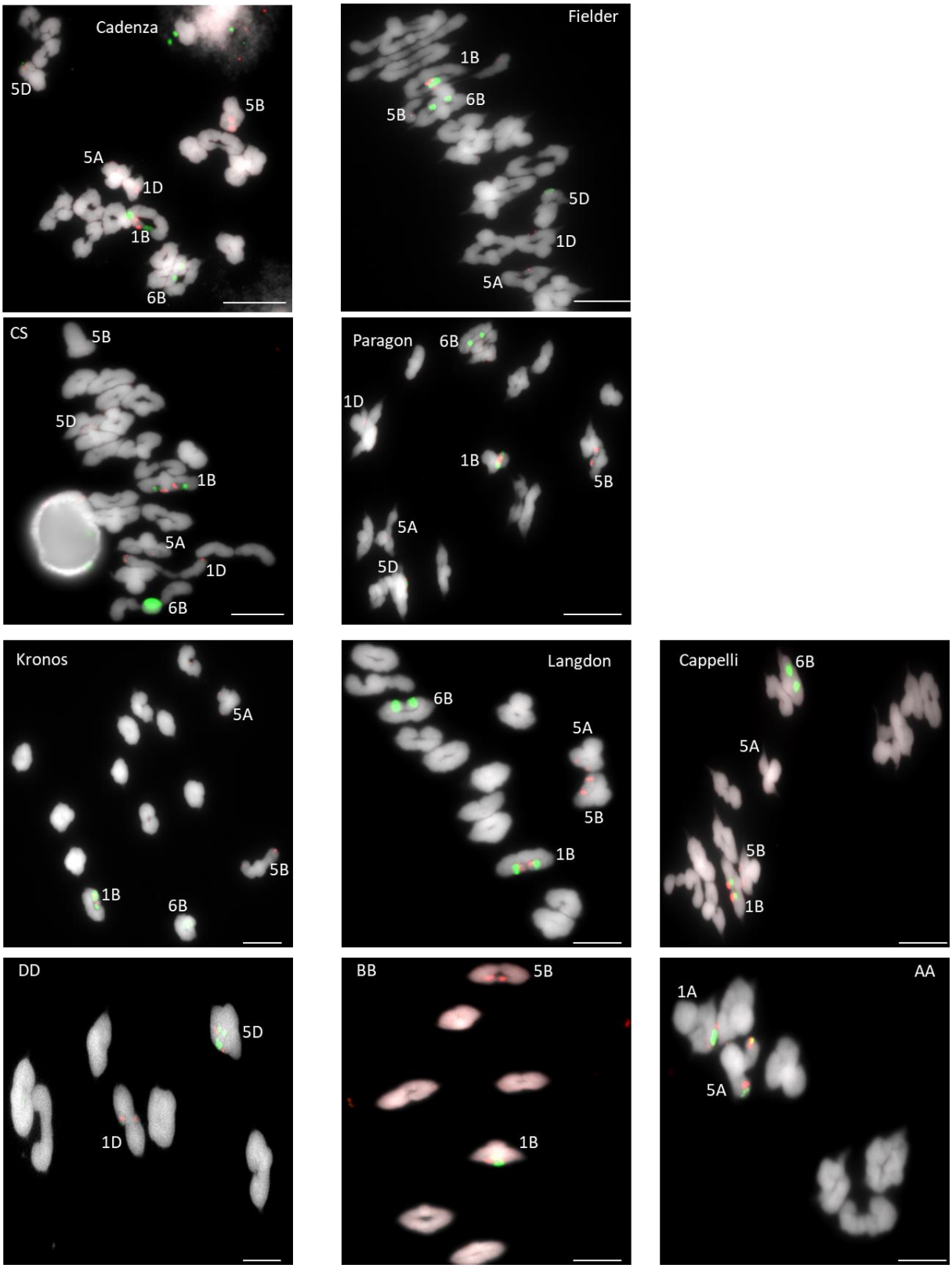

Figure 4.22: FISH o analysis using 45S (green) and 5S (red) rDNA as probes on metaphase I mother pollen cells of hexaploid, tetraploid and diploid wheat species. Identification of chromosomes 1A, 5A, 1B, 5B, 6B, 1D and 5D is indicated. Scale bar = 10 µm.

The FISH analysis showed that it could be possible to identify up to six bivalents in hexaploid wheat cultivars: 5A, 1B, 5B, 6B, 1D and 5D (figure 4.22). In tetraploid cultivars four bivalents: 5A, 1B, 5B and 6B identified. In the diploid ancestral relatives, two bivalents in each: 1A and 5A in *T. monococcum* (AA), 1B and 5B in *Ae. speltoides* (BB), 1D and 5D in *Ae. tauschii* (DD) identified. The mean chiasma frequency was analyzed for each single chromosome pair identified by the 45S and 5S rDNA FISH analysis and comparisons were made among cultivars of the same species and among the different species (with different ploidy level).

4.2.3.2 Chiasma frequency and distribution on chromosome 5A

The mean chiasma frequency on chromosome 5A was carried out in all wheat cultivars and their wild relative *T. monococcum* (AA) (Table 4.20 see appendix). A Kruskal-Wallis test was applied to investigate if the differences observed were statistically significant between them. Interestingly, no significant differences were observed among most of the different materials analyzed (figure 4.23 and 4.24). Only hexaploid cultivar Pg (AABBDD) showed low significant differences on the mean chiasma frequency on chromosome 5A compared to diploid *T. monococcum* (AA) and tetraploid cultivar Kr (AABB) with p values of ($p=0.03$) and ($p=0.04$) respectively.

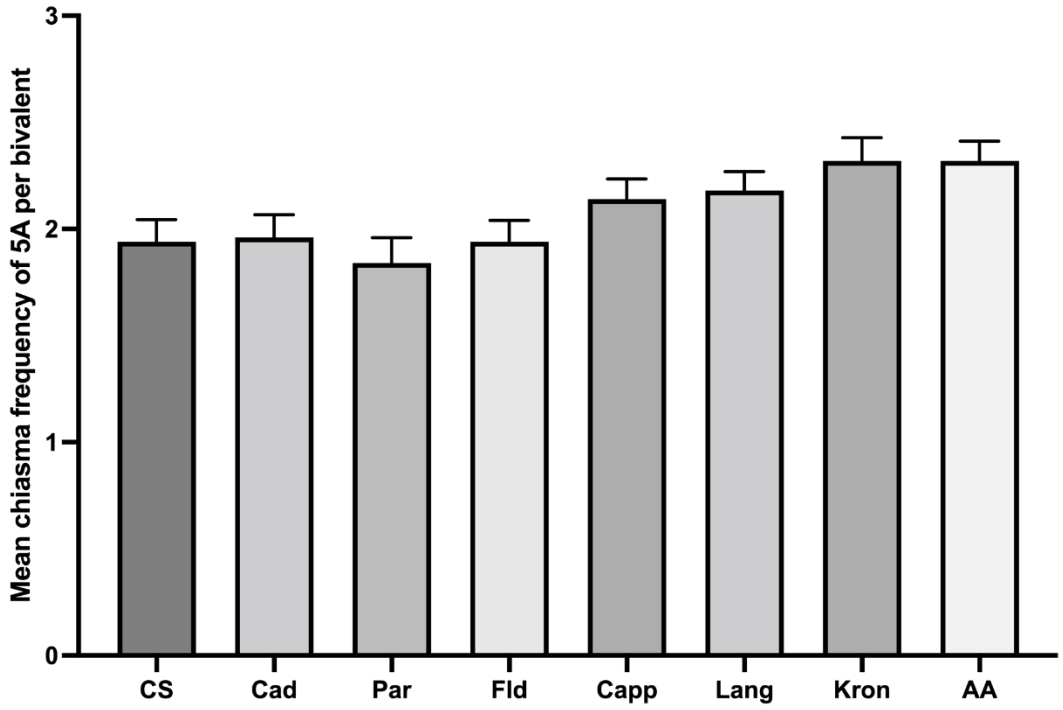

Figure 4.23: Mean chiasma frequency on chromosome 5A in hexaploid, tetraploid and diploid wheats.

	CS	Cad	Par	Fld	Kron	Capp	Lang	AA
CS								
Cad	NS							
Par	NS	NS						
Fld	NS	NS	NS					
Kron	NS	NS	NS	NS				
Capp	NS	NS	NS	NS	NS			
Lang	NS	NS	NS	NS	NS	NS		
AA	NS	NS	*	NS	*	NS	NS	

Figure 4.24: Comparison of the mean chiasma frequency on chromosome 5A in hexaploid, tetraploid and diploid wheats. Hexaploid cultivar Pg (AABBDD) showed low significant differences on the mean chiasma frequency on chromosome 5A compared to diploid *T. monococcum* (AA) and tetraploid cultivar Kr (AABB) with p values of (p=0.03) and (p=0.04) respectively. Kruskal-Wallis test (N=50). (NS p>0.05/ *0.05≥ p > 0.005/ **0.005> p > 0.0005/ ***p < 0.0005) (N=50).

Interestingly, more significant differences were observed when dividing these mean chiasma frequencies on chromosome 5A by their bivalent configurations (rod *vs* ring). The mean chiasma frequency of rod bivalents on chromosome 5A (figure 4.25 and 4.26) and (Table 4.21 see appendix) showed that more significant differences were observed. For instance, hexaploid wheat cultivar Fld showed significant differences on the mean chiasma frequency on rod 5A bivalents with the tetraploid wheat cultivars Lnd (p value = 0.0006) and Cap (p value = 0.0006). Additionally, Fld also showed significant differences with diploid *T. monococcum* (p value = 0.006). Furthermore, significant differences were observed on the mean chiasma frequency on rod 5A bivalents between hexaploid cultivar CS and the two tetraploid cultivars Lnd (p value = 0.009) and Cap (p value = 0.009).

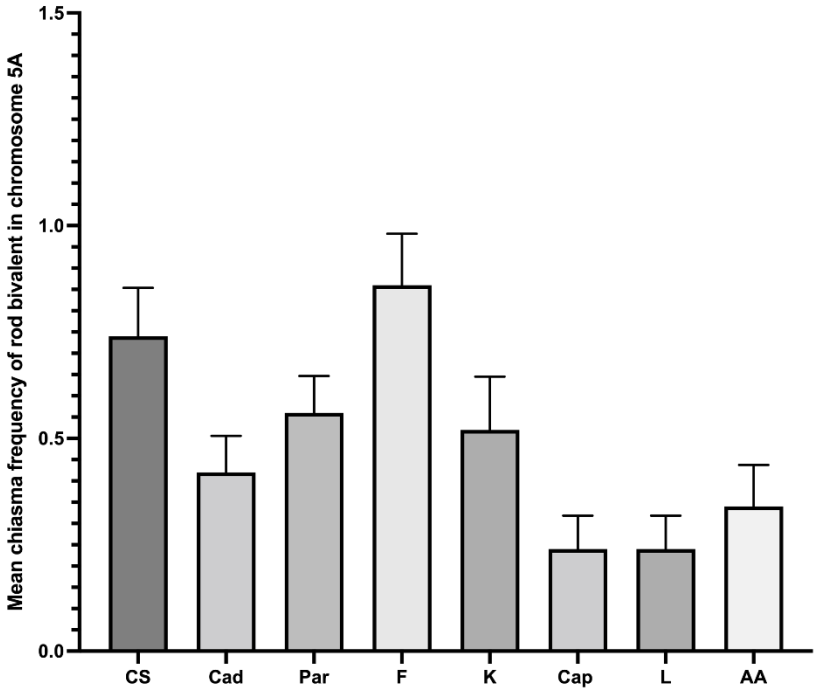

Figure 4.25: Mean chiasma frequency on rod 5A bivalents.

	CS	Cad	Par	Fld	Kron	Capp	Lang	AA
CS								
Cad	NS							
Par	NS	NS						
Fld	NS	NS	NS					
Kron	NS	NS	NS	NS				
Capp	*	NS	NS	**	NS			
Lang	*	NS	NS	**	NS	NS		
AA	NS	NS	NS	*	NS	NS	NS	

Figure 4.26: Comparison of the mean chiasma frequency on rod 5A bivalents. Hexaploid wheat cultivar Fld showed significant differences on the mean chiasma frequency on rod 5A bivalents with the tetraploid wheat cultivars Lnd (p value = 0.0006) and Cap (p value = 0.0006). Fld also showed significant differences with diploid *T. monococcum* (p value = 0.006). Significant differences were observed on the mean chiasma frequency on rod 5A bivalents between hexaploid cultivar CS and the two tetraploid cultivars Lnd (p value = 0.009) and Cap (p value = 0.009). Kruskal-Wallis test (N=50). (NS p>0.05/ *0.05≥ p > 0.005/ **0.005> p > 0.0005/ ***p < 0.0005) (N=50).

The mean chiasma frequency on 5A ring bivalents showed that hexaploid cultivar Fld was significantly different to tetraploid cultivars Lnd (p value = 0.01) and Cap (p value = 0.04). Furthermore, Fld also showed significant differences to diploid AA (p value = 0.01) (figure 4.27 and 4.28) and (Table 4.22 see appendix).

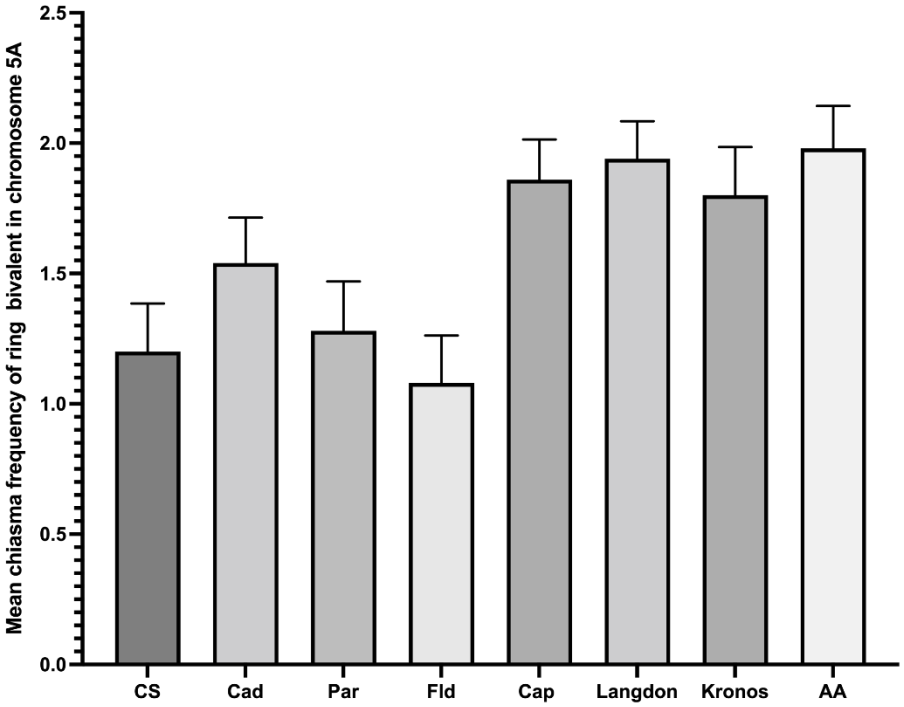

Figure 4.27: Mean chiasma frequency of ring bivalent in chromosome 5A.

	CS	Cad	Par	Fld	Kron	Capp	Lang	AA
CS								
Cad	NS							
Par	NS	NS						
Fld	NS	NS	NS					
Kron	NS	NS	NS	NS				
Capp	NS	NS	NS	*	NS			
Lang	NS	NS	NS	*	NS	NS		
AA	NS	NS	NS	*	NS	NS	NS	

Figure 4.28: Comparison of the mean chiasma frequency of ring bivalent in chromosome 5A. Hexaploid cultivar Fld was significantly different to tetraploid cultivars Lnd (p value = 0.01) and Cap (p value = 0.04). Furthermore, Fld also showed significant differences to diploid AA (p value = 0.01). Kruskal-Wallis test (N=50). (NS p>0.05/ *0.05≥ p > 0.005/ **0.005> p > 0.0005/ ***p < 0.0005) (N=50).

The mean chiasma frequency along different regions (d, i^1, i^2, i^3, p) on chromosome 5A was analyzed in different wheat cultivars and species.

Distal chiasmata at chromosome 5A are the most common among the different species studied. Interestingly, the frequency of distal chiasmata in diploid and tetraploid cultivars were very similar (with means between 1.2 and 1.3). Nevertheless, this mean frequency appeared decreased in hexaploid cultivars (with means between 0.8 and 1). Kruskal-Wallis tests were conducted to analyze if this decrease in hexaploid wheats were significantly different to tetra and diploid wheats, but it showed that distal mean chiasma frequencies in A5 were not significant between diploid, tetraploid and hexaploid wheats (figure 4.29 and 4.30).

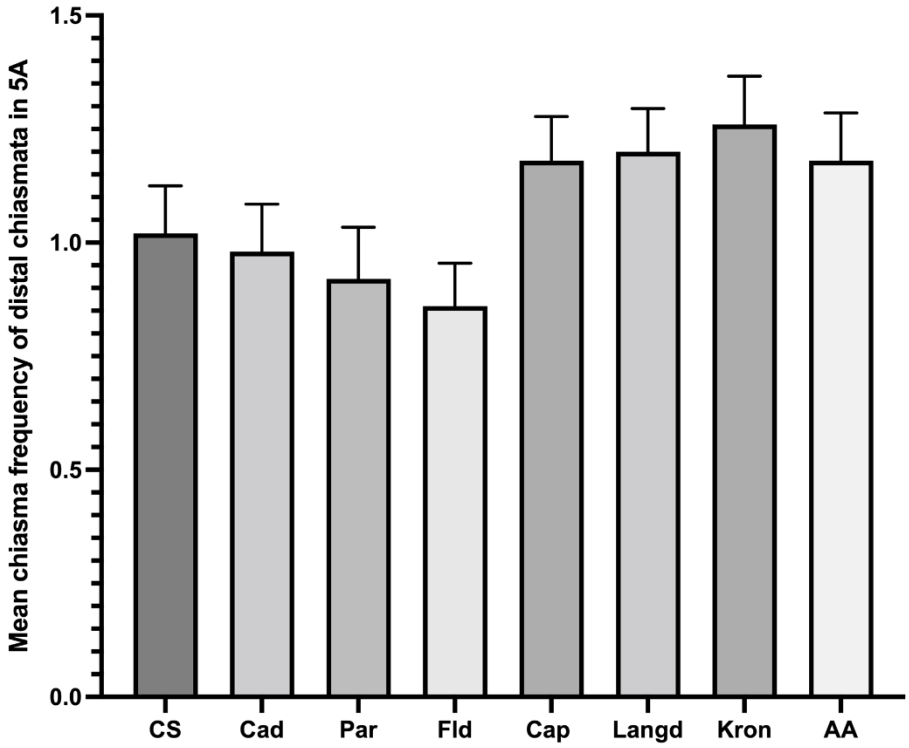

Figure 4.29: Mean chiasma frequency at distal regions on chromosome 5A.

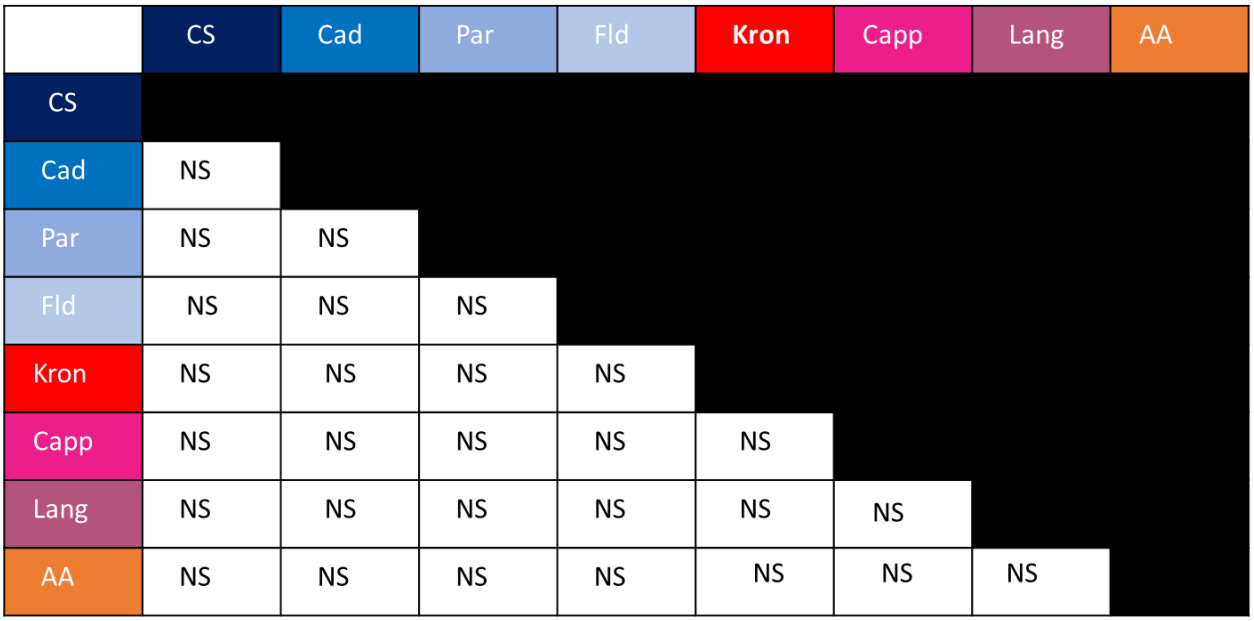

Figure 4.30: Comparison of the mean chiasma frequency at distal regions on chromosome 5A. No significant differences observe between polyploid wheat and their wild relative *T. monococcum*. Kruskal-Wallis test (N=50). (NS p>0.05/ *0.05≥ p > 0.005/ **0.005> p > 0.0005/ ***p < 0.0005) (N=50).

Proximal chiasmata on chromosome 5A appeared to be higher in the tetraploid cultivar Kr (mean of 0.42±0.076) compared to the rest of wheats (with means from 0.1±0.043 to 0.36±0.068). Kr proximal chiasma frequency was significantly different to tetraploid cultivar Cap (p value = 0.01), Fielder (p value = 0.004), Paragon (p value= 0.01) and Cadenza (p value = 0.01) (figure 4.31 and 4.32). Additionally, AA *T. monococcum* show the second highest mean chiasma frequency of proximal chiasmata in chromosome 5A (0.36±0.068). As a result, AA appear to be significantly difference compare to Fielder (p value = 0.03). However, no significant differences were observed between AA and the rest of hexaploid and tetraploid wheat cultivars.

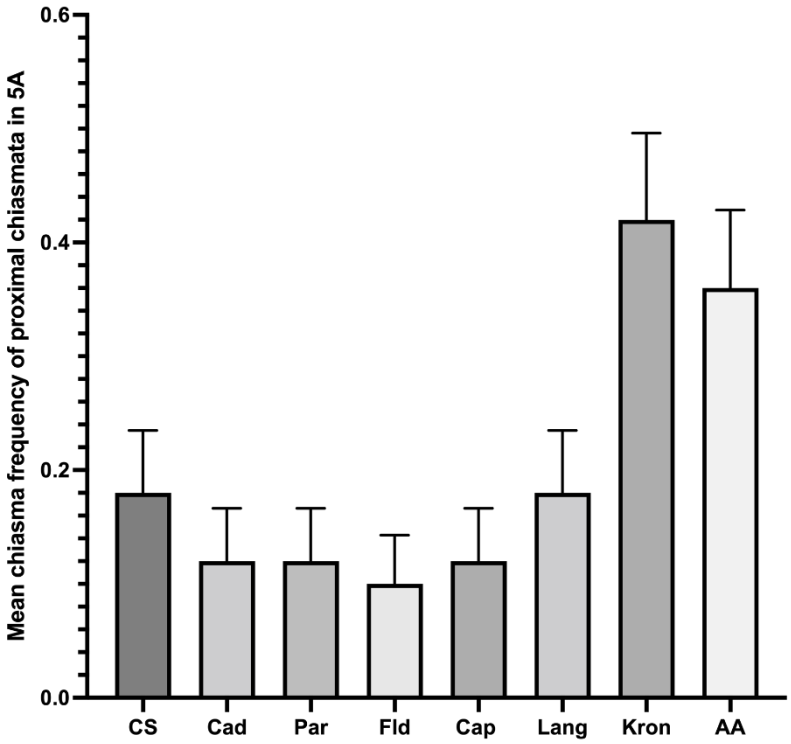

Figure 4.31: Mean chiasma frequency on proximal regions on chromosome 5A.

	CS	Cad	Par	Fld	Kron	Capp	Lang	AA
CS								
Cad	NS							
Par	NS	NS						
Fld	NS	NS	NS					
Kron	NS	*	*	**				
Capp	NS	NS	NS	NS	*			
Lang	NS	NS	NS	NS	NS	NS		
AA	NS	NS	NS	*	NS	NS	NS	

Figure 4.32: Comparison of the mean chiasma frequency on proximal regions on chromosome 5A. Proximal chiasmata on chromosome 5A appeared to be higher in the tetraploid cultivar Kr (mean of 0.42±0.076) compared to the rest of wheats (with means from 0.1±0.043 to 0.36±0.068). Kr proximal chiasma frequency was significantly different to tetraploid cultivar Cap (p value = 0.01), Fielder (p value = 0.004), Paragon (p value= 0.01) and Cadenza (p value = 0.01) (figure 4.27). Also, AA *T. monococcum* show the second highest mean chiasma frequency of proximal chiasmata in chromosome 5A (0.36±0.068). Thus, AA *T. monococcum* appear to be significantly difference compare to Fielder (p

value = 0.03). Finally, no significant differences were observed between AA and the rest of hexaploid and tetraploid wheat cultivars. Kruskal-Wallis test (N=50). (NS p>0.05/ *0.05> p > 0.005/ **0.005> p > 0.0005/ ***p < 0.0005) (N=50).

4.2.3.3 Chiasma frequency and distribution on chromosome 1B

The mean chiasma frequency on chromosome 1B was calculated in all wheat cultivars and their wild relative *Ae. speltoides* (BB) (Table 4.23 see appendix). Welch's ANOVAs were applied to investigate if the differences observed were statistically significant between them (figure 4.33 and 4.34). Interestingly, chiasma frequencies on 1B were significantly different between *Ae. speltoides* (BB) and tetraploid cultivars Kr (p value = 0.04)) and Lnd (p value = 0.001), as well as with hexaploid cultivars CS (p value = 0.003)), Cad (p value = 0.0001)) and Fld (p value = 0.03)).

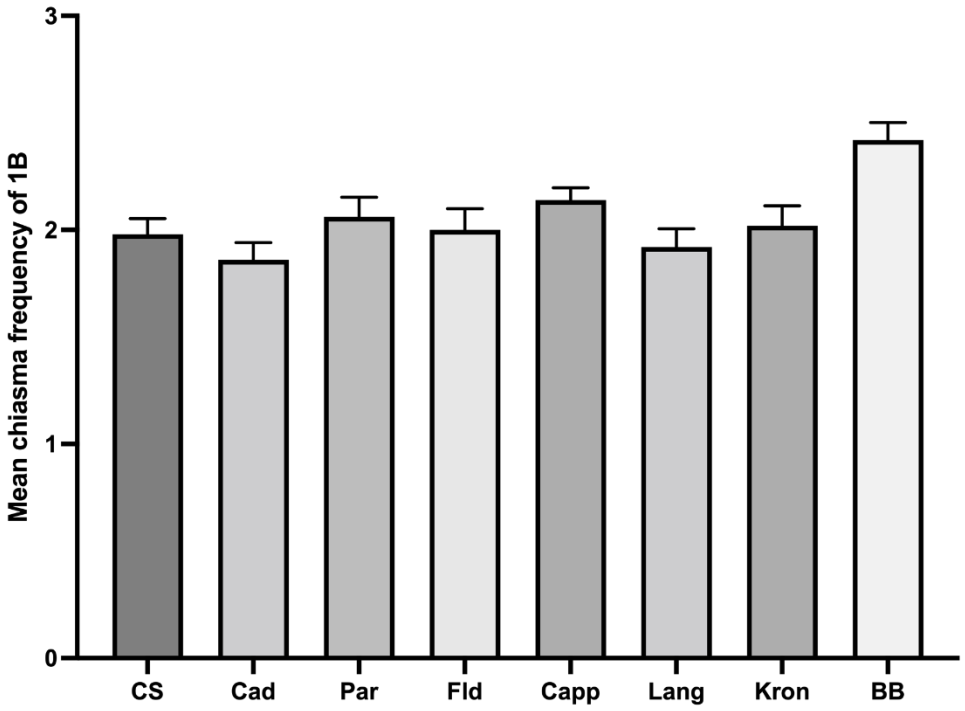

Figure 4.33: Mean chiasma frequency on chromosome 1B in all wheats.

	CS	Cad	Par	Fld	Kron	Capp	Lang	BB
CS								
Cad	NS							
Par	NS	NS						
Fld	NS	NS	NS					
Kron	NS	NS	NS	NS				
Capp	NS	NS	NS	NS	NS			
Lang	NS	NS	NS	NS	NS	NS		
BB	**	***	NS	*	*	NS	**	

Figure 4.34: Comparison of the mean chiasma frequency on chromosome 1B. Mean chiasma frequencies on 1B were significantly different between *Ae. speltoides* (BB) and tetraploid cultivars Kr (p value = 0.04)) and Lnd (p value = 0.001), as well as with hexaploid cultivars CS (p value = 0.003)), Cad (p value = 0.0001)) and Fld (p value = 0.03)). Welch's ANOVA (N=50). (NS p>0.05/ *0.05≥ p > 0.005/ **0.005> p > 0.0005/ ***p < 0.0005) (N=50).

Interestingly, differences were observed when dividing these mean chiasma frequencies on chromosome 1B by their bivalent configurations (rod *vs* ring) (Tables 4.25 and 4.25 see appendix). The mean chiasma frequency of rod bivalents on chromosome 1B (figure 4.35 and 4.36) showed that Fld had the highest mean (0.36±0.0845) whereas Cap had the lowest (0.02±0.02). Tetraploid cultivar Cap (AABB) mean chiasma frequency on chromosome 1B were statistically significant to tetraploid Lnd (p value = 0.02)), and hexaploid cultivars Cad (p value = 0.02) and Fld (p value = 0.007).

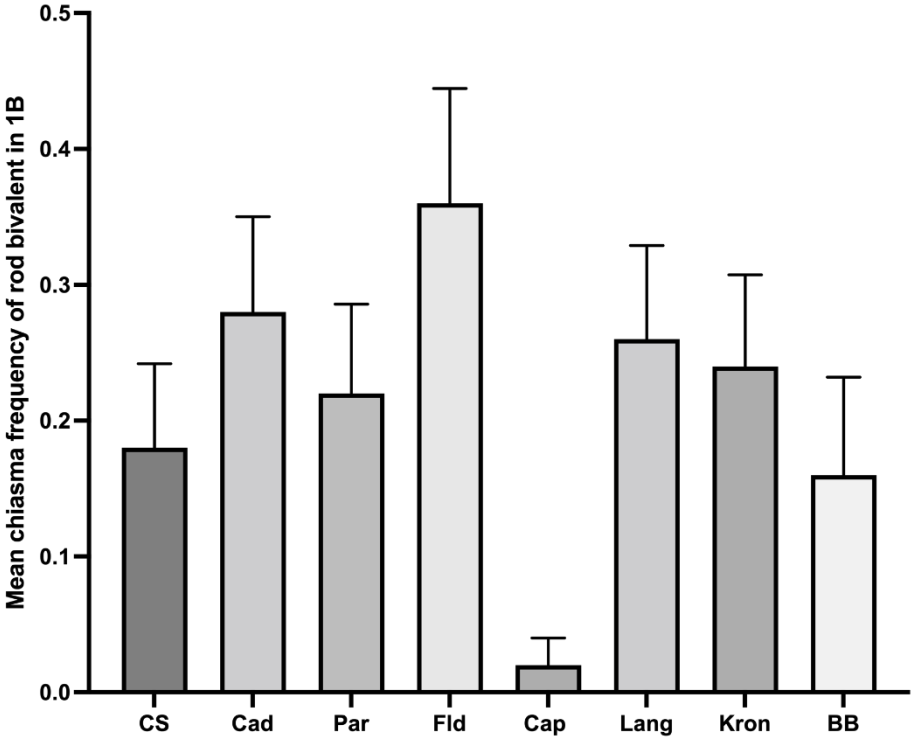

Figure 4.35: Mean chiasma frequency on 1B rod bivalents.

	CS	Cad	Par	Fld	Kron	Capp	Lang	BB
CS								
Cad	NS							
Par	NS	NS						
Fld	NS	NS	NS					
Kron	NS	NS	NS	NS				
Capp	NS	*	NS	**	NS			
Lang	NS	NS	NS	NS	NS	*		
BB	NS	NS	NS	NS	NS	NS	NS	

Figure 4.36: Comparison of the mean chiasma frequency on 1B rod bivalents. Tetraploid cultivar Cap (AABB) mean chiasma frequency on chromosome 1B were statistically significant to tetraploid Lnd (p value = 0.02)), and hexaploid cultivars Cad (p value = 0.02) and Fld (p value = 0.007). Kruskal-Wallis test (N=50). (NS p>0.05/ *0.05≥ p > 0.005/ **0.005> p > 0.0005/ ***p < 0.0005) (N=50).

The mean chiasma frequency of ring bivalents in chromosome 1B showed that tetraploid cultivar Cap (AABB) and *Ae. speltoides* (BB) showed the highest means (2.12±0.0678 and 2.26±0.127) compare to the other materials. The chiasma frequency of *Ae. speltoides* (BB) on chromosome 1B ring configurations showed significant differences to tetraploid cultivar Lnd (p value = 0.007), and hexaploid cultivars Cad (p value = 0.001) and CS (p value = 0.03) (figure 4.37 and 4.38).

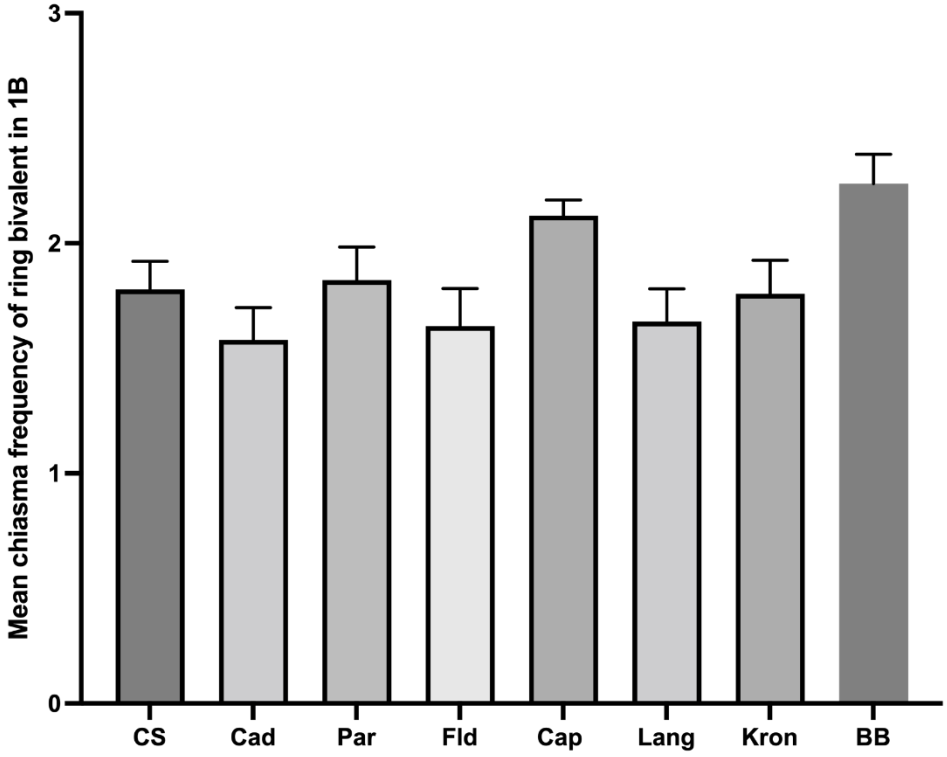

Figure 3.37: Mean chiasma frequency on 1B ring bivalents.

	CS	Cad	Par	Fld	Kron	Capp	Lang	BB
CS								
Cad	NS							
Par	NS	NS						
Fld	NS	NS	NS					
Kron	NS	NS	NS	NS				
Capp	NS	NS	NS	NS	NS			
Lang	NS	NS	NS	NS	NS	NS		
BB	*	***	NS	*	NS	NS	**	

Figure 4.38: **Comparison of the mean chiasma frequency on 1B ring bivalents.** The chiasma frequency of *Ae. speltoides* (BB) on chromosome 1B ring configurations showed significant differences to tetraploid cultivar Lnd (p value = 0.007), and hexaploid cultivars Cad (p value = 0.001) and CS (p value = 0.03). Kruskal-Wallis test (N=50). (NS $p>0.05$/ *$0.05\geq p > 0.005$/ **$0.005> p > 0.0005$/ ***$p < 0.0005$) (N=50).

The mean chiasma frequency along different regions (d, i^1, i^2, i^3, p) on chromosome 1B was analyzed in different wheat cultivars and species. The mean chiasma frequency at different localizations in chromosome 1B were determined. The main purpose of this step was to identify if the mean chiasma at these different locations were different in diploid, tetraploid and hexaploid cultivars.

Distal chiasmata at chromosome 1B are the most common among the different species studied (figure 4.39). Interestingly, the frequency of distal chiasmata in diploid *Ae. speltoides* (BB) appeared to be lower than in the rest of polyploid wheats (0.84 ± 0.104) (Table 4.26 see appendix). Nevertheless, Kruskal-Wallis test showed no significant differences between diploid and polyploid wheats (figure 4.40).

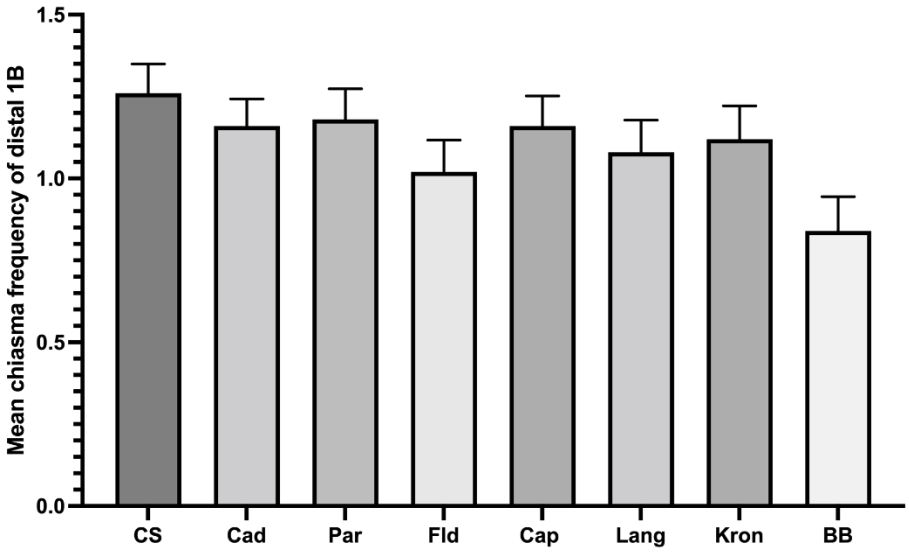

Figure 4.39: Mean chiasma frequency of distal chiasmata in chromosome 1B.

	CS	Cad	Par	Fld	Kron	Capp	Lang	BB
CS								
Cad	NS							
Par	NS	NS						
Fld	NS	NS	NS					
Kron	NS	NS	NS	NS				
Capp	NS	NS	NS	NS	NS			
Lang	NS	NS	NS	NS	NS	NS		
BB	NS	NS	NS	NS	NS	NS	NS	

Figure 4.40: Comparison of the mean chiasma frequency of distal chiasmata in chromosome 1B. No significant differences observe in distal chiasmata in this chromosome. Kruskal-Wallis test (N=50). (NS $p>0.05$/ *$0.05\geq p > 0.005$/ **$0.005> p > 0.0005$/ ***$p < 0.0005$) (N=50).

Interstitial chiasmata at region 2 (i^2) on chromosome 1B seem to be higher in diploid *Ae. speltoides* (BB) (0.44 ± 0.081) than in tetraploid and hexaploid wheats (Table 4.27 see appendix). Mean i^2 chiasma frequency was significantly different between *Ae. speltoides* (BB) and two tetraploid

cultivars Kr (p value = 0.007) and Lnd (p value = 0.03) (figure 4.41 and 4.42). However, no significant differences were observed among the rest of wheat cultivars.

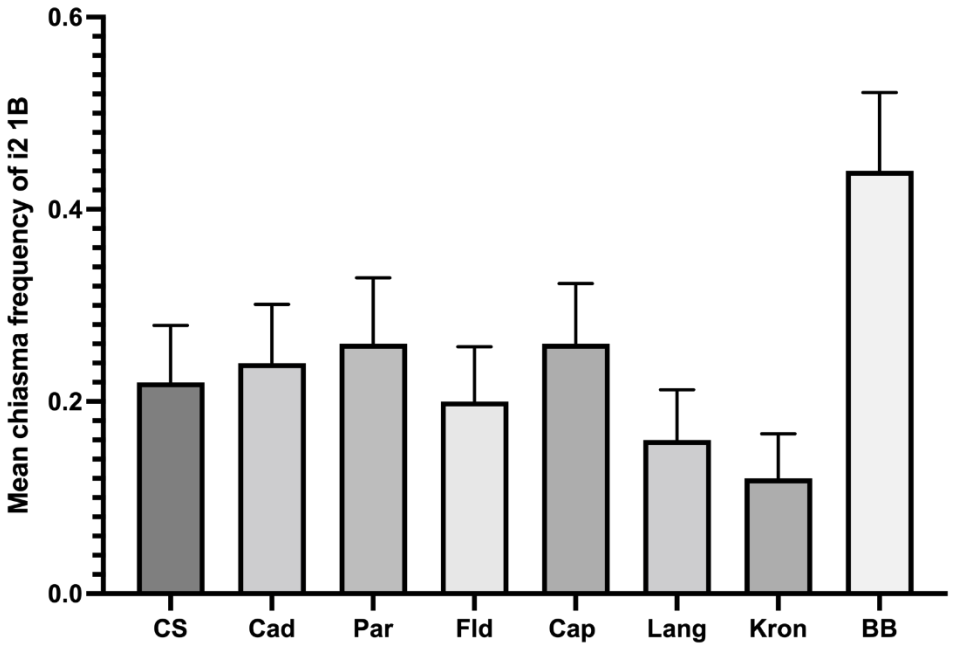

Figure 4.41: Mean chiasma frequency at i^2 in chromosome 1B.

	CS	Cad	Par	Fld	Kron	Capp	Lang	BB
CS								
Cad	NS							
Par	NS	NS						
Fld	NS	NS	NS					
Kron	NS	NS	NS	NS				
Capp	NS	NS	NS	NS	NS			
Lang	NS	NS	NS	NS	NS	NS		
BB	NS	NS	NS	NS	**	NS	*	

Figure 4.42: Comparison of the mean chiasma frequency at i^2 in chromosome 1B. Mean chiasma frequency was significantly different between *Ae. speltoides* (BB) and two tetraploid cultivars Kr (p value = 0.007) and Lnd (p value = 0.03). No significant differences were observed among the rest of wheat cultivars. Kruskal-Wallis test (N=50). (NS p>0.05/ *0.05≥ p > 0.005/ **0.005> p > 0.0005/ ***p < 0.0005) (N=50).

Interstitial chiasmata at region 3 (i^3) of chromosome 1B appeared to be higher in diploid *Ae. speltoides* (BB) (0.38±0.069) than in tetraploid and hexaploid wheats (figure 4.43) (Table 4.28 see appendix). Kruskal-Wallis test showed that *Ae. speltoides* (BB) chiasma frequency at i^3 localization had significant differences to tetraploid cultivars Kr (p value = 0.001), Cap (p value <0.0001) and Lnd (p value <0.0001), as wells as to hexaploid cultivars CS (p value <0.0001), Cad (p value <0.0001) and Pg (p value = 0.03) (figure 4.44).

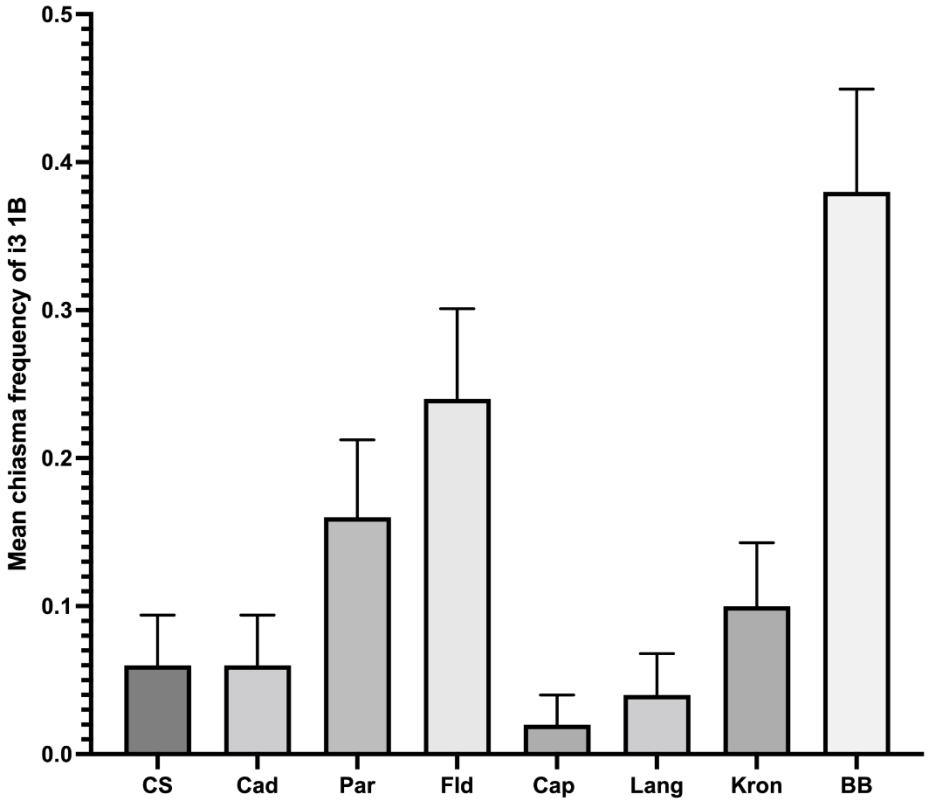

Figure 4.43: Mean chiasma frequency at i^3 in chromosome 1B.

	CS	Cad	Par	Fld	Kron	Capp	Lang	BB
CS								
Cad	NS							
Par	NS	NS						
Fld	NS	NS	NS					
Kron	NS	NS	NS	NS				
Capp	NS	NS	NS	*	NS			
Lang	NS	NS	NS	NS	NS	NS		
BB	****	****	*	NS	**	****	****	

Figure 4.44: Comparison of the mean chiasma frequency at i^3 in chromosome 1B. *Ae. speltoides* (BB) chiasma frequency at i3 localization had significant differences to tetraploid cultivars Kr (p value = 0.001), Cap (p value <0.0001) and Lnd (p value <0.0001), as wells as to hexaploid cultivars CS (p value <0.0001), Cad (p value <0.0001) and Pg (p value = 0.03). Kruskal-Wallis test (N=50). (NS p>0.05/ *0.05≥ p > 0.005/ **0.005> p > 0.0005/ ***p < 0.0005) (N=50).

4.2.3.4 Chiasma frequency and distribution on chromosome 5B

The mean chiasma frequency on chromosome 5B was carried out in all wheat cultivars and their wild relative *Ae. speltoides* (BB) (figure 3.45) (Table 4.29 see appendix). Kruskal-Wallis tests were applied to investigate if the differences observed were statistically significant (figure 4.46). Interestingly, mean chiasma frequencies on 5B were higher in hexaploid cultivar CS (AABBDD) (2.46±0.091) and tetraploid cultivar Cap (AABB) (2.38±0.089). Hexaploid cultivar CS (AABBDD) mean chiasma frequency in 5B showed significant differences to hexaploid cultivar Fld (p value = 0.01), tetraploid cultivar Kr (p value = 0.0003), and diploid *Ae. speltoides* (p value = 0.001). Tetraploid cultivar Cap (AABB) mean chiasma frequency in 5B showed significant differences to hexaploid cultivar Fld (p value = 0.03), and tetraploid cultivar Kr (p value = 0.001), and diploid *Ae. speltoides* (p value = 0.02).

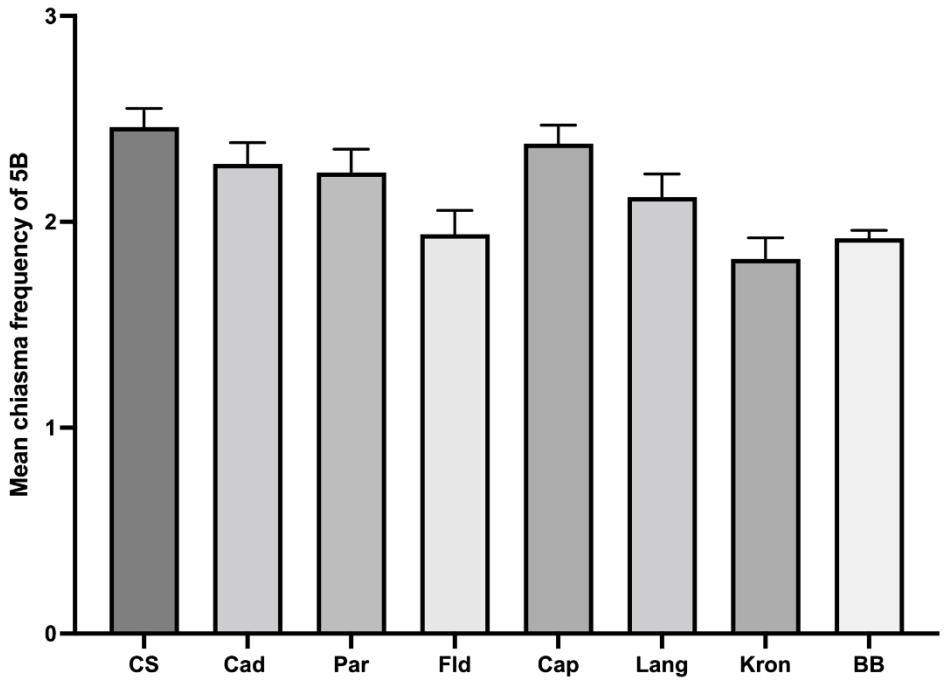

Figure 4.45: Mean chiasma frequency on chromosome 5B in all wheats.

	CS	Cad	Par	Fld	Kron	Capp	Lang	BB
CS								
Cad	NS							
Par	NS	NS						
Fld	**	NS	NS					
Kron	***	*	NS	NS				
Capp	NS	NS	NS	*	**			
Lang	NS	NS	NS	NS	NS	NS		
BB	**	NS	NS	NS	NS	*	NS	

Figure 4.46: Comparison of the mean chiasma frequency on chromosome 5B. Hexaploid cultivar CS (AABBDD) mean chiasma frequency in 5B showed significant differences to hexaploid cultivar Fld (p value = 0.01), tetraploid cultivar Kr (p value = 0.0003), and diploid *Ae. speltoides* (p value = 0.001). Tetraploid cultivar Cap (AABB) mean chiasma frequency in 5B showed significant differences to hexaploid cultivar Fld (p value = 0.03), and tetraploid cultivar Kr (p value = 0.001), and diploid *Ae. speltoides* (p value = 0.02). Kruskal-Wallis test (N=50). (NS p>0.05/ *0.05≥ p > 0.005/ **0.005> p > 0.0005/ ***p < 0.0005) (N=50).

Interestingly, differences could be observed when dividing these mean chiasma frequencies on chromosome 5B by their bivalent configurations (rod *vs* ring) (Tables 4.30 and 4.31 see appendix). The mean chiasma frequency of rod bivalents on chromosome 5B showed that Fld had the highest mean (0.92±0.114) whereas Cap had the lowest (0.16±0.05) (figure 4.47). To investigate whether these differences were significant or not, Kruskal-Wallis tests were conducted among all the different materials. Hexaploid cultivar Fld (AABBDD) was significantly different to all other hexaploid cultivars Pg (p value = 0.002), Cad (p value = 0.0001) and CS (p value = 0.004), and to all tetraploid cultivars Kr (p value = 0.02), Cap (p value <0.0001) and Lnd (p value 0.003), and to *Ae. speltoides* (p value <0.0001) (figure 4.48).

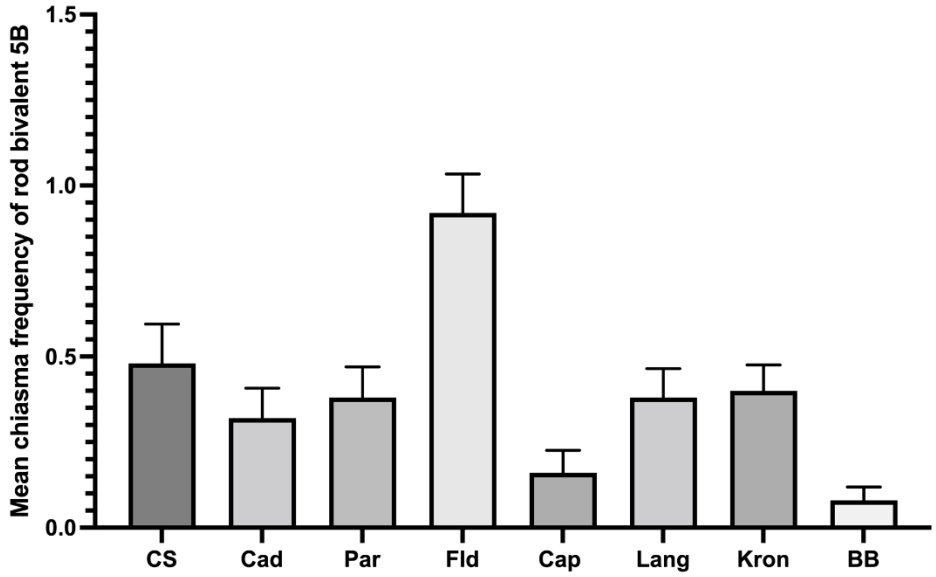

Figure 4.47: Mean chiasma frequency in 5B rod bivalents.

	CS	Cad	Par	Fld	Kron	Capp	Lang	BB
CS								
Cad	NS							
Par	NS	NS						
Fld	**	***	**					
Kron	NS	NS	NS	*				
Capp	NS	NS	NS	****	NS			
Lang	NS	NS	NS	**	NS	NS		
BB	NS	NS	NS	****	NS	NS	NS	

Figure 4.48: Comparison of the mean chiasma frequency in 5B rod bivalents. Hexaploid cultivar Fld (AABBDD) was significantly different to all other hexaploid cultivars Pg (p value = 0.002), Cad (p value = 0.0001) and CS (p value = 0.004), and to all tetraploid cultivars Kr (p value = 0.02), Cap (p value <0.0001) and Lnd (p value 0.003), and to *Ae. speltoides* (p value <0.0001). Kruskal-Wallis test (N=50). (NS p>0.05/ *0.05≥ p > 0.005/ **0.005> p > 0.0005/ ***p < 0.0005) (N=50).

Interestingly, the mean chiasma frequency in 5B ring bivalents showed that Fld had the lowest mean (1.02±0.196) of all materials. Tetraploid cultivar Cap showed the highest mean of chiasma frequency in 5B ring bivalents (2.22±0.135) (figure 4.49). Kruskal-Wallis showed that the differences between hexaploid Fld and tetraploid Cap were significant (p value = 0.0009). In tetraploid cultivars, Cap was also significantly different to Kr (p value = 0.02). Hexaploid cultivar Fld also showed significant differences with CS (p value = 0.005) and Cad (p value = 0.02), and with *Ae. speltoides* (p value = 0.001) (figure 4.50).

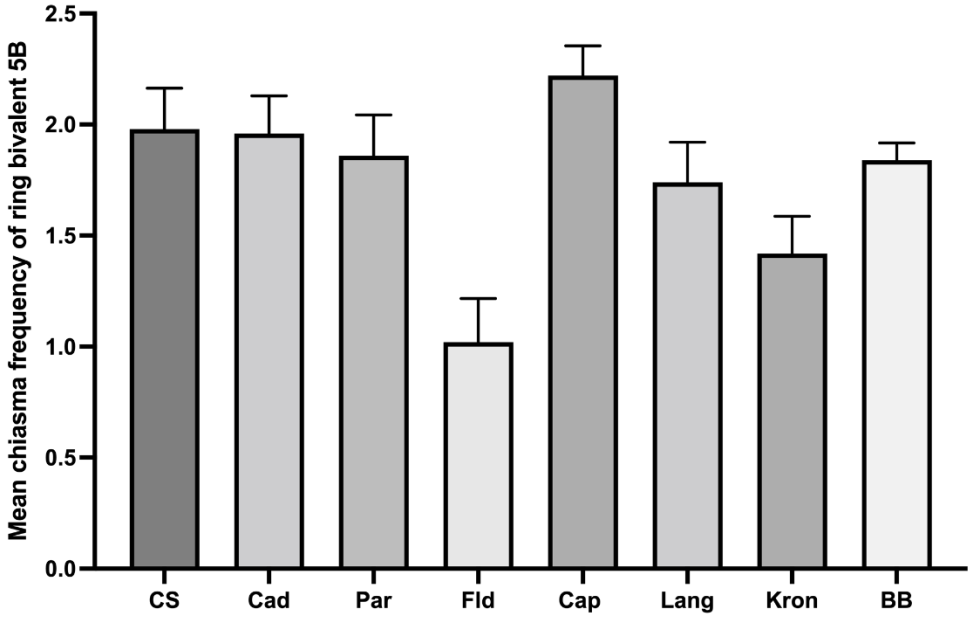

Figure 4.49: Mean chiasma frequency in 5B ring bivalents.

	CS	Cad	Par	Fld	Kron	Capp	Lang	BB
CS								
Cad	NS							
Par	NS	NS						
Fld	**	*	NS					
Kron	NS	NS	NS	NS				
Capp	NS	NS	NS	***	*			
Lang	NS	NS	NS	NS	NS	NS		
BB	NS	NS	NS	NS	NS	NS	NS	

Figure 4.50: Comparison of the mean chiasma frequency in 5B ring bivalents. In tetraploid cultivars, Cap was also significantly different to Kr (p value = 0.02). Hexaploid cultivar Fld also showed significant differences with CS (p value = 0.005) and Cad (p value = 0.02), and with *Ae. speltoides* (p value = 0.001). Fld and Cap showed significant differences (p value <0.0001). Kruskal-Wallis test (N=50).

The mean chiasma frequency along different regions (d, i^1, i^2, i^3, p) on chromosome 5B was further analyzed in different wheat cultivars and species. The mean chiasma frequency at different

localizations in chromosome 5B were conducted. The main purpose of this step was to identify if the mean chiasma at these different locations were different in diploid, tetraploid and hexaploid cultivars.

Distal chiasmata at chromosome 5B were the most common among the different species studied. Interestingly, the frequency of distal chiasmata in diploid *Ae. speltoides* (1.56±0.076) and hexaploid cultivar CS (1.46±0.091) appeared to be the highest among all the material analyzed (figure 4.51) (Table 4.32 see appendix). This is supported by the Kruskal-Wallis tests done that showed significant differences in distal 5B chiasma frequencies (figure 4.52).

Mean distal (d) chiasma frequency on chromosome 5B was significantly different between *Ae. speltoides* (BB) and two tetraploid cultivars Kr (p value <0.0001) and Lnd (p value = 0.02), as well as to hexaploid cultivars Cad (p value = 0.001), Pg (p value = 0.04) and Fld (p value <0.0001). Furthermore, hexaploid cultivar CS was also significantly different to Fld (p value = 0.0004) and Kr (p value = 0.0004). Finally, tetraploid cultivar Cap showed significant differences to Fld (p value = 0.01) and Kr (p value = 0.01).

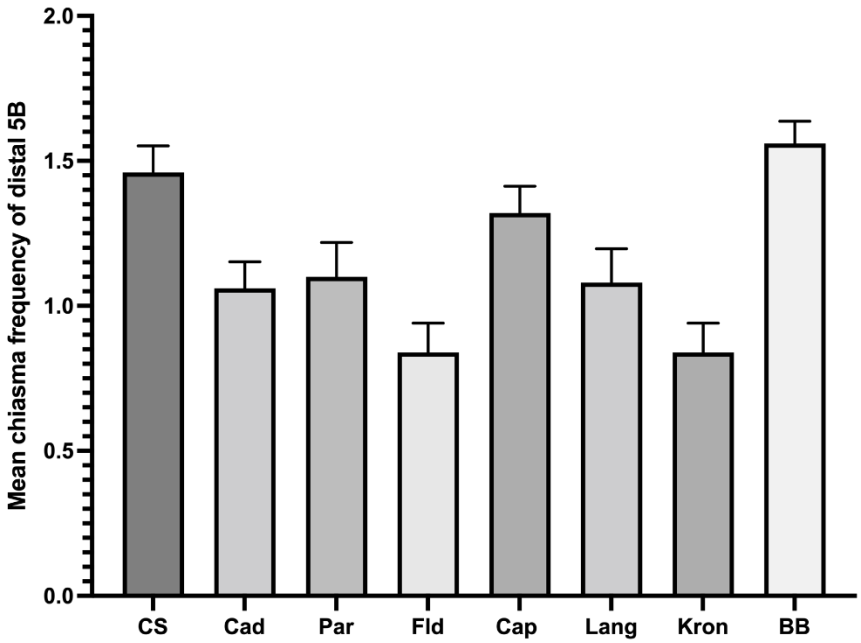

Figure 4.51: Mean chiasma frequency in 5B distal chromosome regions.

	CS	Cad	Par	Fld	Kron	Capp	Lang	BB
CS								
Cad	NS							
Par	NS	NS						
Fld	***	NS	NS					
Kron	NS	NS	NS	NS				
Capp	NS	NS	NS	*	*			
Lang	NS	NS	NS	NS	NS	NS		
BB	NS	**	*	****	****	NS	*	

Figure 4.52: Comparison of the mean chiasma frequency in 5B distal chromosome regions. Mean chiasma frequency on chromosome 5B was significantly different between *Ae. speltoides* (BB) and two tetraploid cultivars Kr (p value <0.0001) and Lnd (p value = 0.02), as well as to hexaploid cultivars Cad (p value = 0.001), Pg (p value = 0.04) and Fld (p value <0.0001). Also, hexaploid cultivar CS was also significantly different to Fld (p value = 0.0004) and Kr (p value = 0.0004). Finally, tetraploid cultivar Cap showed significant differences to Fld (p value = 0.01) and Kr (p value = 0.01). Kruskal-Wallis test (N=50). (NS p>0.05/ *0.05≥ p > 0.005/ **0.005> p > 0.0005/ ***p < 0.0005).

Interstitial region 2 (i^2) chiasmata at chromosome 5B in diploid species *Ae. speltoides* (BB) were never observed (N=50) (figure 4.53) and (Table 4.33 see appendix). Interestingly, mean chiasma frequency Welch's ANOVA analysis showed significant differences between *Ae. speltoides* (BB) and the rest of polyploid wheats (p value <0.0001) (figure 4.54).

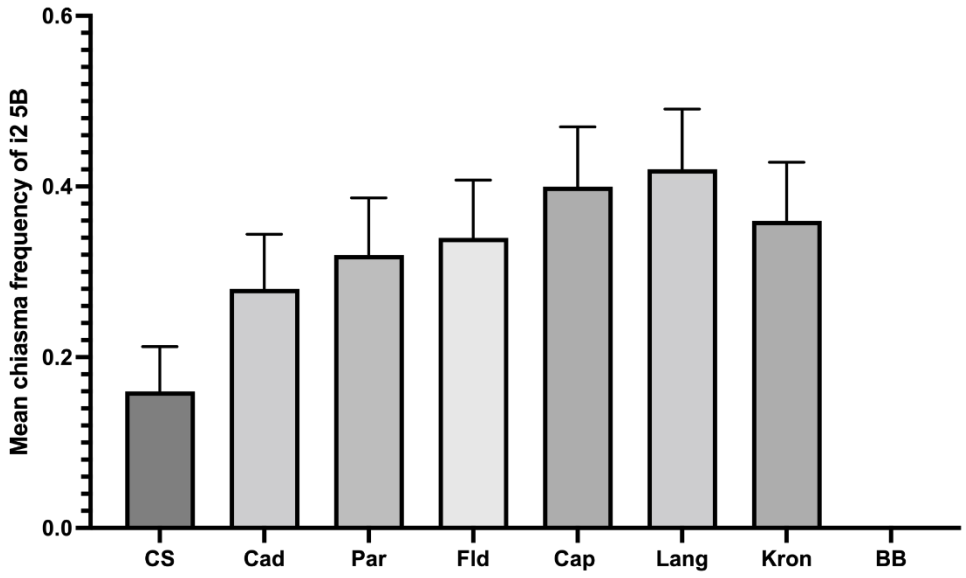

Figure 4.53: Mean chiasma frequency in 5B i^2 chromosome region.

	CS	Cad	Par	Fld	Kron	Capp	Lang	BB
CS								
Cad	NS							
Par	NS	NS						
Fld	NS	NS	NS					
Kron	NS	NS	NS	NS				
Capp	NS	NS	NS	NS	NS			
Lang	NS	NS	NS	NS	NS	NS		
BB	****	****	****	***	***	***	***	

Figure 4.54: Comparison of the mean chiasma frequency in 5B i^2 chromosome region. Significant differences between *Ae. speltoides* (BB) and the rest of polyploid wheats observed in this localization (p value <0.0001). Kruskal-Wallis test (N=50). (NS p>0.05/ *0.05≥ p > 0.005/ **0.005> p > 0.0005/ ***p < 0.0005).

Another interesting chiasma localization and worth investigation was interstitial region 3 (i^3). Similar to i^2, i^3 region was never observed in diploid *Ae. speltoides* (BB) (figure 4.55) and (Table 4.34 see appendix). Kruskal-Wallis tests were conducted and analyzed (figure 4.56). The hexaploid cultivar CS showed the highest mean chiasma frequency at i^3 localization (mean 0.58±0.07) and it was significantly different to all tetraploid cultivars Kr (p value <0.0001), Cap (p value = 0.003) and Lnd (p value = 0.003). Also, *Ae. speltoides* (BB) was significantly different to the rest of polyploid wheats (p value <0.01).

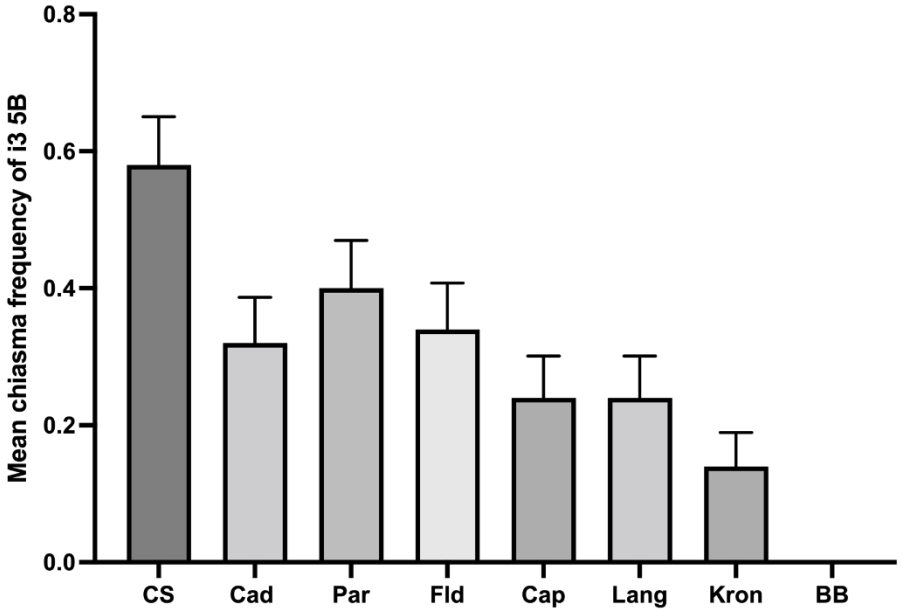

Figure 4.55: Mean chiasma frequency in 5B i[3] chromosome regions.

	CS	Cad	Par	Fld	Kron	Capp	Lang	BB
CS								
Cad	NS							
Par	NS	NS						
Fld	NS	NS	NS					
Kron	***	NS	NS	NS				
Capp	**	NS	NS	NS	NS			
Lang	**	NS	NS	NS	NS	NS		
BB	****	***	****	**	*	*	*	

Figure 4.56: Comparison of the mean chiasma frequency in 5B i[3] chromosome regions. Hexaploid cultivar CS showed the highest mean chiasma frequency at i3 localization (mean 0.58±0.07) and it was significantly different to all tetraploid cultivars Kr (p value <0.0001), Cap (p value = 0.003) and Lnd (p value = 0.003). Also, *Ae. speltoides* (BB) was significantly different to the rest of polyploid wheats. Kruskal-Wallis test (N=50). (NS p>0.05/ *0.05≥ p > 0.005/ **0.005> p > 0.0005/ ***p < 0.0005).

4.2.3.5 Chiasma frequency and distribution on chromosome 1D

The mean chiasma frequency on chromosome 1D was carried out in hexaploid wheat cultivars and their wild relative *Ae. tauschii* (DD) (figure 4.57) (Table 4.35 see appendix). Kruskal-Wallis tests were applied to investigate if the differences observed were statistically significant (figure 4.58) (figure 4.42). Interestingly, mean chiasma frequencies on 1D were lower in *Ae. tauschii* (DD) (mean 1.82±0.054). Diploid *Ae. tauschii* (DD) mean chiasma frequency in 1D showed significant differences to hexaploid cultivars Fld (p value = 0.0002) and Cad (p value = 0.03) but not to Pg (p value = 0.13) or CS (p value = 0.97). CS also showed significant differences with Fld (p value = 0.01).

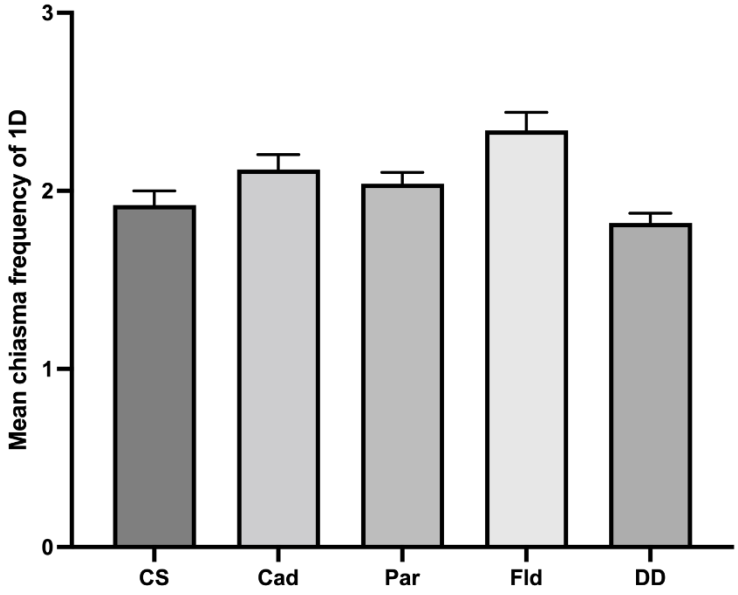

Figure 4.57: Mean chiasma frequency in 1D chromosome in all wheats.

	CS	Cad	Par	Fld	DD
CS					
Cad	NS				
Par	NS	NS			
Fld	*	NS	NS		
DD	NS	*	NS	***	

Figure 4.58: Comparison of the mean chiasma frequency in 1D chromosome in all wheats. *Ae. tauschii* (DD) mean chiasma frequency in 1D showed significant differences to hexaploid cultivars Fld (p value = 0.0002) and Cad (p value = 0.03) but not to Pg (p value = 0.13) or CS (p value = 0.97). CS also showed significant differences with Fld (p value = 0.01). Kruskal-Wallis (N=50). (NS p>0.05/ *0.05≥ p > 0.005/ **0.005> p > 0.0005/ ***p < 0.0005).

Interestingly, not a single significant difference could be observed when dividing these mean chiasma frequencies on chromosome 1D by their bivalent configurations (rod *vs* ring). The mean chiasma frequency of rod and ring bivalents on chromosome 1D (Tables 4.36 and 4.37 see appendix) showed that no significant differences could be observed among the hexaploid cultivars or among *Ae. tauschii* and all the different hexaploid cultivars (figures 4.59 and 4.60) (figures 4.61 and 4.62).

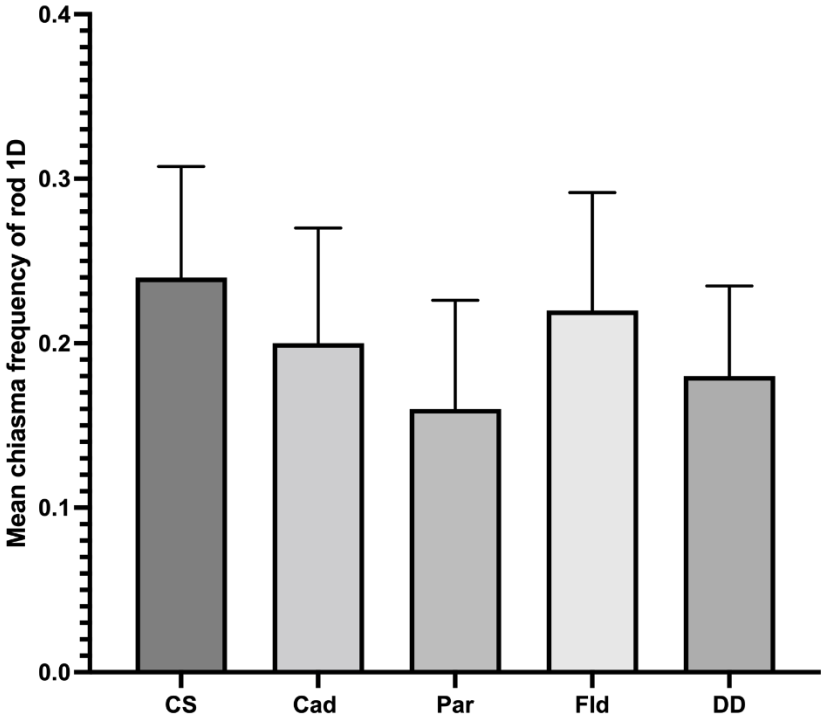

Figure 4.59: Mean chiasma frequency of rod bivalent in chromosome 1D.

	CS	Cad	Par	Fld	DD
CS					
Cad	NS				
Par	NS	NS			
Fld	NS	NS	NS		
DD	NS	NS	NS	NS	

Figure 4.60: Comparison of the mean chiasma frequency of rod bivalent in chromosome 1D. No significant differences observe in rod bivalents. Kruskal-Wallis test (N=50). (NS $p>0.05$/ *$0.05\geq p > 0.005$/ **$0.005> p > 0.0005$/ ***$p < 0.0005$).

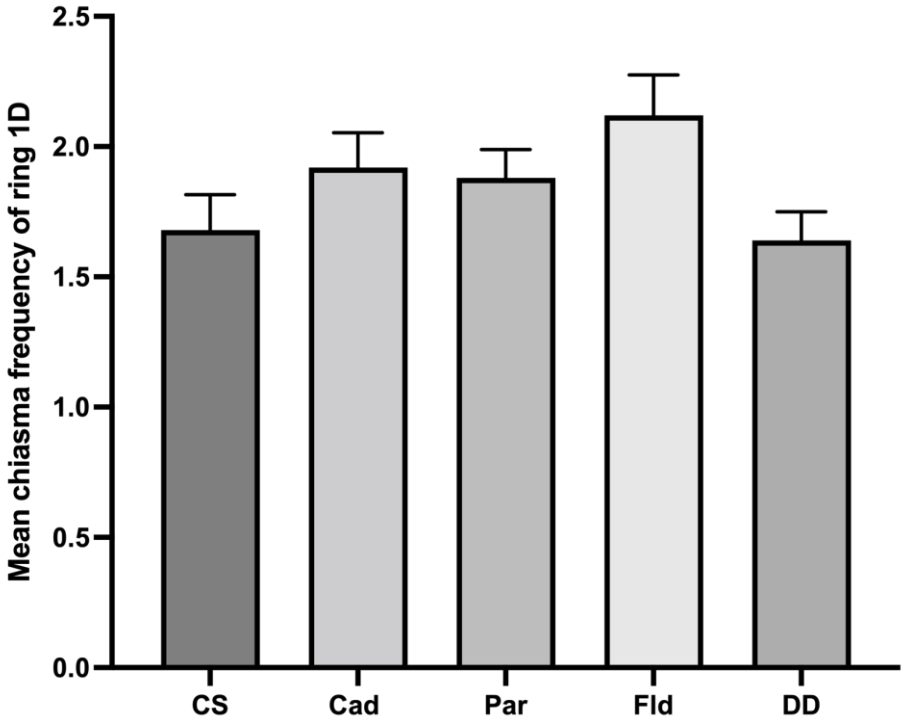

Figure 4.61: Mean chiasma frequency of ring bivalent in chromosome 1D.

	CS	Cad	Par	Fld	DD
CS					
Cad	NS				
Par	NS	NS			
Fld	NS	NS	NS		
DD	NS	NS	NS	NS	

Figure 4.62: Comparison of the mean chiasma frequency of ring bivalent in chromosome 1D. No significant differences observe in ring bivalents. Kruskal-Wallis test (N=50). (NS $p>0.05$/ $*0.05\geq p > 0.005$/ $**0.005> p > 0.0005$/ $***p < 0.0005$).

The mean chiasma frequency along different regions (d, i^1, i^2, i^3, p) on chromosome 1D was further analyzed in different wheat cultivars and species. The mean chiasma frequency at different

localizations in chromosome 1D were conducted. The main purpose of this step was to identify if the mean chiasma at these different locations were different between diploid and hexaploid cultivars.

Distal chiasmata at chromosome 1D were the most common among the different material studied. Interestingly, the frequency of distal chiasmata in diploid *Ae. tauschii* (0.68±0.09) was lower compared to other hexaploid cultivars but Kruskal-Wallis tests showed not significant differences among all the material analyzed.

Mean chiasma frequency in interstitial region 1 (i^1) on chromosome 1D appeared to be higher in *Ae. tauschii* (DD) (mean = 0.62±0.08) (figure 4.63) but Kruskal-Wallis tests showed only statistically significance with hexaploid cultivar Cad (p value = 0.006) (figure 4.64).

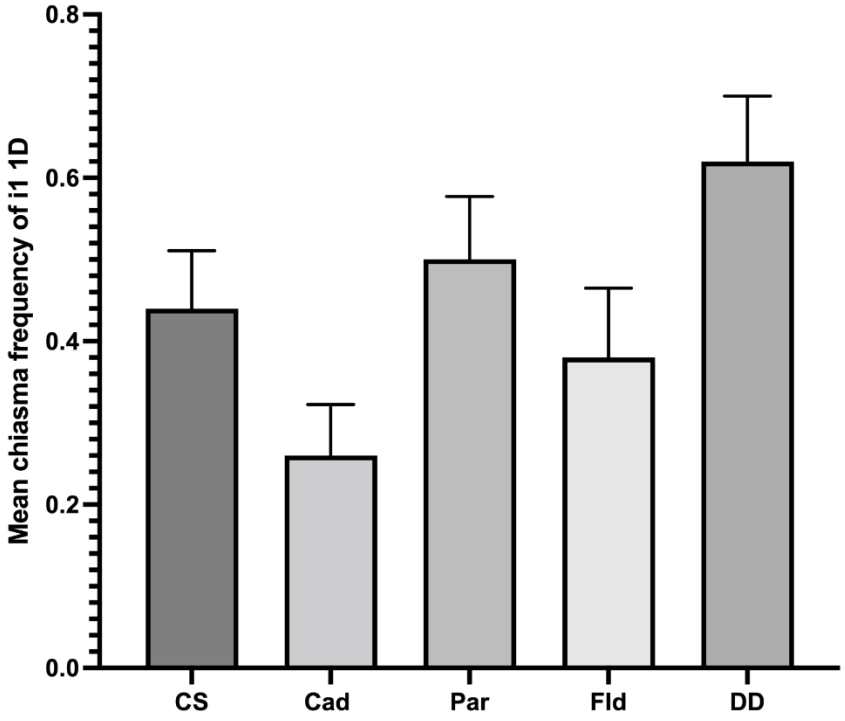

Figure 4.63: Mean chiasma frequency in 1D i^1 chromosome region.

	CS	Cad	Par	Fld	DD
CS					
Cad	NS				
Par	NS	NS			
Fld	NS	NS	NS		
DD	NS	**	NS	NS	

Figure 4.64: Comparison of the mean chiasma frequency in 1D i[1] chromosome region. Mean chiasma frequency in interstitial region 1 (i1) on chromosome 1D was statistically significance with hexaploid cultivar Cad (p value = 0.006). Kruskal-Wallis test (N=50). (NS p>0.05/ *0.05≥ p > 0.005/ **0.005> p > 0.0005/ ***p < 0.0005).

Mean chiasma frequency in proximal regions (p) on chromosome 1D appeared to be absent in *Ae. tauschii* (DD) (figure 4.65) (Table 4.38 see appendix). Interestingly, hexaploid cultivar Fld showed the highest frequency of p chiasmata in chromosome 1D (0.34±0.07) and it was significant different to hexaploid cultivars Pg (p value = 0.01) and CS (p value = 0.001), and to diploid *Ae. tauschii* (p value <0.0001) (figure 4.66).

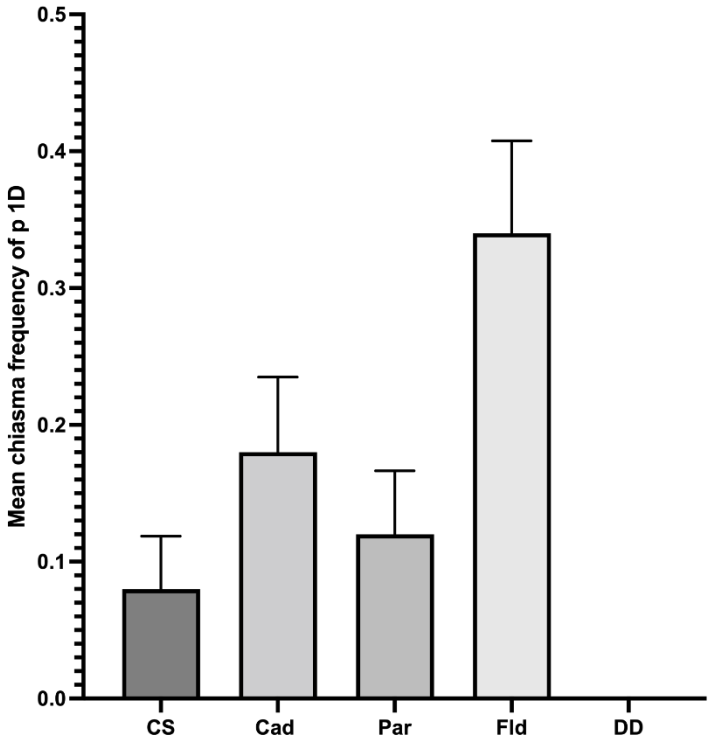

Figure 4.65: Mean chiasma frequency in 1D p chromosome regions.

	CS	Cad	Par	Fld	DD
CS					
Cad	NS				
Par	NS	NS			
Fld	**	NS	*		
DD	***	***	***	***	

Figure 4.66: Comparison of the mean chiasma frequency in 1D p chromosome regions. Hexaploid cultivar Fld was significant different to hexaploid cultivars Pg (p value = 0.01) and CS (p value = 0.001), and to diploid *Ae. tauschii* (p value <0.0001). Kruskal-Wallis test (N=50). (NS p>0.05/ *0.05≥ p > 0.005/ **0.005> p > 0.0005/ ***p < 0.0005).

4.2.3.6 Chiasma frequency and distribution on chromosome 5D

The mean chiasma frequency on chromosome 5D was carried out in hexaploid wheat cultivars and their wild relative *Ae. tauschii* (DD) (figure 4.67) (Table 4.39 see appendix). Kruskal-Wallis tests were applied to investigate if the differences observed were statistically significant between them (figure 4.68). Interestingly, mean chiasma frequencies on 5D was lower in *Ae. tauschii* (DD) (2.14±0.09). Interestingly, diploid *Ae. tauschii* (DD) mean chiasma frequency in 5D showed only a significant difference to hexaploid cultivar CS (p value = 0.009).

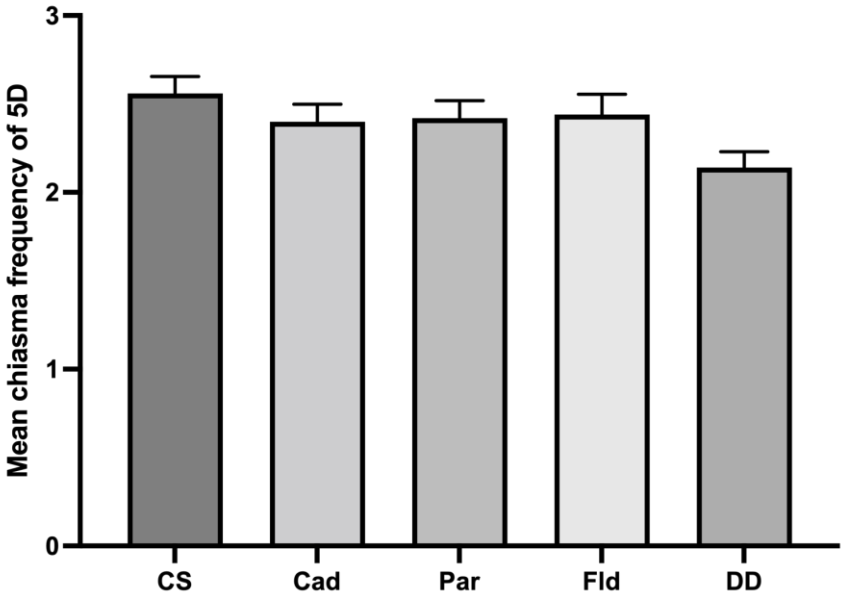

Figure 4.67: Mean chiasma frequency of chromosome 5D.

	CS	Cad	Par	Fld	DD
CS					
Cad	NS				
Par	NS	NS			
Fld	NS	NS	NS		
DD	*	NS	NS	NS	

Figure 4.68: Comparison of the mean chiasma frequency of chromosome 5D in hexaploid cultivars and *Ae. tauschii*. Diploid *Ae. tauschii* (DD) mean chiasma frequency in 5D showed only a significant difference to hexaploid cultivar CS (p value = 0.009). Kruskal-Wallis test (N=50). (NS p>0.05/ *0.05≥ p > 0.005/ **0.005> p > 0.0005/ ***p < 0.0005).

Interestingly, not a single significant difference could be observed when dividing these mean chiasma frequencies on chromosome 5D by their bivalent configurations (rod *vs* ring) (Tables 4.40 and 4.41 see appendix). The mean chiasma frequency of rod (figure 4.69 and 4.70) and ring (figure 4.71 and 4.72) bivalents on chromosome 5D showed that not significant differences were observed among the hexaploid cultivars or among *Ae. tauschii* and all the different hexaploid cultivars.

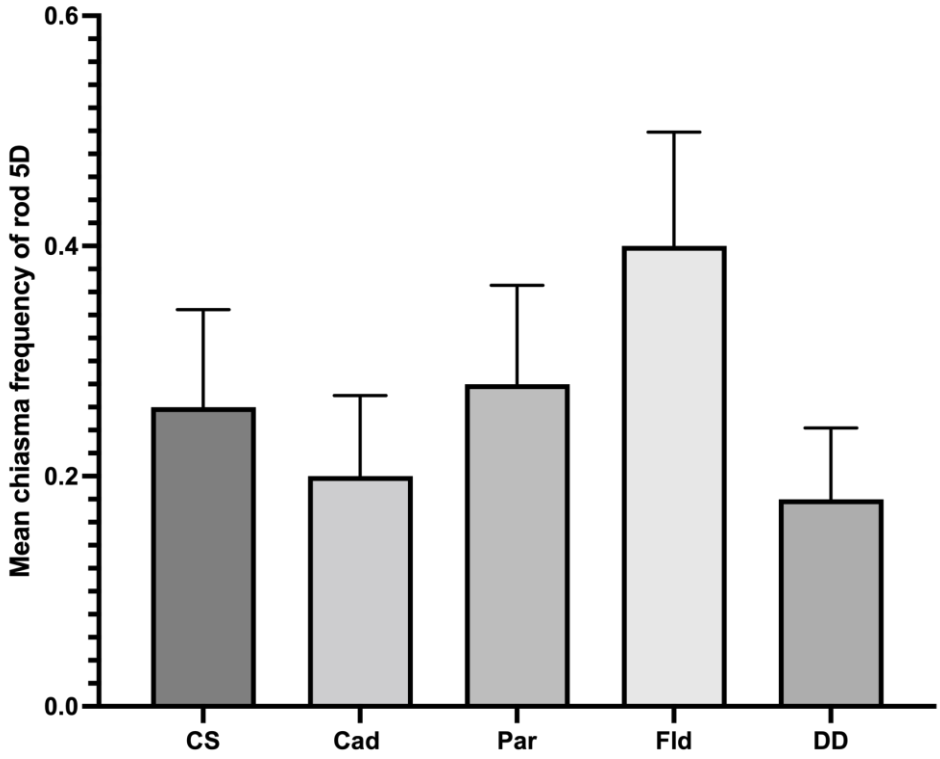

Figure 4.69: Mean chiasma frequency on 5D rod bivalents.

	CS	Cad	Par	Fld	DD
CS					
Cad	NS				
Par	NS	NS			
Fld	NS	NS	NS		
DD	NS	NS	NS	NS	

Figure 4.70: Comparison of the mean chiasma frequency on 5D rod bivalents. No significant differences observe**.** Kruskal-Wallis test (N=50). (NS p>0.05/ *0.05≥ p > 0.005/ **0.005> p > 0.0005/ ***p < 0.0005).

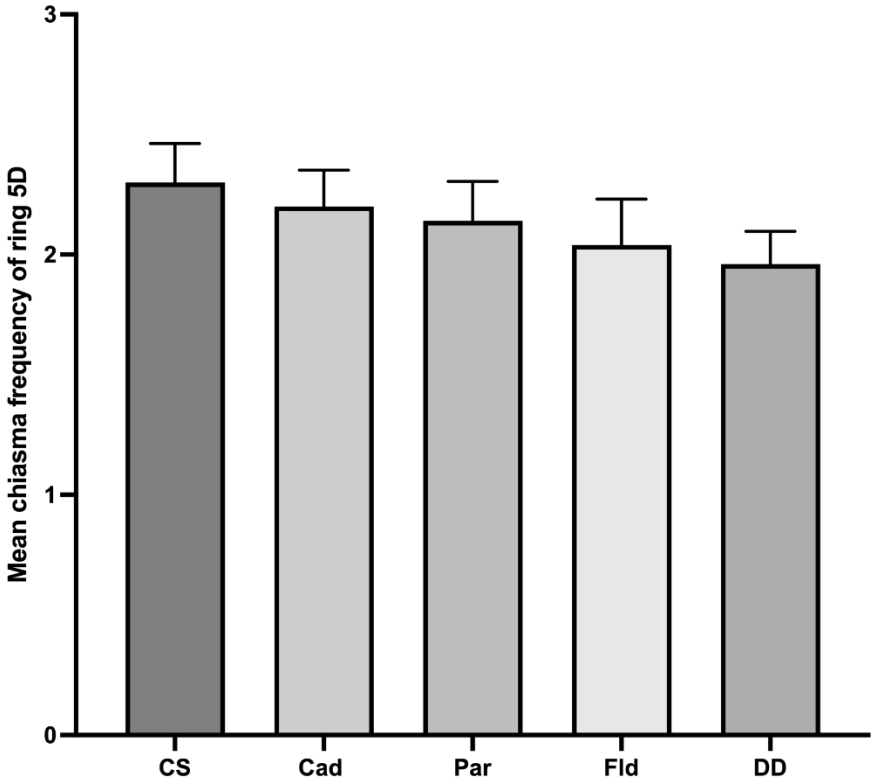

Figure 4.71: Mean chiasma frequency on 5D ring bivalents.

	CS	Cad	Par	Fld	DD
CS					
Cad	NS				
Par	NS	NS			
Fld	NS	NS	NS		
DD	NS	NS	NS	NS	

Figure 4.72: Comparison of the mean chiasma frequency on 5D ring bivalents. No significant differences observed**.** Kruskal-Wallis (N=50). (NS $p>0.05$/ *$0.05\geq p > 0.005$/ **$0.005> p > 0.0005$/ ***$p < 0.0005$).

The mean chiasma frequency along different regions (d, i^1, i^2, i^3, p) on chromosome 5D was further analyzed in different hexaploid wheat cultivars and *Ae. tauschii*. The mean chiasma frequency at different localizations in chromosome 5D were conducted. The main purpose of this step was to identify if the mean chiasma at these different locations were different between diploid and hexaploid cultivars.

Distal chiasmata at chromosome 5D were the most common among the different material studied (figure 4.73). Interestingly, the frequency of distal chiasmata in diploid *Ae. tauschii* (mean = 0.74±0.11) was lower compared to other hexaploid cultivars but Kruskal-Wallis tests showed no significant differences among all the material analyzed (figure 4.74).

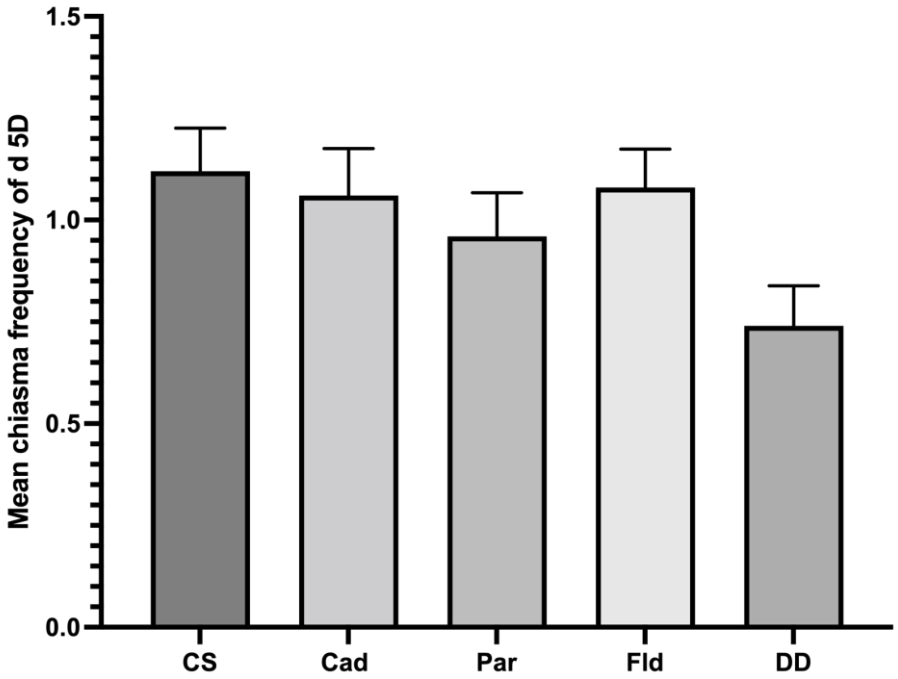

Figure 4.73: Mean chiasma frequency in 5D distal chromosome regions.

	CS	Cad	Par	Fld	DD
CS					
Cad	NS				
Par	NS	NS			
Fld	NS	NS	NS		
DD	NS	NS	NS	NS	

Figure 4.74: Comparison of the mean chiasma frequency in 5D distal chromosome regions. No significant differences observe. Kruskal-Wallis test (N=50). (NS p>0.05/ *0.05≥ p > 0.005/ **0.005> p > 0.0005/ ***p < 0.0005).

Mean chiasma frequency in interstitial region 3 (i^3) on chromosome 5D appeared to be lower in *Ae. tauschii* (DD) (mean = 0.16±0.05) compared to the other hexaploid cultivars (figure 4.75). Interestingly, only hexaploid cultivar Fld showed a significant difference to *Ae. tauschii* (p value = 0.02) (figure 4.76).

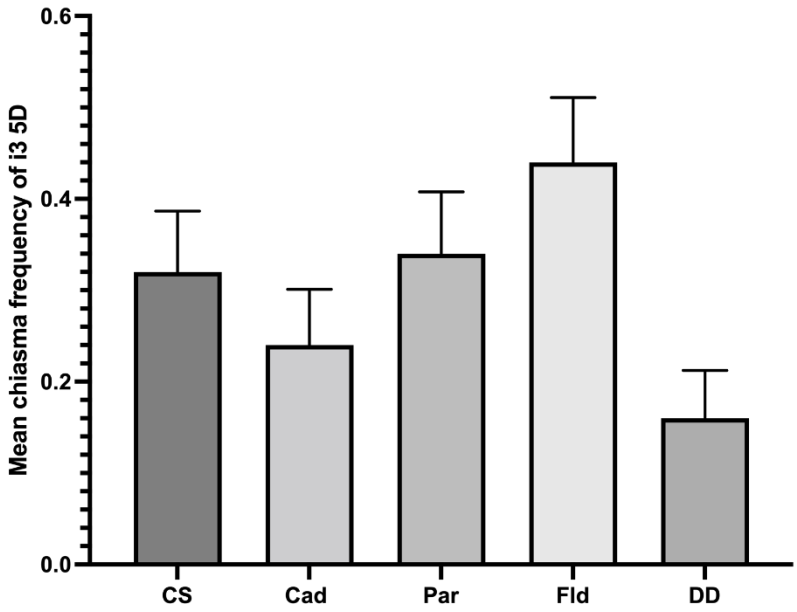

Figure 4.75: Mean chiasma frequency in 5D i^3 chromosome region.

	CS	Cad	Par	Fld	DD
CS					
Cad	NS				
Par	NS	NS			
Fld	NS	NS	NS		
DD	NS	NS	NS	*	

Figure 4.76: Comparison of the mean chiasma frequency in 5D i^3 chromosome region. Hexaploid cultivar Fld showed a significant difference to Ae. tauschii (p value = 0.02). Kruskal-Wallis test (N=50).

The comparison between the mean chiasma frequency (total and per chromosome localization) of specific chromosomes identified by 45S/5S FISH was carried out to investigate if specific chromosomes in wheat have evolved different meiotic behaviours over the evolution of polyploid wheats. The comparison was conducted by comparing the chromosome specific mean chiasma frequency and localization with the overall means of the rest of chromosomes in that species/cultivar. For instance, the mean chiasma frequency of chromosome 5A in CS in (d, i^1, i^2, i^3 and p) localization was compared to the average mean chiasma frequency of CS in (d, i^1, i^2, i^3, and p) localization of all chromosomes.

4.2.3.7 Chromosome 5A

The mean chiasma frequency of chromosome 5A in specific localizations was compare to the overall mean of chiasma frequency in hexaploid and tetraploid and diploid wheats used in this study. In CS, the mean chiasma frequency in 5A was lower in (d, i^1, i^2) localization compared to the overall average in these locations in CS chromosomes, whereas in (i^3 and p) localization the mean chiasma frequency

in 5A was higher compared to the overall average in these two locations in CS chromosomes. Welch's t test was conducted but no significant differences were observed between the mean chiasma frequency of CS-5A compared to the overall average of CS chromosomes at all different localizations (figure 4.77).

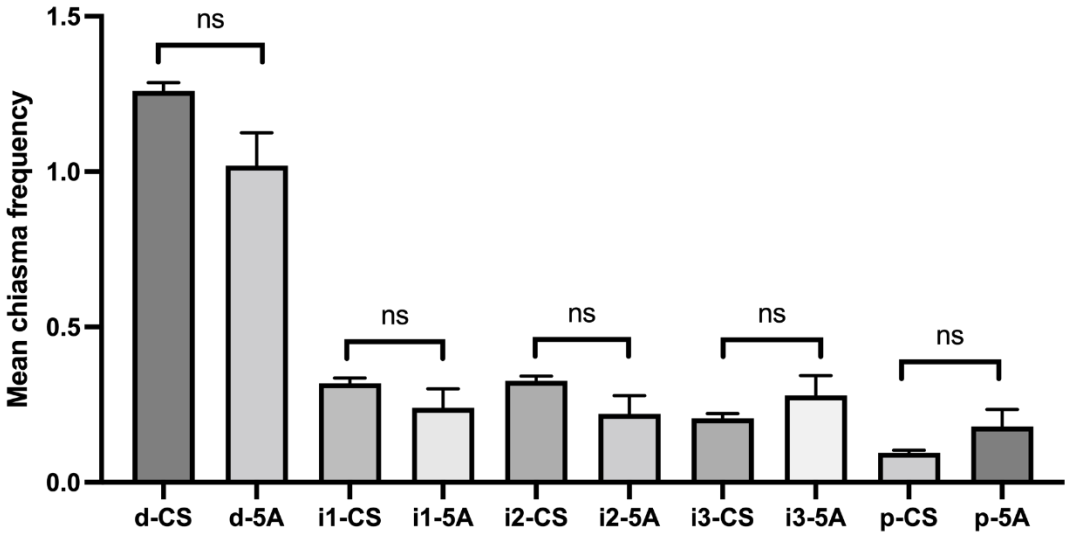

Figure 4.77: Comparison of the mean chiasma frequency between CS-5A chromosome and the overall average in CS chromosomes in different localizations. No significant differences were observed between the mean chiasma frequency of CS-5A compared to the overall average of CS chromosomes at all different localizations. Welch's t test (N=50). (NS $p>0.05$/ *$0.05\geq p > 0.005$/ **$0.005> p > 0.0005$/ ***$p < 0.0005$).

The mean chiasma frequency of Cad-5A was compared to the mean chiasma frequency of the overall average in all chromosomes in Cadenza at different localizations. The mean chiasma frequency at distal regions in chromosome 5A in Cadenza (0.98 ± 0.104) appeared to be significantly lower (Welch's t test, p value = 0.002) compared to the overall average in all the chromosomes in Cad (1.45 ± 0.015). However, the mean chiasma frequency at other chromosome localizations (i^1, i^2, i^3 and

p) appeared to be slightly higher but not significant in chromosome Cadenza-5A compared to the overall Cadenza chromosomes (figure 4.78).

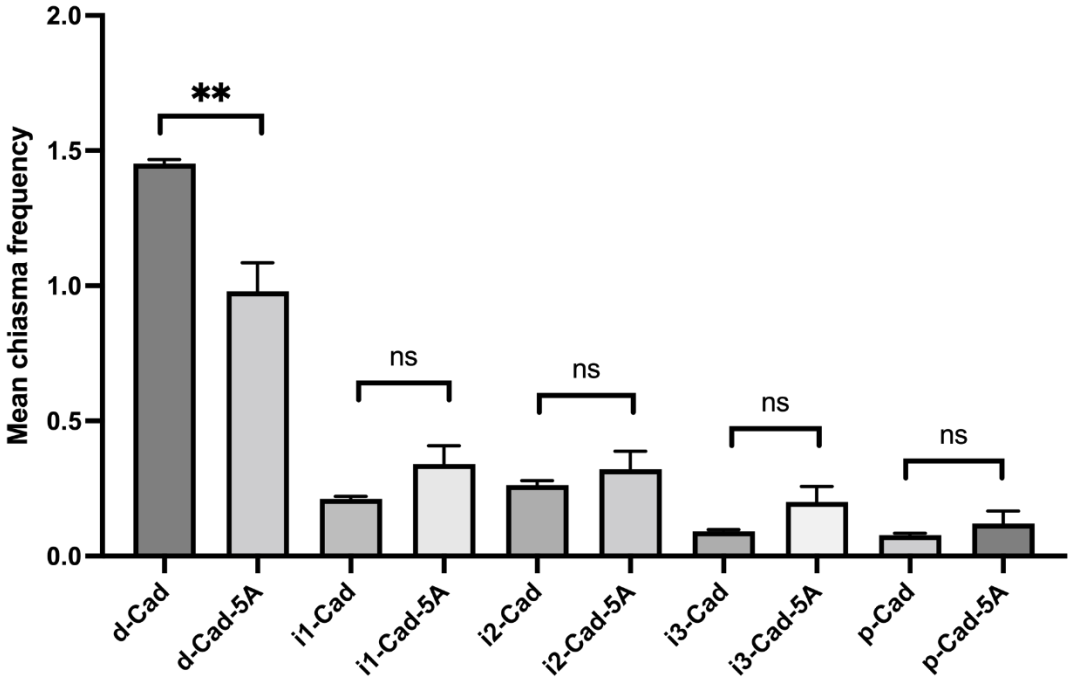

Figure 4.78: Comparison of the mean chiasma frequency between Cadenza-5A and the overall average in Cadenza chromosomes. The mean chiasma frequency at distal regions in chromosome 5A in Cadenza appeared to be significantly lower (p value = 0.002) compared to the overall average in all the chromosomes in Cad. Welch's t test (N=50). (NS p>0.05/ *0.05≥ p > 0.005/ **0.005> p > 0.0005/ ***p < 0.0005).

In Paragon, the mean chiasma frequency of chromosome Paragon-5A was compared to the overall average in Paragon chromosomes at different localizations. The mean chiasma frequency at distal regions in the overall average of Paragon chromosomes (1.305±0.02) appeared to be significantly higher compared to the mean chiasma frequency in Paragon-5A (0.92±0.11) (Welch's t test, p value = 0.01) (figure 4.79).

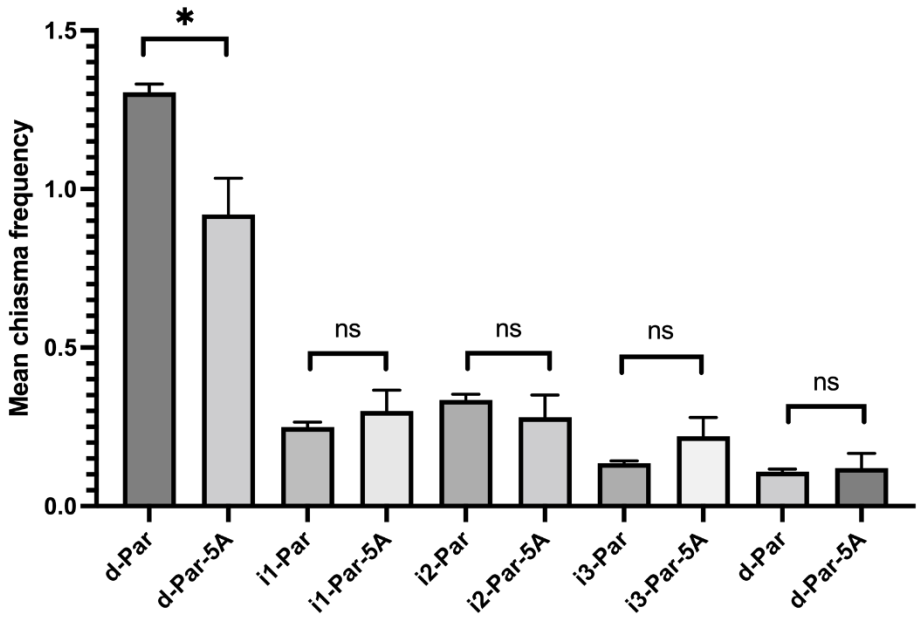

Figure 4.79: Comparison of the mean chiasma frequency between Paragon-5A and the overall average Paragon chromosomes. The mean chiasma frequency at distal regions in the overall average of Paragon chromosomes appeared to be significantly higher compared to the mean chiasma frequency in Paragon-5A. Welch's t test (N=50). (NS $p>0.05$/ $*0.05\geq p > 0.005$/ $**0.005> p > 0.0005$/ $***p < 0.0005$).

In Fielder, the mean chiasma frequency of Fielder-5A (0.86 ± 0.09) was significantly lower compared to the mean chiasma frequency of the overall average of chromosomes at distal regions (1.11 ± 0.02) (Welch's t test, p value =0.02) (figure 4.80).

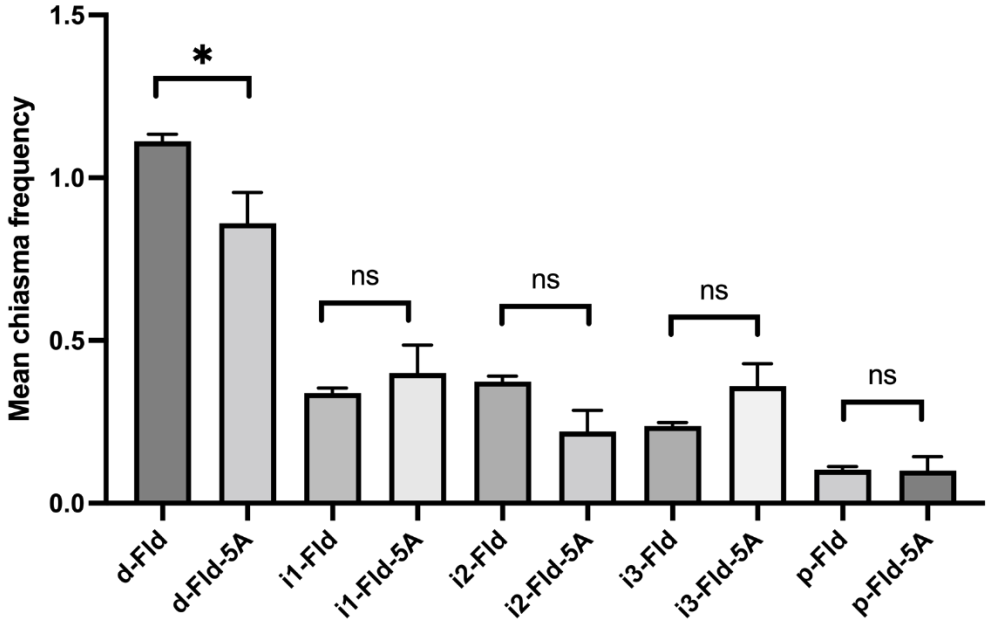

Figure 4.80: Comparison of the mean chiasma frequency between Fielder-5A and the overall average of Fielder chromosomes. The mean chiasma frequency of Fielder-5A was significantly lower compared to the mean chiasma frequency of the overall average of chromosomes at distal regions. Welch's t test (N=50). (NS $p>0.05$/ *$0.05\geq p > 0.005$/ **$0.005> p > 0.0005$/ ***$p < 0.0005$).

The mean chiasma frequency of chromosome 5A was compared to the mean chiasma frequency of the overall average in all chromosomes at different localizations in tetraploid wheat cultivars Kronos, Cappelli and Langdon.

The mean chiasma frequency of Kronos-5A at interstial region 1 (i^1) (0.08 ± 0.03) was significantly lower than the overall average in all chromosomes in Kronos (0.323 ± 0.02) (Welch's t test, p value <0.0001). Nevertheless, at proximal regions, the mean chiasma frequency was significantly higher in Kronos-5A (0.42 ± 0.07) than in the overall average of all chromosomes (0.06 ± 0.01) (Welch's t test, p value = 0.001) (figure 4.81).

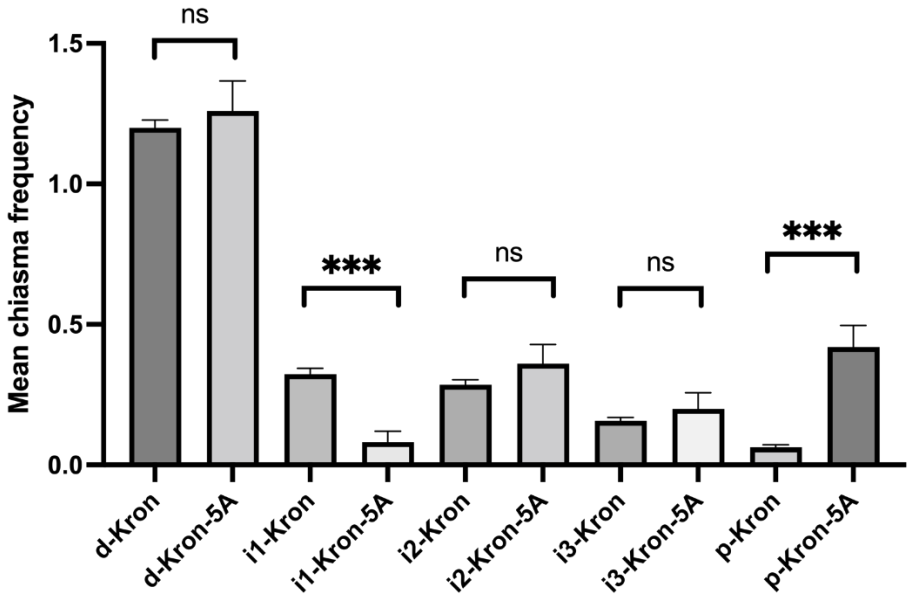

Figure 4.81: Comparison of the mean chiasma frequency between Kronos-5A and Kronos overall average in all chromosomes. The mean chiasma frequency of Kronos-5A at interstial region 1 (i1) was significantly lower than the overall average in all chromosomes in Kronos (p value <0.0001). Nevertheless, at proximal regions, the mean chiasma frequency was significantly higher in Kronos-5A than in the overall average of all chromosomes (p value = 0.001). Welch's t test (N=50). (NS p>0.05/ *0.05≥ p > 0.005/ **0.005> p > 0.0005/ ***p < 0.0005).

In Cappelli and Langdon tetraploid cultivars, the mean chiasma frequency of chromosome 5A in different chromosome localizations appeared to be very similar to the mean chiasma frequency overall chromosome average.

In diploid *T. monococcum* (AA), the mean chiasma frequency of chromosome AA-5A (0.36±0.06) at a proximal localization appeared to be significantly higher than the overall average of all chromosomes at this location (0.097±0.02) (Welch's t test, p value = 0.0005) (figures 4.82).

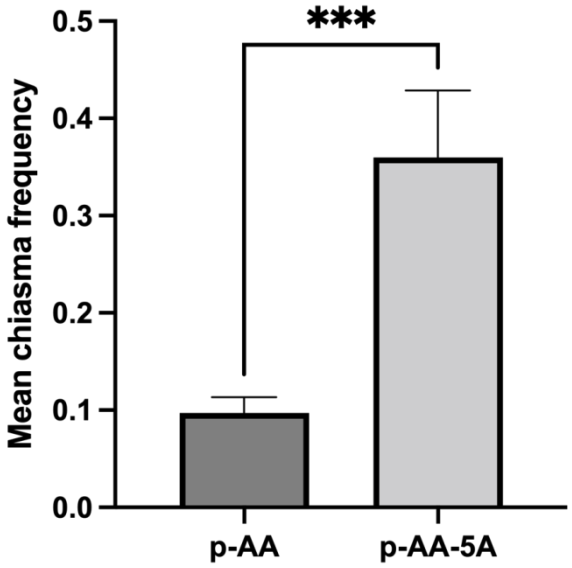

Figure 4.82: Comparison of the mean chiasma frequency in proximal regions between AA-5A and AA overall average of all *T. monococcum* chromosomes. *T. monococcum* (AA), the mean chiasma frequency of chromosome AA-5A at a proximal localization appeared to be significantly higher than the overall average of all chromosomes at this location (p value = 0.0005). Welch's t test (N=50). (NS p>0.05/ *0.05≥ p > 0.005/ **0.005> p > 0.0005/ ***p < 0.0005).

4.2.3.8 Chromosome 1B

The mean chiasma frequency of CS-1B at interstitial region 3 (i^3) (0.06±0.03) was significantly lower than the overall average of all CS chromosomes at this location (0.21±0.01) (Welch's t test, p value = 0.0002) (figures 4.83).

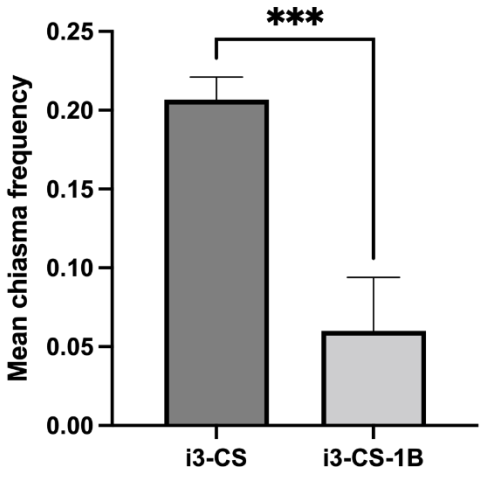

Figure 4.83: Comparison of the mean chiasma frequency between CS-1B and the overall average CS in interstitial regions 3 (i^3). The mean chiasma frequency of CS-1B at interstitial region 3 (i3) was significantly lower than the overall average of all CS chromosomes at this location (p value = 0.0002). Welch's t test (N=50). (NS p>0.05/ *0.05≥ p > 0.005/ **0.005> p > 0.0005/ ***p < 0.0005).

The mean chiasma frequency of Cadenza-1B at distal regions (1.16±0.08) was significantly different to the overall average of all chromosomes at this location (1.45± 0.02) (Welch's t test, p value = 0.001) (figures 4.84).

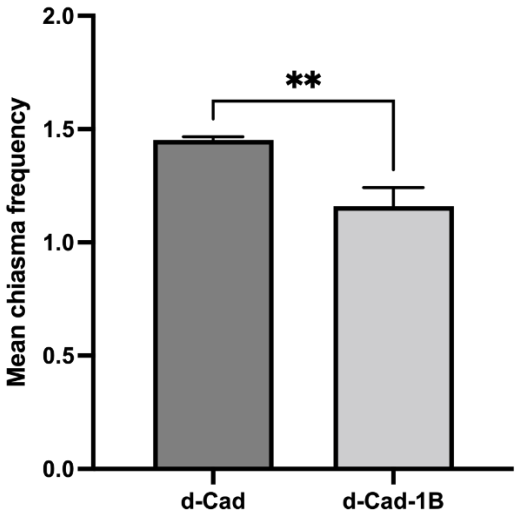

Figure 4.84: Comparison of the mean chiasma frequency at distal (d) and interstitial region 1 (i^1) between Cadenza-1B and the overall average of Cadenza chromosomes in these locations. Welch's t test (N=50). (NS p>0.05/ *0.05≥ p > 0.005/ **0.005> p > 0.0005/ ***p < 0.0005).

The mean chiasma frequency of Paragon-1B showed not significant differences with the overall average of all Paragon chromosomes at the different locations.

The mean chiasma frequency at interstitial region 2 (i^2) of Fielder-1B (0.2±0.05) was significantly lower than the overall average of all the chromosomes at this location (0.37± 0.02) (Welch's t test, p value =0.004) (figures 4.85).

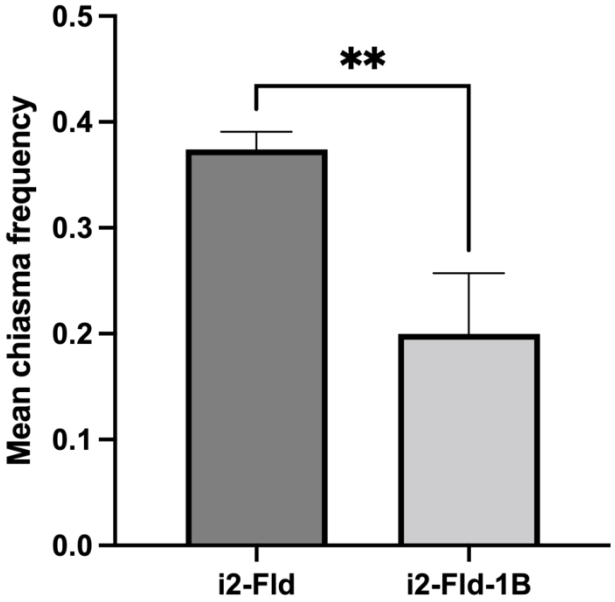

Figure 4.85: Comparison of the mean chiasma frequency at interstitial region 2 (i^2) between Fielder-1B and the overall average of all chromosomes in Fielder. The mean chiasma frequency at interstitial region 2 (i2) of Fielder-1B was significantly lower than the overall average of all the chromosomes at this location (p value =0.004). Welch's t test (N=50). (NS p>0.05/ *0.05≥ p > 0.005/ **0.005> p > 0.0005/ ***p < 0.0005).

In tetraploid cultivar Kronos, the mean chiasma frequency of Kronos-1B at the interstitial region 1 (i^1) (0.54±0.08) was significantly higher than to the overall average in all chromosomes in Kronos in this location (0.32± 0.02) (p value = 0.01). Whereas, the mean chiasma frequency of Kronos-1B at

the interstitial region 2 (i^2) (0.12±0.05) was significantly lower than to the overall average in all chromosomes in Kronos in this location (0.28± 0.02) (p value = 0.001) (figures 4.86).

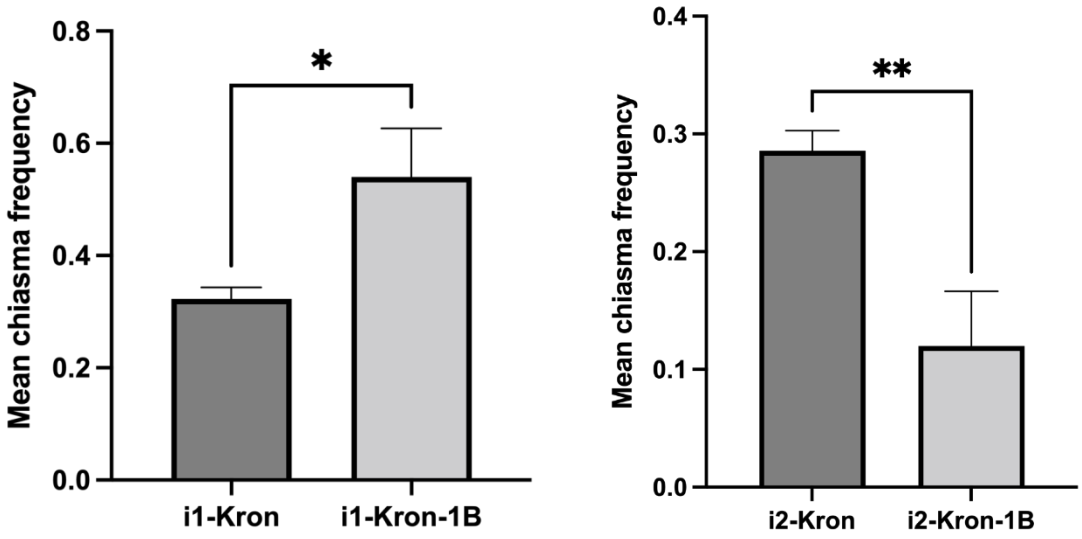

Figure 4.86: Comparison of the mean chiasma frequency at interstitial regions 1 and 2 (i^1 and i^2) between Kronos-1B and the overall average in all chromosomes in Kronos. In tetraploid cultivar Kronos, the mean chiasma frequency of Kronos-1B at the interstitial region 1 (i1) was significantly higher than to the overall average in all chromosomes in Kronos in this location (p value = 0.01). Whereas, the mean chiasma frequency of Kronos-1B at the interstitial region 2 (i2) was significantly lower than to the overall average in all chromosomes in Kronos in this location (p value = 0.001)**.** Welch's t test (N=50). (NS p>0.05/ *0.05≥ p > 0.005/ **0.005> p > 0.0005/ ***p < 0.0005).

The mean chiasma frequency of Cappelli-1B appeared to be significantly higher at the interstitial region 1 (i^1) localization (0.56±0.08) compared to overall average of all Cappelli chromosomes (0.23± 0.01) (p value= 0.0004). Nevertheless, the mean chiasma frequency of Cappelli-1B appeared to be significantly lower at the interstitial region 3 (i^3) localization (0.02±0.02) compared to overall average of all Cappelli chromosomes (0.21±0.01) (p value <0.0001) (figures 4.87).

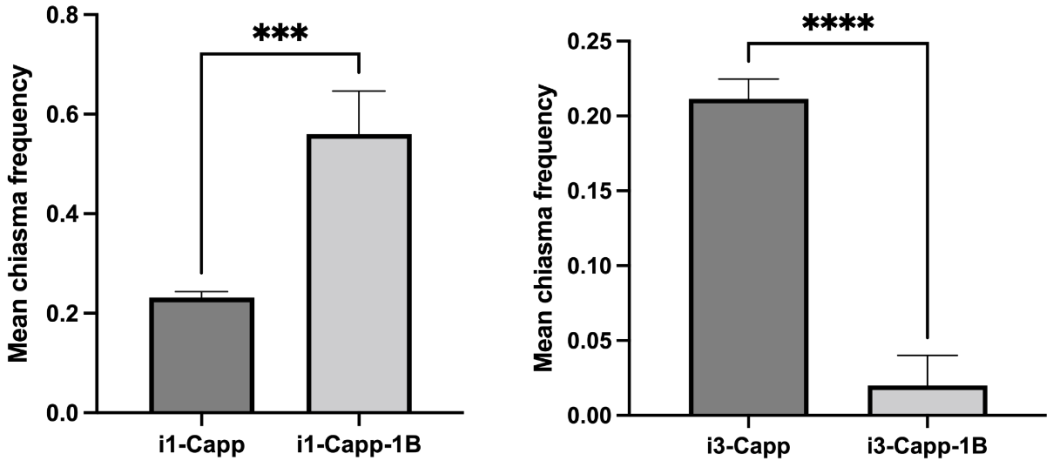

Figure 4.87: Comparison of the mean chiasma frequency at interstitial regions 1 and 3 (i^1 and i^3) in Capelli-1B and the overall average of chromosomes in Cappelli. The mean chiasma frequency of Cappelli-1B appeared to be significantly higher at the interstitial region 1 (i1) localization compared to overall average of all Cappelli chromosomes (p value= 0.0004). Nevertheless, the mean chiasma frequency of Cappelli-1B appeared to be significantly lower at the interstitial region 3 (i3) localization compared to overall average of all Cappelli chromosomes (p value <0.0001). Welch's t test (N=50).

The mean chiasma frequency at interstitial region 1 (i^1) of Langdon-1B (0.52±0.07) was significantly higher than the overall average of all chromosomes in Langdon at this location (0.21±0.01) (p value = 0.005) (figure 4.62). However, the mean chiasma frequencies at interstitial regions 2 and 3 (i^2 , i^3) of Langdon-1B (0.16±0.05 and 0.04±0.02) were significantly lower than the overall average of all chromosomes in Langdon at these locations (0.34±0.02 and 0.21±0.01) (p values = 0.02 and 0.0001, respectively) (figure 4.88).

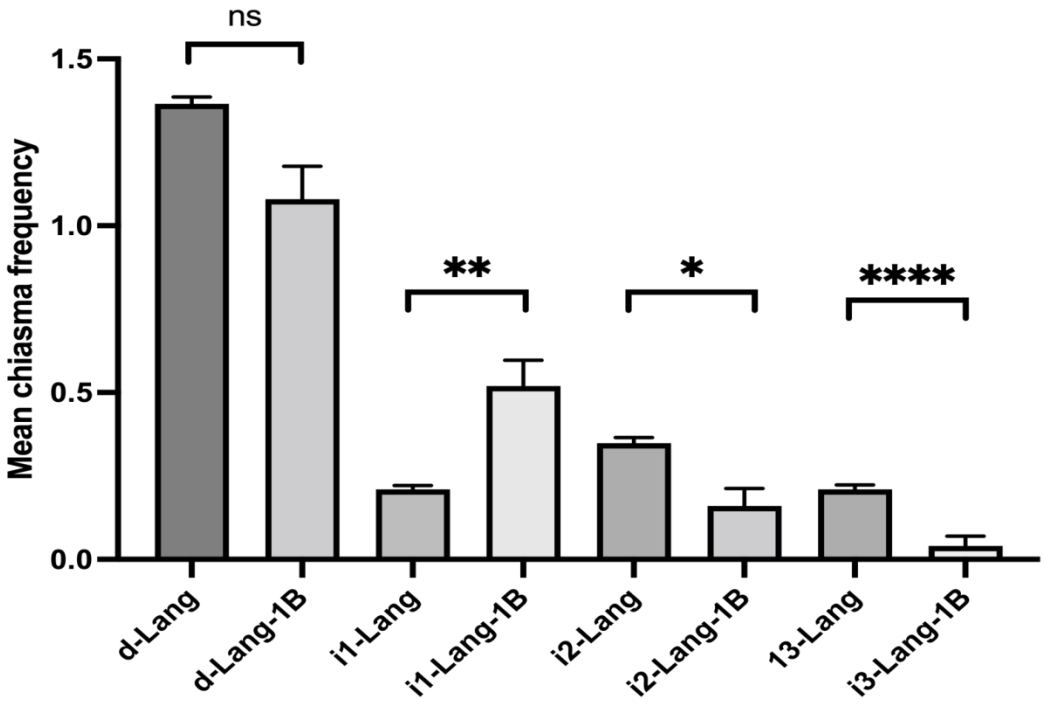

Figure 4.88: Comparison of the mean chiasma frequency at different localizations (d, i^1, i^2 and i^3) between Langdon-1B and the overall average of all chromosomes in Langdon. The mean chiasma frequency at interstitial region 1 (i1) of Langdon-1B was significantly higher than the overall average of all chromosomes in Langdon at this location (p value = 0.005). However, the mean chiasma frequencies at interstitial regions 2 and 3 (i2 , i3) of Langdon-1B were significantly lower than the overall average of all chromosomes in Langdon at these locations (p values = 0.02 and 0.0001, respectively). Welch's t test (N=50). (NS p>0.05/ *0.05≥ p > 0.005/ **0.005> p > 0.0005/ ***p < 0.0005).

In diploid *Ae. speltoides*, the mean chiasma frequency of chromosome BB-1B at distal regions (0.84±0.1) was significantly lower than the overall average of all chromosomes in this location (1.44±0.03) (p value <0.0001). Nevertheless, the mean chiasma frequency of chromosome BB-1B at interstitial region 1 (0.62±0.07) was significantly higher than the overall average of all chromosomes in this location (0.28±0.02) (p value = 0.001) (figure 4.89).

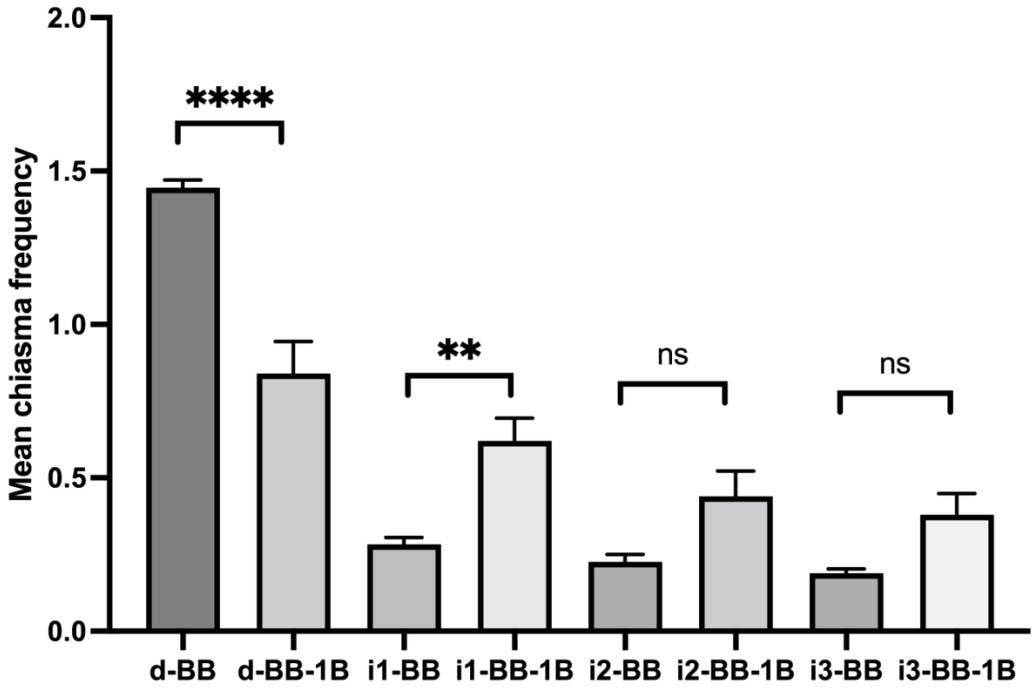

Figure 4.89: Comparison of the mean chiasma frequency of *Ae. speltoides* BB-1B and the overall average of chromosomes in BB in different chromosome localizations. In diploid *Ae. speltoides*, the mean chiasma frequency of chromosome BB-1B at distal regions was significantly lower than the overall average of all chromosomes in this location (p value <0.0001). Nevertheless, the mean chiasma frequency of chromosome BB-1B at interstitial region 1 was significantly higher than the overall average of all chromosomes in this location (p value = 0.001)**.** Welch's t test (N=50). (NS p>0.05/ *0.05≥ p > 0.005/ **0.005> p > 0.0005/ ***p < 0.0005).

4.2.3.9 Chromosome 5B

The mean chiasma frequency of CS-5B at interstitial region 1 (i^1) (0.1±0.04) was significantly lower than the overall average of all chromosomes in this location (0.32±0.02) (p value = 0.0003). Nevertheless, the mean chiasma frequency of CS-5B at interstitial region 3 (i^3) (0.58±0.07) was significantly higher than the overall average of all chromosomes in this location (0.21± 0.01) (p value <0.0001) (figure 4.90).

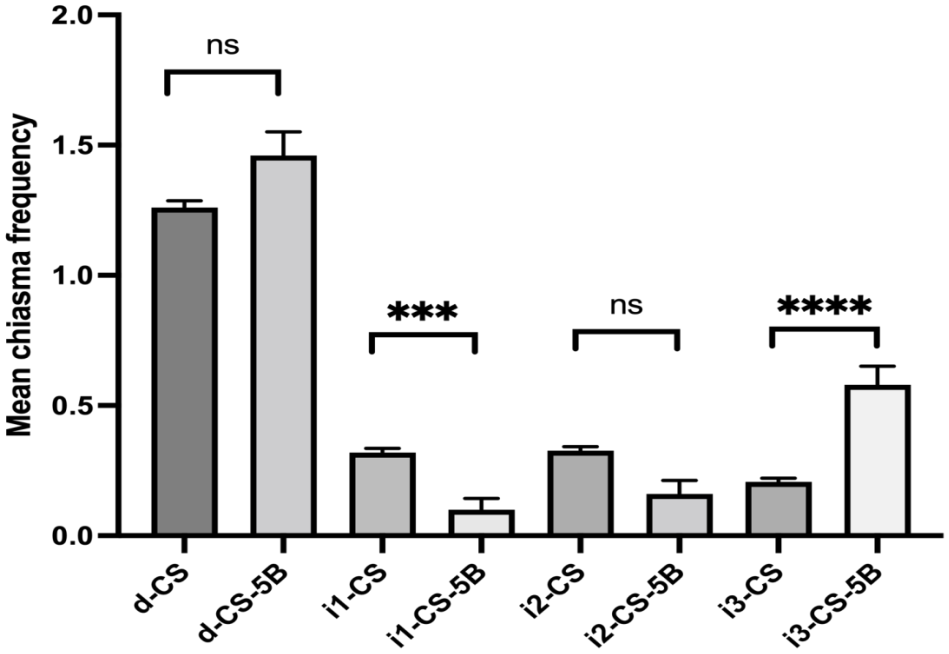

Figure 4.90: Comparison of the mean chiasma frequency between CS-5B and the overall average of all chromosomes in CS at different localizations. The mean chiasma frequency of CS-5B at interstitial region 1 (i1) was significantly lower than the overall average of all chromosomes in this location (p value = 0.0003). Nevertheless, the mean chiasma frequency of CS-5B at interstitial region 3 (i3) was significantly higher than the overall average of all chromosomes in this location (p value <0.0001). Welch's t test (N=50). (NS p>0.05/ *0.05≥ p > 0.005/ **0.005> p > 0.0005/ ***p < 0.0005).

The mean chiasma frequency of Cadenza-5B at distal regions (d) (1.1±0.09) was significantly lower than the overall average of all chromosomes in this location (1.45± 0.02) (p value = 0.004). Nevertheless, the mean chiasma frequency of Cadenza-5B at interstitial regions 1 and 3 (i^1, i^3) (0.42±0.08 and 0.32±0.06) as well as proximal regions (p) (0.2±0.05) were significantly higher than the overall average of all chromosomes in this location in Cadenza (0.21± 0.01, 0.09± 0.01 and 0.07± 0.01) (p value = 0.003 and 0.02) (figure 4.91).

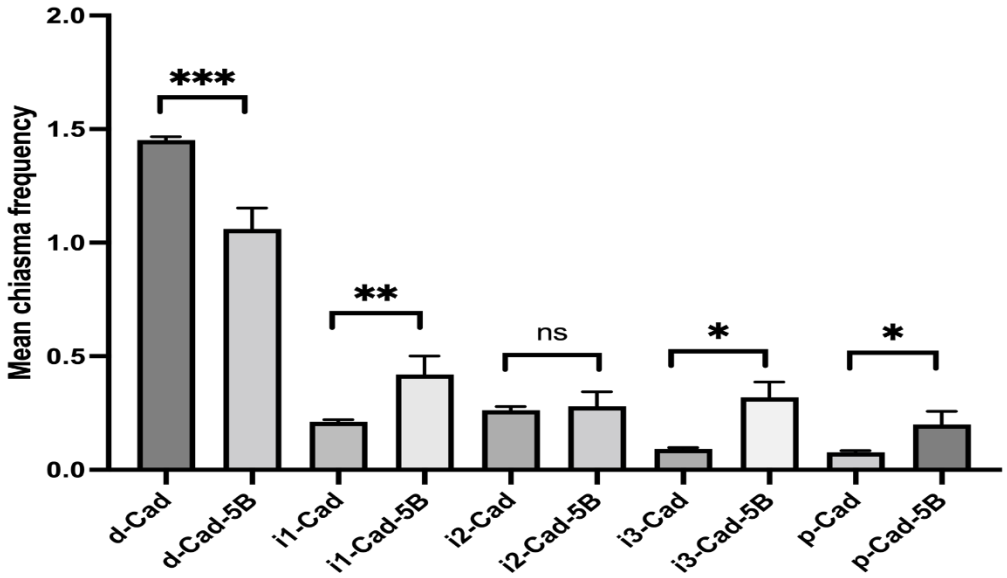

Figure 4.91: Comparison of the mean chiasma frequency in Cadenza-5B and the overall average in all chromosomes in Cadenza at different chromosome localizations. The mean chiasma frequency of Cadenza-5B at distal regions (d) was significantly lower than the overall average of all chromosomes in this location (p value = 0.004). Nevertheless, the mean chiasma frequency of Cadenza-5B at interstitial regions 1 and 3 (i1, i3) as well as proximal regions (p) were significantly higher than the overall average of all chromosomes in this location in Cadenza (p value = 0.003 and 0.02). Welch's t test (N=50). (NS $p>0.05$/ *$0.05\geq p > 0.005$/ **$0.005> p > 0.0005$/ ***$p < 0.0005$).

The mean chiasma frequency of Paragon-5B at interstitial region 3 (i^3) (0.4 ± 0.06) was significantly higher than the overall average of all chromosomes in this location (0.13 ± 0.01) (p value = 0.0004) (figures 4.92).

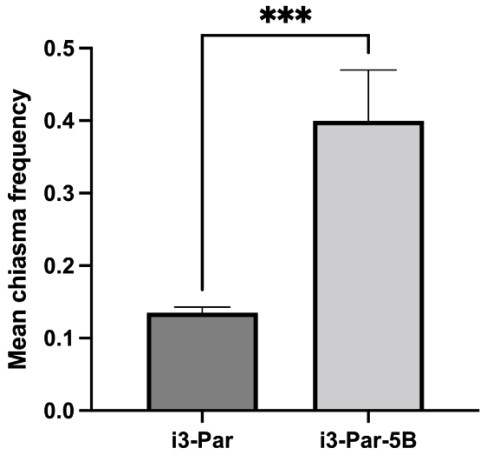

Figure 4.92: Comparison of the mean chiasma frequency in an interstitial region 3 (i^3) in Paragon-5B and the overall average of all chromosomes in Paragon in these locations. The mean chiasma frequency of Paragon-5B at interstitial region 3 (i3) was significantly higher than the overall average of all chromosomes in this location (p value = 0.0004). Welch's t test (N=50). (NS p>0.05/ *0.05≥ p > 0.005/ **0.005> p > 0.0005/ ***p < 0.0005).

The mean chiasma frequencies of Fielder-5B at distal (0.84±0.1) and interstitial region 1 (i^1) (0.18±0.05) were significantly lower than the overall average of all chromosomes in these locations (1.1±0.02 and 0.33± 0.02) (p values 0.01 and 0.007, respectively) (figure 4.93).

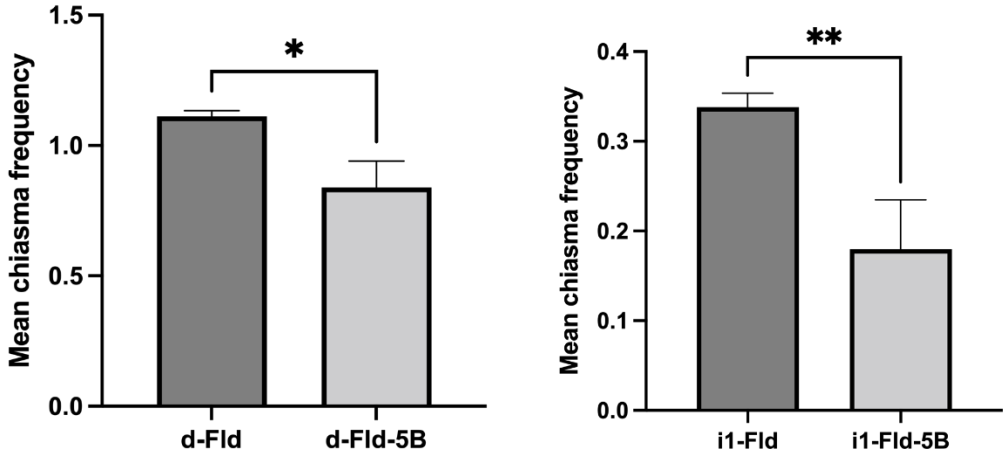

Figure 4.93: Comparison of the mean chiasma frequency in distal and interstitial region 1 (d and i^1) Fielder-5B and the overall average of all chromosomes in Fielder. The mean chiasma frequencies of Fielder-5B at distal and interstitial region 1 (i1) were significantly lower than the overall average of all chromosomes in these locations (p values 0.01 and 0.007, respectively). Welch's t test (N=50). (NS p>0.05/ *0.05≥ p > 0.005/ **0.005> p > 0.0005/ ***p < 0.0005).

The mean chiasma frequency of Kronos-5B at distal regions (d) (0.84±0.1) was significantly lower than the overall average of all chromosomes in this location (1.2±0.02) (p value = 0.001) (figures 4.94).

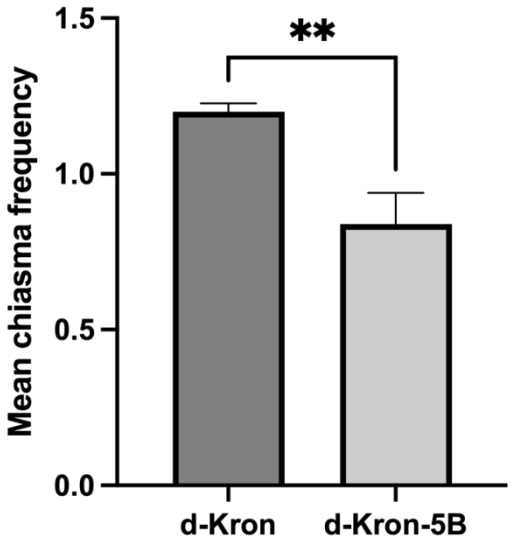

Figure 4.94: Comparison of the mean chiasma frequency at distal regions (d) Kronos-5B and the overall average in all chromosomes in Kronos. The mean chiasma frequency of Kronos-5B at distal regions (d) was significantly lower than the overall average of all chromosomes in this location (p value = 0.001). Welch's t test (N=50). (NS p>0.05/ *0.05≥ p > 0.005/ **0.005> p > 0.0005/ ***p < 0.0005).

The mean chiasma frequencies of Cappelli-5B at all different localizations were not significantly different than the overall average of all chromosomes in these locations.

The mean chiasma frequency of Langdon-5B at distal regions (d) (1.08±0.11) was significantly lower than the overall average of all chromosomes in this location (1.36±0.02) (p value = 0.01) (figures 4.95).

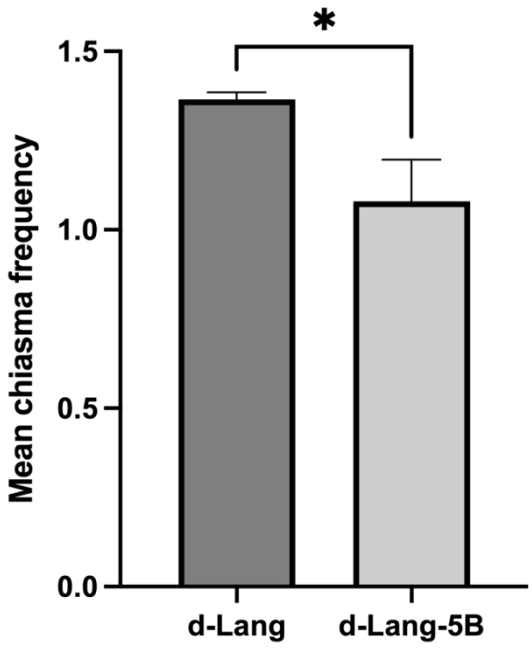

Figure 4.95: Comparison of the mean chiasma frequency at distal regions (d) in Langdon-5B and the overall average of all chromosomes in Langdon. The mean chiasma frequency of Langdon-5B at distal regions (d) was significantly lower than the overall average of all chromosomes in this location (p value = 0.01). Welch's t test (N=50). (NS p>0.05/ *0.05≥ p > 0.005/ **0.005> p > 0.0005/ ***p < 0.0005).

In *Ae. speltoides* (BB), no chiasmata were observed for chromosome 5B in interstitial regions 2 and 3 as well as proximal regions (i^2, i^3 and p), whereas the overall average in the rest of chromosomes showed some chiasmata occurring at these locations.

4.2.3.10 Chromosome 1D

The mean chiasma frequencies of CS-1D at interstitial regions 2 and 3 (i^2 and i^3) (0.14±0.05 and 0.06±0.03) were significantly lower than the overall average of all chromosomes in these locations (0.32± 0.01 and 0.21± 0.01) (p values = 0.0007 and 0.0002, respectively) (figure 4.96).

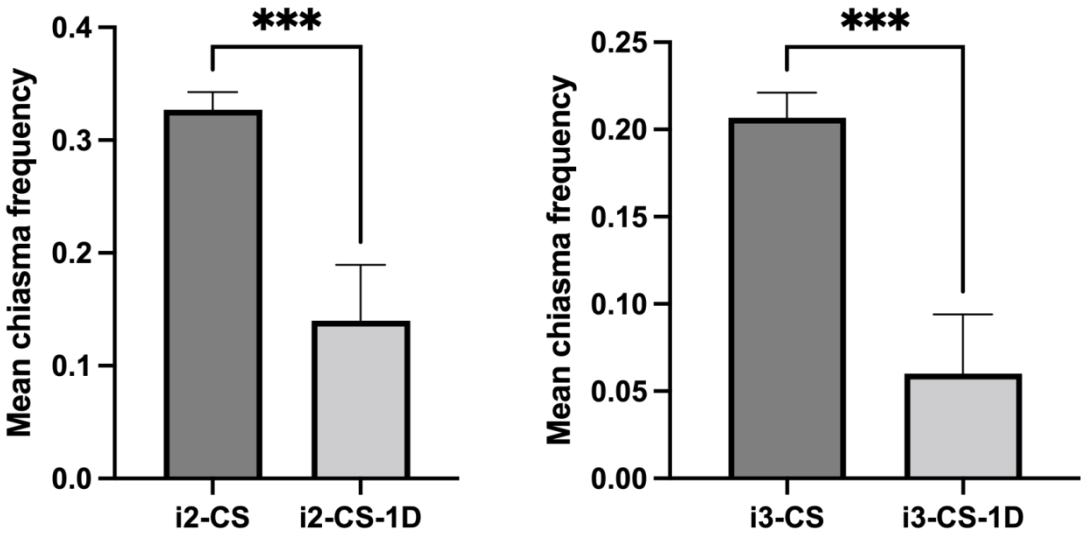

Figure 4.96: Comparison of the mean chiasma frequency at interstitial regions 2 and 3 (i^2 and i^3) in CS-1D and the overall average of all chromosomes in CS. The mean chiasma frequencies of CS-1D at interstitial regions 2 and 3 (i2 and i3) were significantly lower than the overall average of all chromosomes in these locations (p values = 0.0007 and 0.0002, respectively)**.** Welch's t test (N=50). (NS p>0.05/ *0.05≥ p > 0.005/ **0.005> p > 0.0005/ ***p < 0.0005).

The mean chiasma frequencies of Cadenza-1D at different regions were not significantly different to the overall average of all chromosomes in these locations in Cadenza.

The mean chiasma frequency of Paragon-1D at interstitial region 1 (i^1) (0.5±0.07) was significantly higher than the overall average of all chromosomes in this location (0.25± 0.02) (p value = 0.002). However, the mean chiasma frequencies of Paragon-1D at interstitial regions 2 and 3 (i^2 and i^3) (0.08±0.03 and 0.04±0.02) were significantly lower than the overall average of all chromosomes in these locations (0.335± 0.02 and 0.135± 0.01) (p values<0.0001 and 0.001) (figure 4.97).

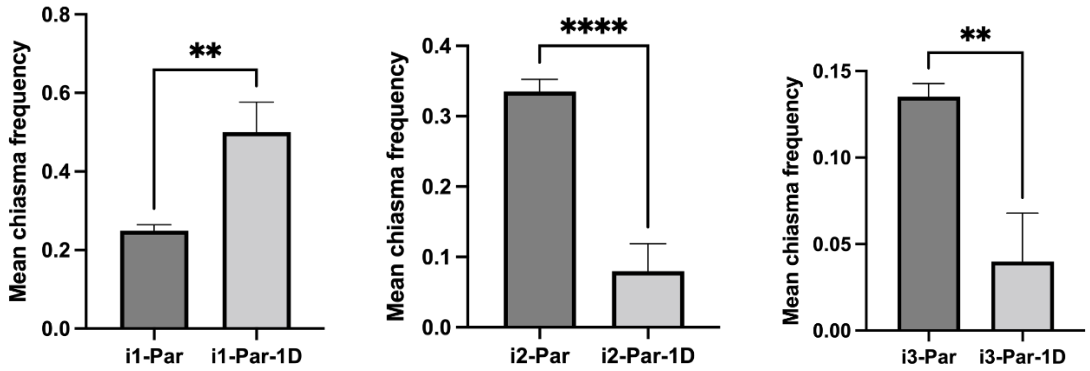

Figure 4.97: Comparison of the mean chiasma frequencies at interstitial regions 1, 2 and 3(i^1, i^2 and i^3) in Paragon-1D and the overall average of all chromosomes in Paragon. The mean chiasma frequency of Paragon-1D at interstitial region 1 (i1) was significantly higher than the overall average of all chromosomes in this location (p value = 0.002). However, the mean chiasma frequencies of Paragon-1D at interstitial regions 2 and 3 (i2 and i3) were significantly lower than the overall average of all chromosomes in these locations (p values<0.0001 and 0.001). Welch's t test (N=50). (NS p>0.05/ *0.05≥ p > 0.005/ **0.005> p > 0.0005/ ***p < 0.0005).

The mean chiasma frequency of Fielder-1D at proximal regions (p) (0.34±0.0.6) was significantly higher than the overall average of all chromosomes in this location (0.1±0.01) (p value = 0.001) (figures 4.98).

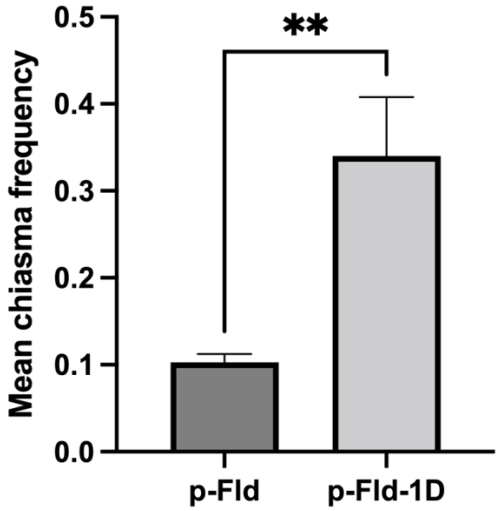

Figure 4.98: Comparison of the mean chiasma frequencies at proximal region in Fielder-1D and the overall average of all chromosomes in Fielder. The mean chiasma frequency of Fielder-1D at proximal regions (p) was significantly higher than the overall average of all chromosomes in this location (p value = 0.001). Welch's t test (N=50). (NS p>0.05/ *0.05≥ p > 0.005/ **0.005> p > 0.0005/ ***p < 0.0005).

The mean chiasma frequency of diploid *Ae. tauschii* (DD)-1D at interstitial region 1 (i^1) (0.62±0.08) was significantly higher than the overall average of all chromosomes in this location (0.36± 0.03) (p value = 0.005). However, the mean chiasma frequencies of *Ae. tauschii* (DD)-1D at interstitial regions 2 and 3 (i^2 and i^3) (0.08±0.03 and 0) and proximal (p) (0±0) were significantly lower than the overall average of all chromosomes in these locations (p values = 0.0001, <0.0001 and <0.0001, respectively) (figure 4.99).

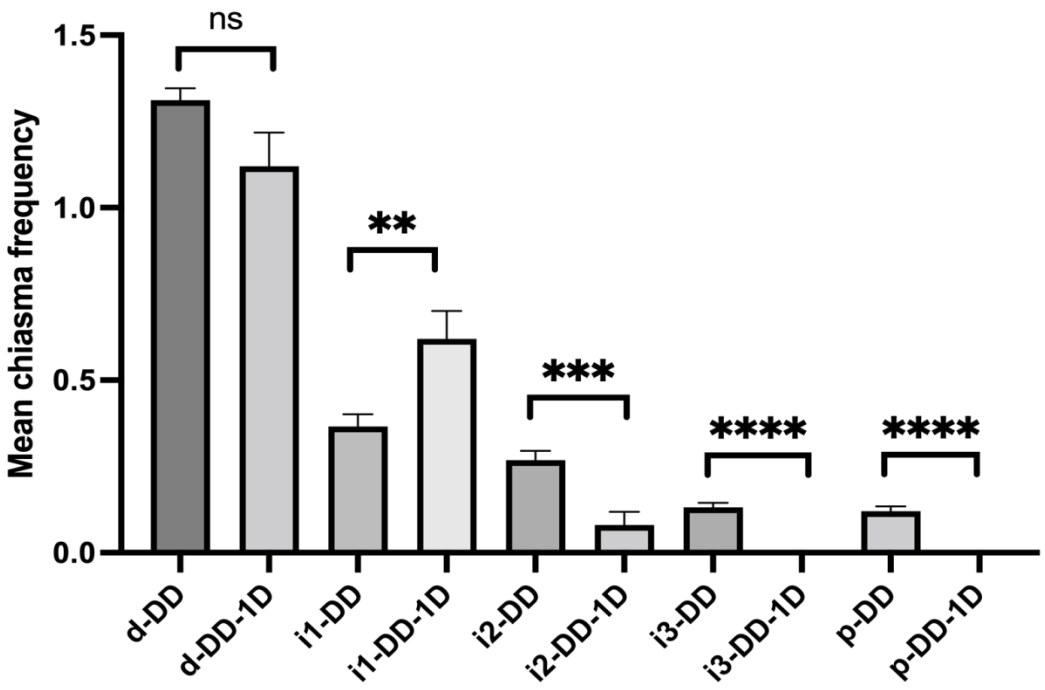

Figure 4.99: Comparison of the mean chiasma frequency in *Ae. tauschii* DD-1D and in the overall average of all chromosomes in different chromosome localizations. The mean chiasma frequency of diploid *Ae. tauschii* (DD)-1D at interstitial region 1 (i1) was significantly higher than the overall average of all chromosomes in this location (p value = 0.005). However, the mean chiasma frequencies of *Ae. tauschii* (DD)-1D at interstitial regions 2 and 3 (i2 and i3) and proximal (p) were significantly lower than the overall average of all chromosomes in these locations (p values = 0.0001, <0.0001 and <0.0001, respectively). Welch's t test (N=50). (NS p>0.05/ *0.05≥ p > 0.005/ **0.005> p > 0.0005/ ***p < 0.0005).

4.2.3.11 Chromosome 5D

The mean chiasma frequency of CS-5D at proximal regions (p) (0.42±0.07) was significantly higher than the overall average of all chromosomes in this location (0.09± 0.01) (p value <0.0001) (figure 4.100).

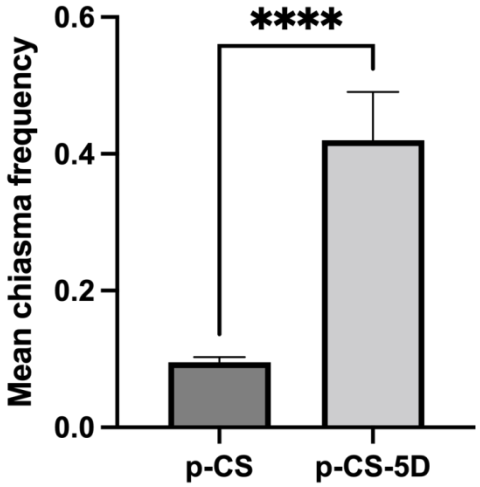

Figure 4.100: Mean chiasma frequency at proximal regions (p) of CS-5D and the overall average of all chromosomes in CS. The mean chiasma frequency of CS-5D at proximal regions (p) was significantly higher than the overall average of all chromosomes in this location (p value <0.0001). Welch's t test (N=50).

The mean chiasma frequency of Cadenza-5D at distal regions (d) (1.1±0.11) was significantly lower than the overall average of all chromosomes in this location (1.45±0.01) (p value = 0.001). Nevertheless, the mean chiasma frequencies of Cadenza-5D at interstitial regions 1 and 3 (i^1 and i^3) (0.42±0.09 and 0.24±0.06) as well as proximal regions (p) (0.32±0.06) were significantly higher than the overall average of all chromosomes in these locations (p values = 0.02, 0.01 and 0.0007, respectively) (figure 4.101).

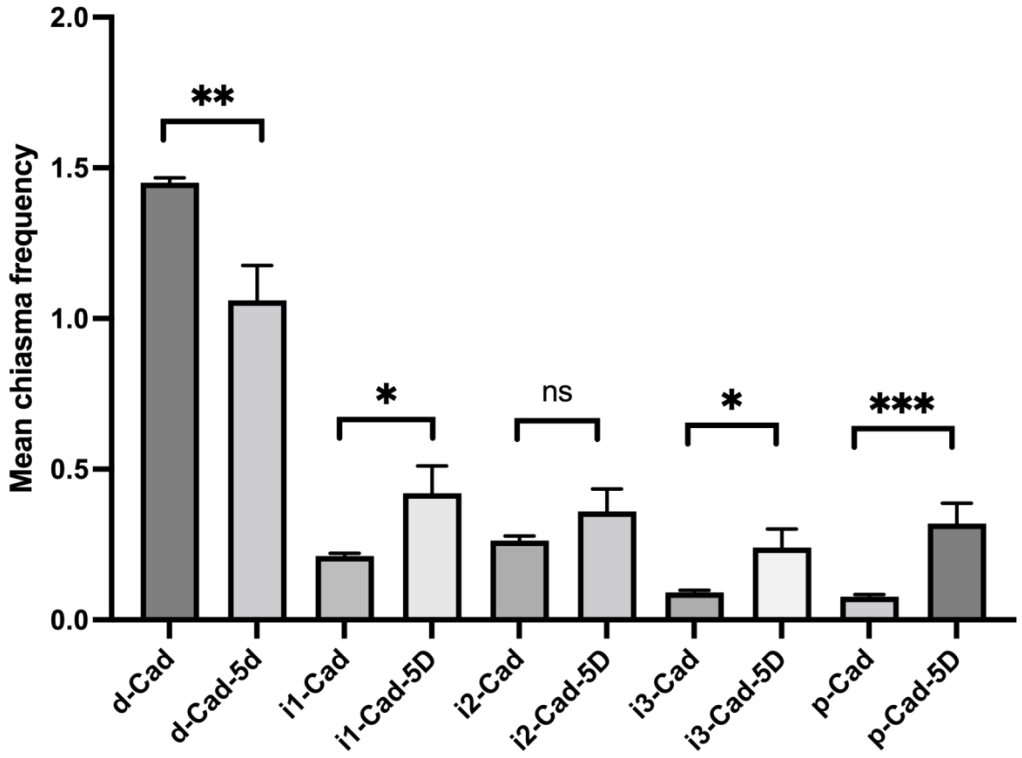

Figure 4.101: Comparison of the mean chiasma frequency of Cadenza-5D and the overall average of all chromosomes in Cadenza at different chromosome localizations. The mean chiasma frequency of Cadenza-5D at distal regions (d) was significantly lower than the overall average of all chromosomes in this location (p value = 0.001). Nevertheless, the mean chiasma frequencies of Cadenza-5D at interstitial regions 1 and 3 (i1 and i3) as well as proximal regions (p) were significantly higher than the overall average of all chromosomes in these locations (p values = 0.02, 0.01 and 0.0007, respectively). Welch's t test (N=50). (NS $p>0.05$/ *$0.05\geq p > 0.005$/ **$0.005> p > 0.0005$/ ***$p < 0.0005$).

The mean chiasma frequency of Paragon-5D at distal regions (d) (0.96 ± 0.1) was significantly lower than the overall average of all chromosomes in this location (1.3 ± 0.02) (p value = 0.002). Nevertheless, the mean chiasma frequencies of Paragon-5D at interstitial region 3 (i^3) (0.34 ± 0.06) as well as proximal regions (p) (0.28 ± 0.06) were significantly higher than the overall average of all chromosomes in these locations (p values = 0.004 and 0.01, respectively) (figure 4.102).

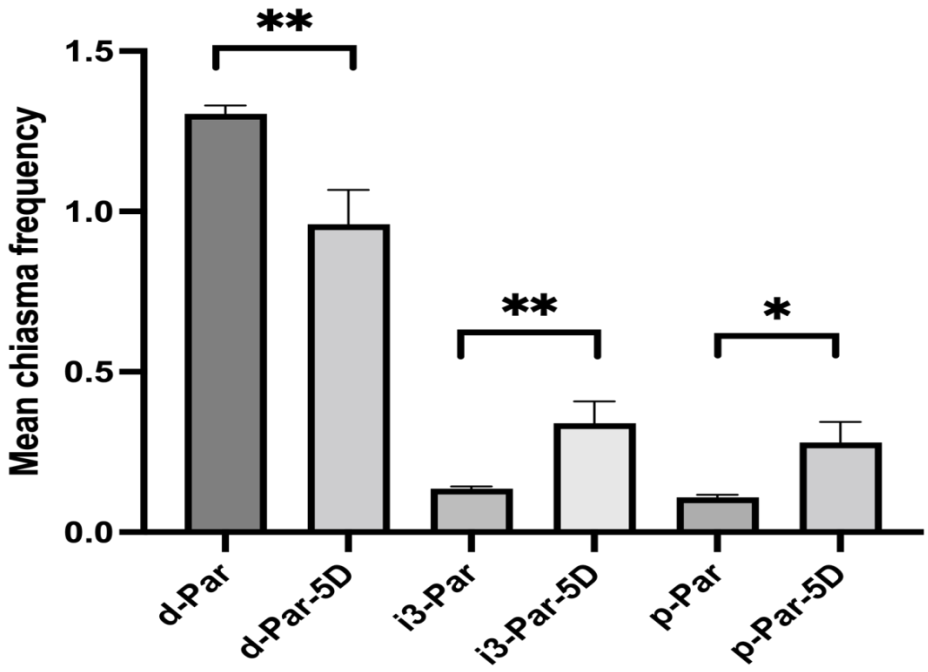

Figure 4.102: Comparison of the mean chiasma frequency at distal, interstitial region 3 and proximal regions (d,i^3 and p) in Paragon-5D and the overall average of all chromosomes in Paragon. The mean chiasma frequency of Paragon-5D at distal regions (d) was significantly lower than the overall average of all chromosomes in this location (p value = 0.002). Nevertheless, the mean chiasma frequencies of Paragon-5D at interstitial region 3 (i3) as well as proximal regions (p) were significantly higher than the overall average of all chromosomes in these locations (p values = 0.004 and 0.01, respectively). Welch's t test (N=50). (NS p>0.05/ *0.05≥ p > 0.005/ **0.005> p > 0.0005/ ***p < 0.0005).

The mean chiasma frequencies of Fielder-5D at interstitial region 3 (i^3) (0.44±0.07) as well as proximal regions (p) (0.28±0.06) were significantly higher than the overall average of all chromosomes in these locations (p values = 0.006, and 0.008, respectively) (figure 4.103).

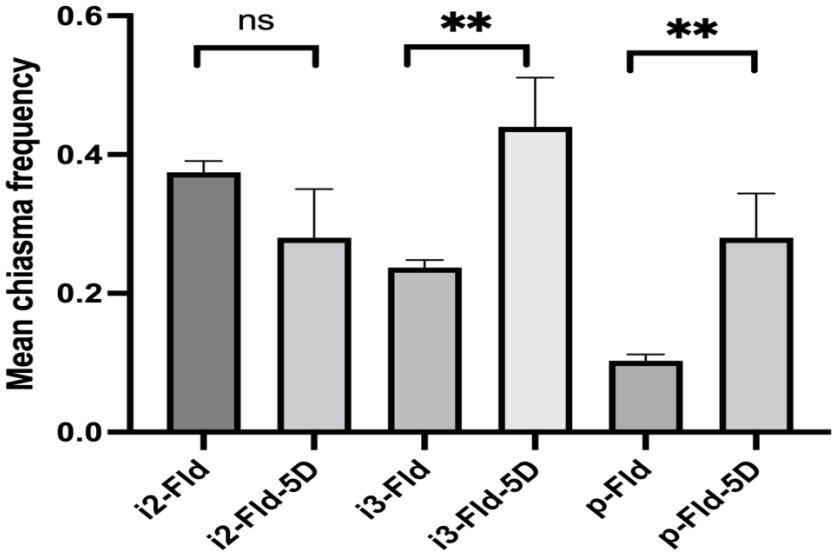

Figure 4.103: Comparison of the mean chiasma frequency at different interstitial 2 and 3 regions and proximal regions (i^2, i^3 and p) in Fielder-5D and the overall average of all chromosomes in Fielder in these locations. The mean chiasma frequencies of Fielder-5D at interstitial region 3 (i3) as well as proximal regions (p) were significantly higher than the overall average of all chromosomes in these locations (p values = 0.006, and 0.008, respectively). Welch's t test (N=50).

The mean chiasma frequency of diploid *Ae. tauschii* DD-5D at distal regions (d) (0.74±0.09) was significantly lower than the overall average of all chromosomes in this location (1.31± 0.03) (p value <0.0001). Nevertheless, the mean chiasma frequency of DD-5D at interstitial region 2 (i^2) (0.56±0.07) was significantly higher than the overall average of all chromosomes in this location (0.26± 0.02) (p value = 0.0003) (figure 4.104).

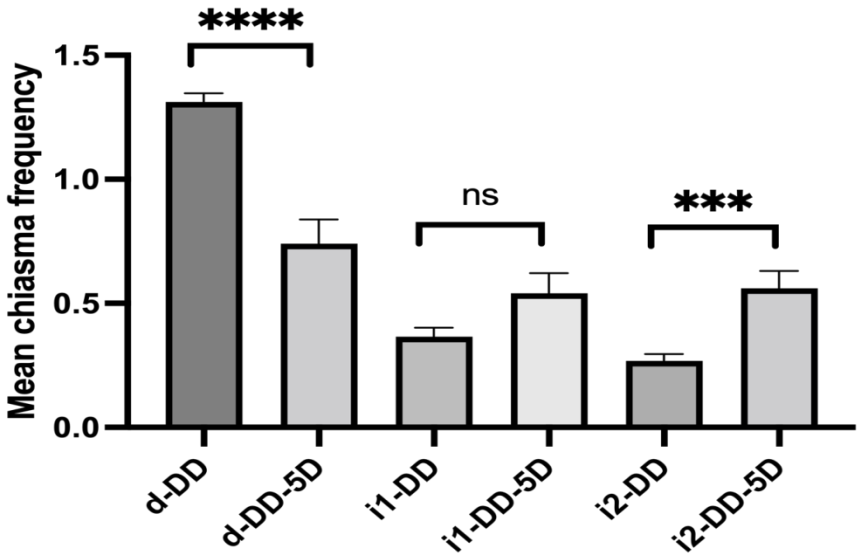

Figure 4.104: Comparison of the mean chiasma frequency at distal and interstitial regions 1 and 2 (d, i^1 and i^2) in *Ae. tauschii* DD-5D and the overall average of all chromosomes at these locations. The mean chiasma frequency of diploid *Ae. tauschii* DD-5D at distal regions (d) was significantly lower than the overall average of all chromosomes in this location (p value <0.0001). Nevertheless, the mean chiasma frequency of DD-5D at interstitial region 2 (i2) was significantly higher than the overall average of all chromosomes in this location (p value = 0.0003). Welch's t test (N=50). (NS p>0.05/ *0.05≥ p > 0.005/ **0.005> p > 0.0005/ ***p < 0.0005) (N=50).

4.3 Discussion

4.3.1 Meiotic Recombination in Wheat species: systematic chiasma frequency comparisons.

In this thesis we have analyzed meiotic recombination in different wheat species from different ploidy levels, the mean chiasma frequency was analyzed in 4 different cultivars in hexaploid wheat (CS, Cad, Pg, Fld), 3 different cultivars in tetraploid wheat (Kr, Cap, Lnd) and 3 diploid species closely related to the A (*T. monococcum*), B (*Ae. speltoides*) and D (*Ae. tauschii*) genome ancestors. Metaphase I bivalent configurations were identified and chiasmata number and localization quantified in all the different materials. Chiasmata analysis have been broadly used as an evaluating approach to analyze recombination events across the whole genome and within each chromosome (Sanchez Moran et al., 2001, Sanchez-Moran et al., 2002, Sybenga, 2012, Sybenga, 1975). In *Arabidopsis*, analysis of the mean chiasma frequency in accession were conducted (Sanchez-Moran et al., 2001). The author found out that mean chiasma frequency was significantly difference between them. A later analysis of the comparison of the mean chiasma frequency between nine *Arabidopsis* accession was conducted (Lopez et al., 2011). The author found out that the mean chiasma frequency between the nine accession were significantly difference. A recent study in three accession in *Arapidopsis* (two wild type and one hybrid) shows that the mean chiasma frequency of accession Col were significantly higher compare to accession Ler (Parra-Nunez et al., 2018). The author explains that in Col/Ler hybrid the mean chiasma frequency was statistically difference compare to Col and Ler means. In wheat, there has been different mean chiasma frequency reported in different emmer tetraploid wheats (Patil and Deodiker, 1972) and hexaploid wheats and their hybrids (Driscoll *et al*., 1979). In these two studies the significant differences were observe between different wheat species and their hybrids. However, these tetraploid and hexaploid wheat studies were conducted to analyse

differences among different species such as *T. durum, T. turgidum, T. dicoccum* and others without any emphasis in the comparison of the mean chiasma frequency within each species and ploidy level and chiasma localization within them.

In this work, it has been observed that different wheat varieties from the same ploidy level showed significant differences in the mean chiasma frequency and chiasmata localization. This is consistence to have been observed in *Arabidopsis* (Sanchez-Moran et al., 2001; Lopez et al., 2011) and in wheat (Driscoll et al., 1979). Thus, in this analysis, it is found that hexaploid cultivars CS showed the highest mean chiasma frequency and that the chiasmata location was more widely distributed along the chromosomes with higher numbers of interstitial and proximal chiasmata compared to Cadenza and Paragon. In fact, Cadenza and Paragon both are UK wheat and both shows almost the same mean chiasma frequency with no significant differences reported between them. This is consistent to what have been reported in the two related *Arabidopsis* accession Pro-0 and Sol-0 (Lopez et al., 2011) with no significant differences reported between them. Additionally, tetraploid cultivar Cap showed the highest mean chiasma frequency being significantly different to the mean in Kr. Moreover, chiasmata localization in Cap showed more broadly distributed recombination along the chromosome arms with more interstitial and proximal chiasmata compared to Kr. It is worth to mention that tetraploid and hexaploid wheats evolve in genome duplication following hybridization and this might affect in several genetic rearrangement and change in the genome contents which might directly or indirectly affect the CO/chiasmata number in both of them. Surprisingly, the three diploid species supposed to be closely related to the ancestral donors of the wheat genomes (*T. monococcum* (AA), *Ae. speltoides* (BB) and *Ae. tauschii* (DD)) did not show any significant differences on mean chiasma frequency between each other. This might be due to the genome stabilisation (not involve in hybridisation or duplication) which result in non-significant differences between them in the mean chiasma frequency analysis.

It is important to highlight that the majority of chiasmata in all wheat species from different ploidy level are localized to the distal regions of the chromosome and they are far more abundant than interstitial and proximal chiasmata. Remarkably, interstitial and proximal chiasmata could be observed in ring bivalents in both chromosome arms in some wheat cultivars but not in others (e.g.: presence in CS but not in Cad). Wheats with more interstitial and proximal chiasmata (such SC and Cappelli) will be useful cultivars for plant breeder in terms of having more meiotic recombination compare to the other wheat cultivars also in terms of using them in an introgression process with wild relatives' species.

4.3.2 Differences in chiasma frequency and distribution on specific chromosomes labelled by FISH among different ploidy levels

Applying FISH with 45S and 5S rDNA probes to the wheat chromosomes allowed us to identify specific chromosomes in the different species studied: 5A, 1B, 5B, 6B, 1D and 5D in hexaploid *T. aestivum* (AABBDD) cultivars (CS, Cad, Pag, Fld); 5A, 1B, 5B and 6B in tetraploid *T. durum* (AABB) cultivars (Kr, Cap, Lnd); 1A and 5A in diploid *T. monococcum* (AA); 1B and 5B in diploid *Ae. speltoides* (BB); 1D and 5D in diploid *Ae. tauschi* (DD) Mean chiasma frequency in specific chromosomes labelled by 45S and 5S FISH probes has been carried out before in Arabidopsis and barley (Higgins et al., 2012, Sanchez-Moran et al., 2002). For instance, in *Arabidopsis*, it is found that the mean chiasma frequency in chromosome 1 was higher whereas chromosome 2 and 4 showed the lowest mean chiasma frequency (Sanchez-Moran et al., 2001, Sanchez-Moran et al., 2002). In wheat hybrids, the analysis of meiotic recombination of chromosomes has been done by using C-banding (Rodriguez *et al*., 2000).

Analyzing the mean chiasma frequency in specific chromosomes in wild type wheat cultivars has revealed significant differences among them. This result is consistence to what have been reported in

Arapidopsis (Lopez et al., 2011; Parra-Nunez et al., 2018; Sanchez-Moran et al., 2001). For instance, chromosome 5B has showed a significant difference between CS and Fld in hexaploid wheat and between Cap and Kr in tetraploid wheat. Additionally, the mean chiasma frequency of chromosome 5B in ring and rod bivalents showed significant differences between different wheat cultivars from the same and different ploidy levels. For instance, Cap showed the highest mean of chiasma frequency in ring bivalent whereas Fld showed the lowest mean of chiasma frequency for chromosome 5B. In contrast, tetraploid cultivar Fld (AABB) showed the highest mean chiasma frequency in rod bivalents whereas the diploid *Ae. speltoides* (BB) showed the lowest mean of chiasma frequency. The exact reasons that cause differences in the mean chiasma frequency in different wheats cultivars and in their individual chromosome were not known but different possible reasons could be discussed.

4.3.3 Possible reasons causing differences in the mean chiasma frequency

There are some possible reasons that might cause differences in the mean chiasma frequency like how the origin of these cultivars might have an impact in the meiosis progression on them. For instance, CS is well known to be used as a laboratory hexaploid model whereas Cadenza has been used more in breeding programs in field trials. Environmental conditions in labs and fields are very different, and the evolution of these two cultivars might have been very different in the last century. In a field with different abiotic and biotic stresses Cadenza might have evolved differently than CS and this could have had an impact in meiotic recombination among other things. Additionally, being in a field with an open pollination system might lead to introgression with other plants and that might have important effects to the meiotic recombination. In this study, some multivalents (trivalents and quadrivalents) and univalents appeared in some individual spikes in Cadenza whereas no multivalents or univalents were observed in CS (figure 4.79). The data showed in this thesis for the cultivar

Cadenza was obtained from plants not showing multivalents or univalents but the presence of these configurations at metaphase I in some plants might be showing different chromosome rearrangements among the Cadenza cultivar chromosomes which could have an impact in meiotic recombination.

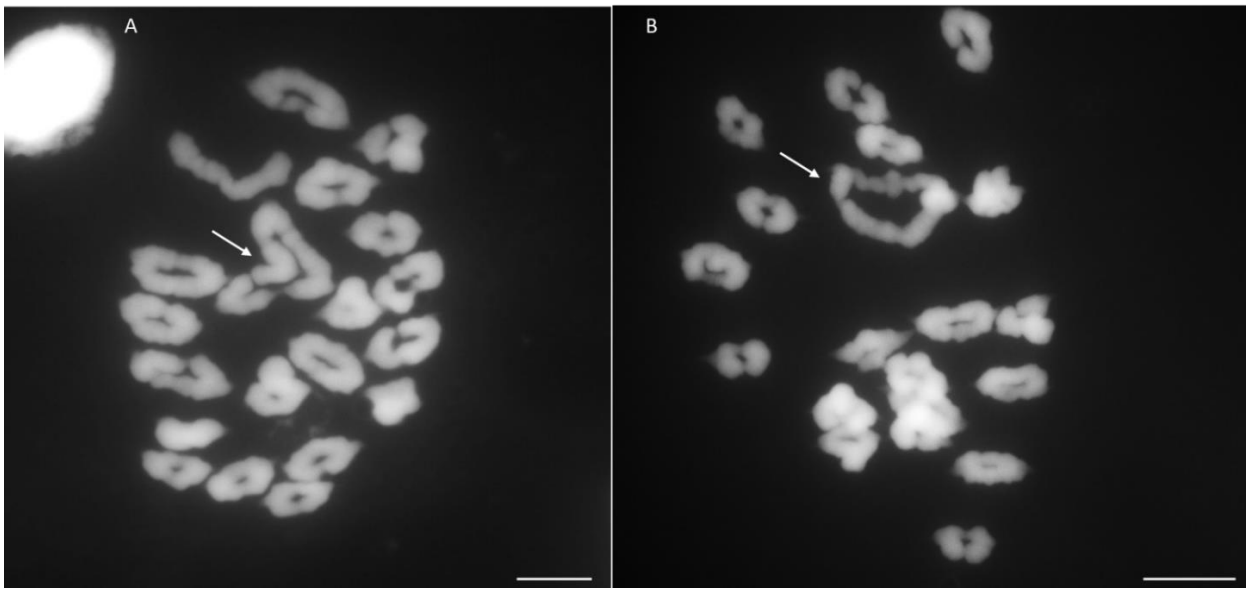

Figure 4.105: Microphotographs of Cadenza pollen mother cells at metaphase I with multivalents (quadrivalents indicated by an arrow). DAPI staining of chromosomes. Scale bar = 10µm.

Chromatin condensation has also been reported to play an important role in meiotic recombination and chiasmata formation (Choi *et al*., 2013). It is thought that chromatin architecture allows the activation of meiotic protein in euchromatinic regions rather than heterochromatinic regions (Choi *et al*., 2013). In wheat COs hotspots have been identified to be associated with sub-class II DNA transposons such as *Mariner* and *Mutator* and euchromatin H3K27me3 (Darrier *et al*., 2017; Tock *et al*., 2021). Thus, it is possible that chromatin condensation and different genome components such as DNA transposons, repetitive sequences, DNA methylation, euchromatin and heterochromatin play important roles in CO formation in wheat. It could be possible that different localization of these components along the different chromosome regions in different cultivars could lead to changes in

meiotic recombination in these regions. It is possible that the whole genome sequence in different wheat cultivars could facilitate the identification of some of these elements that could explain the differences in chiasmata localization observed on these cultivars. A recent whole genome sequence in hexaploid wheat cultivar CS has been published (Consortium *et al*., 2018). Thus, the whole genome sequence of the other wheat cultivars could allow in a near future the analysis and comparison of all these elements and their effect in meiotic recombination.

Chapter 5. Manipulating Meiotic Recombination in Wheats

5.1 Introduction

The meiotic recombination process is tightly controlled in plants. From over hundreds or even thousand DSBs, only 10-15% of them are processed into COs producing a restricted number of chiasmata (1-3) per chromosome pair. In Arabidopsis (2n=10), ~150 DSBs are formed in early prophase I and only ~10 COs were formed at late prophase I (Sanchez-Moran *et al*., 2007). Whereas, in hexaploid wheat (2n=6X=AABBDD=42), ~2,000 DSBs are formed but only produce ~42 COs (Osman *et al*., 2021). Additionally, in cereals such as wheat, barley and rye these COs seem to accumulate around the distal regions of the chromosomes (close to telomeres) which provides a linkage-drag to the plant breeders. Based on these limitations of the number and localization of COs, it is necessary to be able to attempt different methodologies to manipulate meiotic recombination in plants such as cereals. This seems to be a high priority for the plant breeders. In plants, meiotic recombination can be manipulated by several strategies such as: i) altering abiotic stresses; ii) manipulating epigenetic factors; iii) overexpression and/or down-regulation (mutations) of meiotic proteins; iv) chemical manipulation (inhibition/induction).

Abiotic stresses such as temperature has revealed to produce a significant change in chiasma location. For instance, increasing temperature to 28^{o}C has showed an increase in recombination frequency in *Arabidopsis* (Francis *et al*., 2007). Additionally, in barley increasing temperature resulted in the redistribution of the chiasmata from distal to more interstitial regions (Higgins *et al*., 2012). Moreover, in wheat a recent study has revealed that altering temperature resulted in significant differences in recombination frequency (Coulton *et al*., 2020).

Moreover, altering epigenetic factors has been also used in plant meiosis. Yelina and collaborators (2012) by mutating CG Methyltransferase 1 (MET1) in Arabidopsis obtained a significant increase in COs in euchromatic regions. In contrast, mutation of non-CG chromomethylase (CMT3) and

histone 3 lysine 9 demethylation (H3K9me2) resulted in a significant increase in COs in proximal regions (Underwood *et al*., 2018). Recently, in wheat using Virus-induced gene silencing (VIGS) to mutate MET1 resulted in the redistribution of meiotic recombination in euchromatic regions with no effect on recombination to heterochromatic regions (Raz *et al.*, 2021*).*

Furthermore, another strategy of manipulating meiotic recombination that has been broadly used is down regulating anti-recombinases (e.g.: FANCM, FIGL1, RECQ4) or overexpressing proteins involved in COs formation (e.g.: HEI10). For instance, in *Arabidopsis* down regulating (mutant alleles) of anti-recombinases such as *fancm*, *figl1* and *recq4* results in an increase of COs specifically Class II COs (Crismani *et al*., 2012; Girard *et al*., 2015; Séguéla-Arnaud *et al*., 2015). In addition to this, overexpression of ZMM protein HEI10 increases the Class I COs (Ziolkowski *et al*., 2017). Furthermore, overexpression of HEI10 in combination with down regulation of anti-recombinase RECQ4 resulted in a huge increase in COs in Arabidopsis (Serra *et al*., 2018). A recent study in Arabidopsis has also reported that downregulating the SC central element protein ZYP1 can produce an increased in COs formation (Capilla-Pérez *et al*., 2021). Thus, in different plant species such as rice, pea and tomato down regulating Recq4 resulted in an increase of meiotic recombination (Mieulet *et al.*, 2018). Moreover, in brassicas down regulating Fancm also resulted in an increase of COs (Blary and Jenczewski, 2019). However, manipulating these type of meiotic proteins usually are accompanied by other meiotic abnormalities such as the appearance of univalents at metaphase I, chromosome bridges at anaphase I and/or fragmentation at metaphase I/anaphase I. Additionally, most of COs increases seem to be restricted to euchromatic distal regions with no much effect to the heterochromatic interstitial and proximal regions (Serra *et al*., 2018).

Many different approaches have been explored to manipulate meiotic recombination in the model plant species *Arabidopsis*, however plant species with a larger genome such as hexaploid wheats have not been fully explored. Because of the large genome size and the extra copies of alleles (up to six in

hexaploid wheats), it is very challenging to manipulate meiotic proteins in wheats (Da Ines *et al*., 2020). However, some small progress has been made recently in manipulating meiotic proteins in wheat. For instance, using VIGS has allowed to regulate the expression of XRCC2 (anti-recombinase) resulting in an increase of meiotic recombination in interstitial regions in tetraploid wheats (Raz *et al.,* 2021). Additionally, VIGS mutation was used to down regulate FANCM by the same authors but they didn't find any change to meiotic recombination. However, a recent study by Desjardins and collaborators (2022) indicated that *fancm* mutation resulted in ~30% increase in COs in hexaploid wheats.

Historically, an important locus in wheat that has been exploited over more than 6 decades to manipulate meiotic recombination between wheat and their wild relative species by hybridization has been the *Ph1* (Pairing homologues) locus. A *ph1* mutant was identified and characterised by Sears in 1957 and years later a similar mutant *ph2* mutant was identified by Mello-Sampayo in 1971. The *Ph* locus in wheat is responsible for the diploid-like behavior of meiotic chromosomes during metaphase I by ensuring homologous recombination and preventing homoeologous recombination during meiosis. *Ph1* locus is localized in the long arm of chromosome 5B whereas the *Ph2* locus is localized in the short arm of chromosome 3D. Deletion of these two loci results in homoeologous recombination during metaphase I. Due to this phenotype, the exploitation of these mutants has been widely used in wheat breeding programs. In the absence of the *Ph1* locus, hybridization between wheat and their wild relatives such as rye allows homoeologous recombination between them during metaphase I and the exchange of genetic material (introgression). Recently, two major meiotic genes have been identified in the *Ph1* and *Ph2* loci in wheat. These genes are *Zip4* in *Ph1* (Rey *et al*., 2017; 2018) and Msh7 in *Ph2* (Serra *et al*., 2021). Additionally, CRISPR-Cas9 mutation of *TaZip4-B2* showed an identical phenotype to Sears *ph1b* mutant suggesting that TaZIP4-B2 is responsible for controlling homologous recombination and avoiding recombination among homoeologous

chromosomes (Rey *et al*., 2018). *TaZip4-B2* has been shown to play two major roles in homologous recombination, firstly by ensuring pairing and synapsis between homologous chromosomes, and secondly by preventing homoeologous recombination between non-homologous chromosomes (Martín *et al*., 2021). A recent study reported a separation-of-function mutant for ZIP4 in wheat allowing crossover between related chromosomes in hybrids but being meiotically stable in wheat. This mutation known as *Tazip4-ph1d* has normal chromosome segregation during anaphase I and can conserve full fertility (Martín *et al*., 2021). *Msh7-3D* has been identified to be a major meiotic protein involved in the *Ph2* locus (Serra *et al*., 2021). Msh7 belongs to the mismatch repair group of proteins and in Arabidopsis promotes the formation of COs by forming a heterodimer with Msh2 (Desjardins *et al*., 2022). However, wheat *msh7*-3D mutation results in an increase of homoeologous recombination (multivalent formation during metaphase I) between wheat and their wild relative *(*Serra *et al*., 2021). In conclusion, progress has been made in manipulating meiotic recombination in wheats however more analysis and characterization of meiotic proteins such as Hei10, Figl1 and Recq4 need to be further explored in wheat.

Another strategy to manipulate meiotic recombination is by using chemical inhibitors or inductors. In this chapter, we have explored the use of chemicals affecting DNA replication. The chemicals used were hydroxyurea (HU) and Suberoylanilide Hydroxyamic Acid (SAHA). HU is a widely used chemical to block DNA replication through the inhibition of ribonucleotide reductase (RNR) (Timson, 1975). The role of HU has been studied in meiosis in budding yeast and its found to inhibit the DNA replication during S-phase (Simchen *et al.*, 1976). The mechanism of HU inhibiting DNA replication is explained by the fact that HU prevents the dNTPs from association with the DNA polymerase in replication forks during the S-phase (Koç *et al*., 2004). SAHA is an inhibitor of histone deacetylase (HDACi) and is broadly applied in medicine as an anti-cancer drug (Conti *et al*., 2010). In humans SAHA has been reported to decrease the speed of replication forks and activating non-

active regions of replication (Conti *et al*., 2010). It is worth to mention that the effect of HU and SAHA in wheat meiosis is never been explored. It is already reported that in barley and wheat the early meiotic events such as pairing and synapsis seems to be synchronised with the DNA replication starting at telomeric regions and progressing towards the interstitial and proximal regions (Higgins *et al*., 2012; Osman *et al*., 2021). Thus, the treatments with HU and SAHA may result in the manipulation of DNA replication progression and could affect the spatio-temporal progression of meiosis and the distal bias of meiotic recombination.

5.2 Results

In this chapter, we have analyzed hexaploid wheat *ph1b* mutant in CS, tetraploid wheat *ph1c* in Cappelli and chromosome substitution line 5B-5D in Langdon (chromosome 5B replaced by chromosome 5D). We have analyzed the mean chiasma frequency and compared them to the wild type genomic background (CS, Cappelli and Langdon). FISH analysis using 45S and 5S rDNA probes was carried out to analyze specific chromosomes. Additionally, immunolocalisation analysis of Asy1 and Zyp1 proteins was carried out to investigate changes in the spatio-temporal progression of meiosis in these mutants. Meiotic time course analysis using BrdU, and telomere FISH with immunecytology analysis was carried out in CS *ph1b*.

Moreover, the effect of inhibitor chemicals HU and SAHA were also investigated to determine how these treatments affected the mean chiasma frequency and chiasmata localization in Cadenza (hexaploid wheat). HEI10 immunolocalization and quantification was carried out for HU treatments and compared to Cadenza wild type (WT) controls.

5.2.1 Analysis of *ph1b* mutant in hexaploid wheat

In addition to the two main configurations observed at metaphase I in the WT (rod and ring bivalents), CS *ph1b* mutant also shown univalents and multivalents at metaphase I (figure 5.1). A total of 1,000 bivalents (687 ring bivalents and 235 rod bivalents), 45 multivalents and 33 univalents (figure 5.1C). The mean chiasma frequency per cell in CS *ph1b* mutant was 36.06 $\pm$ 0.5. Comparison between mean chiasma frequency of CS *ph1b* mutant and CS WT was conducted using Welch's t test and the results showed that the mean chiasma frequency was significantly different between them with (p value <0.0001) (figure 5.2).

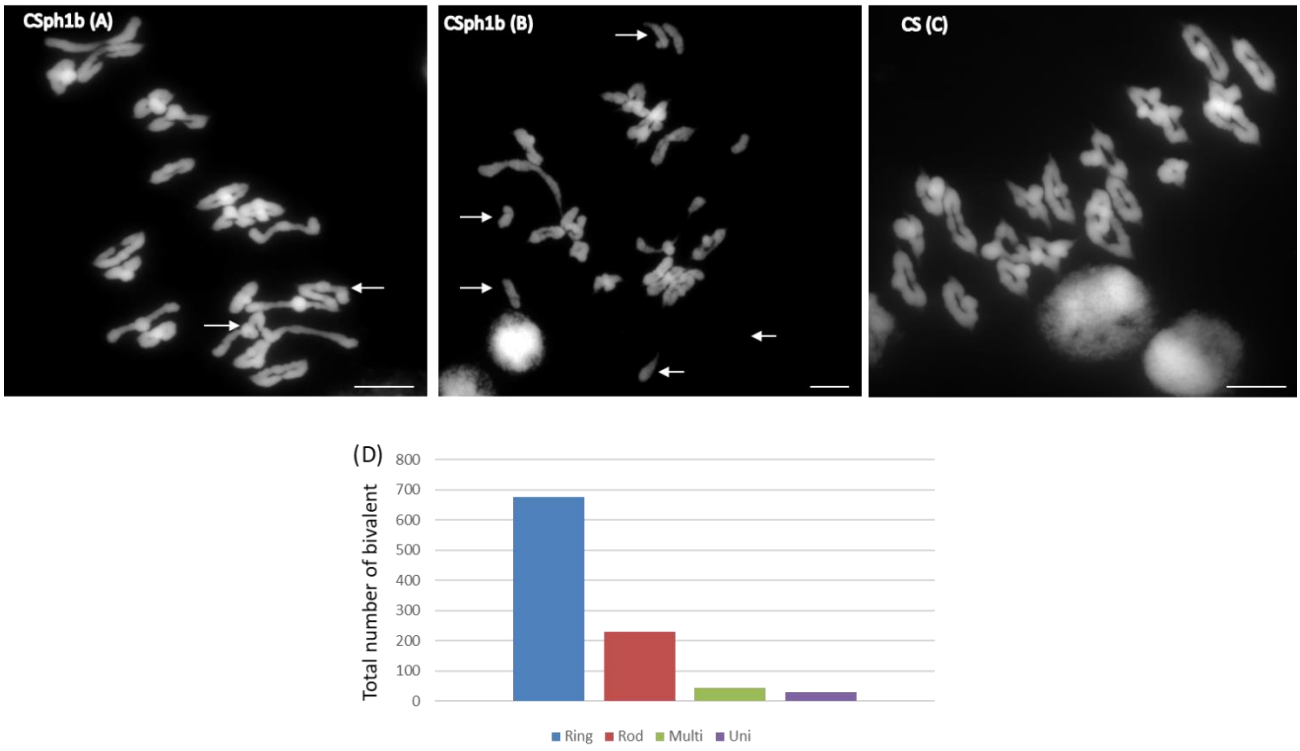

Figure 5.1: DAPI staining of CS *ph1b* mutant and CS wild type and the different configurations observed at metaphase I chromosomes. (A & B) Microphotograps of pollen mother cells at metaphase I of CS *ph1b* mutant. (A) Arrows points to multivalents. (B) Arrows point to univalents. (C) Microphotograps of pollen mother cell at metaphase I in CS wild type with only ring bivalent. (D) Diagram of total number of rings, rods, multivalents and univalents in CS *ph1b*. Scale Bar = 10µm.

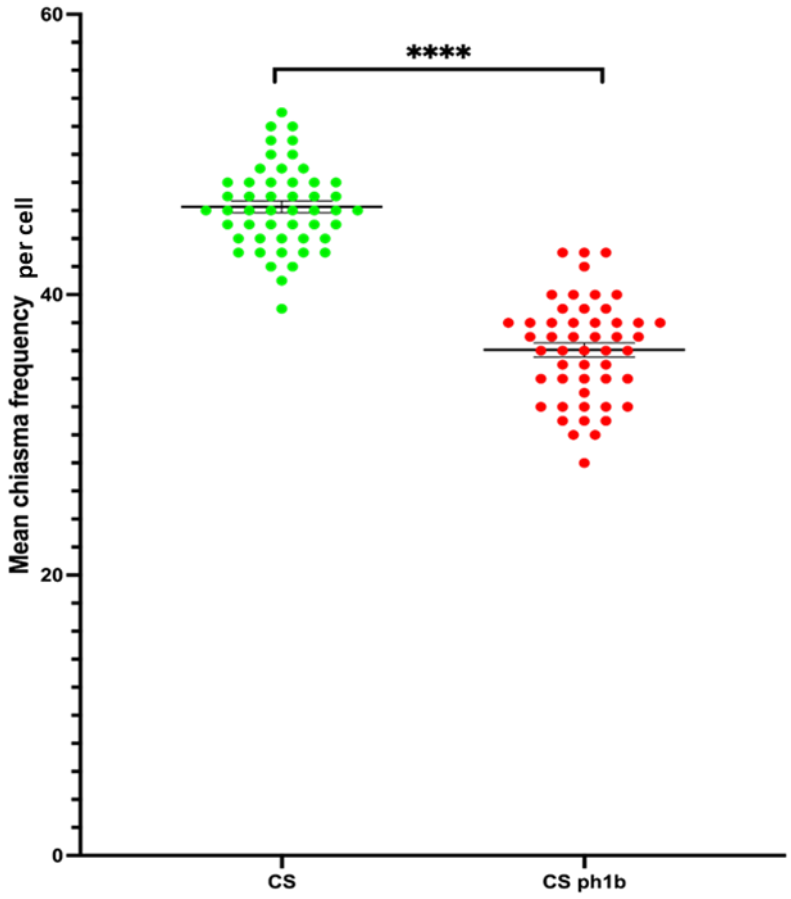

Figure 5.2: Comparison of the mean chiasma frequency per cell between CS and CS *ph1b*. The mean chiasma frequency per cell in CS *ph1b* was significantly lower compared CS WT (Welch's t test $p<0.0001$, N=50).

Chiasmata localization in CS *ph1b* is shown in figure 5.3. Most of the chiasmata appeared to be distal in rod and ring bivalents. This followed by i^1 and i^2 which both appeared to be moderate in both rod and ring bivalents. Whereas, the i^3 and p chiasmata appeared to be very low in rod and ring bivalents. In addition to this, chiasmata in interstitial and proximal region of both chromosome arms were observed in this mutant (figure 5.3).

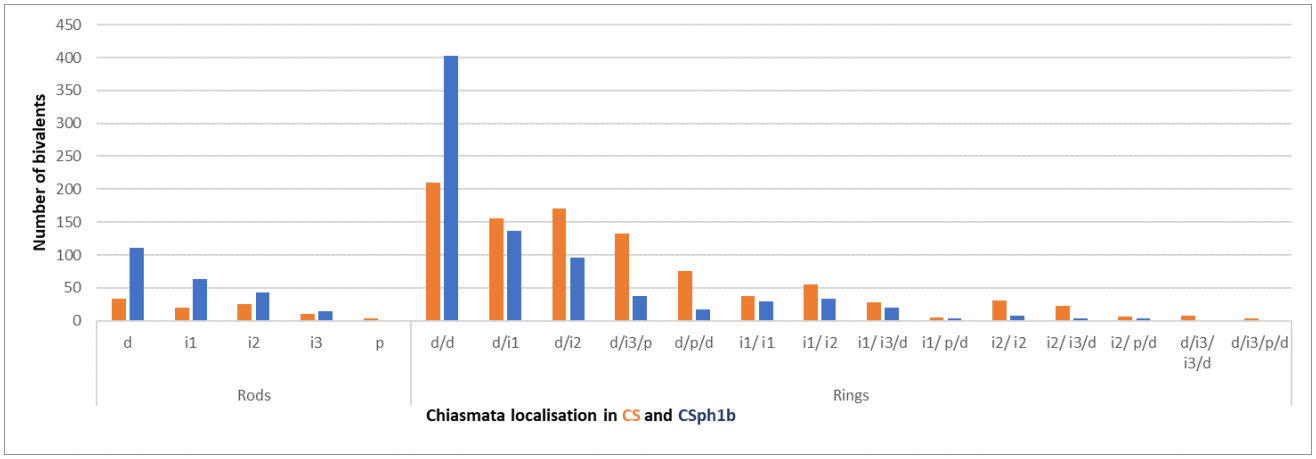

Figure 5.3: Distribution of CS wild type and CS *ph1b* bivalents based on chiasmata localization. The number of rod bivalents are higher in CSph1b in (d, i^1, i^2) region compare to CS wild type. However, the number of ring bivalents were higher in CS wild type compare CSph1b in all localization except in (d/d) localization.

Furthermore, the mean chiasma number per bivalent in CS *ph1b* (1.6±0.02) was significantly lower than in CS WT (2.2±0.02) (p value <0.0001) (figure 5.4). In *CS ph1b* a total of 31/50 (62%) cells showed multivalents as a consequence of homoeologous recombination. Furthermore, a total of 20/50 (40%) cells showed univalents.

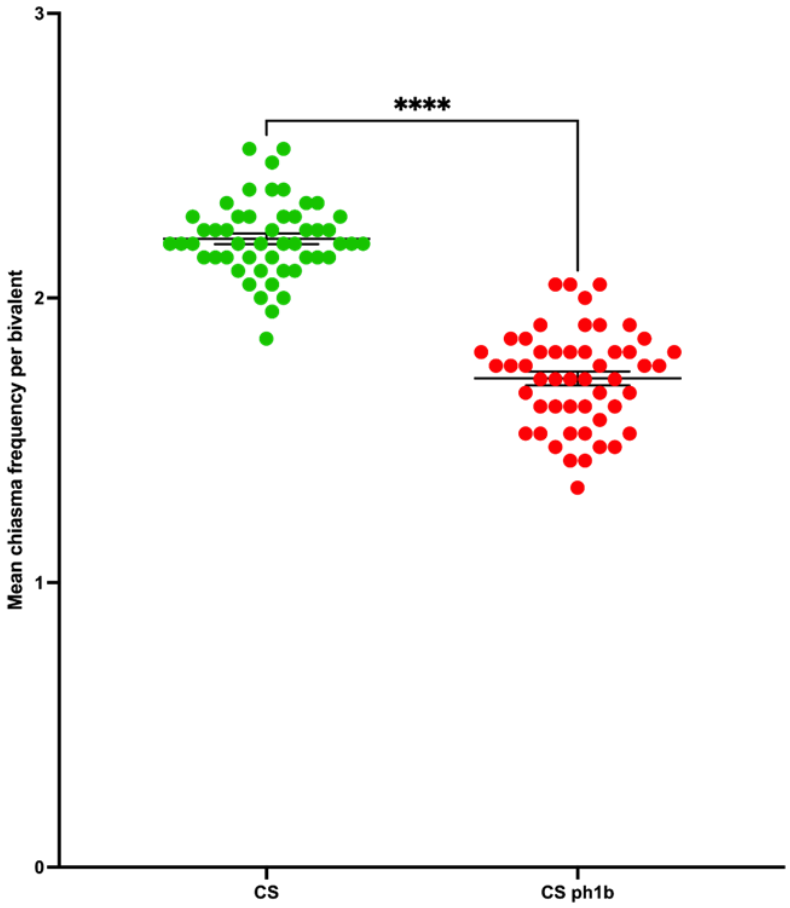

Figure 5.4: Mean chiasma frequency per bivalent in CS WT and CS *ph1b* mutant (N=50). The mean chiasma frequency per bivalent in CS *ph1b* was significantly lower compared CS WT. Welsh's t test (p value <0.0001).

We further investigated the spatio-temporal polarization of meiotic progression events in CS *ph1b*. Thus, the immunolocalization with ASY1 and ZYP1 proteins was conducted and revealed variation in the axis formation and SC elongation. About 60% of the meiocytes showed normal pairing and synapsis whereas about 40% showed defects in synapsis progression (figure 5.5). In these meiocytes that show defects in synapsis the ASY1 and ZYP1 signals appeared to be dotty instead of linear as in WT (figure 5.5D). The polarization of ASY1 and ZYP1 was restricted to the telomeric region but a delay of synapsis progression was observed. To test this observation telomere DNA probe was used to do FISH in combination with immunolocalisation of ZYP1.

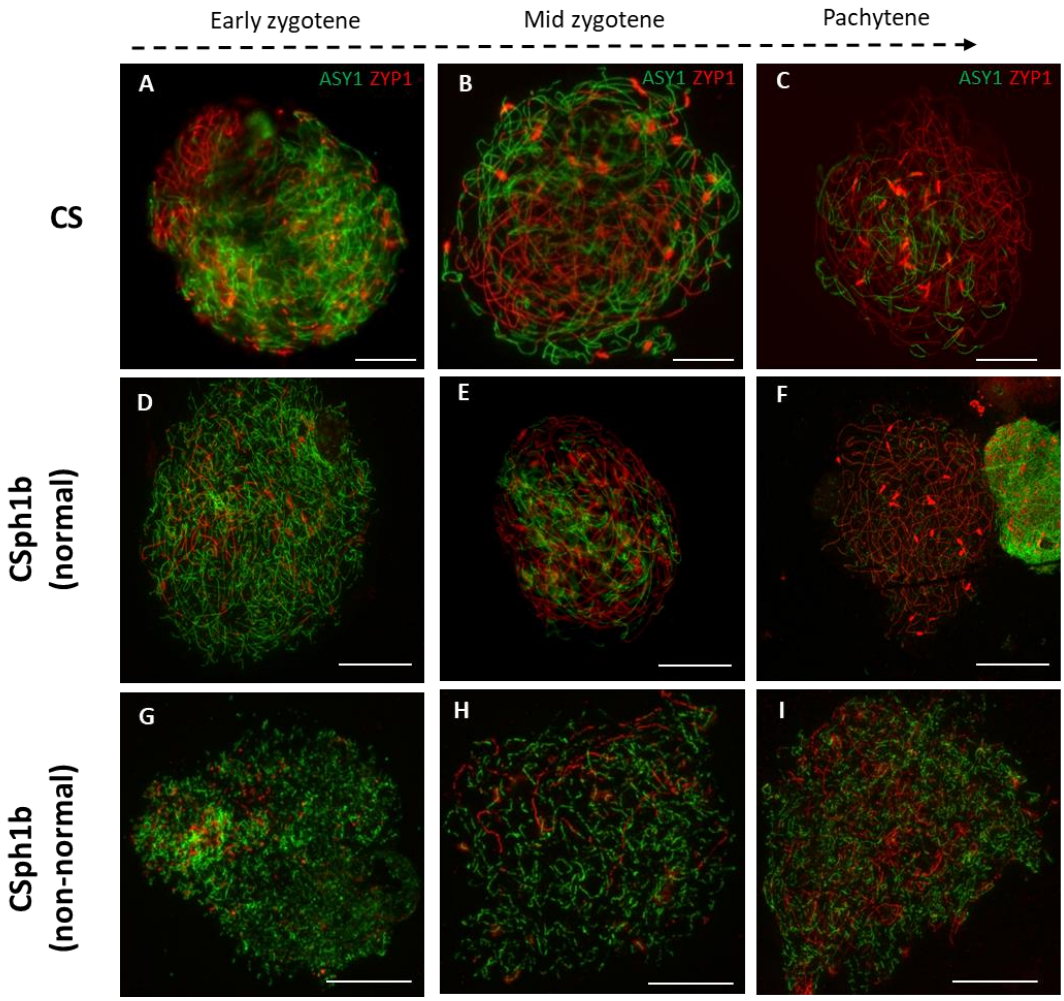

Figure 5.5: Immunolocalization of ASY1 and ZYP1 in CS WT and CS *ph1b* in early zygotene to pachytene stages. In CS WT, (A) Early zygotene, (B) Mid-zygotene and (C) Late zygotene (normal synapsis). In *CS ph1b* (D, E and F) normal synapsis. In CS *ph1b* (G) Early zygotene (non-normal), Asy1 signal appears to be dotty and not linearize normally. (H) Mid-zygotene and (I) Late zygotene. Scale bar = 10µm.

The chronology of meiosis was analyzed in CS *ph1b* mutant by using BrdU (figure 5.6). Meiotic time course revealed that meiotic progression in CS *ph1b* is delayed. For instance, at 33h CS *ph1b* appears to be at early zygotene whereas in CS at 33h the meiocytes are almost in mid or late zygotene (figure 5.6E). Additionally, at 44h CS *ph1b* reach diplotene whereas CS reach metaphase I at 39h which indicates a delay in meiosis specifically at prophase I in CS *ph1b*. Finally, at 48h CS *ph1b* reaches tetrad stage whereas this stage is reached at 43h in CS wild type.

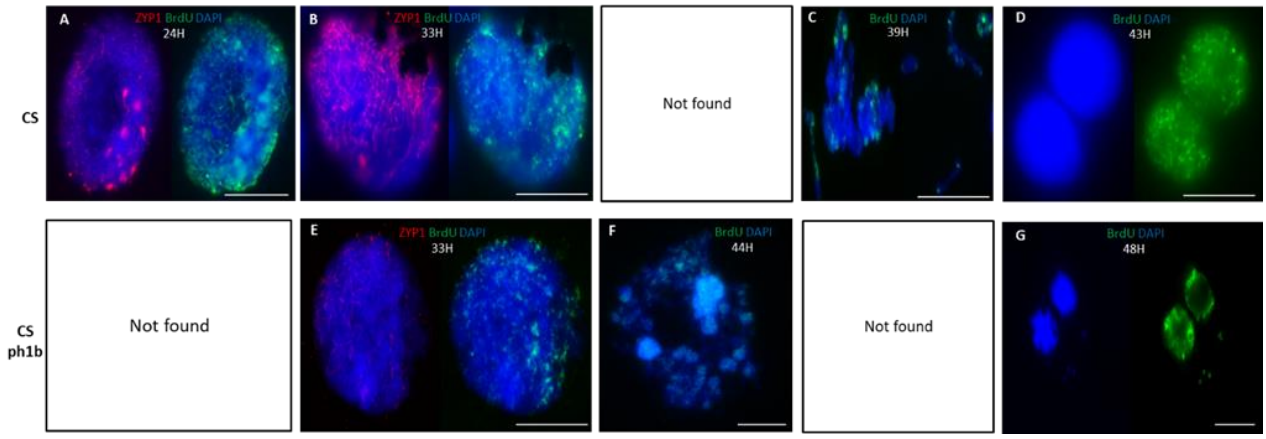

Figure 5.6: Meiotic time course for CS *ph1b* and CS WT. In CS, (A) Early zygotene, (B) Late zygotene, (C) Metaphase 1 and (D) Tetrad. In CS *ph1b*, (E) early zygotene, (f) diplotene and (g) Tetrad. Meiotic time course revealed that meiotic progression in CS ph1b is delayed. For instance, at 33h CS ph1b appears to be at early zygotene whereas in CS at 33h the meiocytes are almost in mid or late zygotene (figure 5.6E). Additionally, at 44h CS ph1b reach diplotene (figure 5.6.F) whereas CS reach metaphase I at 39h (figure 5.6.C) which indicates a delay in meiosis specifically at prophase I in CS ph1b. Finally, at 48h CS ph1b reaches tetrad stage (figure 5.6.G) whereas this stage is reached at 43h in CS wild type (figure 5.6.D). Scale bar = 10µm.

5.2.1.1 Telomere FISH with immunolocalization of ZYP1 protein

The telomere DNA probe FISH in combination with immunolocalisation of ZYP1 protein was applied to the CS WT and CS *ph1b* to compare synapsis initiation and elongation. In early zygotene when the telomere bouquet is still visible the synapsis stretches appear to be further polymerized in CS WT compared to CS *ph1b* (figure 5.7). In mid-zygotene the telomere bouquet starts to disperse and the SC continues to elongate normally in CS WT, however, the SC is not polymerized to the same length in CS *ph1b* (figure 5.7). Finally, in late-zygotene and pachytene the SC completes polymerization, with telomeres completely dispersed, in CS WT whereas in the CS *ph1b* the SC formation is not fully completed even when the telomere is fully dispersed in the entire cell (figure 5.7).

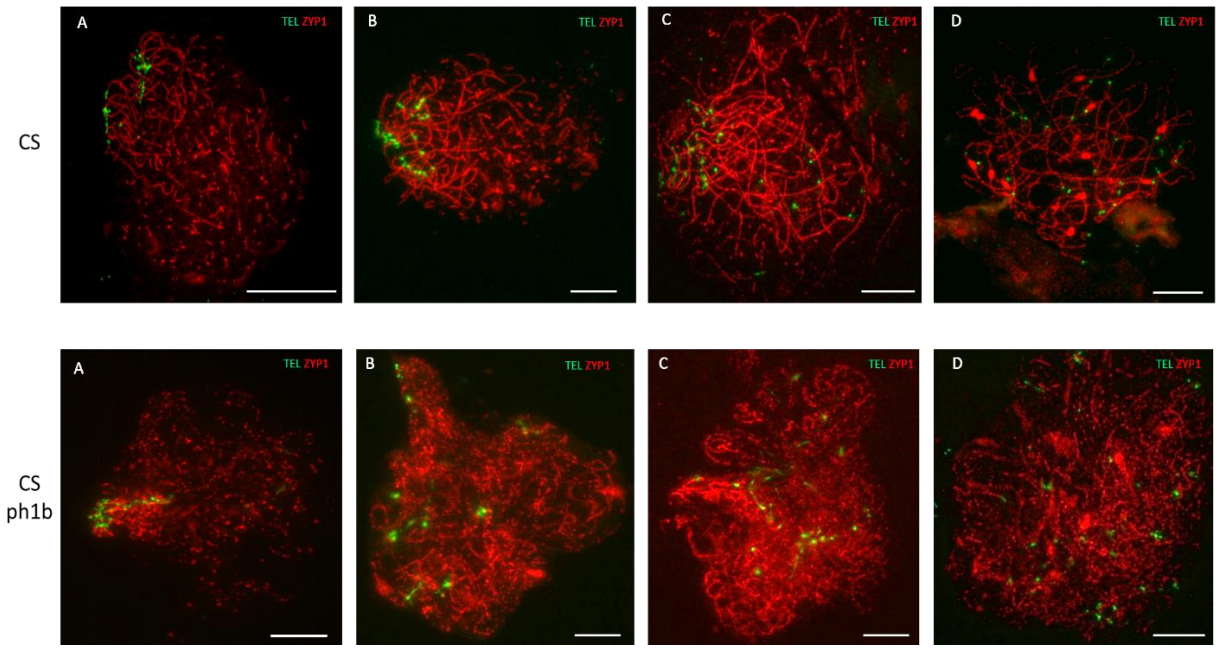

Figure 5.7: Telomere FISH (green) in combination with immunolocalisation of ZYP1(red) in CS and CS *ph1b*. (A) early zygotene, (B) mid-zygotene, (C and D) late zygotene. In early zygotene when the telomere bouquet is still visible the synapsis stretches appear to be further polymerized in CS WT compared to CS ph1b (figure 5.7. A). In mid-zygotene the telomere bouquet starts to disperse and the SC continues to elongate normally in CS WT, however, the SC is not polymerized to the same length in CS ph1b (figure 5.7. B). Finally, in late-zygotene and pachytene the SC completes polymerization, with telomeres completely dispersed, in CS WT whereas in the CS ph1b the SC formation is not fully completed even when the telomere is fully dispersed in the entire cell (figure 5.7. C and D). Scale bar = 10µm.

FISH with rDNA 45S and 5S were applied to metaphase I meiocytes slide of CS *ph1b* mutant to identify specific chromosomes and to analyze their mean chiasma frequency and chiasmata localization (figure 5.8).

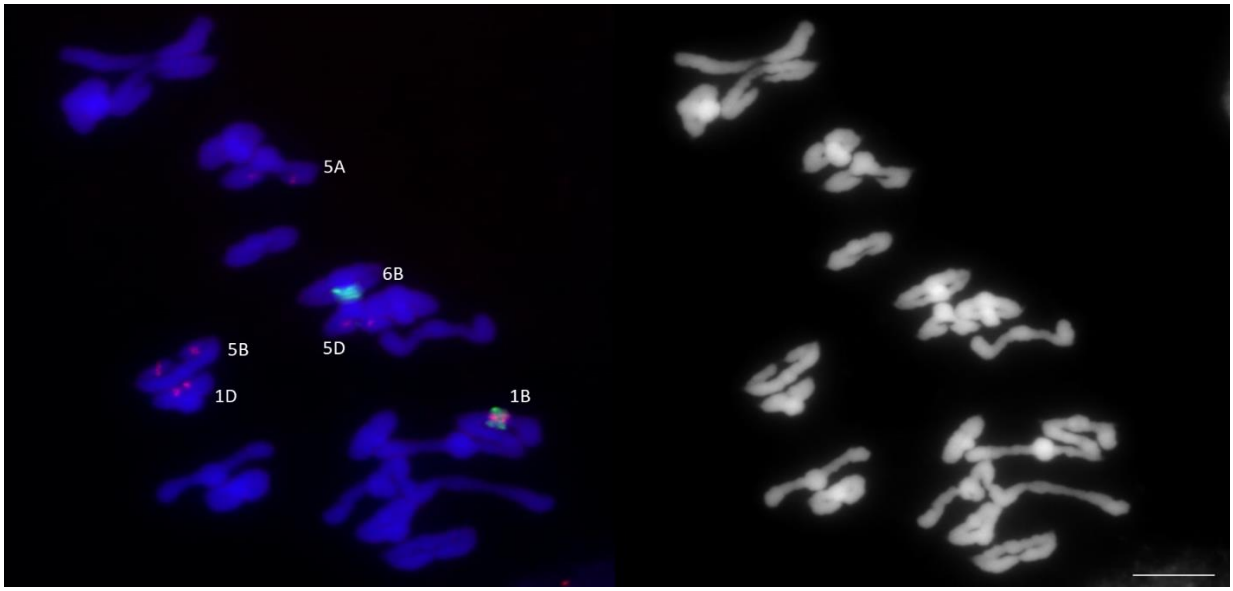

Figure 5.8: FISH with rDNA 45S (green) and 5S probes (red) in CS *ph1b*. Scale bar = 10µm.

5.2.1.2 Mean Chiasma Frequency per Chromosome

The mean chiasma frequency in specific chromosomes identified by FISH showed significant lower values in each chromosome of CS *ph1b* to the mean of the same chromosome in CS WT (Table 5.1 see appendix) and (figure 5.9).

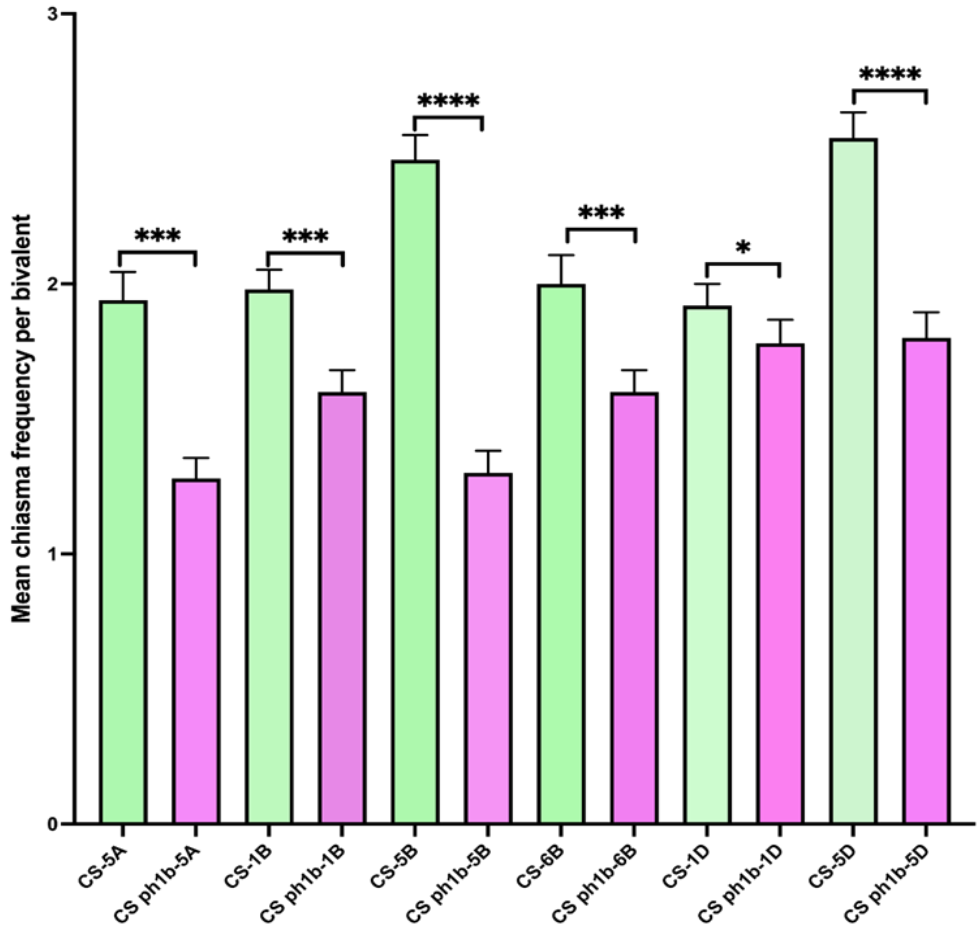

Figure 5.9: Comparison of the mean chiasma frequency in chromosomes 5A, 1B, 5B, 6B, 1D and 5D in CS WT and CS *ph1b*. The mean chiasma frequency in specific chromosomes identified by FISH showed significant lower values in each chromosome of CS ph1b to the mean of the same chromosome in CS WT. (One-way Welch's ANOVA test, N=50).

In CS *ph1b*: Chromosome 5A was involved in homeologous recombination in 3/50 (6%) cells and 2/50 (4%) cells as univalents. Chromosome 1B was involved in homeologous recombination in 7/50 (14%) cells and 1/50 (2%) cells as univalents. Chromosome 5B was involved in homeologous recombination in 4/50 (8%) cells and 2/50 (4%) cells as univalents. Chromosome 6B was involved in homeologous recombination only in 1/50 (2%) cells and 2/50 (4%) cells as univalents. Chromosome 1D was involved in homeologous recombination in only 1/50 (2%) cells and never was observed as univalents (0% cells). Chromosome 5D was never involved in homeologous recombination nor as univalents (0%) cells.

5.2.2 Analysis of *ph1c* mutant in tetraploid wheat

In addition to the rod and ring configurations observed in Cappelli WT, Cappelli *ph1c* mutant showed multivalents and univalents at metaphase I (figure 5.10). The mean chiasma frequency of Cappelli *ph1c* (24.1 ± 0.45) was significantly lower compared to Cappelli WT (32.82 ± 0.35) (Welch's t test, p value <0.0001) (figure 5.11).

In Cappelli *ph1c* a total of 4/50 (8%) cells showed multivalents as a consequence of homoeologous recombination. Furthermore, a total of 26/50 (52%) cells showed univalents.

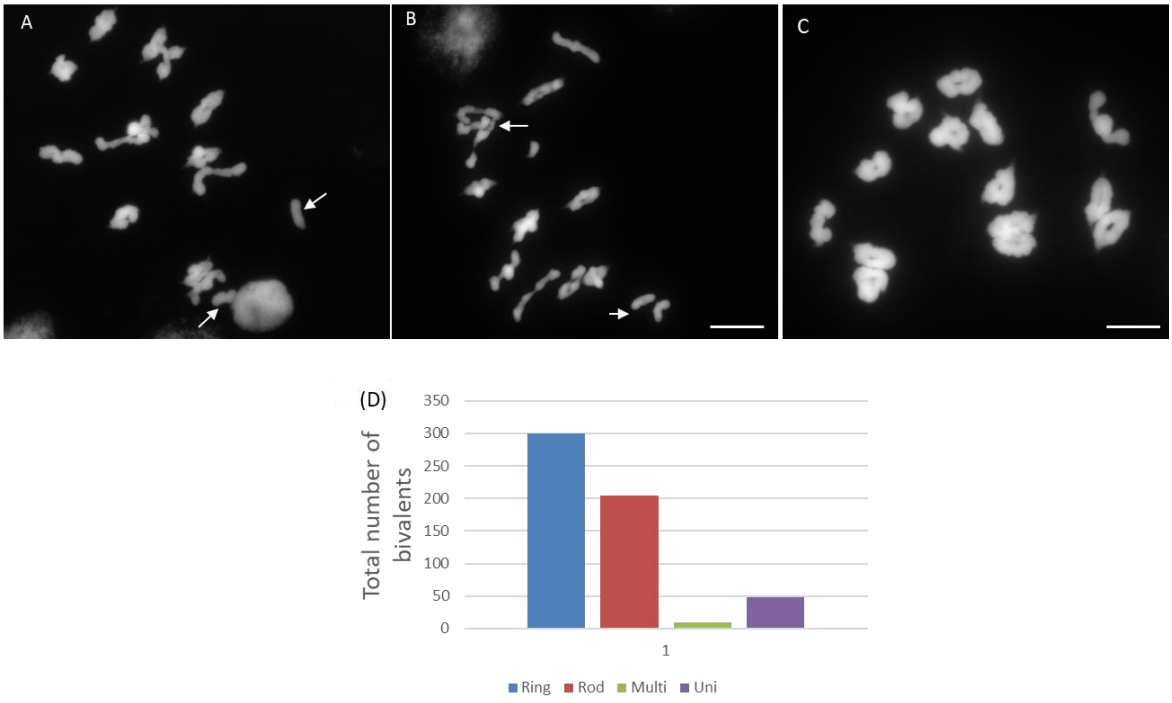

Figure 5.10: DAPI staining of Cappelli *ph1c* mutant and the different configurations observed at metaphase I chromosomes. (A & B) Microphotograps of pollen mother cells at metaphase I of Cappelli *ph1c* mutant. (A) Arrows points to univalents. (B) Arrows point to multivalent and to univalents. (C) Microphotograps of pollen mother cells of metaphase I of Cappelli wild type only ring and rod bivalent observe. (D) Diagram of total number of rings, rods, multivalents and univalents in Cappelli *ph1c*. Scale Bar = 10µm.

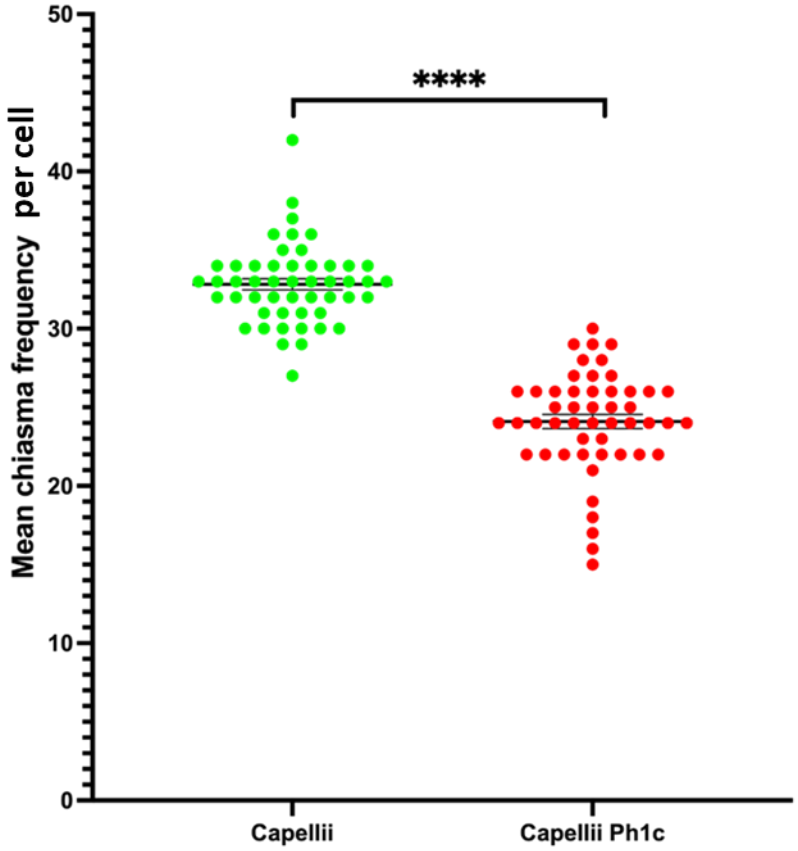

Figure 5.11: Comparison of the mean chiasma frequency per cell in Cappelli WT and Cappelli *ph1c*. Mean chiasma frequency per cell in Cappelli *ph1c* was significantly lower compare to Cappelli WT (Welch's t test $p<0.0001$, N=50).

Chiasmata localizations were listed in figure 5.12 The majority of chiasmata were localized at distal regions in both ring and rod bivalents. This distal localization was followed by a moderate number of chiasmata in interstitial regions 1 and 2 (i^1 and i^2) in both ring and rod bivalents. The lowest number of bivalents where in localizations closer to centromeres (i^3 and p).

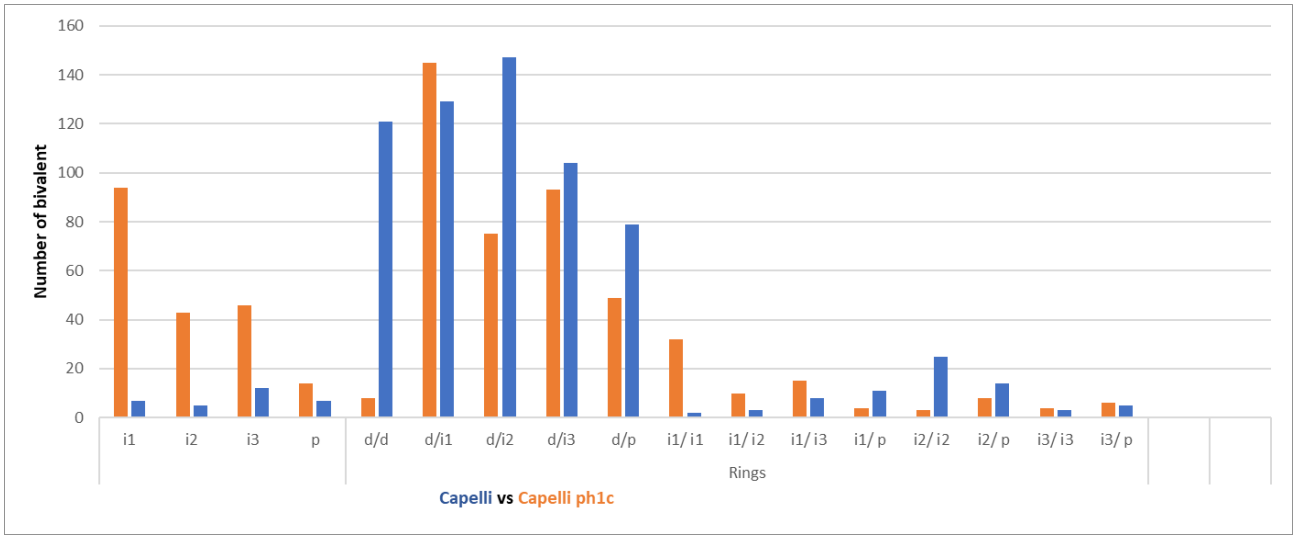

Figure 5.12: Distribution of Cappelli wild type and Cappelli *ph1c* bivalents based on chiasmata localization. Cappelli *ph1c* appear to be higher in the number of rod bivalent. However, Cappelli wild type contain higher number of ring bivalents with in an interstitial and proximal localization.

The mean chiasma frequency per bivalent in Cappelli *ph1c* was (1.72±0.032) and it was significantly lower to Cappelli WT (2.43±0.02)) (Welch's t test, p value <0.0001) (figure 5.13).

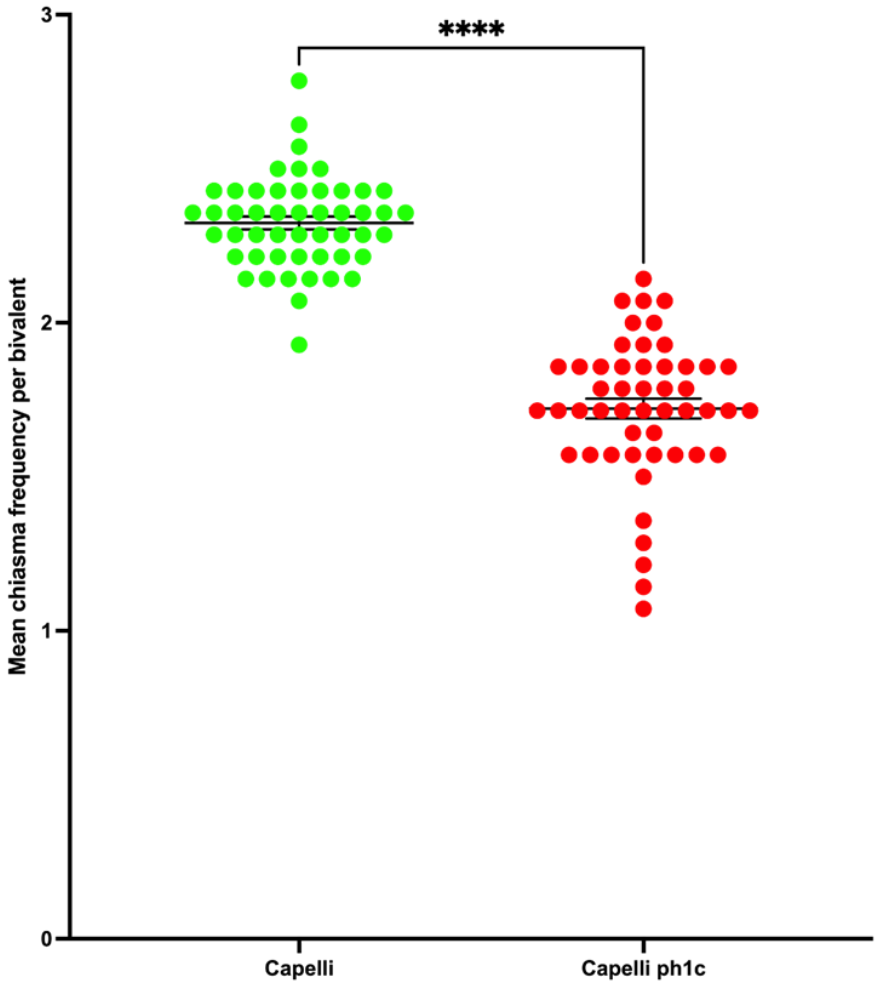

Figure 5.13: Mean chiasma frequency per bivalent in Cappelli WT and Cappelli *ph1c* (N=50). Mean chiasma frequency per bivalent in Cappelli *ph1c* was significantly lower compare to Cappelli WT Welsh's t test (p value <0.0001).

The spatio-temporal meiotic progression was also investigated in Cappelli WT and Cappelli *ph1c* mutant by immunolocalization of ASY1 and ZYP1 proteins. Most of the meiocytes showed normal chromosome axis and SC formation from early zygotene to pachytene (figure 5.14).

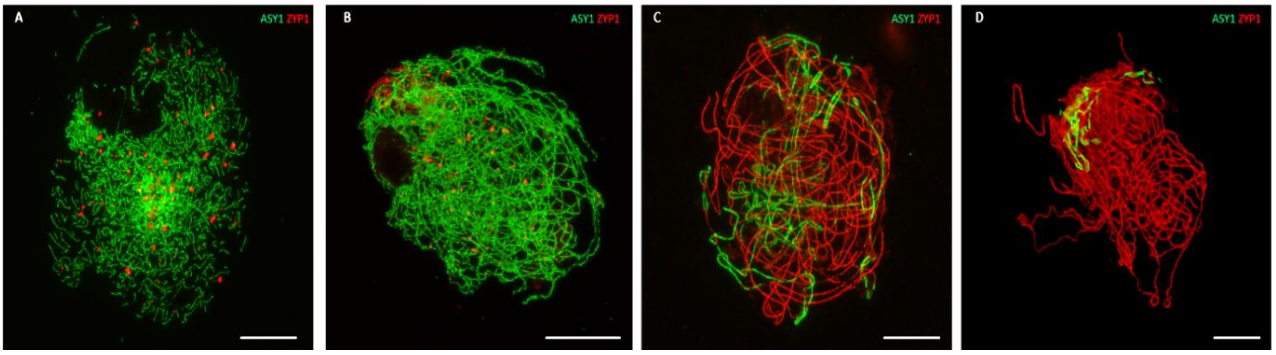

Figure 5.14: Spatio-Temporal progression of meiosis in Cappelli *ph1c* with ASY1 (green) and ZYP1 (red) immunolocalization showed normal chromosome axis (ASY1) and SC (ZYP1) polymerization. (A) leptotene, (B) early zygotene, (C) mid-late zygotene and (D) pachytene. Scale bar = 10µm.

A total of four chromosomes could be identified using 45S and 5S rDNA probes and FISH in tetraploid Cappelli WT and Cappelli *ph1c* mutant: 5A, 1B, 5B and 6B (figure 5.15). The mean chiasma frequency of each chromosome in Cappelli *ph1c* was significantly lower to the mean chiasma frequency of each chromosome in Cappelli WT (Table 5.2 see appendix) and (figure 5.16).

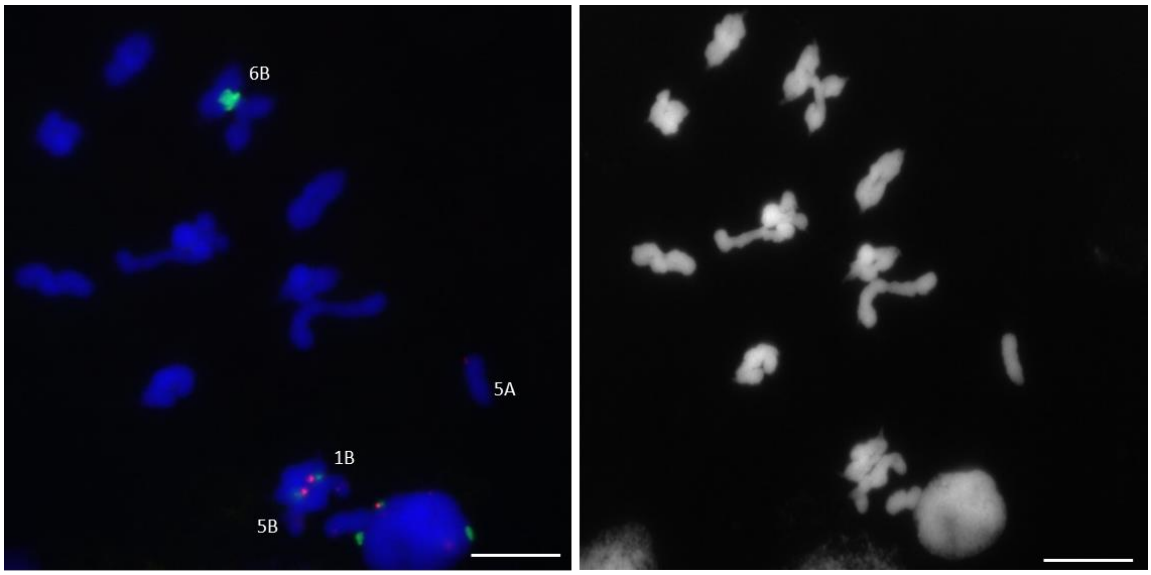

Figure 5.15: FISH with 45S (green) and 5S (red) rDNA probes in Cappelli WT and *ph1c*. Scale bar = 10µm.

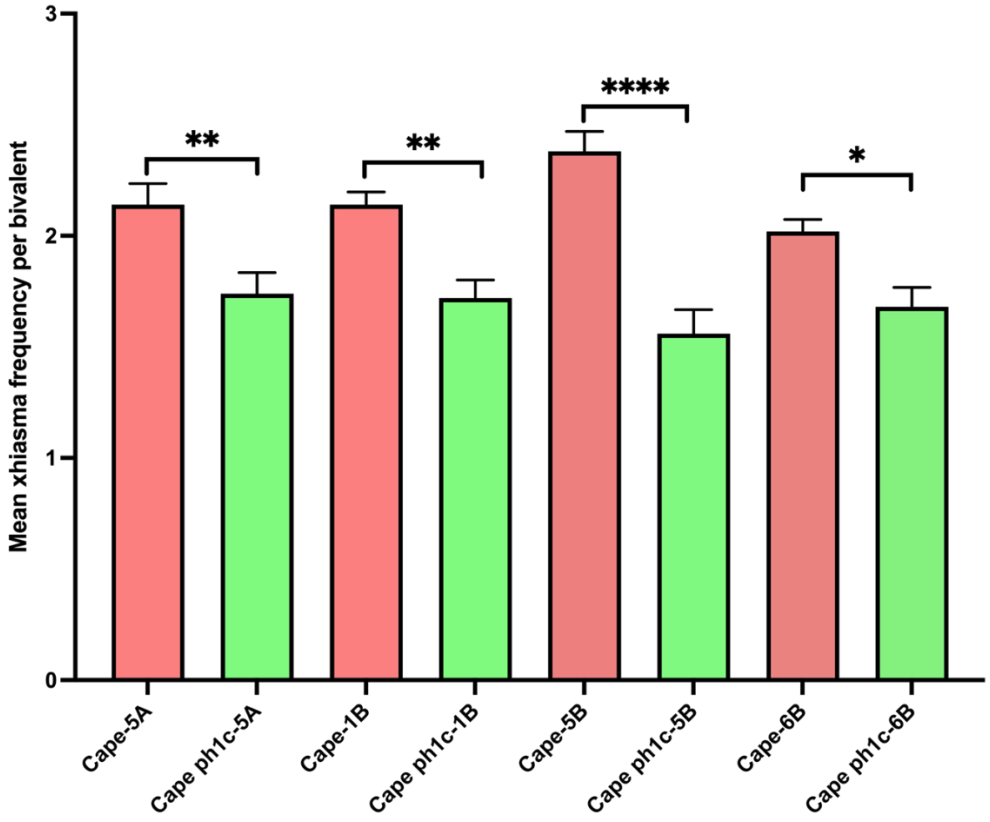

Figure 5.16: Comparison of the mean chiasma frequency in chromosomes 5A, 1B, 5B and 6B in Cappelli WT and Cappelli *ph1c* Welch's t test, N=50).

In Cappelli *ph1c*: Chromosome 5A was involved in homoeologous recombination in 1/50 (2%) cells and 2/50 (4%) cells as univalents. Chromosome 1B was involved in homoeologous recombination in 2/50 (4%) cells and 1/50 (2%) cells as univalents. Chromosome 5B was involved in homoeologous recombination in 2/50 (4%) cells and 4/50 (8%) cells as univalents. Chromosome 6B was never involved in homoeologous recombination (0% cells) and 1/50 (2%) cells as univalents.

5.2.3 Analysis of substitution line 5D (5B) in tetraploid wheat cultivar Langdon

This phenotype showed the same effect as CS *ph1b* and Cappelli *ph1c* with homoeologous recombination at metaphase I due to the absence of chromosome 5B and therefore the *Ph1* locus. As reported for *ph1b* and *ph1c* mutants, ring and rod bivalents were observed as well as univalents and multivalents Langdon 5D (5B) (Figure 5.17). Moreover, the mean chiasma frequency of Langdon 5D (5B) (21.84 $\pm$ 0.43) was significantly lower to the Langdon WT (31.8 $\pm$ 0.33) (Welch's t test, p value <0.0001) (figure 5.18). In Langdon 5D (5B) a total of 3/50 (6%) cells showed multivalents as a consequence of homoeologous recombination. Furthermore, a total of 25/50 (50%) cells showed univalents.

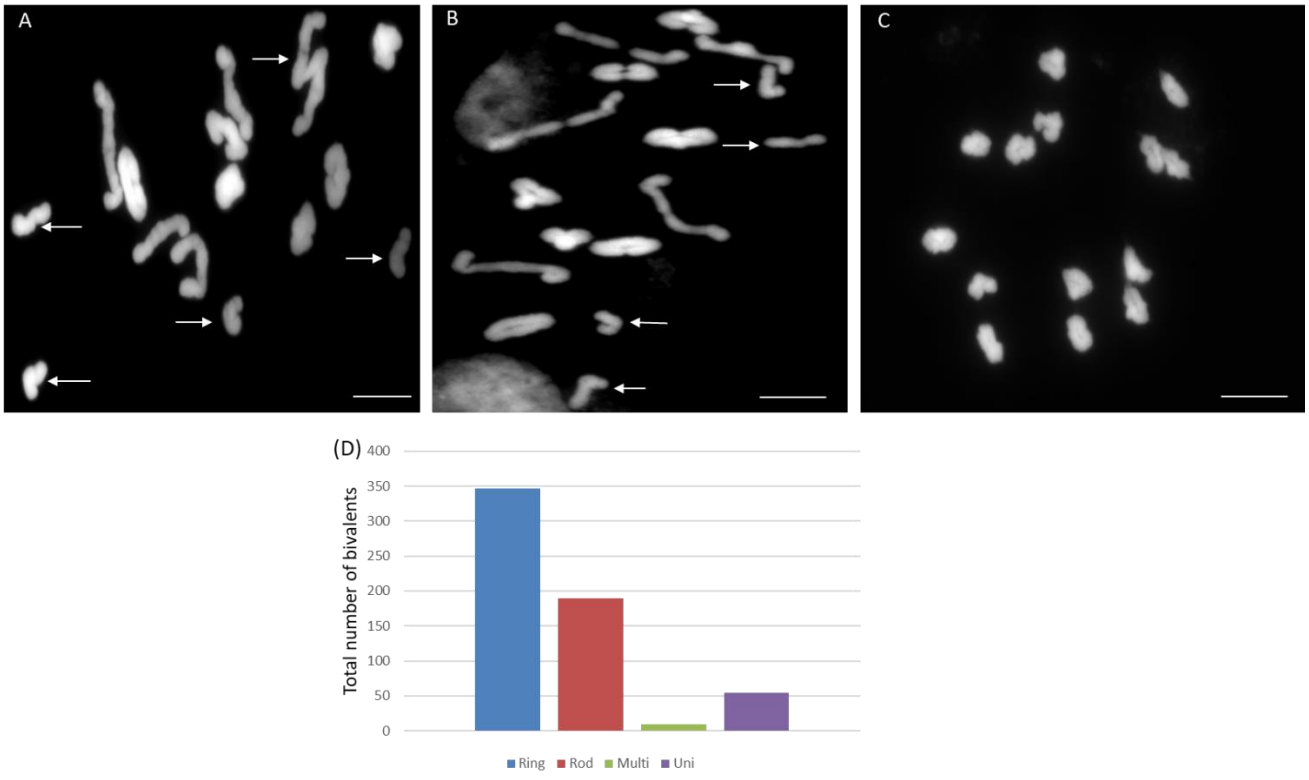

Figure 5.17: DAPI staining of Langdon 5D (5B) mutant and Langdon wild type of different configurations observed at metaphase I chromosomes. (A & B) Microphotographs of pollen mother cells at metaphase I of Langdon 5D (5B). (A) Arrows points to univalent and multivalent. (B) Arrows point to univalents. (C) Microphotographs of

pollen mother cell of Langdon wild type only ring bivalent observe. (D) Diagram of total number of rings, rods, multivalents and univalents in Langdon 5D (5B). Scale Bar = 10μm.

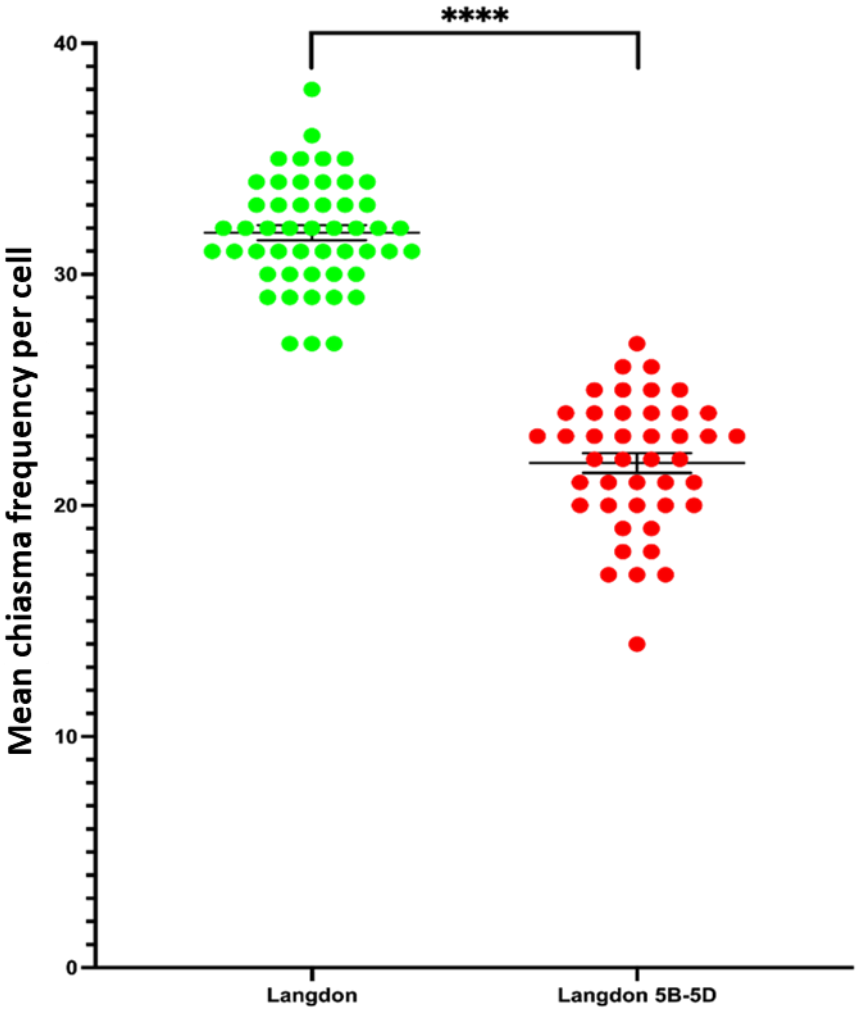

Figure 5.18: Comparison of the mean chiasma frequency per cell between Langdon WT and Langdon 5D (5B). Mean chiasma frequency of Langdon 5D (5B) was significantly lower compared to Langdon WT. (Welch's t test $p<0.0001$, N=50).

The distribution of chiasmata localization is listed in (figure 5.19). The majority of chiasmata were distal in both ring and rod bivalents. This was followed by a moderate number of i^1 and i^2 chiasmata. The i^3 and p chiasmata showed the lowest number in ring bivalents whereas none of these chiasmata localization could be observed in rod bivalents.

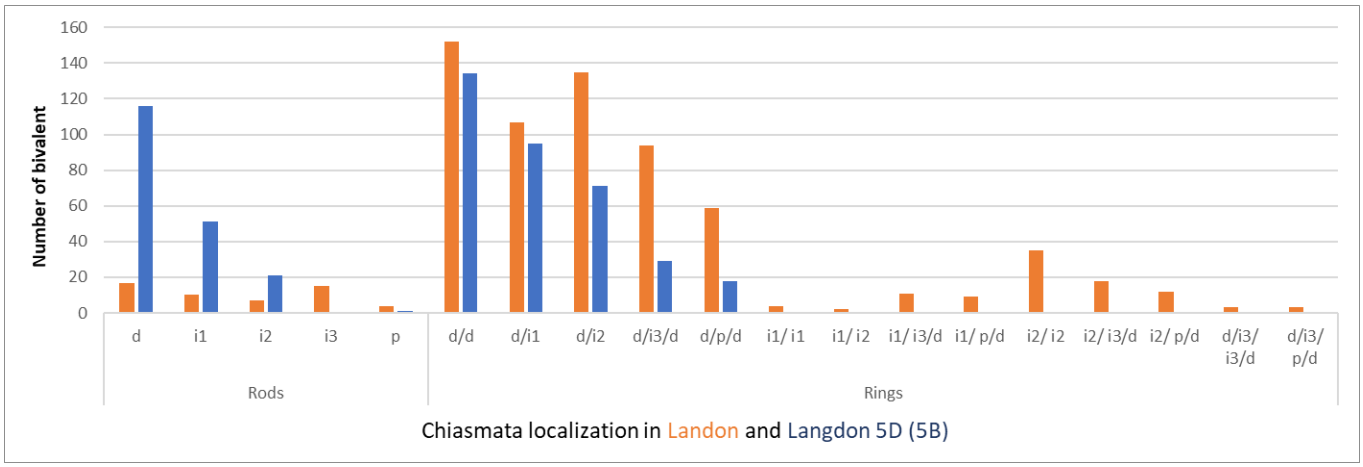

Figure 5.19: Distribution of chiasmata localization in Langdon wild type and Langdon 5D (5B). Langdon 5D (5B) show higher number of rod bivalent. However, Langdon wild type contains higher number of ring bivalent with more interstitial and proximal chiasmata. Bivalent with interstitial and proximal chiasmata never observed in Langdon 5D (5B).

The mean chiasmata frequency per bivalent was analyzed (figure 5.20). As a result, the mean chiasma frequency in Langdon 5D(5B) (1.56 ± 0.03)) was significantly lower compared to the mean of Langdon WT (2.27 ± 0.02; Welsh's t test, p value <0.0001).

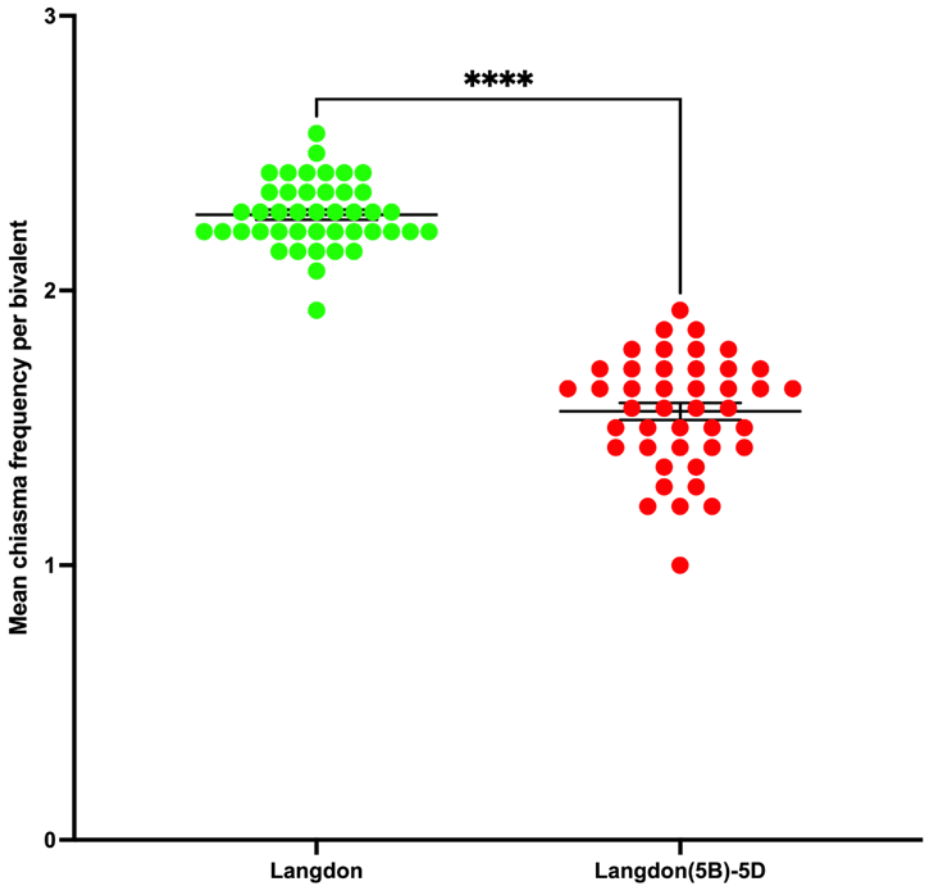

Figure 5.20: Mean chiasmata per bivalents in Langdon WT was significantly higher compared to Langdon 5D (5B). (N=50). Welsh's t test (p value <0.0001).

Spatial-temporal meiotic progression polarization of Langdon 5D(5B) was investigated using immunolocalizatio of Asy1 and Zyp1. About 40% of the meiocytes showed defects in the chromosome axis and SC formation (figure 5.21 A-F). However, 60% of the meiocyte showed normal progression (figure 5.21 G-I). This result indicates that replacing chromosome 5B by chromosome 5D showed a partial defect to the chromosome axis and SC formation in this mutant.

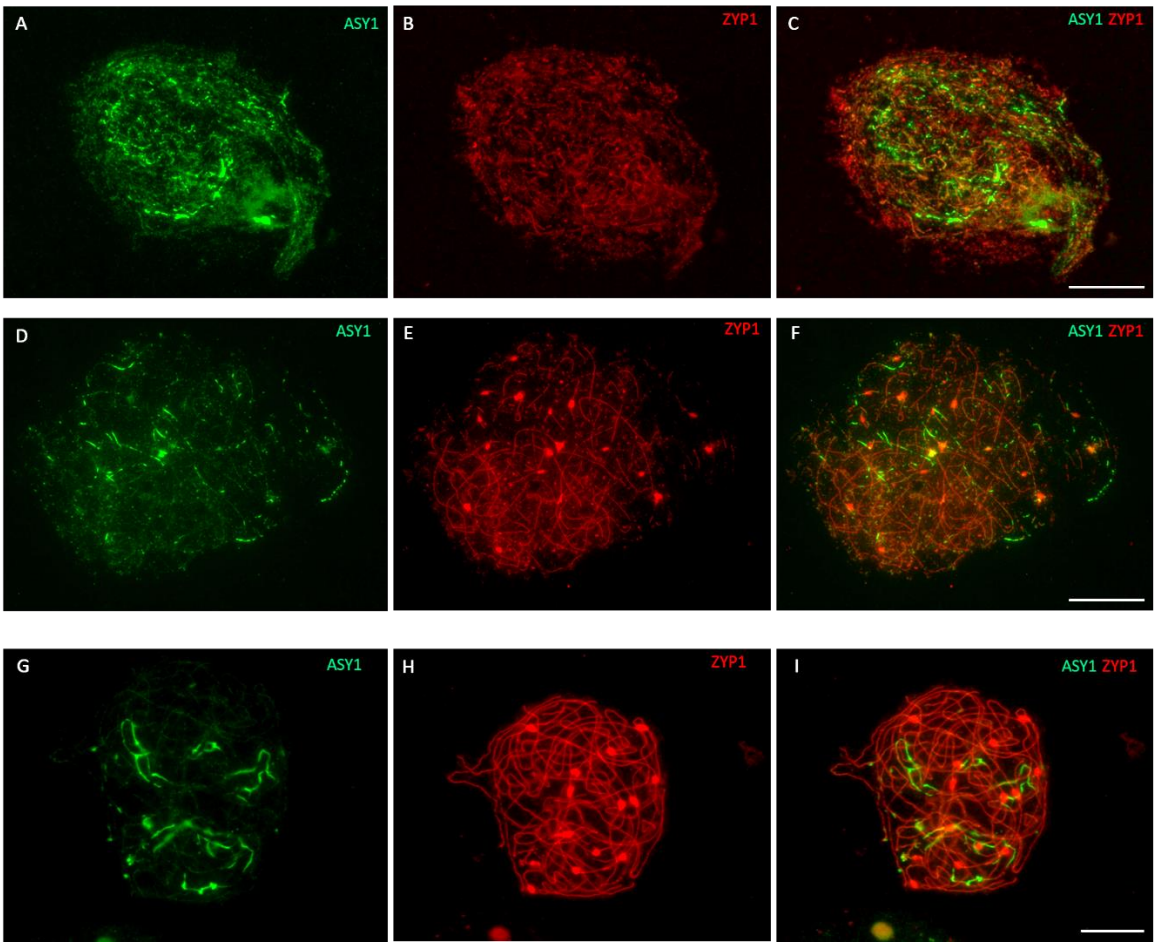

Figure 5.21: Immunolocalization with ASY1 and ZYP1 in Langdon 5D(5B). (A-F) show defect in chromosome axis and SC formation (A and D) ASY1 signal only, (B and E) ZYP1 signal only and (C and F) merge of the both signals. (G-I) show normal chromosome axis and SC formation (G) ASY1 signal only, (H) ZYP1 signal only and (I) merge of the both signals. Scale bar = 10µm.

FISH with 45S and 5S rDNA allowed us to distinguish four chromosomes: 1A, 1B, 5D and 6B (figure 5.22). The mean chiasma frequency of each chromosome was conducted and compare the mean chiasma frequency of the FISH chromosomes in Langdon WT (Welch's t test) (Table 5.3 see appendix) and (figure 5.23). As a result, the mean chiasma frequency of the FISH chromosomes was significantly lower in Langdon 5D(5B) compared to the mean of each chromosome in Langdon WT. In Langdon 5D(5B): Chromosome 5A appeared as univalents in 7/50 (14%) cells. Chromosome 1B appeared as univalents in 6/50 (12%) cells. Chromosome 6B appeared as univalents in 3/50 (6%)

cells. Chromosome 5D appeared as univalents in 5/50 (10%) cells and had a mean chiasma frequency of (1.56±0.12).

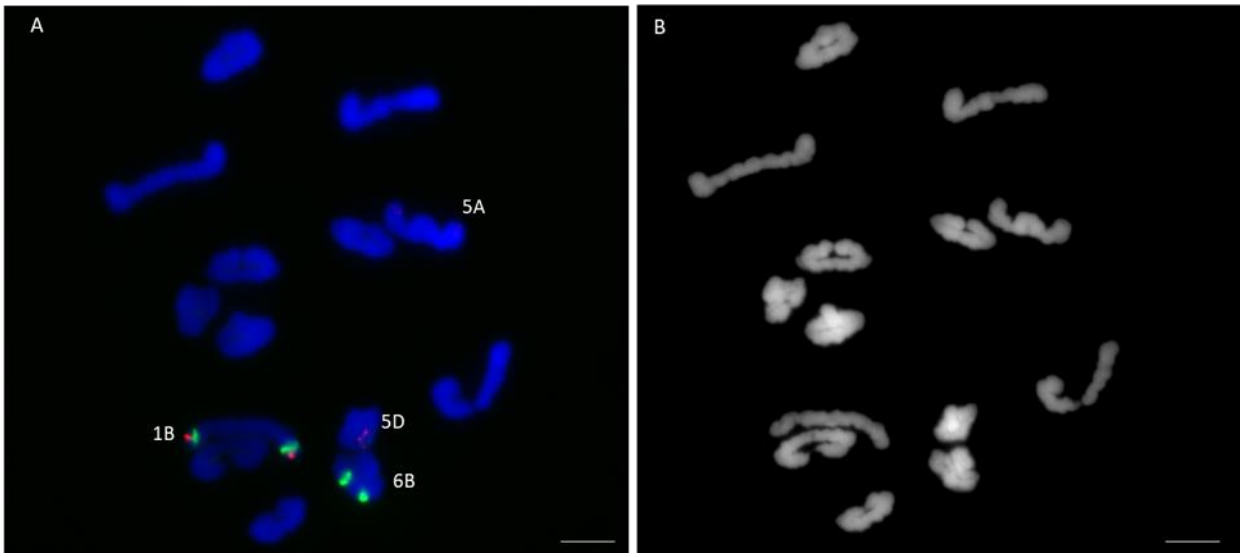

Figure 5.22: (A) FISH with 45s(green) and 5s(red) in Langdon 5D(5B). (B) DAPI spread image. Scale bar = 10µm.

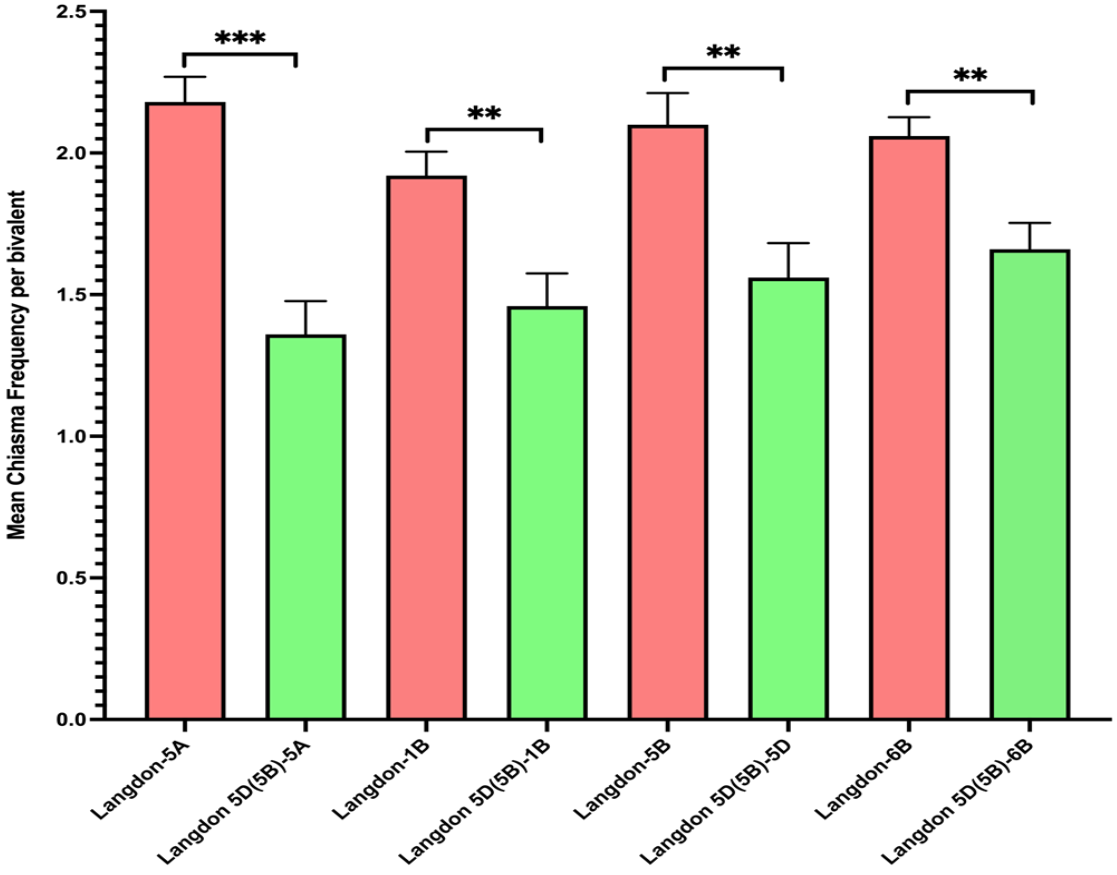

Figure 5.23: Comparison of the mean chiasma frequency of the chromosomes 5A, 1B, 5B and 6B in Langdon WT and Langdon 5D. The mean chiasma frequency of the FISH chromosomes was significantly lower in Langdon 5D(5B) compared to the mean of each chromosome in Langdon WT (5B). (Welch's t test $p<0.001$, N=50).

5.2.4 Analysis of HU treatment in hexaploid cultivar Cadenza

In this chapter, HU was used (0.5 mM) to affect DNA replication in order to manipulate meiotic recombination in wheat. The effect of HU was analyzed in metaphase I pollen mother cells by scoring chiasma frequency and their localization. The effect of HU in wheat meiotic recombination can be classified to three categories. First, a few cells showed sever defects in chiasmata formation and this might be due to the time of HU incorporated to the cell (before the starting of the DNA replication) (figure 5.24 A and B). Second, about 1% of the chromosomes appeared as univalent in about 10% of

the total number of the cell (N=50) at metaphase I but interstitial and proximal chiasmata could be observed in those cell (up to five bivalents) (figure 5.24 C and D). Third, bivalents appeared to be normal at metaphase I with an observation of interstitial and proximal chiasmata in some bivalents (up to five bivalents) (figure 5.24 E and F). Additionally, bivalents with interstitial and proximal chiasmata in both chromosome arms could be observed in Cadenza treated with HU (figure 5.24 E and F).

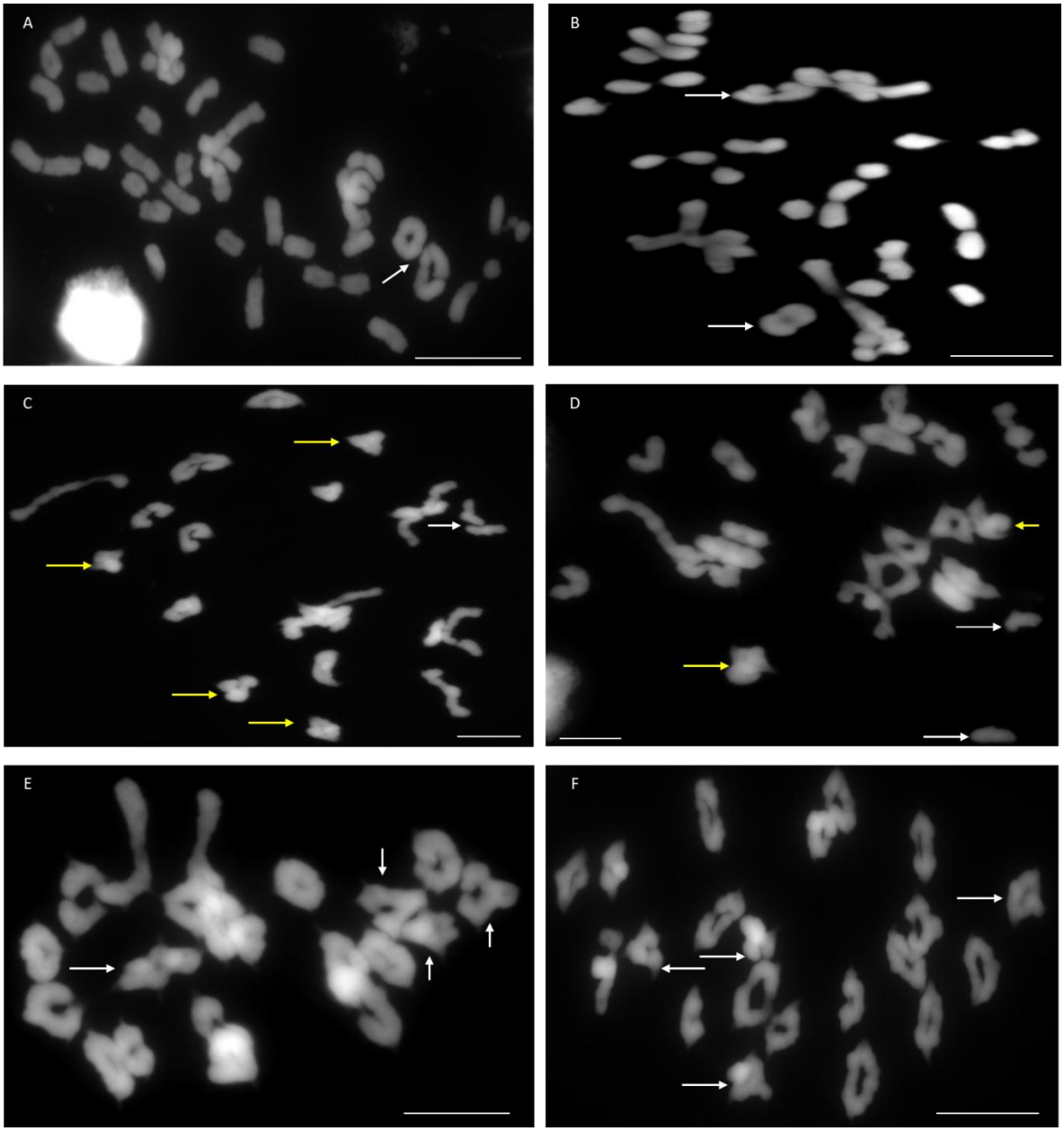

Figure 5.24: Metaphase I of Cadenza treated with HU. (A and B) Cells with a huge defect in bivalents formation with only 2 to 3 bivalents observed (indicated by an arrow). (C and D) univalents can be observed in these cells (indicated by white arrows) and bivalents with an interstitial and proximal chiasma observed in both arms (indicated by yellow arrow). (E and F) normal bivalent formation with some bivalents containing an increase of interstitial and proximal chiasmata (indicated by an arrows).

Moreover, the mean chiasma frequency of Cadenza HU (40.7±0.44) was significantly lower compared to the mean of Cadenza WT (44.2±0.25) (figure 5.4.1) (Welch's t test $p<0.0001$, N=47).

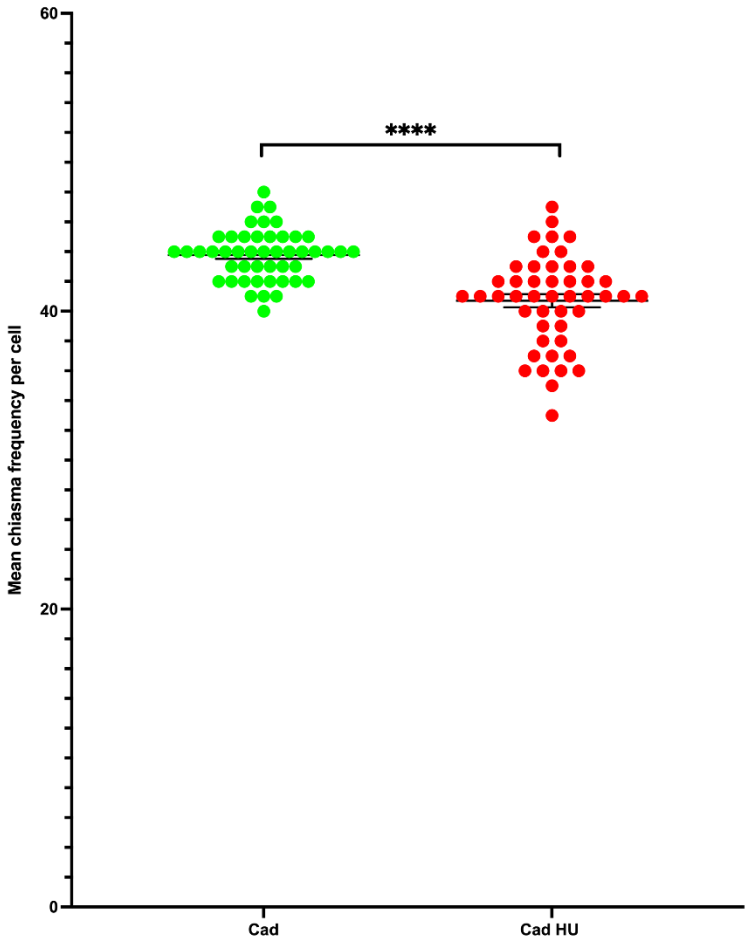

Figure 5.25: Comparison of the mean chiasma frequency of Cadenza WT and Cadenza treated with HU. The mean chiasma frequency of Cadenza HU was significantly lower compared to the mean of Cadenza WT. (Welch's t test $p<0.0001$, N=47).

The chiasmata localization in Cadenza HU appeared to be more widely distributed along the chromosome arms (both arms) compared to Cadenza WT (figure 5.26). In the ring bivalents, the (d/d) bivalent configurations seem to be reduced in Cadenza HU compared to Cadenza WT. In the (d/i^1) bivalent configuration the mean number was almost equal in both of them. In the ($d/i^3/d$ and d/p/d) the bivalent number was higher in Cadenza WT compared to Cadenza treated with HU. However, interestingly the number of bivalents with chiasmata in both chromosome arms was higher in Cadenza HU compared to Cadenza WT. In Cadenza HU, bivalents with interstitial and proximal chiasmata in both arms could be found in different localizations such as (i^1/i^1, i^1/i^2, $i^1/p/d$, i^2/i^2 and $d/i^3/p/d$).

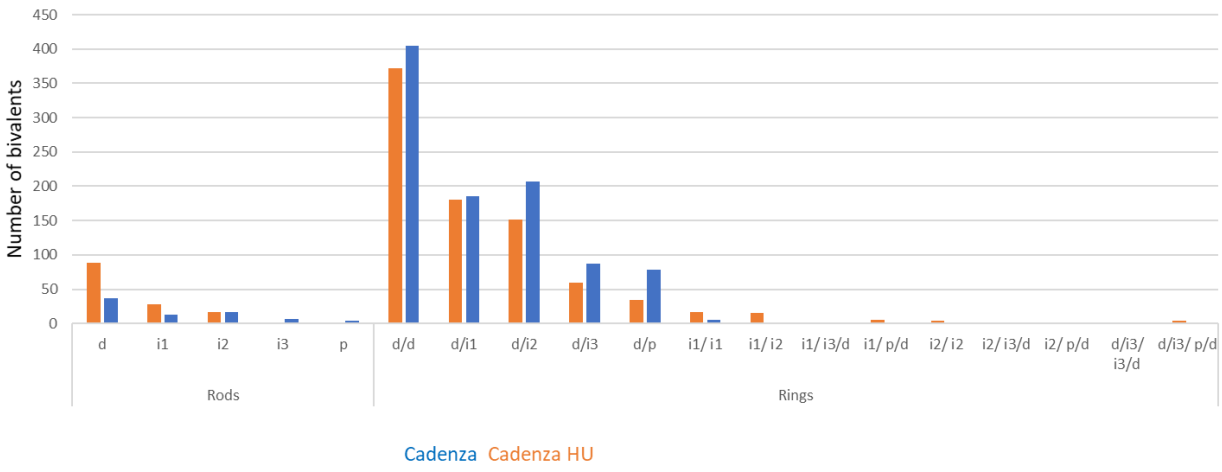

Figure 5.26: Chiasmata localization in Cadenza and Cadenza HU. Bivalents with interstitial and proximal chiasmata in both chromosome arms observed in Cadenza HU whereas this shape of bivalents not observed in the wild type.

However, d and i^1 rods appeared to be higher in Cadenza HU compared to Cadenza WT. In contrast, i^2 rod bivalents appeared to be equal in both of them. Surprisingly, no i^3 or p rod bivalents were observed in Cadenza HU.

The immunolocalization of HEI10 in combination with ZYP1 at late diplotene was applied to the Cadenza HU. The HEI10 foci were more distributed along the chromosome arms with up to five foci observed in some chromosome pairs (figure 5.27).

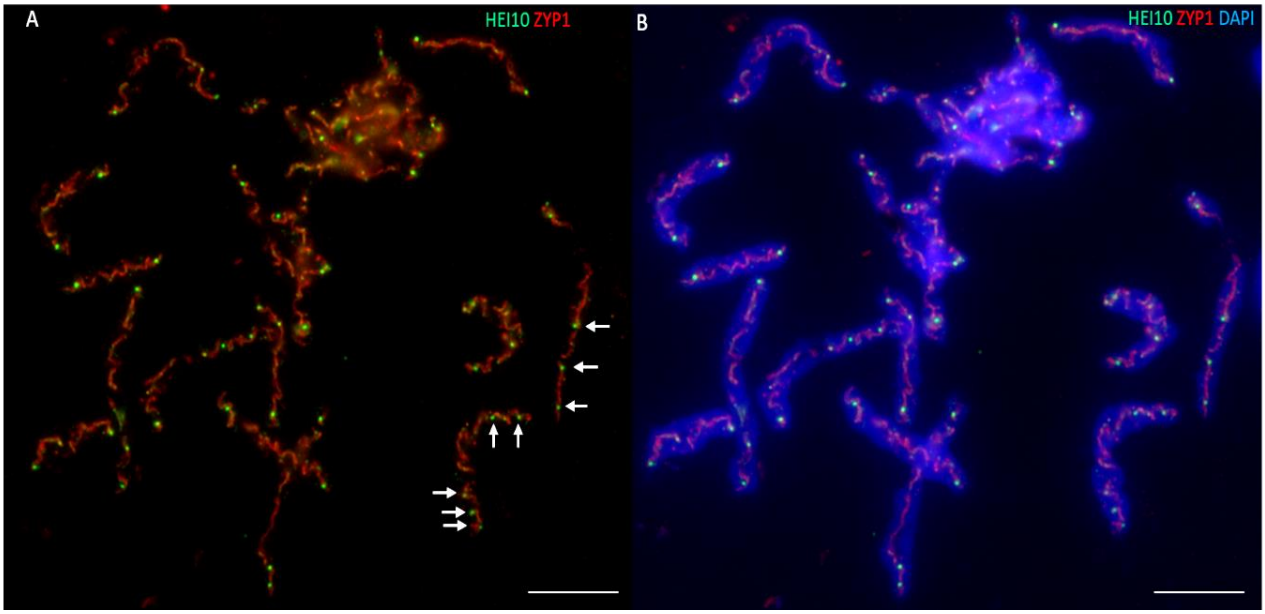

Figure 5.27:Immunolocalization of Hei10(green) with combination of Zyp1(red). (A) Zyp1 with Hei10 foci only (arrows indicate Hei10 foci in two bivalents). (B) Zyp1 with Hei10 foci with DAPI. A close HEI10 foci (indicated by arrows) observed in this treatment whereas these close foci not observed in Cadenza WT. Scale bar = 10μM.

After the observation of the high number of HEI10 foci in some bivalents, the analysis of the mean of HEI10 foci was conducted and compared to the mean number of HEI10 foci in Cadenza WT. The mean number of HEI10 foci in Cadenza HU (46$\pm$0.7) was significantly higher compared to Cadenza WT (43$\pm$0.6) (Welch's t test $p<0.002$, N=30) (figure 5.28).

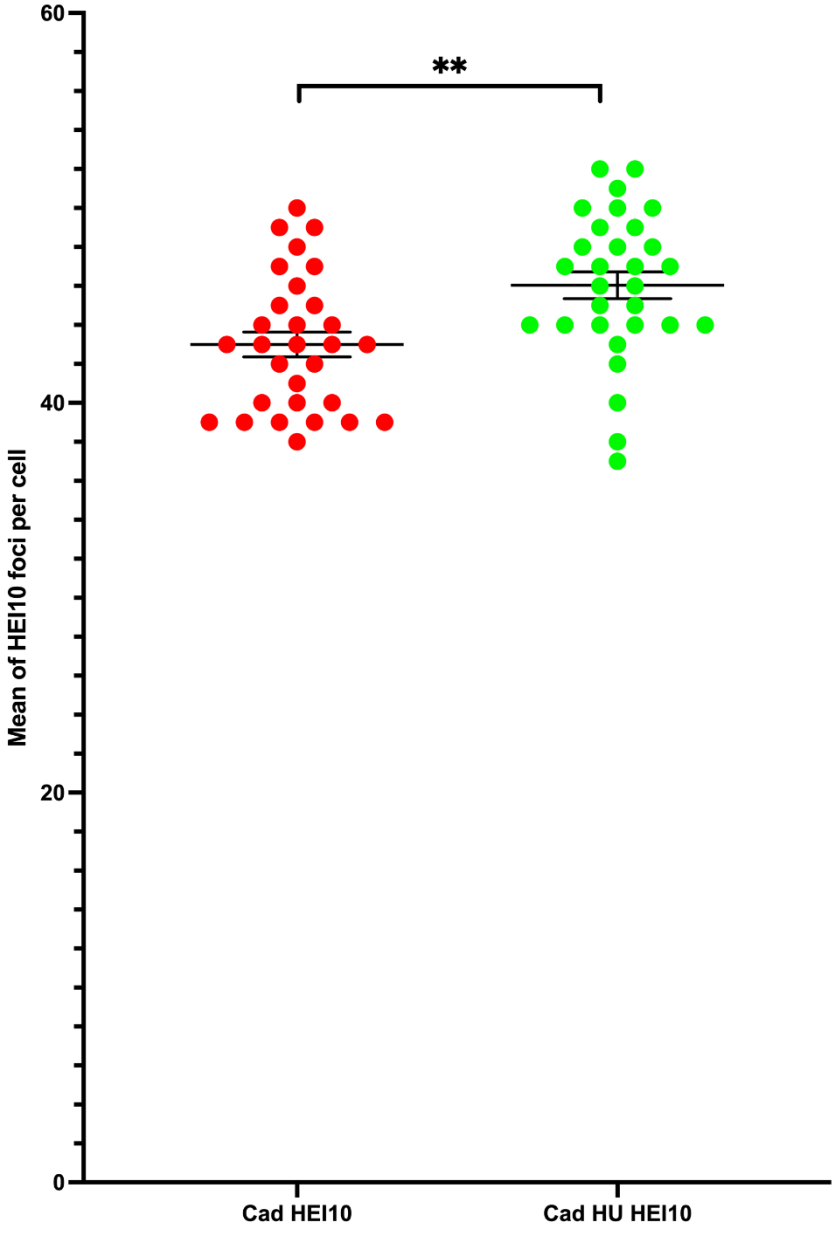

Figure 5.28:Comparison of the mean of the HEI10 foci in Cadenza WT and Cadenza HU. The mean number of HEI10 foci in Cadenza HU was significantly higher compared to Cadenza WT (Welch's t test $p<0.002$, N=30).

FISH analysis with rDNA 45S and 5S probes allowed us to identify chromosomes 5A, 1B, 5B, 6B, 1D and 5D (figure 5.29).

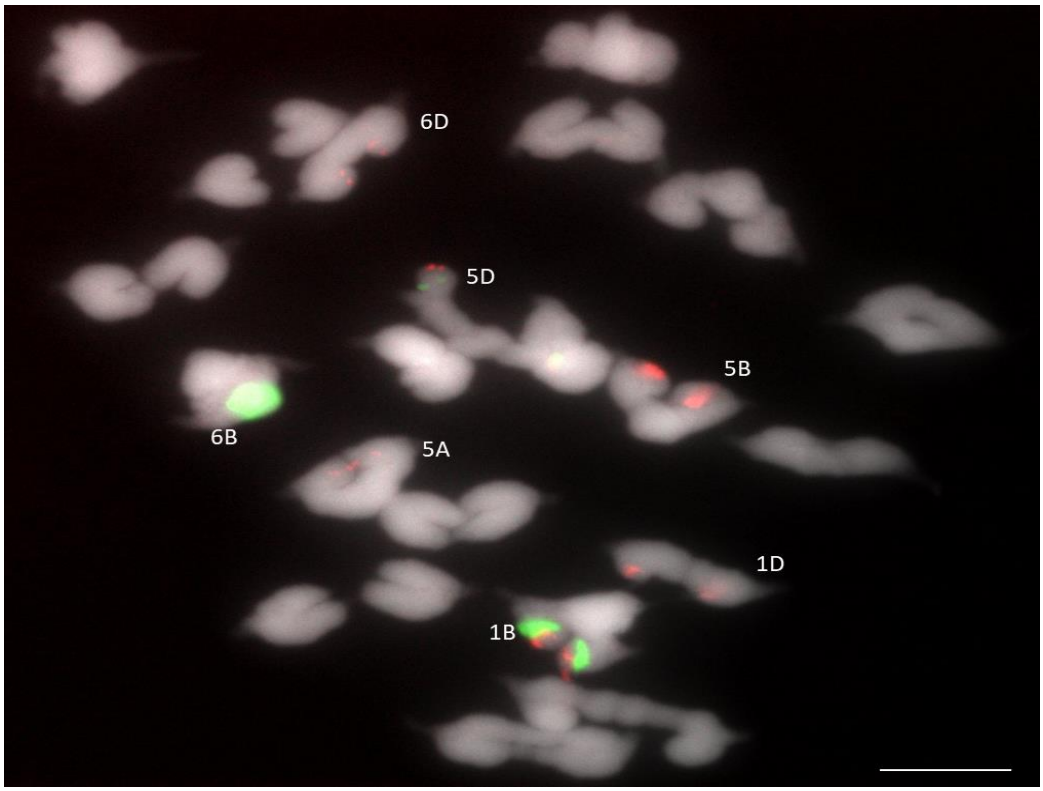

Figure 5.29: FISH with 45s(green) and 5s(red) in Cadenza HU. Scale bar = 10µm.

Moreover, the mean chiasma frequency of the chromosomes 5A, 1B, 5B, 6B, 1D and 5D in Cadenza HU and Cadenza WT were analysed. As a result, no significant differences were observed between the FISH chromosomes in Cadenza HU and Cadenza WT except on chromosome 5B which showed a low significant difference between them (One-way Welch's ANOVA test, p value = 0.02, N=32; figure 5.30).

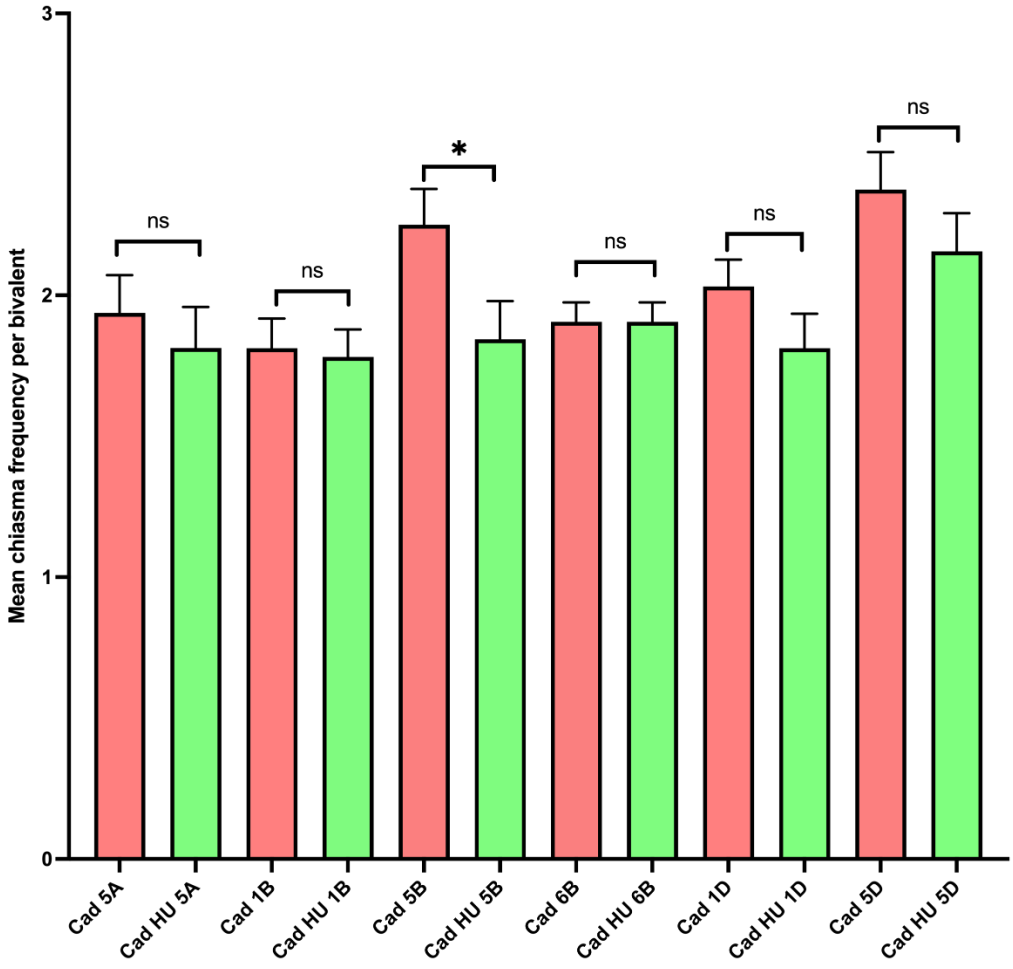

Figure 5.30: Comparison of the mean chiasma frequency of the FISH chromosome in Cadenza and Cadenza HU. Only chromosome 5B which showed a low significant difference between them. (One-way Welch's ANOVA, N=32).

5.2.4.1 Chromosome 5D

Starting with chromosome 5D, the chiasmata localization in this chromosome is listed in figure 5.31. Chiasmata are more distributed in chromosome 5D in Cadenza HU compared to Cadenza wild type. In ring bivalent, interstitial and proximal chiasmata appeared in both chromosome arms in Cadenza HU whereas this was not observed in Cadenza WT. The new localization of chiasmata in chromosome 5D are (i^1/i^1, i^1/i^2, i^1/i^3/p, i^1/p/d, i^2/i^2, i^2/i^3/d and i^2/p/d).

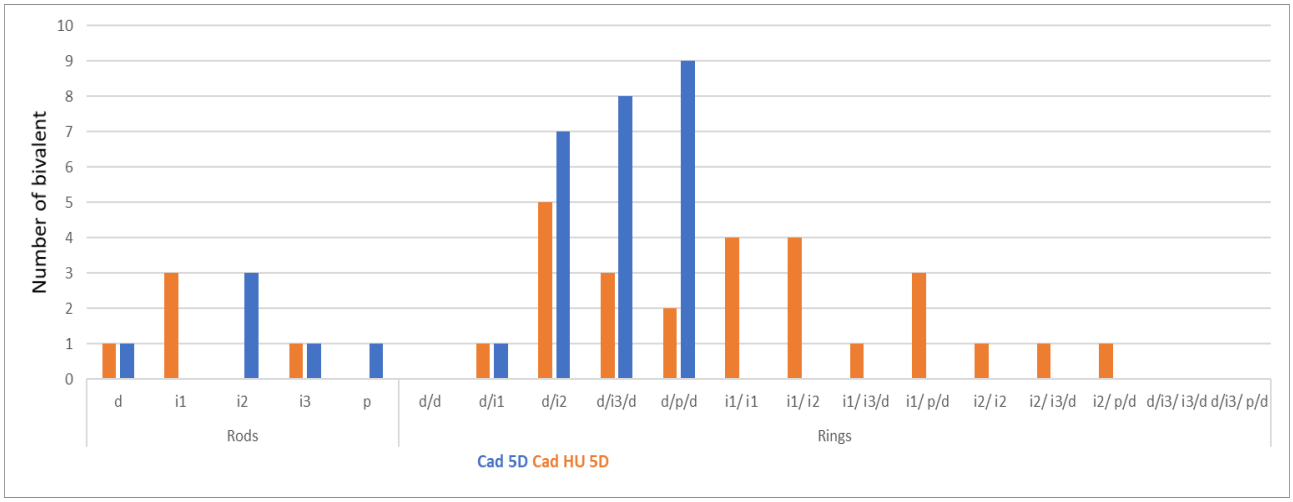

Figure 5.31:Distribution of chiasmata per bivalent in chromosome 5D in Cadenza and Cadenza HU. High number of chromosome 5D with more interstatitial and proximal chiasmata in both chromosome arm observed in Cadenza HU with no observation to these number of chromosome 5D in Cadenza WT.

Chiasmata occurred in both chromosome arms in chromosome 6B in Cadenza HU whereas no chiasmata were observed in both arms in Cadenza wild type for this chromosome (figure 5.32). The new chiasmata localization is (i^1/i^2 and $i^1/p/d$). In addition, the d/d ring chiasmata number was reduced in Cadenza HU whereas d/i^2 chiasmata increase in this plant compared to the wild type.

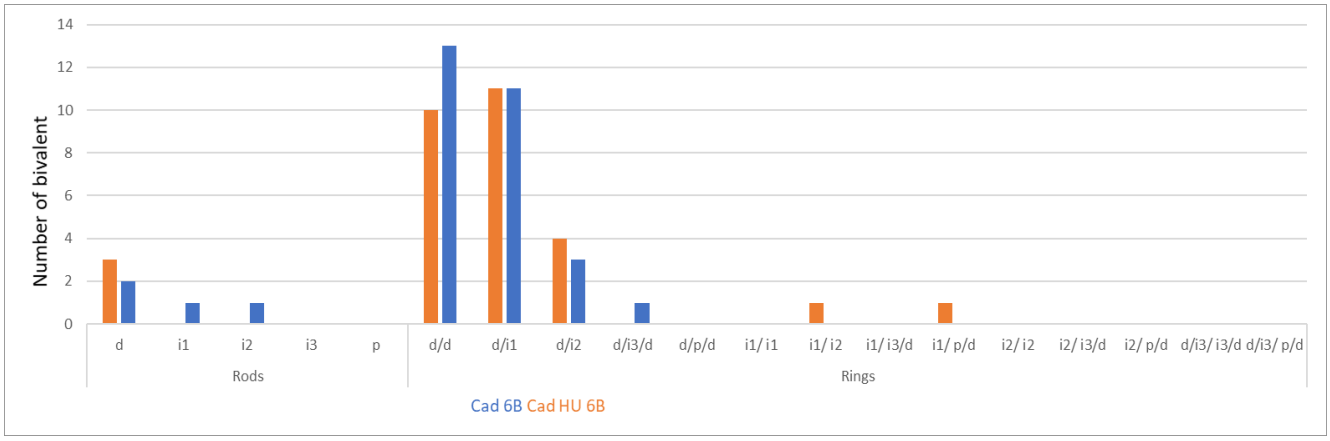

Figure 5.32: Distribution of chiasmata per bivalent in chromosome 6B in Cadenza and Cadenza HU. The new chiasmata localization is (i1/i2 and i1/p/d) in Cadenza HU chromosome 5D.

The chiasmata localization in chromosome 1B occurred at both chromosome arms in this chromosome in Cadenza HU (Figure 5.33). The new chiasmata localization is (i^1/i^1). In addition, bivalent with interstitial and proximal such as (d/i^1 and d/p/d) chiasmata increase in this chromosome in Cadenza HU compared to the wild type.

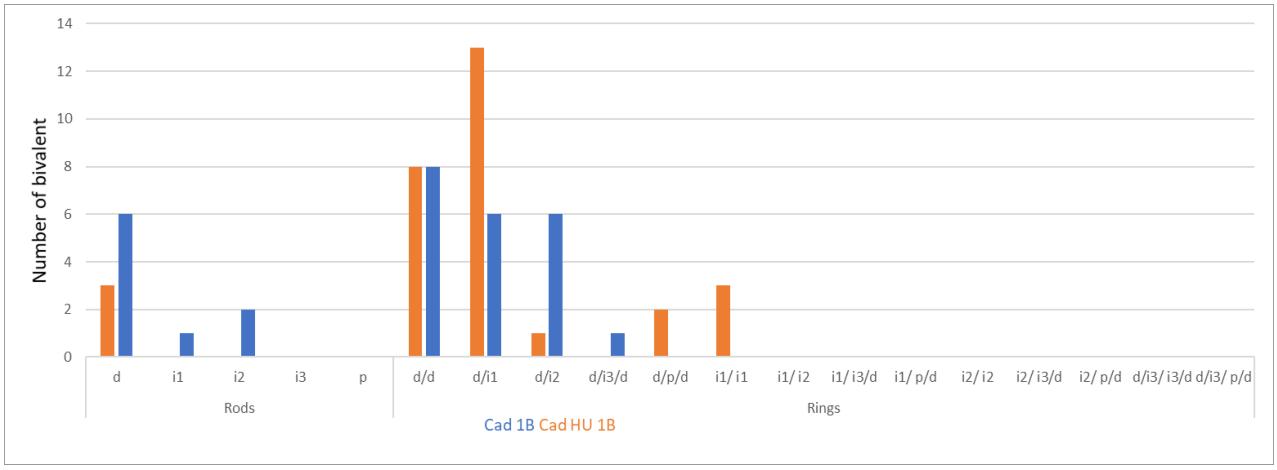

Figure 5.33: Distribution of chiasmata per bivalent in chromosome 1B in Cadenza and Cadenza HU. The new chiasmata localization is (i1/i1) in Cadenza HU chromosome 1B.

In conclusion, HU in Cadenza has showed a clear change pattern in chiasmata localization without any significant effect to the total number of chiasmata in the cell. Additionally, in specific chromosomes detected by FISH chiasmata localization was changed in some chromosomes such as 5D, 1B and 6B. Thus, the mean chiasma frequency of the FISH chromosome does not reflect any significant change between Cadenza and Cadenza HU.

5.2.5 Analysis of SAHA treatment in hexaploid cultivar Cadenza

SAHA (0.1mM) was injected to wheat to affect DNA replication to manipulate meiotic recombination and chiasmata localization in wheat. The metaphase I cells analyzed in this treatment showed rod and

ring bivalents in most of the cell, however, univalents also could be observed in some cells too (figure 5.34). The mean chiasma frequency of Cadenza SAHA (41.28±0.42) was significantly lower compared to Cadenza WT (43.78±0.23) (Welch's t test p value <0.0001, N=50) (figure 5.35).

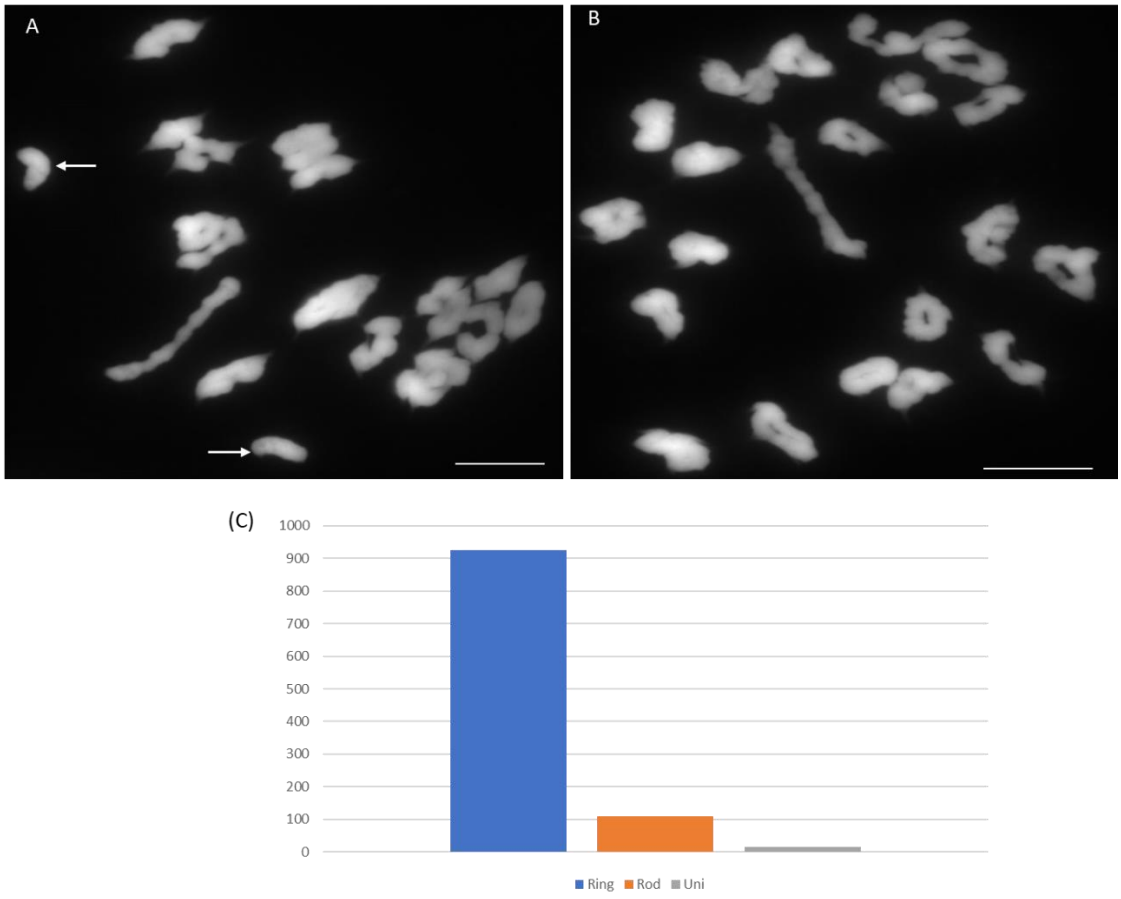

Figure 5.34: Metaphase l in Cadenza SAHA. (A) univalent observe and indicates by an arrow, (B) rod and ring bivalent only and (C) number of rings, rods and univalent in Cadenza SAHA. Scale bar = 10µm.

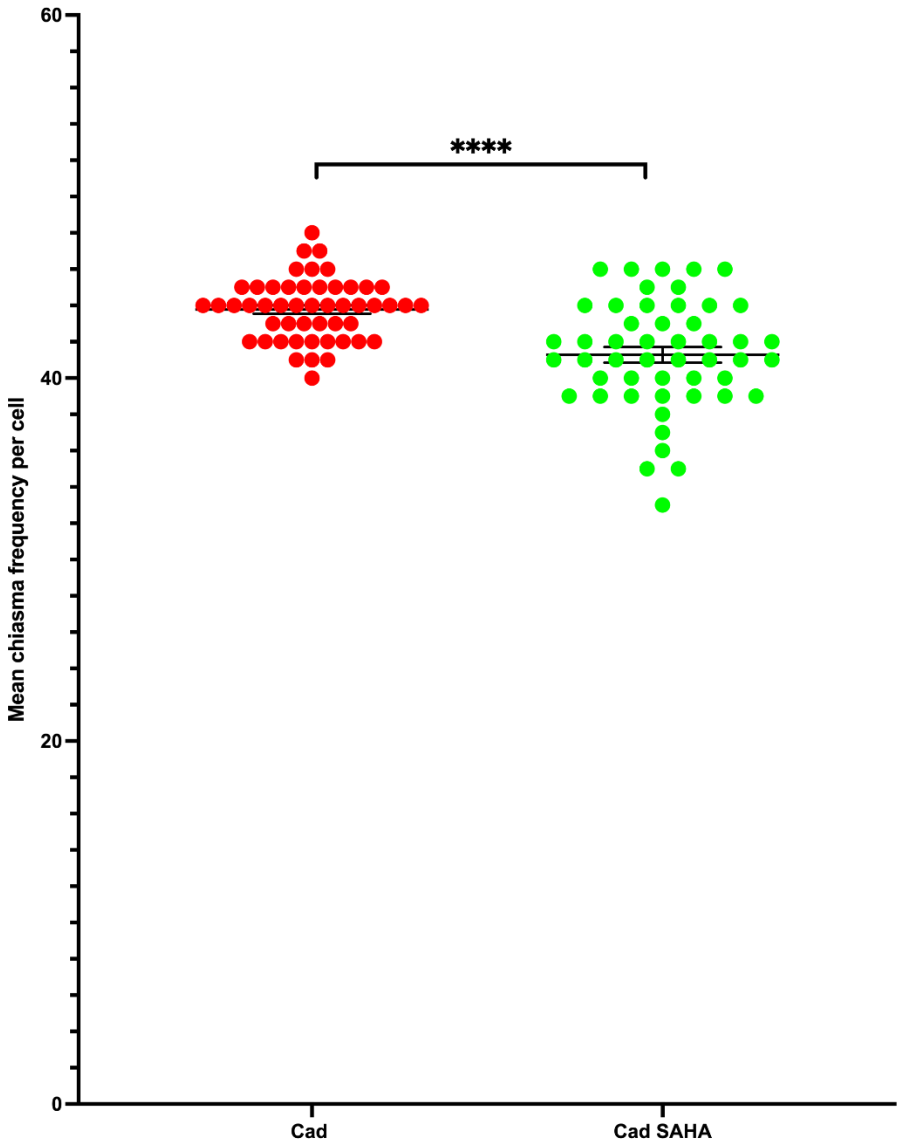

Figure 5.35: Comparison of the mean chiasma frequency in Cadenza WT and Cadenza treated with SAHA. The mean chiasma frequency of Cadenza SAHA was significantly lower compared to Cadenza WT. (Welch's t test $p<0.0001$, N=50).

Chiasmata localization in Cadenza SAHA was compared Cadenza WT. Chiasmata localization seem to occur in a new location in the chromosomes in these treated plants (figure 5.36). The new chiasmata localization produced new bivalent configurations: i^1/i^1 and i^1/i^2. Other chiasmata localization observed in these plants were $i^1/p/d$, i^2/i^2 and $i^2/p/d$ but the numbers observed with these chiasmata localizations was very low (up to four bivalents) in each location.

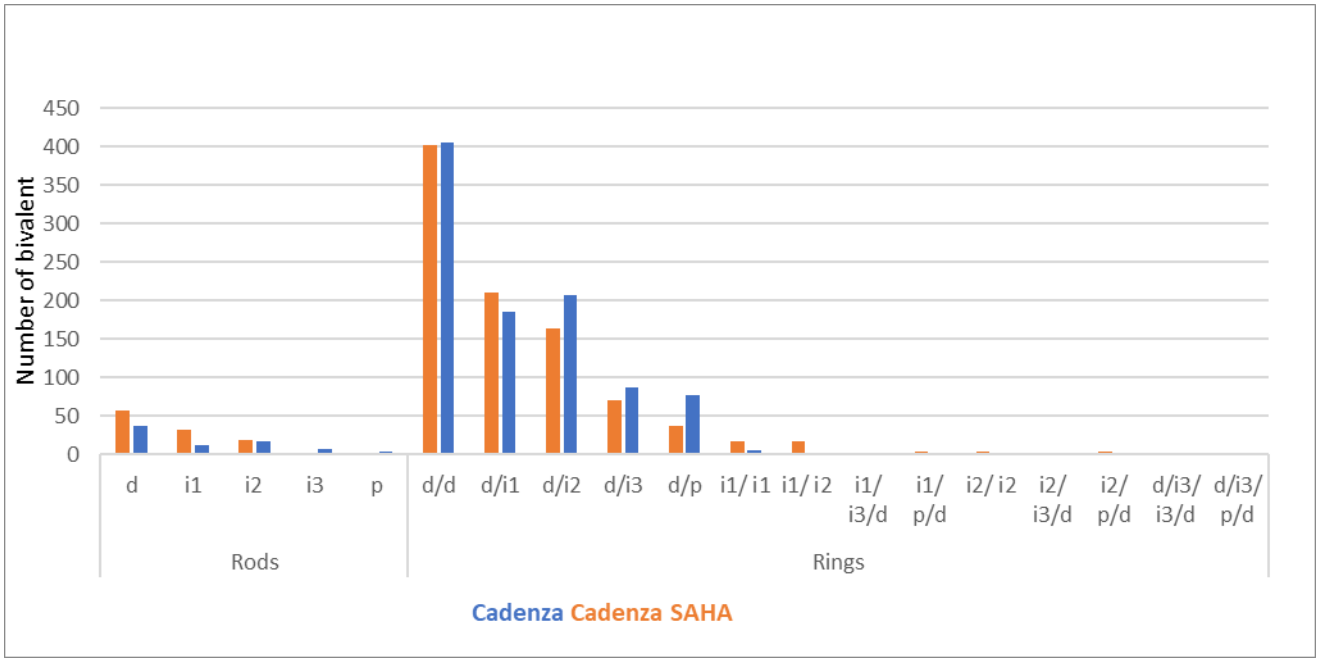

Figure 5.36: Distribution of chiasmata localization in Cadenza WT and Cadenza SAHA. The new chiasmata localization produced new bivalent configurations: i^1/i^1 and i^1/i^2. Other chiasmata localization observed in these plants were i^1/p/d, i^2/i^2 and i^2/p/d.

Furthermore, the number of distal chiasmata in rod and ring bivalents in Cadenza SAHA was almost similar to Cadenza WT. Additionally, a slight increase in d/i^1 bivalents in Cadenza SAHA in both rod and ring bivalents. However, there was a reduction in chiasmata localization in d/i^2, d/i^3/d and d/p/d in Cadenza SAHA compared to the WT (figure 5.36).

FISH probes were used to label six chromosomes: 5A, 1B, 5B, 6B, 1D and 5D (figure 5.37). No significant differences could be observed in chromosomes 5A, 1B, 6B and 1D (figure 5.38) Nevertheless, the mean chiasma frequencies in 5B and 5D chromosomes were significantly lower in Cadenza SAHA compared to Cadenza WT (p values = 0.03).

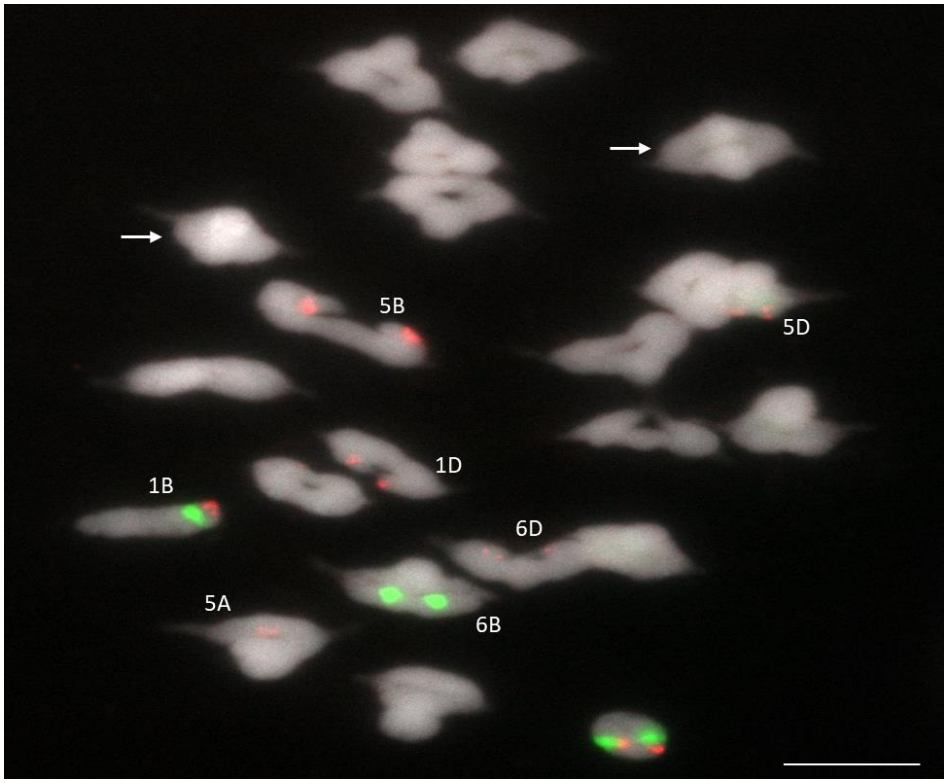

Figure 5.37: FISH with 45S(green) and 5S(red) rDNA probes in Cadenza SAHA. Two ring bivalents with interstitial chiasmata in both arms (indicated by arrows). Scale bar = 10µm.

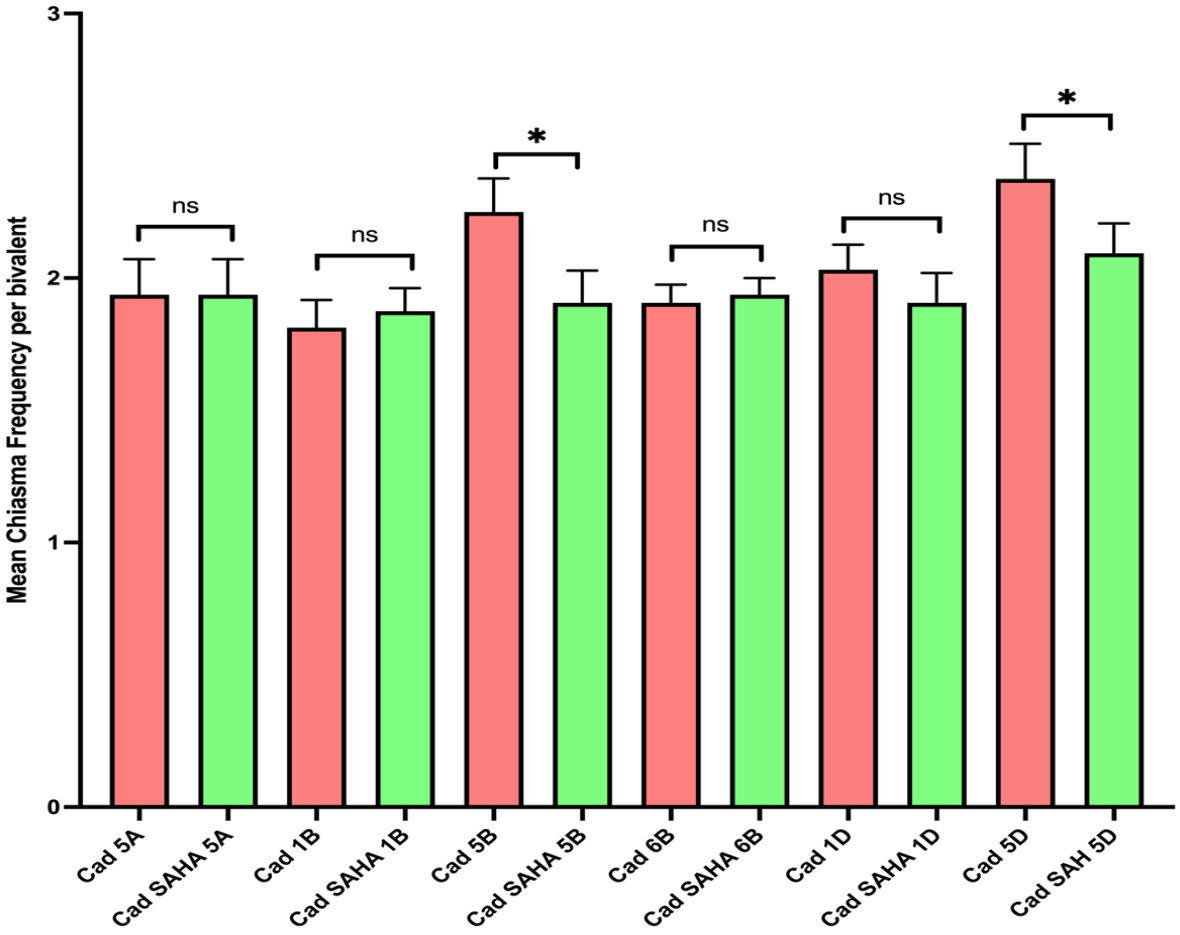

Figure 5.38: Comparison of the mean chiasma frequency of Cadenza WT and Cadenza SAHA FISH chromosomes. The mean chiasma frequencies in 5B and 5D chromosomes were significantly lower in Cadenza SAHA compared to Cadenza WT (Welch's t test, N=50).

5.3 Discussion

In this chapter, we have tried to analyse different methodologies to manipulate meiotic recombination in allopolyploid wheats. From classical mutations, *ph1b* and *ph1c*, to chemical treatments. Our analysis of the outcome of these methods have shown promising opportunities to achieve the required meiotic recombination manipulation needed for plant breeders to produce the next generation of crops.

5.3.1 Hexaploid wheat *ph1b* mutant allows homeologous recombination with a great cost to synapsis and homologous recombination

CS *ph1b* mutant was first identified by Sears (1977) as a deletion of 59.3 Mb on the long arm of chromosome 5B (Alabdullah *et al*., 2021).

The metaphase I chiasma analysis of CS *ph1b* has showed the presence of univalents and multivalents as well as normal bivalent configurations, rods and rings. This result is consistent with previous studies (Robert *et al*., 1999). In addition, the mean chiasma frequency of CS *ph1b* mutant was significantly lower than in CS WT, probably due to the presence of univalents (with obviously 0 chiasma) and multivalents (with an average of 2-3 chiasmata). Interestingly, the maximum number of multivalents observed per meiocyte was 3 (affecting 6 pairs of homologous chromosomes) whereas the minimum number of multivalents observed per meiocyte was just 1 (affecting only 2 pairs of homologous chromosomes). Additionally, the maximum number of univalents observed per meiocyte was 4 (affecting 2 bivalents) whereas the minimum number of univalents per meiocytes was 2 (affecting only 1 bivalent). Furthermore, when quantifying both, the appearance of univalents and multivalents per meiocyte together, it is observed that the maximum number per meiocyte was 3 multivalents and 4 univalents (affecting a total of 8 pairs of homologous chromosomes). From all

these observations it can be concluded that the effect of *ph1b* mutation was producing a limited number of bivalents (between 6-8 bivalents per meiocyte). Thus, about 40% of homologous pairs showed abnormal metaphase I configurations (multivalents and univalents) whereas about 60% of homologous pairs showed normal bivalent configurations (rod and ring). This observation is consistence to previous reports (Martín *et al*., 2014). It is thought that the role of *Ph1b* locus is to promote homologous pairing rather than preventing homoeologous pairing, however, deletion of *ph1b* results in limited (not all) homoeologous pairing and also limited synapsis (Martín *et al*., 2014).

Analysis of the spatio-temporal polarization of the meiotic progress in CS *ph1b* was conducted by using immunolocalisation of meiotic proteins ASY1 and ZYP1, as well as FISH using telomere DNA probe. This analysis in CS *ph1b* showed that meiosis progresses like in CS WT, from telomeric regions to more centromeric regions. Furthermore, it also showed that in CS *ph1b* about 40% of meiocytes did not show normal synapsis (ZYP1 polymerization). Why is the *ph1b* mutation affecting some meiocytes more than others? It was thought that the *Ph1* locus prevents synapsis between homoeologues, however, in wheat-rye hybrids, when only homeologous chromosomes are present, synapsis appears to be completed (Martín *et al*., 2017). Additionally, these authors also reported that even in *ph1b* mutant the synapsis is completed between homologous and homoeologous with the only difference that in *ph1b* mutant synapsis appears to be delayed compared to the WT (Martín *et al*., 2017).

We would like to emphasize that this 40% of meiocytes without full synapsis observed in the *ph1b* mutant seems to correlate with the 40% of homologous pairs that showed abnormal metaphase I configurations (multivalents and univalents). Moreover, the observation in delay in synapsis observed in *ph1b* in previous studies (Martín *et al*., 2017) was also observed by using FISH with telomere DNA probes combined with immunolocalisation of ZYP1. Synapsis progression seems to be delayed in *ph1b* mutant.

Furthermore, the meiotic time course with BrdU also showed a significant delay in meiotic progression in the *ph1b* mutant. The time taken to be complete meiosis in the *ph1b* mutant was about 48h. This is 5h longer than in CS WT (which takes about 43h). Additionally, analyzing the progression of prophase I in more detail allowed us to observe than in CS *ph1b* completion to metaphase I took about 43h whereas in CS WT it took about 39h. At 33h, CS *ph1b* appeared to be at early zygotene (initiation of synapsis) whereas CS WT seemed to be at mid/late zygotene (nearly full synapsis). This supports the idea that in *ph1b* mutant the synapsis progression is delayed and this brings a further delay in the meiotic completion of up to 5h.

FISH analysis of specific chromosomes in CS *ph1b* showed that the mean chiasma frequency of each identified chromosome was significantly lower to the same chromosome in CS WT. These identified chromosomes in CS *ph1b* showed that the reduction of chiasmata was correlated with the presence of univalents and multivalents of the same chromosomes. For instance, chromosome 5B which usually appears with 2-3 chiasmata in CS WT, in *ph1b* mutant appeared as a rod bivalent with 1 single chiasma in most of the cells and also as a pair of univalents in some other meiocytes. It was reported that many meiotic genes could be involved in the *Ph1* region.

CO formation has been related to the SC polymerization (synapsis) of homologous chromosomes. Recently, a correlation between ZIP4 and this role of the SC was found in budding yeast (Pyatnitskaya *et al*., 2022). ZIP4 seems to directly interact with ECM11 which is a SC central element protein that is present in DSBs attached to chromosome axis. ZIP4-ECM11 interaction ensures SC polymerization from DSB sites selected to progress to COs (Pyatnitskaya *et al*., 2022).

5.3.2 Tetraploid wheat *ph1c* mutant allows homeologous recombination with a great cost to homologous recombination but not synapsis

Cappelli *ph1c* mutant was first identified by Giorgi in 1978. This mutant contains a deletion in the long arm of chromosome 5B in the tetraploid wheat *T. durum* cultivar Cappelli (Giorgi, 1978).

Similarly to the analysis in CS *ph1b* mutant, tetraploid Cappelli *ph1c* mutant showed a significant decrease in the mean chiasma frequency compared to Cappelli WT. This significant decrease is also correlated to the presence of univalents and multivalents at metaphase I. However, the number of multivalents observed in Cappelli *ph1c* was lower compared to the number of multivalents observed in CS *ph1b*. This observation is consistent with what has been reported previously in *ph1c* mutant (Sanchez-Moran *et al*., 2001).

In contrast to hexaploid CS *ph1b* mutant, tetraploid Cappelli *ph1c* shows normal and fully completed synapsis at prophase I. It might be possible that the extra D genome present in CS *ph1b* (AABBDD) could make the synapsis progression more challenging compared to what happens in Cappelli *ph1c* (AABB). For instance, it has been reported that about 90% of homoeologous recombination that occurs in CS *ph1b* mutant it does happen between A and D genomes (Sánchez-Morán *et al.*, 2001). However, in tetraploid Cappelli *ph1c* only A and B genomes are present and this might be the reason of the lower number of multivalents. It is worth mentioning that due to poor growth and constraints in seed numbers further analysis of the meiosis time course in Cappelli *ph1c* by BrdU could not conducted.

The mean chiasma frequency of each identified chromosome by rDNA FISH analysis in Cappelli *ph1c* was significantly lower than the mean chiasma frequency of each of these chromosomes in Cappelli WT. This was identical to what it was observed in CS *ph1b* mutant. Thus, even if synapsis progression seems to be closer to the WT in *ph1c*, the effect on homologous recombination is maintained in the tetraploid mutant.

5.3.3 Tetraploid wheat substitution line 5D (5B) in cultivar Langdon allows homeologous recombination with a great cost to synapsis and homologous recombination

Langdon substitution line 5D(5B) with an extra chromosome 5D instead of chromosome 5B was developed by Joppa and Williams in 1979. It was developed as a result of a cross between monosomic 5B line with disomic 5D line of tetraploid wheat (Langdon) (Joppa and Williams, 1979). This line has been mostly use to introgress traits from wild relatives into tetraploid wheat. For instance, a study by (Othmeni *et al.*, 2022) used Langdon 5D(5B) to introgress *A. tauschii* (DD) genome traits into tetraploid wheat because the D genome contains desirable traits such as resistance to some abiotic and biotic stresses (Jia *et al*., 2013).

The mean chiasma frequency in Langdon 5D(5B) is significantly lower compared to Langdon WT. This reduction in the mean chiasma frequency coincides with the presence of univalents and multivalents at metaphase I in the Lnd 5D(5B) substitution line. Additionally, the immunolocalisation analysis of ASY1 and ZYP1 in this line showed defects in synapsis in about 40% of the meiocytes which was identical to the CS *ph1b* mutant. The number of univalents observed in this line in total of 50 cells was higher (55) compared to Cappelli *ph1c* (47) and CS *ph1b* (31). This high number of univalents might be due to the whole absence of chromosome 5B in Langdon 5D(5B) instead of partly deleted chromosome 5B in Cappelli *ph1c* and CS *ph1b*. The mean chiasma frequency of each identified chromosome by rDNA FISH analysis in the substitution line Lnd 5D(5B) showed to be significantly lower than in Lnd WT. Interestingly, in CS *ph1b* the percentage of cells with multivalents was much higher than in Cappelli *ph1c* and Langdon 5D(5B) (Table 5.4). Whereas the percentage of cells with univalents was very similar in all these materials (Table 5.5).

% cells	5A	1B	5B	6B	1D	5D	Any
ph1b	6	14	8	2	2	0	62
ph1c	2	4	4	0			8
5D(5B)	0	0		0		0	6

Table 5.1: Percentage of cells with multivalents involving 5A, 1B, 5B, 6B, 1D, 5D or any chromosome in CS *ph1b*, Cappelli *ph1c* and Langdon 5D(5B).

% cells	5A	1B	5B	6B	1D	5D	Any
ph1b	4	2	4	4	0	0	40
ph1c	4	2	8	2			52
5D(5B)	14	12		6		10	50

Table 5.2: Percentage of cells with univalents involving 5A, 1B, 5B, 6B, 1D, 5D or any chromosome in CS *ph1b*, Cappelli *ph1c* and Langdon 5D(5B).

5.3.4 HU treatment in hexaploid cultivar Cadenza has effects in chiasma frequency and localization

We decided to explore the manipulation of DNA replication to affect meiotic recombination in wheats. The spatio-temporal polarizing meiotic progression observed in cereals (Higgins *et al*., 2012; Osman *et al.*, 2021) starts very early on just as DNA replication progress from telomeres towards more interstitial regions along the chromosomes.

We decided to use HU to affect DNA replication in the hexaploid wheat cultivar Cadenza (Cad). HU is widely used to block DNA replication through the inhibition of ribonucleotide reductase (RNR) (Timson, 1975). The mechanism of limiting DNA repair by HU can be explained by the role of RNT activating the transformation of NDP to dNDP which results in limiting the formation of dNDP

(Nordlund and Reichard, 2006). HU seems to prevent dNTP from associating with the DNA polymerase at replication forks during the S-phase (Koç *et al*., 2004). HU treatment has been used during meiosis in budding yeast and its found to inhibit DNA replication during the pre-meiotic S-phase (Simchen *et al.*, 1976).

Moreover, the number of initiation sites for DNA synthesis seems to be affected by RNR activity (Wheeler *et al*., 2005). However, under the action of HU the RNR activity will be affected resulting in an accumulation of a huge number of DNA synthesis initiation sites at replication forks Subsequently, new replication forks are formed as a protection mechanism to guarantee continuation of the DNA replication process (Ercilla *et al*., 2020).

In this thesis chapter, the effect of HU on chiasma frequency and distribution was studied in hexaploid wheat. In Cadenza, the ring bivalents always contained distal chiasmata in one chromosome arm and distal, interstitial and/or proximal in the other chromosome arm. However, in Cadenza HU the observation of interstitial, or even proximal, chiasmata in one chromosome arm and interstitial or proximal chiasmata in the other arm was observed in some ring bivalents at metaphase I. It is worth to mention here that not all meiocytes showed the same response to the chemical treatment and this might be due to limitations and constraints of the methodology (not all the cells might be exposed equally to the chemical). Furthermore, wheat spikes contain cells at different meiotic stages, with HU could only affecting cells undergoing DNA replication. HU could be accumulating DNA synthesis at replication forks during the pre-meiotic S phase. Following this, when the cells are able to reactivate the replication forks at different sites of the chromosomes through the cell protection mechanism it might result in the formation of more initiation sites of meiotic progression, including sites in more interstitial/proximal regions.

The appearance of univalents and a significant lower chiasma frequency in Cadenza HU might be related to the effect of HU at CO sites where DNA replication is needed. Surprisingly, not fragmentation was observed, implying that HU DNA replication inhibition only affects COs (Class I and Class II).

Even though, the mean chiasma frequency is significant lower in Cadenza HU compared to Cadenza WT, the chiasmata localization appears to be more broadly distributed along the chromosome arms in Cadenza HU. To investigate this observation in more depth, Hei10 immunolocalization was carried out. This showed that in Cadenza HU the HEI10 foci number was significantly higher compared to Cadenza WT. It is possible that chiasmata counting could underestimate the CO number in Cadenza HU. For example, configuration i^2/i^2 (a ring bivalent containing 2 chiasmata, one in interstitial region 2 [i^2] in one arm and another in a similar i^2 region in the other arm) was quantified as a 2 chiasmata configuration but with HEI10 foci it was possible to identify bivalents with two foci close to each other at distal and i^2 regions. These close positioned foci observed at HU treatment could indicate a lessening of CO interference.

The analysis of HEI10 foci in Cadenza HU shows that the mean number of HEI10 foci at late diplotene is significantly higher than in untreated Cadenza. This is correlated with a significant decrease of chiasma frequency in Cadenza HU. These results can be explained by different ways:

- Firstly, the chiasmata count at metaphase I could have been understimated in Cadenza treated with HU. As reported before, bivalent configurations with distal and interstitial or proximal chiasmata in the same chromosome arm were observed. In these situations, we quantified the minimum number of chiasmata to explain the configuration (in this chromosome arms it counted as two chiasmata, one distal and another interstitial or proximal). Furthermore, in situations when an interstitial i^3 or a proximal chiasma occurs in a chromosome arm is easy

to recognise if there is another distal chiasma or not in that chromosome arm by the shape of the configuration. Nevertheless, with interstitial i^1 and i^2 chiasmata is very difficult, to the point that any double d/i^1 or d/i^2 in the same chromosome arm never counted. Our observations using HEI10 immunolocalization on diplotene bivalents have shown clear examples of bivalents with i^2 chiasma in one chromosome arm and another i^2 chiasma in the other in Cadenza HU that I would have counted at metaphase I as an i^2/i^2 configuration with a total of 2 chiasmata. Nevertheless, HEI10 foci images shows that in these configurations there can be two foci very close to each other during diplotene passing from a configuration with only 2 chiasmata to a bivalent with 3-4 HEI10 foci which could have been classified at metaphase I as $d/i^2/i^2/d$.

- Secondly, it might be possible that not all HEI10 foci observed at diplotene progress to chiasmata under the effect of HU. One of the close observations to this is reported by Martin et al (2014) in *ph1b* mutant in hexaploid wheat. is the authors reported that the number of MLH1 foci (Class I COs) in *ph1b* mutant is higher during pachytene than the number of chiasmata observed at metaphase I (Martín *et al*., 2014). Interestingly, in untreated CS and Cadenza the HEI10 foci number seems to be highly elevated compared to the chiasma frequency measured at metaphase I. These elevated numbers of HEI10 foci would mean that in Chinese Spring ~96% of COs are Class I whereas in Cadenza ~98% of COs are Class I. These percentage of Class I COs seems to be very elevated when compared to Arabidopsis (~85%) (Higgins *et al*., 2004; 2008; Osman *et al*., 2021) and other species like *Oryza sativa*, *Solanum lycopersicum*, *Brassica napus* and *Triticum turgidum subsp. durum* (Higgins *et al*., 2004, 2008b; Luo *et al*., 2013; Anderson *et al*., 2014; Wang *et al*., 2016; Gonzalo *et al*., 2019; Desjardins *et al*., 2020). Furthermore, it has been shown that in Cadenza (Osman *et al*., 2021) the immunolocalisation of another Class I CO mark, MLH3 foci at late pachytene was smaller

than HEI10 foci to the point that the ratio gets reduced to ~87% of Class I COs when using MLH3 foci as the Class I CO marker. All this could be pointing that HEI10 might be involved in processing other structures not just Class I COs. Interestingly, *zmm* mutants for *Msh4* and *Msh5* genes in tetraploid wheat variety Kronos (Desjardin *et al*., 2020) showed that the residual chiasmata (Class II COs) in these mutants was about 15% of the WT with similar values than in Arabidopsis and other plant species (Higgins *et al*., 2004, 2008b; Luo *et al*., 2013; Anderson *et al*., 2014; Wang *et al*., 2016; Gonzalo *et al*., 2019; Desjardin *et al*., 2020). Furthermore, these authors observed that in Kronos the mean number of HEI10 foci per cell was 28.9 ± 0.64 (Desjardin *et al*., 2020). A value higher than the chiasma frequency observed (26.22 ± 0.24) in the same article. These observations could lead to think that indeed the authors might have been underestimating COs numbers by quantifying chiasma frequency. Nevertheless, the authors also did immunolocalization of HEI10 foci in *msh4/msh5* mutants in Kronos and surprisingly they found residual signals on the chromosomes (~3 foci/cell) and although most of them look smaller and fainter, at least 17.6% looked similar to those observed in the WT (Desjardin *et al*., 2020). This could indicate that perhaps HEI10 in wheats is not a very good Class I marker as it could be labelling other structures.

5.3.5 SAHA treatment in hexaploid cultivar Cadenza has effects in chiasma frequency but limited effects in chiasmata localization

SAHA is an inhibitor of histone deacetylases (HDACi) and it has been used in human cell culture to delay the speed of the replication forks and to activate the replication in different dormant regions (Conti *et al.*, 2010). This is the first study to date to analyze the effect of SAHA in DNA replication and meiotic recombination in wheat. SAHA affects replication forks which means that it would be more effective in early DNA replication initiation (S phase). The result in this thesis have shown that

SAHA has a low effect in chiasmata localization but the mean chiasma frequency was significantly lower in SAHA treated Cadenza cells compared to the non-treated. Again, this decrease on recombination seems to be also related to the appearance of univalents and a significant increase in the number of rod bivalents in this treatment. Again, the presence of univalents and absence of fragmentation at metaphase I might be pointing that SAHA influences on COs but not in NCOs.

The effect of HU in chiasmata localization was higher compared to the effect of the SAHA. Thus, in Cadenza HU 40 cells out of 50 cells showed at least one bivalent with interstitial chiasmata in both chromosome arms whereas in Cadenza SAHA 25 cells showed at least one bivalent with interstitial chiasmata in both arms. FISH analysis to identify some specific chromosomes showed that SAHA treated Cadenza presented mean chiasma frequencies in 5B and 5D chromosomes were significantly lower than in no treated Cadenza.

Chapter 6. General Discussion and Conclusions

The purpose of this study has been to systematically analyse meiotic recombination through analysing chiasma frequency and localization in different wheat cultivars from different ploidy levels (tetraploid and hexaploid) and in wheat wild ancestor relatives (diploid). Additionally, the analysis of wheat mutants such as CS *ph1b*, Cappelli *ph1c* and Langdon substitution line 5D(5B) were conducted in this study. Finally, the analysis of chemical treatments (HU and SAHA) to manipulate meiotic recombination was also conducted.

6.1 Relationship between genetic markers and COs frequency

Different hexaploid wheat map lengths have been reported in the literature. A high-density genetic map of a CSxSQ1 cross showed a length of 3,522 cM, equivalent to 70 COs per meiosis or about 3.3 COs per bivalent (Quarrie et al., 2005). Using inbred lines, the genetic map length was estimated to be 4,558.55 cM, this would equate to 91 COs per meiosis or about 4.3 COs per bivalent (Qu et al., 2021). These numbers are up to double the numbers that observed by chiasma frequency in this thesis (higher value was observed in CS (46 COs per cell / 2.2 COs per bivalent). These anomalies to estimate CO frequency per meiosis using genetic map lengths have been observed in different organisms. For instance in *Arabidopsis thaliana*, differences in map lengths have been shown using different techniques: a high resolution map of inbred lines reported a map length of 422.5 cM (8,45 COs per meiosis, about 1.69 COs per bivalent) (Singer et al., 2006); a genome-wide sequencing showed a map length of 575 cM (11.5 COs per meiosis, about 2.3 COs per bivalent) (Giraut et al., 2011); a more recent high-density genetic map using RNA-seq has shown an intermediate map length of 471.7 cM (9.4 COs per meiosis, about 1.88 COs per bivalent) (Serin et al., 2017). Interestingly, this later number is very similar to that reported using chiasma frequency (9.24 COs per cell) (Sanchez-Moran et al., 2001). Nevertheless, the association of recombination frequencies (COs) from

map distances contains some problems. The additive nature of the genetic map lengths between different markers to obtain the full genomic genetic map have several constraints: COs rates are distributed differentially along the chromosomes (more frequent in distal regions than close to the centromere), more than one CO can occur between two markers and recombination can be missed, the map distance over a long interval is estimated by the addition of smaller intervals and this makes the association with recombination frequency not sufficient clear. Different functions have been used to model for these constraints, among them Haldane's function and Kosambi's map function are the most common used. Nevertheless, in some species (humans and stickleback fishes) these functions have shown to be unable to predict recombination frequencies from map distances (Kivikoski et al., 2023). The author's results showed that the association between map distance and recombination frequency depends of different parameters in the organism in question and it is not possible to have a universal solution making the estimations very difficult (Kivikoski et al., 2023). Thus, in hexaploid wheat the high number of COs per meiosis estimated by using map distances could be overestimating COs due to different constraints of genetic mapping but we are also aware that it could be possible that we might be underestimating some of these COs by counting chiasmata at metaphase I bivalents.

6.2 Differences and similarities in chiasmata localization in wheat

In cultivated tetra and hexaploid wheats and in their wild diploid relatives, the cytological analysis revealed that the most preferred location for chiasmata was at distal regions (close to telomeres). However, all these wheat cultivars and species also showed some interstitial and proximal chiasmata. Distal chiasmata in wheat have been accounted as one of the most common barriers to plant breeders

because it restricts allelic variation during meiosis. In fact, there are many studies showing that interstitial and proximal regions in wheat chromosomes might contain genetic regions that could be important to improve wheat breeding programmes. Based on this, manipulating meiotic recombination in wheat could be seen as one of the most important solutions to improve wheat breeding programmes and to provide tools to generate the new crops in a near future that will be needed to ensure Food Security and survive climate change.

In wild type wheat, there are two main forms of bivalents at metaphase I: rod bivalents with at least one chiasma occurring in only one of the chromosome arms between the homologous chromosomes and ring bivalents with at least two chiasmata occurring in both arms (at least one chiasma per chromosome arm between the two homologous chromosomes) (Sybenga, 1975). In all cultivated wheat and wild relatives, the majority of bivalent shapes are rings with a few rods (figure 6.1).

The chromosome length can be divided in distal (d) regions (close to telomere), proximal (p) regions (close to centromeres) and everything in between as interstitial (i) regions. Wheat chromosomes are of such a big size that we have been able to classify different interstitial regions (i^1, i^2 and i^3) being i^1 the closer to telomeres and i^3 the closer to centromeres but not as close to them as the proximal regions. Identifying different bivalent configurations at metaphase I has facilitated the quantification of the numbers of chiasmata and their localization on wheat chromosomes. The analysis of wheat configurations at metaphase I showed that most chiasmata in wheat are occurring at distal regions with very moderate numbers occurring at interstitial regions and low numbers at proximal regions. Furthermore, this analysis allowed us to identify the mean chiasma frequency and the chiasmata localization in different wheat cultivars and species and compared them. Our data has showed significant differences between them.

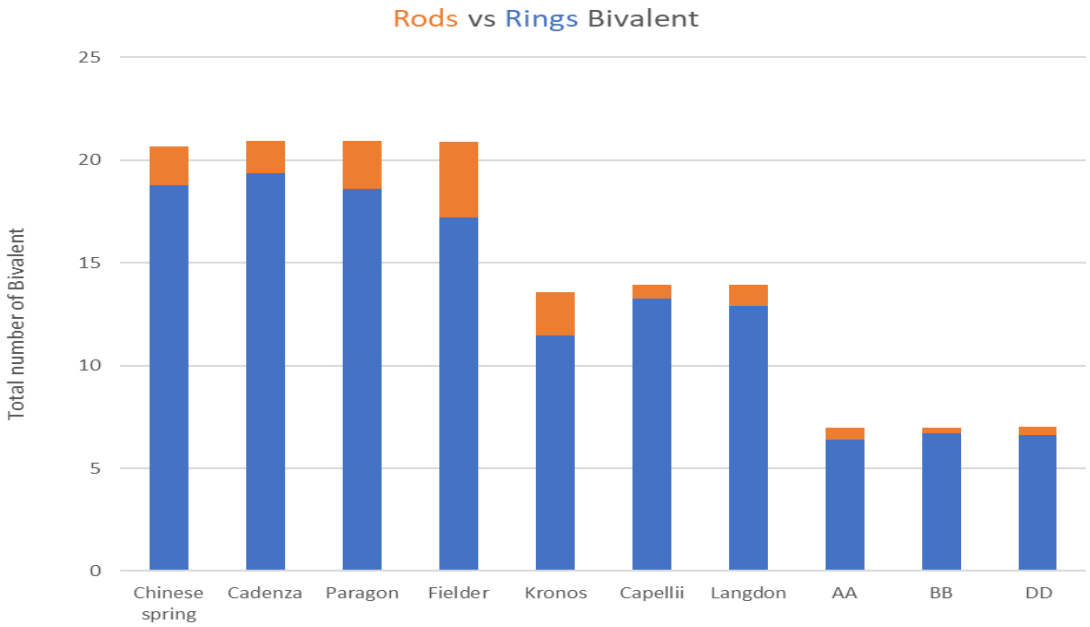

Figure 6.1: Number of ring and rod bivalents in all cultivated wheats and their wild relatives studied.

6.3 Chiasma frequency in cultivated wheats

The mean chiasma frequency in hexaploid wheat cultivars showed significant differences among some of them (summary of mean chiasma frequency significance in Table 6.1). For instance, CS mean chiasma frequency was significantly higher compared to Cadenza's mean chiasma frequency. Additionally, in tetraploid wheat Cappelli mean chiasma frequency was significantly higher compared to Kronos mean chiasma frequency. Furthermore, the chiasmata localization in tetraploid and hexaploid wheats showed significant differences between them when they compare to each other. For instance, Kronos and Fielder cultivars show lower numbers on distal chiasmata whereas CS and Cappelli show the highest number on proximal chiasmata compare to the other wheat cultivars. Surprisingly, the mean chiasma frequency in diploid wheat relatives did not show significant differences among them.

			Mean Chiasma Frequency …															
			... per cell				… per bivalent				... per ring				... per rod			
6X	CS	6X	CS	Cad	Pg	Fld	CS	Cad	Pg	Fld	CS	Cad	Pg	Fld	CS	Cad	Pg	Fld
		4X	Kr	Cap	Lnd		Kr	Cap	Lnd		Kr	Cap	Lnd		Kr	Cap	Lnd	
		2X	AA	BB	DD		AA	BB	DD		AA	BB	DD		AA	BB	DD	
	Cad	6X	CS	Cad	Pg	Fld	CS	Cad	Pg	Fld	CS	Cad	Pg	Fld	CS	Cad	Pg	Fld
		4X	Kr	Cap	Lnd		Kr	Cap	Lnd		Kr	Cap	Lnd		Kr	Cap	Lnd	
		2X	AA	BB	DD		AA	BB	DD		AA	BB	DD		AA	BB	DD	
	Pg	6X	CS	Cad	Pg	Fld	CS	Cad	Pg	Fld	CS	Cad	Pg	Fld	CS	Cad	Pg	Fld
		4X	Kr	Cap	Lnd		Kr	Cap	Lnd		Kr	Cap	Lnd		Kr	Cap	Lnd	
		2X	AA	BB	DD		AA	BB	DD		AA	BB	DD		AA	BB	DD	
	Fld	6X	CS	Cad	Pg	Fld	CS	Cad	Pg	Fld	CS	Cad	Pg	Fld	CS	Cad	Pg	Fld
		4X	Kr	Cap	Lnd		Kr	Cap	Lnd		Kr	Cap	Lnd		Kr	Cap	Lnd	
		2X	AA	BB	DD		AA	BB	DD		AA	BB	DD		AA	BB	DD	
4X	Kr	6X	CS	Cad	Pg	Fld	CS	Cad	Pg	Fld	CS	Cad	Pg	Fld	CS	Cad	Pg	Fld
		4X	Kr	Cap	Lnd		Kr	Cap	Lnd		Kr	Cap	Lnd		Kr	Cap	Lnd	
		2X	AA	BB	DD		AA	BB	DD		AA	BB	DD		AA	BB	DD	
	Cap	6X	CS	Cad	Pg	Fld	CS	Cad	Pg	Fld	CS	Cad	Pg	Fld	CS	Cad	Pg	Fld
		4X	Kr	Cap	Lnd		Kr	Cap	Lnd		Kr	Cap	Lnd		Kr	Cap	Lnd	
		2X	AA	BB	DD		AA	BB	DD		AA	BB	DD		AA	BB	DD	
	Lnd	6X	CS	Cad	Pg	Fld	CS	Cad	Pg	Fld	CS	Cad	Pg	Fld	CS	Cad	Pg	Fld
		4X	Kr	Cap	Lnd		Kr	Cap	Lnd		Kr	Cap	Lnd		Kr	Cap	Lnd	
		2X	AA	BB	DD		AA	BB	DD		AA	BB	DD		AA	BB	DD	
2X	AA	6X	CS	Cad	Pg	Fld	CS	Cad	Pg	Fld	CS	Cad	Pg	Fld	CS	Cad	Pg	Fld
		4X	Kr	Cap	Lnd		Kr	Cap	Lnd		Kr	Cap	Lnd		Kr	Cap	Lnd	
		2X	AA	BB	DD		AA	BB	DD		AA	BB	DD		AA	BB	DD	
	BB	6X	CS	Cad	Pg	Fld	CS	Cad	Pg	Fld	CS	Cad	Pg	Fld	CS	Cad	Pg	Fld
		4X	Kr	Cap	Lnd		Kr	Cap	Lnd		Kr	Cap	Lnd		Kr	Cap	Lnd	
		2X	AA	BB	DD		AA	BB	DD		AA	BB	DD		AA	BB	DD	
	DD	6X	CS	Cad	Pg	Fld	CS	Cad	Pg	Fld	CS	Cad	Pg	Fld	CS	Cad	Pg	Fld
		4X	Kr	Cap	Lnd		Kr	Cap	Lnd		Kr	Cap	Lnd		Kr	Cap	Lnd	
		2X	AA	BB	DD		AA	BB	DD		AA	BB	DD		AA	BB	DD	

Table 6.1: Statistical significant differences in mean chiasma frequency per cell, per bivalent, per ring and per rod bivalents. Species/varieties comparisons are indicated by different colour codes: N.S. ($p > 0.05$) in black, significant differences ($p \leq 0.05$) higher in green, significant differences ($p \leq 0.05$) lower in red.

6.3.1 Mean chiasma frequency per bivalent allows to compare different ploidy level species

Calculating mean chiasma frequency per bivalent has allowed us to systematically compare all different wheat cultivars and species. The mean chiasma frequency per bivalent shows significant differences among different wheat cultivars and species (Table 6.1). Furthermore, mean chiasma frequency could be inferred for different chromosome regions d, i1, i2, i3 and p (Table 6.2).

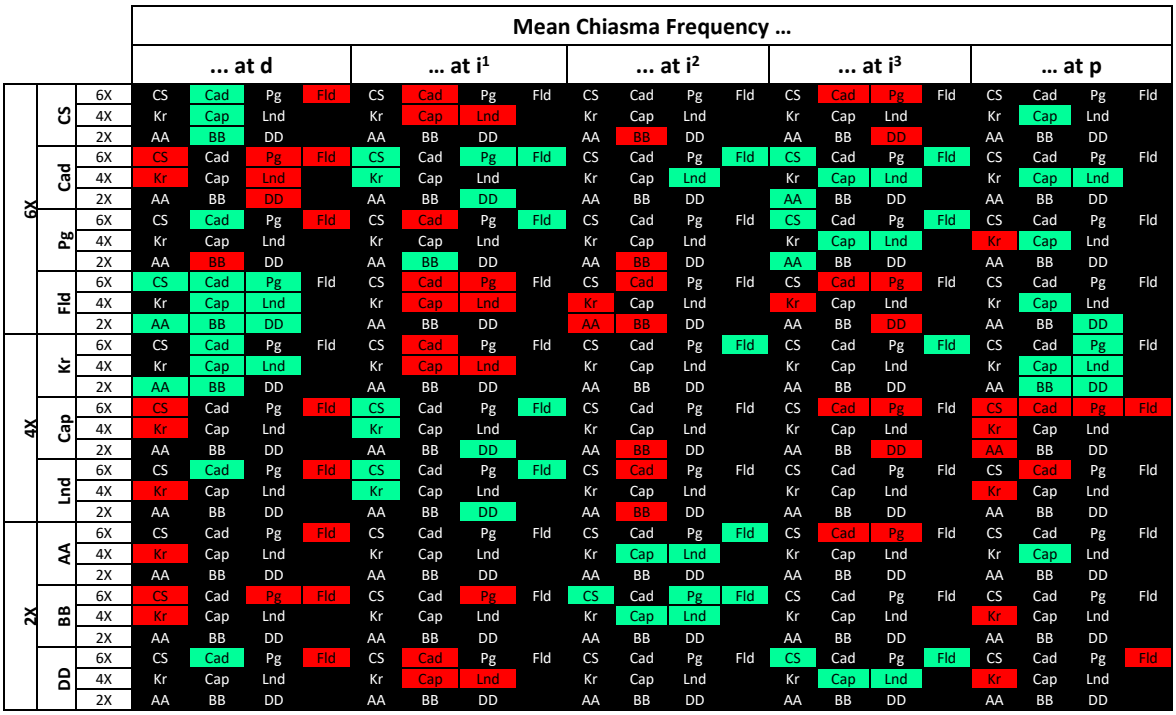

			Mean Chiasma Frequency …																			
			… at d				… at i^1				… at i^2				… at i^3				… at p			
6X	CS	6X	CS	Cad	Pg	Fld	CS	Cad	Pg	Fld	CS	Cad	Pg	Fld	CS	Cad	Pg	Fld	CS	Cad	Pg	Fld
		4X	Kr	Cap	Lnd		Kr	Cap	Lnd		Kr	Cap	Lnd		Kr	Cap	Lnd		Kr	Cap	Lnd	
		2X	AA	BB	DD		AA	BB	DD		AA	BB	DD		AA	BB	DD		AA	BB	DD	
	Cad	6X	CS	Cad	Pg	Fld	CS	Cad	Pg	Fld	CS	Cad	Pg	Fld	CS	Cad	Pg	Fld	CS	Cad	Pg	Fld
		4X	Kr	Cap	Lnd		Kr	Cap	Lnd		Kr	Cap	Lnd		Kr	Cap	Lnd		Kr	Cap	Lnd	
		2X	AA	BB	DD		AA	BB	DD		AA	BB	DD		AA	BB	DD		AA	BB	DD	
	Pg	6X	CS	Cad	Pg	Fld	CS	Cad	Pg	Fld	CS	Cad	Pg	Fld	CS	Cad	Pg	Fld	CS	Cad	Pg	Fld
		4X	Kr	Cap	Lnd		Kr	Cap	Lnd		Kr	Cap	Lnd		Kr	Cap	Lnd		Kr	Cap	Lnd	
		2X	AA	BB	DD		AA	BB	DD		AA	BB	DD		AA	BB	DD		AA	BB	DD	
	Fld	6X	CS	Cad	Pg	Fld	CS	Cad	Pg	Fld	CS	Cad	Pg	Fld	CS	Cad	Pg	Fld	CS	Cad	Pg	Fld
		4X	Kr	Cap	Lnd		Kr	Cap	Lnd		Kr	Cap	Lnd		Kr	Cap	Lnd		Kr	Cap	Lnd	
		2X	AA	BB	DD		AA	BB	DD		AA	BB	DD		AA	BB	DD		AA	BB	DD	
4X	Kr	6X	CS	Cad	Pg	Fld	CS	Cad	Pg	Fld	CS	Cad	Pg	Fld	CS	Cad	Pg	Fld	CS	Cad	Pg	Fld
		4X	Kr	Cap	Lnd		Kr	Cap	Lnd		Kr	Cap	Lnd		Kr	Cap	Lnd		Kr	Cap	Lnd	
		2X	AA	BB	DD		AA	BB	DD		AA	BB	DD		AA	BB	DD		AA	BB	DD	
	Cap	6X	CS	Cad	Pg	Fld	CS	Cad	Pg	Fld	CS	Cad	Pg	Fld	CS	Cad	Pg	Fld	CS	Cad	Pg	Fld
		4X	Kr	Cap	Lnd		Kr	Cap	Lnd		Kr	Cap	Lnd		Kr	Cap	Lnd		Kr	Cap	Lnd	
		2X	AA	BB	DD		AA	BB	DD		AA	BB	DD		AA	BB	DD		AA	BB	DD	
	Lnd	6X	CS	Cad	Pg	Fld	CS	Cad	Pg	Fld	CS	Cad	Pg	Fld	CS	Cad	Pg	Fld	CS	Cad	Pg	Fld
		4X	Kr	Cap	Lnd		Kr	Cap	Lnd		Kr	Cap	Lnd		Kr	Cap	Lnd		Kr	Cap	Lnd	
		2X	AA	BB	DD		AA	BB	DD		AA	BB	DD		AA	BB	DD		AA	BB	DD	
2X	AA	6X	CS	Cad	Pg	Fld	CS	Cad	Pg	Fld	CS	Cad	Pg	Fld	CS	Cad	Pg	Fld	CS	Cad	Pg	Fld
		4X	Kr	Cap	Lnd		Kr	Cap	Lnd		Kr	Cap	Lnd		Kr	Cap	Lnd		Kr	Cap	Lnd	
		2X	AA	BB	DD		AA	BB	DD		AA	BB	DD		AA	BB	DD		AA	BB	DD	
	BB	6X	CS	Cad	Pg	Fld	CS	Cad	Pg	Fld	CS	Cad	Pg	Fld	CS	Cad	Pg	Fld	CS	Cad	Pg	Fld
		4X	Kr	Cap	Lnd		Kr	Cap	Lnd		Kr	Cap	Lnd		Kr	Cap	Lnd		Kr	Cap	Lnd	
		2X	AA	BB	DD		AA	BB	DD		AA	BB	DD		AA	BB	DD		AA	BB	DD	
	DD	6X	CS	Cad	Pg	Fld	CS	Cad	Pg	Fld	CS	Cad	Pg	Fld	CS	Cad	Pg	Fld	CS	Cad	Pg	Fld
		4X	Kr	Cap	Lnd		Kr	Cap	Lnd		Kr	Cap	Lnd		Kr	Cap	Lnd		Kr	Cap	Lnd	
		2X	AA	BB	DD		AA	BB	DD		AA	BB	DD		AA	BB	DD		AA	BB	DD	

Table 6.2: Statistical significant differences in mean chiasma frequency per d, per i^1, per i^2, per i^3 and per p localisation. Species/varieties comparisons are indicated by different colour codes: N.S. ($p > 0.05$) in black, significant differences ($p \leq 0.05$) higher in green, significant differences ($p \leq 0.05$) lower in red.

Our results show that the mean chiasma frequency is significant different between wheat cultivars in the same species and ploidy level (e.g.: hexaploid *T. aestivum* cultivars CS vs Cadenza; tetraploid *T. durum* cultivars Cappelli vs Kronos). Furthermore, also significant differences could be observed between wheat species with different ploidy level (e.g.: hexaploid CS vs tetraploid Kronos).

To understand why there were differences among cultivars on the same species, two wheat hexaploid cultivars with the same ploidy level that showed significant differences in the mean chiasma frequency were further analysed: CS vs Cadenza. Different methodologies were used to get a broader picture of these differences: Immuno-cytological localization of meiotic chromosome axis protein ASY1 and SC central element ZYP1, meiotic time course using a combined BrdU staining and

immunolocalisation of ZYP1, FISH analysis to identify telomere regions and immunolocalisation of Class I COs using Hei10 antibodies at late diplotene.

6.4 Identification of specific chromosomes by FISH and the systematic analysis of their evolution through different ploidy levels

FISH analysis with 45S and 5S rDNA probes has allowed us to identify specific chromosomes in diploid, tetraploid and hexaploid wheats. In hexaploid *T. aestivum* wheat (AABBDD) chromosomes 5A, 1B, 5B, 6B, 1D and 5D were identified. In tetraploid *T. durum* wheat (AABB) chromosomes 5A, 1B, 5B and 6B were identified. In diploid species *T. monococcum* (AA) two chromosomes 1A and 5A were identified. In diploid species *Ae. speltoides* (BB) another two chromosomes were distinguished 1B and 5B. In diploid species *Ae. tauschii* (DD) another two chromosomes were also distinguished 1D and 5D. The mean chiasma frequency has been analysed in each chromosome and compared to the mean chiasma frequency of the same chromosome in different cultivars of the same species and even to other species at different ploidy levels.

For instance, chromosome 5B mean chiasma frequency shows significant differences between wheats from the same ploidy level (e.g.: CS vs Fielder) and between different species with different ploidy level (e.g.: Cappelli vs Fielder). The reason of why this chromosome 5B is behaving differently in term of chiasma number and localization in wheat from the same ploidy level is unknown. It might be possible that chromosome structure has an important influence to chiasmata formation and localization on them, something that whole genome sequence comparisons would be able to find.

The whole genome duplication process that occurs during the formation of a polyploid could cause changes in chromosome structure (chromosome rearrangements) and even in the genome size. For instance, chromosome 5B which usually appears as a ring bivalent with d/d chiasmata in the diploid

species *Ae. speltoides* (BB). However, chromosome 5B in tetraploid and hexaploid wheats usually appears as ring bivalent with interstitial and proximal chiasmata indicating an increase in the chiasmata number and changes in the localization in this chromosome. In contrast, chromosome 1B appears as a ring bivalent with always an interstitial chiasma in diploid *Ae. speltoides* (BB) whereas in tetra and hexaploid wheats this chromosome appears usually as a rod bivalent or a ring with d/d chiasmata. This situation in these two chromosomes, 5B and 1B, shows a different tendency in chiasma frequency and distribution during the polyploidization process of wheats. One of the possible reasons to explain these opposite tendencies in these chromosomes could be due to chromosome rearrangements (e.g.: translocations) following the hybridisation process during the polyploidization of wheats. It might be that some of the active recombination regions move from one chromosome to another. It was reported that translocation and inversion in wheat appears to be different in different wheat cultivars from the different geographical regions (Badaeva *et al.*, 2007). Interestingly, analysing chiasma frequency and distribution in different terminal deletion lines in hexaploid wheat has showed that these distal deletions obligate to move the chiasmata to more proximal positions that are now located in distal regions (Naranjo, 2015).

6.4.1 Chromosome 5B

Chromosome 5B is an important chromosome in wheat specifically in the meiosis field because it carries one of the most important loci in homologous pairing *Ph1* locus. This *Ph1* locus maintains the diploid like behaviour in tetra and hexaploid wheats. It has recently been characterized one of the most important genes in allopolyploid meiosis which if mutated produces identical effects than those observed in the *Ph1b*, the gene is *Zip4* (Rey *et al*., 2017; Rey *et al*., 2018). The *Ph1* locus is localised at the long arm of chromosome 5B. In diploid ancestral species of wheat, *Ae. speltoides*, chromosome

5B usually appears as a ring bivalent with a few as a rod bivalent. The main location of chiasmata in these ring or rod bivalents is distal in this diploid species. In tetra and hexaploid wheat cultivars, the long arm of chromosome 5B show almost always an interstitial or a proximal chiasma in ring and rod bivalents. It is observed that the chiasmata location in the long arm usually is inherited as a block in tetra and hexaploid wheats. Additionally, it is observed that when chromosome 5B appear as ring bivalent with i3 or p chiasmata, the total number of chiasmata in the same cell is increased (e.g.: CS and Cappelli) whereas when this chromosome 5B appears as a rod bivalent the total number of chiasmata are reduced in the cells (e.g.: Kronos). Based on this observation, it can be conclude that increasing chiasmata number in chromosome 5B might cause an increase to the total chiasmata number in the cells whereas reduction in chiasmata formation in chromosome 5B might cause a general decrease in the total chiasmata number in the cell. Another observation compatible with this situation is that when chromosome 5B appears as a ring bivalent with i3 or p chiasmata the total number of ring bivalents is usually increased in that cell whereas when this chromosome appear as rod bivalent the number of rod bivalents is increased in the cell. A clear example of chromosome 5B behaviour is that one observed in hexaploid cultivar CS and tetraploid cultivar Cappelli which show the highest mean chiasma frequency compared to the other lines analysed and in these two cultivars the mean chiasma frequency of chromosome 5B is the highest compared to the others. In contrast, in hexaploid cultivar Fielder and tetraploid cultivar Kronos highest number of rod bivalents were observed and the mean chiasma frequency of chromosome 5B in these two cultivars showed to be the lowest compared to the other cultivars.

6.5 *Ph1* locus effect on meiotic recombination in polyploid wheats

Disruptions to chromosome 5B by deleting a fragment of its long arm allowed to identify the *Ph1* locus in tetra and hexaploid wheats. In these deletions, homeologous recombination was observed at metaphase I cells. Similar effects were also observed in lines where chromosome 5B was replaced. Additionally, the ring and rod bivalent configurations among the homologous chromosomes are still present in this mutant indicating that the effect of *Ph1* locus on homoeologous recombination is restricted to a specific number of chromosomes (around 8 pairs out of 21). It is observed that pairing and synapsis in this mutant is completed but that there is a delay in the time that takes meiosis to complete specifically during prophase I. The BrdU analysis showed us that diakinesis (last stage of prophase I) in CS wild type was achieved at 37h whereas the same stage was reached at 44h in CS *ph1b* mutant. Telomere-FISH in combination with immunolocalisation of Zyp1 shows that synapsis initiates during the telomere bouquet formation in CS wild type whereas synapsis initiates after telomere bouquet dispersal in CS *ph1b*. Based on these results it is possible that in the CS *ph1b* mutant the pairing process is delayed due to difficulty of homologous chromosome recognition which result in homoeologous pairing. It is reported that *ph1b* seems to affect histone H1 phosphorylation which results in affecting chromatin condensation. Disruption to chromatin condensation could result in a delay of meiotic progression specifically delay synapsis and allow homoeologous recombination to form instead of homologous recombination (Greer *et al*., 2012).

6.5.1 *Ph1* locus effect in specific chromosomes

The mean chiasma frequency of all identified chromosomes using rDNA FISH probes showed significant differences in all wheat mutants (*ph1b* and *ph1c*) as well as in the substitution line 5D(5B). The formation of univalents and multivalents decreases the chiasmata number per chromosome in

these mutants. The genetic rearrangement observed in these mutants might be the reason of this reduction in chiasma frequency (Sanchez-Moran *et al.*, 2001).

Recently, a separation-of-function *zip4* mutant in hexaploid wheat has been identified with allows crossover between related chromosomes in hybrids but in the hexaploid wheat chromosomes is meiotically stable and fully fertile (Martín et al., 2021).

6.6 The effect of HU in meiotic recombination in wheat

HU treatment has been analysed in wheat meiotic recombination in this study. Chiasmata localization appears to be more widely distributed along the chromosomes. The metaphase I configurations observed after HU treatment show that bivalents with interstitial chiasmata in both arms could be observed in Cadenza. Additionally, some bivalents with proximal chiasmata in both arms were also observed but their number was still low. These new configurations with interstitial or proximal chiasmata in both arms have never been observed in the cultivar Cadenza. This might indicate that HU treatment and effect on DNA replication could change chiasma localization in hexaploid wheat. In contrast, the mean chiasma frequency is not increase in Cadenza HU but actually significantly decreased compared to the mean chiasma frequency of untreated Cadenza. The main reason of decreasing mean chiasma frequency in Cadenza HU could be associated to the presence of univalents and an increase of the number of rod bivalents in some cells. HU is affecting ribonucleotide reductase activity at replication forks which can results in the accumulation of initiation sites for DNA synthesis. This new initiation sites for DNA replication at the pre-meiotic S phase seem to correlate with the presence of new chiasmata positions in Cadenza treated with HU. However, the observation of univalents at metaphase I could be explained by the effect of HU at meiotic stages after the S-phase where DNA replication is necessary to process DSBs and the recombination intermediates.

Interestingly, not fragmentation could be observed in Cadenza HU, so it seems that HU might be affecting DNA replication in COs intermediates but not in the NCOs and therefore some COs are lost but not fragmentation found. This has been correlated in our lab with pulse treatments with HU at different time points in *Arabidopsis*.

6.7 Agricultural recommendation for wheat breeder

In this thesis, the analysis of the mean chiasma frequency and chiasmata localization of different wheat cultivars from different ploidy levels was performed based on the chiasmata count observed at metaphase I configuration. It is reported that chiasmata in wheat are distally distributed, resulting in limitations in the allelic variation. The analysis of the mean chiasma frequency of different wheats showed that distal chiasmata is the main feature between different wheat cultivars. However, these analyses showed some cultivars contained fewer distal chiasmata compared to others (e.g., CS vs Cadenza). This observation would be very important to the wheat breeder to have an idea that some wheat cultivars have less distal chiasmata and might be used in wheat breeding programmes instead of other wheat. Additionally, wheat cultivars with more interstitial and proximal chiasmata were also observed (e.g., CS and Cappelli). Thus, these cultivars can be exploited by wheat breeders in the introgression process with wheat wild relatives that contain desirable traits for wheat breeding programmes.

It is important to mention that this analysis was only done in a few cultivars of tetraploid and hexaploid wheats and it showed significant differences in chiasma frequency and localization between them. So, it would be recommended that expanding this analysis to cover more cultivars of spring and winter wheats from different ploidy levels might result in discovering some wheat cultivars behaving better than others in terms of chiasma frequency and distribution. Moreover, analysing

wheat cultivars from different geographical and environmental regions could result in the identification of new cultivars that behave better during meiosis.

Based on mean chiasma frequency and chiasmata localization analyses in this study, I would recommend wheat breeder to grow Chinese Spring hexaploid wheat and Cappelli tetraploid wheat. These wheat cultivars show the highest mean chiasma frequency and chiasma localization appear to be more distributed in both of them. Thus, Cappelli is highly resistant to biotic and abiotic stresses, contains a high concentration of free phenols, which contribute to its health-promoting potential (Danelli et al., 2009 and Van Bueren et al., 2011). Nevertheless, Chinese Spring identified to contain several weaknesses such as shattering (grain not stay in the spike after the spike dried), susceptibility to the most of wheat disease and insects and difficulty to be adopted to the most important wheat preferable region around the world (Sears and Miller, 1985).

6.8 Conclusions

- Wheat meiotic bivalent configurations at metaphase l can be accurately classified and the chiasma frequency and distribution correctly inferred. All this is achieved by identifying different shapes of bivalents at metaphase I. These different shapes, also known as bivalent configurations, have been identified and classified according to different facts:
    - Sister Chromatid Cohesion (SCC) is preserved along all the chromosome arms and centromeres throughout the bivalent at metaphase I.
    - Bivalents are co-orientated at the equatorial part of the cell due to the tension achieved by the attachment of the meiotic spindle to the chromosome centromeric kinetochores.
    - The position of the chiasmata is the exact position where the CO occurred. The configuration shape depends on the number and localization of chiasmata along the

bivalent. Different regions on the chromosomes arms were identified: distal (close to telomeres), interstitial (1, 2, 3) and proximal (close to centromeres).

- The time of meiotic progression seems to be related to the ploidy level in wheats. By BrdU time course analysis, it is found that hexaploid *T. aestivum* (AABBDD) cultivars CS and Cadenza finalize meiosis at 43h, whereas tetraploid *T. durum* (AABB) cultivar Cappelli reaches complete meiosis at 41h, and *T. monococcum* (AA) completes meiosis in just 39h. It is interesting that there is an extra 2h period for complete meiosis at each ploidy level (2h more than diploids at tetraploids, and 2h more than tetraploids at hexaploids). This increase in the time it takes meiosis to complete might be related to the extra complexity of having an extra genome could have in different events during meiosis like DNA replication, initiation of recombination (homologous chromosome search), pairing and even synapsis.
- The spatio-temporal polarization of meiotic progression is conserved among the different ploidy levels in wheat species. Chromosome axis formation and SC polymerization were analysed and both begin at telomeric regions and as prophase I advances their polymerization/assembly progresses from these telomeric regions towards the centromeres. This behaviour is conserved among all the different wheat species and cultivars analysed in this thesis independently of ploidy level (*T. monococcum* (AA), *T durum* var. Cappelli (AABB), *T. aestivum* (AABBDD) var. CS and var. Cadenza).
- *T. aestivum* var. CS chiasma frequency is significantly higher than the one observed in *T. aestivum* var Cadenza. This increase on meiotic recombination in CS does not seem to arise from a Class I CO increase as HEI10 foci number is not significantly different from Cadenza.
- Analysis of HEI10 foci at diplotene and chiasma frequency in *T. aestivum* var CS and Cadenza showed that the percentage of Class I COs is higher in this species (96-98% of Class I COs) compared to Arabidopsis (~85%).

- A systematic chiasma frequency per cell analysis on different ploidy levels in wheat species were conducted:
    - In hexaploid *T. aestivum* (AABBDD): CS has showed significant differences in the mean chiasma frequency with Cadenza and Paragon cultivars. Whereas no significant differences were observed when comparing it to Fielder. In addition, Cadenza showed significant differences in chiasma frequency with Fielder whereas no significant differences were observed between Cadenza and Paragon.
    - In tetraploid *T. durum* (AABB), Kr appeared to be significantly different in mean chiasma frequency to Cap and Lnd. Moreover, Cap and Lnd showed a moderate significant difference in the mean chiasma frequency between them.
    - In diploid ancestor relative species, *T. monococcum* (AA), *Ae. speltoides* (BB) and *Ae. tauschii* (DD) no significant differences on chiasma frequency per cell was found among these species.
- Mean chiasma frequency per bivalent allows to compare different ploidy level wheat species. This analysis was conducted by dividing the total number of chiasmata per cell by the total number of bivalents present in each cell. Thus, in diploid species the mean chiasma frequency was divided by 7, in tetraploids by 14 and in hexaploids by 21. The systematic analysis showed interesting differences among the material analysed (figure 6.3):
    - In hexaploid wheat (AABBDD), the mean chiasma frequency per bivalent in:
        - CS was significantly different to Cadenza and Paragon varieties in hexaploidy wheat (AABBDD), to Kronos and Cappelli varieties in tetraploid wheat (AABB), and to diploid *Ae. speltoides* (BB).
        - Cadenza was significantly different to CS and Fielder in hexaploid wheat (AABBDD), to Kronos, Cappelli and Langdon in tetraploid wheat (AABB),

and to diploid *T. monococcum* (AA), *Ae. speltoides* (BB) and *Ae. tauschii* (DD).

- Paragon was significantly different to CS in hexaploid wheat (AABBDD), to Kronos, Cappelli and Langdon in tetraploid wheat (AABB), and to diploid *T. monococcum* (AA), *Ae. speltoides* (BB) and *Ae. tauschii* (DD).
- Fielder was significantly different to Cadenza in hexaploidy wheat (AABBDD), to Kronos, Cappelli and Langdon tetraploid wheat (AABB); and to diploid *Ae. speltoides* (BB).

- In tetraploid wheat (AABB), the mean chiasma frequency per bivalent in:
  - Kronos was significantly different to all wheat species and varieties analysed with different ploidy level.
  - Cappelli was significantly different to all wheat species and cultivars analysed with the exception of diploid *Ae. speltoides* (BB) that was not significant.
  - Langdon was significantly different to Cadenza, Paragon and Fielder in hexaploid wheat (AABBDD), to Kronos and Cappelli in tetraploid wheat (AABB), and to diploid *Ae. tauschii* (DD).
- In diploid species, the mean chiasma frequency per bivalent in:
  - *T. monococcum* (AA) was significantly different to Cadenza and Paragon in hexaploid wheat (AABBDD), to Kronos and Cappelli in tetraploid wheat (AABB).
  - *Ae. speltoides* (BB) was significantly different to CS, Cadenza, Paragon and Fielder hexaploid wheat (AABBDD), to Kronos tetraploid wheat (AABB), and to diploid *Ae. tauschii* (DD).

    - Ae. tauschii (DD) was significantly to Cadenza and Paragon hexaploid wheat (AABBDD), to Kronos, Cappelli and Langdon tetraploid wheat (AABB), and to diploid *Ae. speltoides* (BB).

- The mean chiasma frequency at different chromosome locations were identified and analyzed. Most chiasmata were located in the distal regions of the chromosomes close to telomeres. The next most common localization was in the interstitial region 2 (i^2) followed by i^1 region. Finally, i^3 and proximal p regions of the chromosomes contained the lowest chiasma frequency. Interestingly, significant differences could be identified by chiasma frequency in specific regions that were not significant on chiasma frequency per bivalent. For instance, CS chiasma frequency at distal regions was significantly different to Fielder but CS chiasma frequency per bivalent didn't show this difference. Thus, identifying chiasma localization opens a new level of comparisons among different wheat varieties, species and even mutants.
- Identification of specific chromosomes by rDNA 45S and 5S probes FISH allowed us to systematic analyse the chiasma frequency and distribution on chromosomes 5A, 1B, 5B, 6B, 1D and 5D in wheat and to study their different behavior at different ploidy levels (2X, 4X and 6X). This analysis allowed us to establish that different chromosomes behave different that the rest according to mean chiasma frequency and their distribution. For example, chromosome 5A had a significant decreased chiasma frequency in Paragon compared to Kronos, but the mean chiasma frequency per bivalent observed in Paragon was significantly higher than in Kronos. Thus, chromosome 5A behaves in a opposite way than the rest of bivalents in Kronos and Paragon.
- Hexaploid wheat *ph1b* mutant allows homoeologous recombination among different genome chromosomes but with a great cost to synapsis and homologous recombination.

- Tetraploid wheat *ph1c* mutant also allows homoeologous recombination but with a great cost to homologous recombination but not to synapsis (not errors found in ZYP1 polymerization).
- Tetraploid wheat substitution line 5D(5B) in cultivar Langdon also allows homoeologous recombination but with a great cost to synapsis and homologous recombination. Could the synapsis errors be due to the 5D extra pair of chromosomes?
- *Ph1* locus effect seems to decrease chiasma frequency in all the specific chromosomes identified by rDNA FISH in *ph1b*, *ph1c* and 5D (5B) substitution line.
- HU treatment in the hexaploid cultivar Cadenza decreases chiasma frequency but HEI10 foci are significantly increased in numbers suggesting an increase of Class I COs. Furthermore, HU treatment alters the chiasma localization by producing new bivalent configurations not observed without the treatment.

SAHA treatment in the hexaploid cultivar Cadenza decreases chiasma frequency but it had not significant effects in chiasmata localization.

References

AARONSOHN, A. 1910. *Agricultural and botanical explorations in Palestine*, US Government Printing Office.

AGARWAL, S. & ROEDER, G. S. 2000. Zip3 provides a link between recombination enzymes and synaptonemal complex proteins. *Cell,* 102**,** 245-55.

AL-KAFF, N., KNIGHT, E., BERTIN, I., FOOTE, T., HART, N., GRIFFITHS, S. & MOORE, G. 2008. Detailed dissection of the chromosomal region containing the Ph1 locus in wheat Triticum aestivum: with deletion mutants and expression profiling. *Ann Bot,* 101**,** 863-72.

ALABDULLAH, A. K., BORRILL, P., MARTIN, A. C., RAMIREZ-GONZALEZ, R. H., HASSANI-PAK, K., UAUY, C., SHAW, P. & MOORE, G. 2019. A Co-Expression Network in Hexaploid Wheat Reveals Mostly Balanced Expression and Lack of Significant Gene Loss of Homeologous Meiotic Genes Upon Polyploidization. *Front Plant Sci,* 10**,** 1325.

ALABDULLAH, A. K., MOORE, G. & MARTÍN, A. C. 2021. A duplicated copy of the meiotic gene ZIP4 preserves up to 50% pollen viability and grain number in polyploid wheat. *Biology,* 10**,** 290.

ALBINI, S. & JONES, G. 1988. Synaptonemal complex spreading in Allium cepa and Allium fistulosum. II. Pachytene observations: the SC karyotype and the correspondence of late recombination nodules and chiasmata. *Genome,* 30**,** 399-410.

ALLERS, T. & LICHTEN, M. 2001. Differential timing and control of noncrossover and crossover recombination during meiosis. *Cell,* 106**,** 47-57.

ARMSTRONG S. (2013). A time course for the analysis of meiotic progression in Arabidopsis thaliana. Methods in molecular biology (Clifton, N.J.), 990, 119–123. https://doi.org/10.1007/978-1-62703-333-6_12

ARMSTRONG, S. J., & JONES, G. H. 2003. Meiotic cytology and chromosome behaviour in wild-type Arabidopsis thaliana. Journal of experimental botany, 54(380), 1–10. https://doi.org/10.1093/jxb/erg034

ARMSTRONG, S., FRANKLIN, F. & JONES, G. 2003. A meiotic time-course for Arabidopsis thaliana. *Sexual Plant Reproduction,* 16**,** 141-149.

ARMSTRONG, S. J., CARYL, A. P., JONES, G. H. & FRANKLIN, F. C. H. 2002. Asy1, a protein required for meiotic chromosome synapsis, localizes to axis-associated chromatin in Arabidopsis and Brassica. *Journal of cell science,* 115**,** 3645-3655.

ATCHESON, C. L., DIDOMENICO, B., FRACKMAN, S., ESPOSITO, R. E. & ELDER, R. T. 1987. Isolation, DNA sequence, and regulation of a meiosis-specific eukaryotic recombination gene. *Proc Natl Acad Sci U S A,* 84**,** 8035-9.

BALBONI, M., YANG, C., KOMAKI, S., BRUN, J., & SCHNITTGER, A. (2020). COMET Functions as a PCH2 Cofactor in Regulating the HORMA Domain Protein ASY1. Current biology : CB, 30(21), 4113–4127.e6. https://doi.org/10.1016/j.cub.2020.07.089

Balfourier, F., Bouchet, S., Robert, S., De Oliveira, R., Rimbert, H., Kitt, J., Choulet, F., International Wheat Genome Sequencing Consortium, BreedWheat Consortium, & Paux, E. (2019). Worldwide phylogeography and history of wheat genetic diversity. *Science advances*, *5*(5), eaav0536. https://doi.org/10.1126/sciadv.aav0536

BARAKATE, A., HIGGINS, J. D., VIVERA, S., STEPHENS, J., PERRY, R. M., RAMSAY, L., COLAS, I., OAKEY, H., WAUGH, R. & FRANKLIN, F. C. H. 2014. The synaptonemal complex protein ZYP1 is required for imposition of meiotic crossovers in barley. *The Plant Cell,* 26**,** 729-740.

BAUDAT, F., BUARD, J., GREY, C., FLEDEL-ALON, A., OBER, C., PRZEWORSKI, M., COOP, G. & DE MASSY, B. 2010. PRDM9 is a major determinant of meiotic recombination hotspots in humans and mice. *Science,* 327**,** 836-40.

BENAVENTE, E., & SYBENGA, J. 2004. The relation between pairing preference and chiasma frequency in tetrasomics of rye. Genome, 47(1), 122–133. https://doi.org/10.1139/g03-134

BENNETT, M. D. 1972. Nuclear DNA content and minimum generation time in herbaceous plants. *Proceedings of the Royal Society of London. Series B. Biological Sciences,* 181**,** 109-135.

BENNETT, M. D. 1977. The time and duration of meiosis. *Philosophical Transactions of the Royal Society of London. B, Biological Sciences,* 277**,** 201-226.

BENNETT, M. D. & SMITH, J. B. 1976. Nuclear dna amounts in angiosperms. *Philos Trans R Soc Lond B Biol Sci,* 274**,** 227-74.

Berchowitz, L. E., & Copenhaver, G. P. (2009). Visual markers for detecting gene conversion directly in the gametes of Arabidopsis thaliana. *Methods in molecular biology (Clifton, N.J.)*, *557*, 99–114. https://doi.org/10.1007/978-1-59745-527-5_8

BERCHOWITZ L. E., FRANCIS K. E., BEY A. L., COPENHAVER G. P., The role of AtMUS81 in interference-insensitive crossovers in *A. thaliana.* PLoS Genet. 3, e132 (2007).

BERGERAT, A., DE MASSY, B., GADELLE, D., VAROUTAS, P. C., NICOLAS, A. & FORTERRE, P. 1997. An atypical topoisomerase II from Archaea with implications for meiotic recombination. *Nature,* 386**,** 414-7.

BHULLAR, R., NAGARAJAN, R., BENNYPAUL, H., SIDHU, G. K., SIDHU, G., RUSTGI, S., VON WETTSTEIN, D. & GILL, K. S. 2014. Silencing of a metaphase I-specific gene results in a phenotype similar to that of the Pairing homeologous 1 (Ph1) gene mutations. *Proc Natl Acad Sci U S A,* 111**,** 14187-92.

BISHOP, D. K., & ZICKLER, D. (2004). Early decision; meiotic crossover interference prior to stable strand exchange and synapsis. Cell, 117(1), 9–15. https://doi.org/10.1016/s0092-8674(04)00297-1

BLARY, A. & JENCZEWSKI, E. 2019. Manipulation of crossover frequency and distribution for plant breeding. *Theoretical and Applied Genetics,* 132**,** 575-592.

BÖRNER, G. V., BAROT, A. & KLECKNER, N. 2008. Yeast Pch2 promotes domainal axis organization, timely recombination progression, and arrest of defective recombinosomes during meiosis. *Proceedings of the National Academy of Sciences,* 105**,** 3327-3332.

BÖRNER, G. V., KLECKNER, N. & HUNTER, N. 2004. Crossover/noncrossover differentiation, synaptonemal complex formation, and regulatory surveillance at the leptotene/zygotene transition of meiosis. *Cell,* 117**,** 29-45.

BORRILL, P., HARRINGTON, S. A. & UAUY, C. 2019. Applying the latest advances in genomics and phenomics for trait discovery in polyploid wheat. *The Plant Journal,* 97**,** 56-72.

BOVERI T., 1889. Ein geschlechtlich erzeugter Organismus ohne mütterliche Eigenschaften. Gesel. für Morph. und Physiol. München 5: 73–83 (translated by T. H. Morgan 1893, as “An organism produced sexually without characteristics of the mother”). Am. Nat. 27: 222–232

BOVERI T., 1904. Results Concerning the Chromosome Substance of the Cell Nucleus, p. 65 Fischer, Jena, Germany (in German)

BRIDGES C. B. 1914. Direct proof through non-disjunction that the sex-linked genes of Drosophila are borne by the X-chromosome. Science 40: 107–109

CAI, X., DONG, F., EDELMANN, R. E. & MAKAROFF, C. A. 2003. The Arabidopsis SYN1 cohesin protein is required for sister chromatid arm cohesion and homologous chromosome pairing. *J Cell Sci,* 116**,** 2999-3007.

CAPILLA-PÉREZ, L., DURAND, S., HUREL, A., LIAN, Q., CHAMBON, A., TAOCHY, C., SOLIER, V., GRELON, M. & MERCIER, R. 2021. The synaptonemal complex imposes crossover interference and heterochiasmy in Arabidopsis. *Proceedings of the National Academy of Sciences,* 118**,** e2023613118.

CHAMBON, A., WEST, A., VEZON, D., HORLOW, C., DE MUYT, A., CHELYSHEVA, L., RONCERET, A., DARBYSHIRE, A., OSMAN, K. & HECKMANN, S. 2018. Identification of ASYNAPTIC4, a component of the meiotic chromosome axis. *Plant Physiology,* 178**,** 233-246.

CHAPMAN, C. G., & KIMBER, G. 1992. Developments in the meiotic analysis of hybrids. II. Amended models for tetraploids. Heredity, 68 (Pt 2), 105–113.

CHELYSHEVA, L., DIALLO, S., VEZON, D., GENDROT, G., VRIELYNCK, N., BELCRAM, K., ROCQUES, N., MÁRQUEZ-LEMA, A., BHATT, A. M., HORLOW, C., MERCIER, R., MÉZARD, C. & GRELON, M. 2005. AtREC8 and

AtSCC3 are essential to the monopolar orientation of the kinetochores during meiosis. *J Cell Sci,* 118**,** 4621-32.

CHELYSHEVA, L., GENDROT, G., VEZON, D., DOUTRIAUX, M. P., MERCIER, R. & GRELON, M. 2007. Zip4/Spo22 is required for class I CO formation but not for synapsis completion in Arabidopsis thaliana. *PLoS Genet,* 3**,** e83.

CHELYSHEVA, L., VEZON, D., CHAMBON, A., GENDROT, G., PEREIRA, L., LEMHEMDI, A., VRIELYNCK, N., LE GUIN, S., NOVATCHKOVA, M. & GRELON, M. 2012. The Arabidopsis HEI10 is a new ZMM protein related to Zip3. *PLoS genetics,* 8**,** e1002799.

CHOI, K., ZHAO, X., KELLY, K. A., VENN, O., HIGGINS, J. D., YELINA, N. E., HARDCASTLE, T. J., ZIOLKOWSKI, P. A., COPENHAVER, G. P., FRANKLIN, F. C., MCVEAN, G. & HENDERSON, I. R. 2013. Arabidopsis meiotic crossover hot spots overlap with H2A.Z nucleosomes at gene promoters. *Nat Genet,* 45**,** 1327-36.

Choi, K., Yelina, N. E., Serra, H., & Henderson, I. R. (2017). Quantification and Sequencing of Crossover Recombinant Molecules from Arabidopsis Pollen DNA. *Methods in molecular biology (Clifton, N.J.), 1551*, 23–57. https://doi.org/10.1007/978-1-4939-6750-6_2

CHOI, K., ZHAO, X., TOCK, A. J., LAMBING, C., UNDERWOOD, C. J., HARDCASTLE, T. J., SERRA, H., KIM, J., CHO, H. S. & KIM, J. 2018. Nucleosomes and DNA methylation shape meiotic DSB frequency in Arabidopsis thaliana transposons and gene regulatory regions. *Genome research,* 28**,** 532-546.

CHOULET, F., ALBERTI, A., THEIL, S., GLOVER, N., BARBE, V., DARON, J., PINGAULT, L., SOURDILLE, P., COULOUX, A., PAUX, E., LEROY, P., MANGENOT, S., GUILHOT, N., LE GOUIS, J., BALFOURIER, F., ALAUX, M., JAMILLOUX, V., POULAIN, J., DURAND, C., BELLEC, A., GASPIN, C., SAFAR, J., DOLEZEL, J., ROGERS, J., VANDEPOELE, K., AURY, J. M., MAYER, K., BERGES, H., QUESNEVILLE, H., WINCKER, P. & FEUILLET, C. 2014. Structural and functional partitioning of bread wheat chromosome 3B. *Science,* 345**,** 1249721.

CHUA, P. R. & ROEDER, G. S. 1998. Zip2, a meiosis-specific protein required for the initiation of chromosome synapsis. *Cell,* 93**,** 349-359.

COMAI, L. 2005. The advantages and disadvantages of being polyploid. *Nature reviews genetics,* 6**,** 836-846.

Copenhaver, G. P., Keith, K. C., & Preuss, D. (2000). Tetrad analysis in higher plants. A budding technology. *Plant physiology*, *124*(1), 7–16. https://doi.org/10.1104/pp.124.1.7CREIGHTON H. MCCLINTOCK B., 1931. A correlation of cytological and genetical crossing-over in *Zea Mays*. Proc. Natl. Acad. Sci. USA 17: 492–497

CREIGHTON, H. B. & MCCLINTOCK, B. 1935. The correlation of cytological and genetical crossing-over in Zea mays. A corroboration. *Proceedings of the National Academy of Sciences,* 21**,** 148-150.

CRISMANI, W., GIRARD, C., FROGER, N., PRADILLO, M., SANTOS, J. L., CHELYSHEVA, L., COPENHAVER, G. P., HORLOW, C. & MERCIER, R. 2012. FANCM limits meiotic crossovers. *Science,* 336**,** 1588-90.

CROW, E. W. & CROW, J. F. 2002. 100 years ago: Walter Sutton and the chromosome theory of heredity. *Genetics,* 160**,** 1-4.

Clift, D. and Marston, A.L., 2011. The role of shugoshin in meiotic chromosome segregation. *Cytogenetic and genome research*, *133*(2-4), pp.234-242.

DARLINGTON, C.D. 1929. Chromosome behaviour and structural hybridity in the Tradescantieae. Journal of Genetics 21, 207-286.

DARLINGTON, C.D. 1932. Recent advances in cytology. London: J. and A. Churchill

DARLINGTON, C.D. 1935. The internal mechanics of the chromosomes. I, II and III. Proc. Roy. Soc. London B., 118: 33-96.

DARLINGTON, C.D. and LA COUR, L. 1941. The genetics of embryo-sac development. Ann. Bot. N.S., 5: 547-562.

DA INES, O., ABE, K., GOUBELY, C., GALLEGO, M. E. & WHITE, C. I. 2012. Differing requirements for RAD51 and DMC1 in meiotic pairing of centromeres and chromosome arms in Arabidopsis thaliana. *PLoS genetics,* 8**,** e1002636.

DE LOS SANTOS T, HOLLINGSWORTH NM (1999) Red1p, a MEK1-dependent phosphoprotein that physically interacts with Hop1p during meiosis in yeast. Journal of Biological Chemistry 274: 1783–1790.

DE LOS SANTOS, T., HUNTER, N., LEE, C., LARKIN, B., LOIDL, J. & HOLLINGSWORTH, N. M. 2003. The Mus81/Mms4 endonuclease acts independently of double-Holliday junction resolution to promote a distinct subset of crossovers during meiosis in budding yeast. *Genetics,* 164**,** 81-94.

DE MASSY, B. 2013. Initiation of meiotic recombination: how and where? Conservation and specificities among eukaryotes. *Annu Rev Genet,* 47**,** 563-99.

DE MUYT, A., PEREIRA, L., VEZON, D., CHELYSHEVA, L., GENDROT, G., CHAMBON, A., LAINÉ-CHOINARD, S., PELLETIER, G., MERCIER, R., NOGUÉ, F. & GRELON, M. 2009. A high throughput genetic screen identifies new early meiotic recombination functions in Arabidopsis thaliana. *PLoS Genet,* 5**,** e1000654.

DE MUYT, A., VEZON, D., GENDROT, G., GALLOIS, J. L., STEVENS, R. & GRELON, M. 2007. AtPRD1 is required for meiotic double strand break formation in Arabidopsis thaliana. *Embo j,* 26**,** 4126-37.

DESJARDINS, S. D., OGLE, D. E., AYOUB, M. A., HECKMANN, S., HENDERSON, I. R., EDWARDS, K. J., & HIGGINS, J. D. 2020. MutS homologue 4 and MutS homologue 5 Maintain the Obligate Crossover in Wheat Despite Stepwise Gene Loss following Polyploidization. Plant physiology, 183(4), 1545–1558. https://doi.org/10.1104/pp.20.00534

DESJARDINS, S. D., SIMMONDS, J., GUTERMAN, I., KANYUKA, K., BURRIDGE, A. J., TOCK, A. J., SANCHEZ-MORAN, E., FRANKLIN, F. C. H., HENDERSON, I. R., EDWARDS, K. J., UAUY, C., & HIGGINS, J. D. 2022. FANCM promotes class I interfering crossovers and suppresses class II non-interfering crossovers in wheat meiosis. Nature communications, 13(1), 3644. https://doi.org/10.1038/s41467-022-31438-6

Dinelli, G., Carretero, A.S., Di Silvestro, R., Marotti, I., Fu, S., Benedettelli, S., Ghiselli, L. and Gutiérrez, A.F., 2009. Determination of phenolic compounds in modern and old varieties of durum wheat using liquid chromatography coupled with time-of-flight mass spectrometry. *Journal of Chromatography A*, *1216*(43), pp.7229-7240.

DOBSON MJ, PEARLMAN RE, KARAISKAKIS A, SPYROPOULOS B, MOENS PB (1994) Synaptonemal complex proteins: occurrence, epitope mapping and chromosome disjunction. Journal of Cell Science 107: 2749–2760.

DONG, C., WHITFORD, R. & LANGRIDGE, P. 2002. A DNA mismatch repair gene links to the Ph2 locus in wheat. *Genome,* 45**,** 116-124.

DRISCOLL, C., BIELIG, L. & DARVEY, N. 1979. An analysis of frequencies of chromosome configurations in wheat and wheat hybrids. *Genetics,* 91**,** 755-767.

DROUAUD, J., MERCIER, R., CHELYSHEVA, L., BÉRARD, A., FALQUE, M., MARTIN, O., ZANNI, V., BRUNEL, D. & MEZARD, C. 2007. Sex-specific crossover distributions and variations in interference level along Arabidopsis thaliana chromosome 4. *PLoS genetics,* 3**,** e106.

Drouaud, J., & Mézard, C. (2011). Characterization of meiotic crossovers in pollen from Arabidopsis thaliana. *Methods in molecular biology (Clifton, N.J.)*, *745*, 223–249. https://doi.org/10.1007/978-1-61779-129-1_14

DUBOIS, E., DE MUYT, A., SOYER, J. L., BUDIN, K., LEGRAS, M., PIOLOT, T., DEBUCHY, R., KLECKNER, N., ZICKLER, D. & ESPAGNE, E. 2019. Building bridges to move recombination complexes. *Proc Natl Acad Sci U S A,* 116**,** 12400-12409.

EL BAIDOURI M., F. MURAT, M. VEYSSIERE, M. MOLINIER, R. FLORES, L. BURLOT, M. ALAUX, H. QUESNEVILLE, C. PONT, J. SALSE. 2017. Reconciling the evolutionary origin of bread wheat (Triticum aestivum) New Phytol., 213 (2017), pp. 1477-1486

FAN QQ, PETES TD. 1996. Relationship between nuclease-hypersensitive sites and meiotic recombination hot spot activity at the HIS4 locus of Saccharomyces cerevisiae. Mol Cell Biol 16: 2037–2043.

FAO, F. 2017. The future of food and agriculture–Trends and challenges. *Annual Report,* 296**,** 1-180.

FAWCETT DW (1956) The fine structure of chromosomes in the meiotic prophase of vertebrate spermatocytes. J Biophys Biochem Cytol 2:403–406

FAO, IFAD, UNICEF, WFP and WHO. 2018. The State of Food Security and Nutrition in the World 2018.

Building climate resilience for food security and nutrition. Rome, FAO.
FERDOUS, M., HIGGINS, J. D., OSMAN, K., LAMBING, C., ROITINGER, E., MECHTLER, K., ARMSTRONG, S. J., PERRY, R., PRADILLO, M. & CUÑADO, N. 2012. Inter-homolog crossing-over and synapsis in Arabidopsis meiosis are dependent on the chromosome axis protein AtASY3. *PLoS genetics,* 8**,** e1002507.
FRANCE, M. G., ENDERLE, J., RÖHRIG, S., PUCHTA, H., FRANKLIN, F. C. H. & HIGGINS, J. D. 2021. ZYP1 is required for obligate cross-over formation and cross-over interference in Arabidopsis. *Proceedings of the National Academy of Sciences,* 118**,** e2021671118.
Francis, K. E., Lam, S. Y., Harrison, B. D., Bey, A. L., Berchowitz, L. E., & Copenhaver, G. P. (2007). Pollen tetrad-based visual assay for meiotic recombination in Arabidopsis. *Proceedings of the National Academy of Sciences of the United States of America*, *104*(10), 3913–3918. https://doi.org/10.1073/pnas.0608936104
FU, T. K., & SEARS, E. R. (1973). The Relationship between Chiasmata and Crossing over in TRITICUM AESTIVUM. Genetics, 75(2), 231–246. https://doi.org/10.1093/genetics/75.2.231
FUSSELL, C. P. The Rabl orientation: A prelude to synapsis. 1987.
GALL, J. G. & PARDUE, M. L. 1969. Formation and detection of RNA-DNA hybrid molecules in cytological preparations. *Proceedings of the National Academy of Sciences,* 63**,** 378-383.
GB, D. 1972. Inter-specific variations in chiasma frequencies and terminalization in emmer wheats. *Cytologia,* 37**,** 225-234.
GERLACH, W. & DYER, T. 1980. Sequence organization of the repeating units in the nucleus of wheat which contain 5S rRNA genes. *Nucleic Acids Research,* 8**,** 4851-4865.
GERLACH, W. L. & BEDBROOK, J. R. 1979. Cloning and characterization of ribosomal RNA genes from wheat and barley. *Nucleic Acids Res,* 7**,** 1869-85.
GIORGI B (1978) A homoeologous pairing mutant isolated in Triticum durum cv 'Cappelli'. Mutat Breed Newsl 11:4–5
GIORGI B AND BOZZINI A. 1969. Karyotype analysis in Triticum. I Analisi of Triticum turgidum (L.) Thell. and some related tetraploid wheats. Cariologia 22: 249-258.
Giraut, L., Falque, M., Drouaud, J., Pereira, L., Martin, O. C., & Mézard, C. (2011). Genome-wide crossover distribution in Arabidopsis thaliana meiosis reveals sex-specific patterns along chromosomes. *PLoS genetics*, *7*(11), e1002354. https://doi.org/10.1371/journal.pgen.1002354
GORNICKI P., H. ZHU, J. WANG, G.S. CHALLA, Z. ZHANG, B.S. GILL, W. LI. 2014. The chloroplast view of the evolution of polyploid wheat New Phytol., 204 (2014), pp. 704-714
GREER, E., MARTÍN, A. C., PENDLE, A., COLAS, I., JONES, A. M., MOORE, G. & SHAW, P. 2012. The Ph1 locus suppresses Cdk2-type activity during premeiosis and meiosis in wheat. *The Plant Cell,* 24**,** 152-162.
GRÉGOIRE V. 1904. Reduction of the chromosome number and maturation divisions (La réduction numérique des chromosomes et les cinèses de maturation). Cellule 21: 297–314 (in French)
GRIFFITHS, S., SHARP, R., FOOTE, T. N., BERTIN, I., WANOUS, M., READER, S., COLAS, I. & MOORE, G. 2006. Molecular characterization of Ph1 as a major chromosome pairing locus in polyploid wheat. *Nature,* 439**,** 749-52.
GUO, J., GAO, D., GONG, W., LI, H., LI, J., LI, G., SONG, J., LIU, J., YANG, Z. & LIU, C. 2019. Genetic diversity in common wheat lines revealed by fluorescence in situ hybridization. *Plant Systematics and Evolution,* 305**,** 247-254.
HALDANE J. B. S. 1931. The cytological basis of genetical interference. Cytologia (Tokyo) 3: 54–65
HARTUNG, F., SUER, S. & PUCHTA, H. 2007a. Two closely related RecQ helicases have antagonistic roles in homologous recombination and DNA repair in Arabidopsis thaliana. *Proc Natl Acad Sci U S A,* 104**,** 18836-41.
HARTUNG, F., WURZ-WILDERSINN, R., FUCHS, J., SCHUBERT, I., SUER, S. & PUCHTA, H. 2007b. The catalytically active tyrosine residues of both SPO11-1 and SPO11-2 are required for meiotic double-strand break induction in Arabidopsis. *Plant Cell,* 19**,** 3090-9.

HESLOP-HARRISON, J. 2000. Comparative genome organization in plants: from sequence and markers to chromatin and chromosomes. *The Plant Cell,* 12**,** 617-635.

HEYTING, C. 1996. Synaptonemal complexes: structure and function. *Curr Opin Cell Biol,* 8**,** 389-96.

HIGGINS, J. D., ARMSTRONG, S. J., FRANKLIN, F. C. & JONES, G. H. 2004. The Arabidopsis MutS homolog AtMSH4 functions at an early step in recombination: evidence for two classes of recombination in Arabidopsis. *Genes Dev,* 18**,** 2557-70.

HIGGINS, J. D., BUCKLING, E. F., FRANKLIN, F. C. & JONES, G. H. 2008. Expression and functional analysis of AtMUS81 in Arabidopsis meiosis reveals a role in the second pathway of crossing-over. *Plant J,* 54**,** 152-62.

HIGGINS, J. D., VIGNARD, J., MERCIER, R., PUGH, A. G., FRANKLIN, F. C., & JONES, G. H. 2008. AtMSH5 partners AtMSH4 in the class I meiotic crossover pathway in Arabidopsis thaliana, but is not required for synapsis. The Plant journal : for cell and molecular biology, 55(1), 28–39. https://doi.org/10.1111/j.1365-313X.2008.03470.x

HIGGINS, J. D., OSMAN, K., JONES, G. H. & FRANKLIN, F. C. H. 2014. Factors underlying restricted crossover localization in barley meiosis.

HIGGINS, J. D., PERRY, R. M., BARAKATE, A., RAMSAY, L., WAUGH, R., HALPIN, C., ARMSTRONG, S. J. & FRANKLIN, F. C. H. 2012. Spatiotemporal Asymmetry of the Meiotic Program Underlies the Predominantly Distal Distribution of Meiotic Crossovers in Barley. *The Plant Cell,* 24**,** 4096-4109.

HIGGINS, J. D., SANCHEZ-MORAN, E., ARMSTRONG, S. J., JONES, G. H. & FRANKLIN, F. C. 2005. The Arabidopsis synaptonemal complex protein ZYP1 is required for chromosome synapsis and normal fidelity of crossing over. *Genes Dev,* 19**,** 2488-500.

HIRANO, T. 2002. The ABCs of SMC proteins: two-armed ATPases for chromosome condensation, cohesion, and repair. *Genes Dev,* 16**,** 399-414.

HIRANO, T. 2012. Condensins: universal organizers of chromosomes with diverse functions. *Genes Dev,* 26**,** 1659-78.

HOBOLTH, P. 1981. Chromosome pairing in allohexaploid wheat var. Chinese Spring. Transformation of multivalents into bivalents, a mechanism for exclusive bivalent formation. *Carlsberg Research Communications,* 46**,** 129-173.

HOLLINGSWORTH, N. M. & BRILL, S. J. 2004. The Mus81 solution to resolution: generating meiotic crossovers without Holliday junctions. *Genes & development,* 18**,** 117-125.

HOWELL, E. C. & ARMSTRONG, S. 2013. Using sequential fluorescence and genomic in situ hybridization (FISH and GISH) to distinguish the A and C genomes in Brassica napus. *Methods Mol Biol,* 990**,** 25-34.

HUNTER, N. & KLECKNER, N. 2001. The single-end invasion: an asymmetric intermediate at the double-strand break to double-holliday junction transition of meiotic recombination. *Cell,* 106**,** 59-70.

HUSKINS C.L. 1931. A cytological study of Vilmorin's unfixable dwarf wheat. J Genetics 25: 113-124.

JACKSON, N., SANCHEZ-MORAN, E., BUCKLING, E., ARMSTRONG, S. J., JONES, G. H. & FRANKLIN, F. C. 2006. Reduced meiotic crossovers and delayed prophase I progression in AtMLH3-deficient Arabidopsis. *Embo j,* 25**,** 1315-23.

JAUHAR, P. P., RIERA-LIZARAZU, O., DEWEY, W. G., GILL, B. S., CRANE, C. F., & BENNETT, J. H. 1991. Chromosome pairing relationships among the A, B, and D genomes of bread wheat. TAG. Theoretical and applied genetics. Theoretische und angewandte Genetik, 82(4), 441–449. https://doi.org/10.1007/BF00588597

JAUHAR, P., ALMOUSLEM, A., PETERSON, T. & JOPPA, L. 1999. Inter-and intragenomic chromosome pairing in haploids of durum wheat. *Journal of heredity,* 90**,** 437-445.

JENCZEWSKI, E. & ALIX, K. 2004. From diploids to allopolyploids: the emergence of efficient pairing control genes in plants. *Critical Reviews in Plant Sciences,* 23**,** 21-45.

JENKINS, G. & REES, H. 1991. Strategies of bivalent formation in allopolyploid plants. *Proceedings of the Royal Society of London. Series B: Biological Sciences,* 243**,** 209-214.

JI, Y., STELLY, D. M., DE DONATO, M., GOODMAN, M. M. & WILLIAMS, C. G. 1999. A candidate recombination modifier gene for Zea mays L. *Genetics,* 151**,** 821-830.

JOLIVET, S., VEZON, D., FROGER, N. & MERCIER, R. 2006. Non conservation of the meiotic function of the Ski8/Rec103 homolog in Arabidopsis. *Genes to Cells,* 11**,** 615-622.

JONES G. H. 1971. The analysis of exchanges in tritium-labeled meiotic chromosomes. II. Stethophyma grossum. Chromosoma 34: 367–382

JONES, G.H. 1977. A test for early terminalisation of chiasmata in diplotene spermatocytes of Schistocerca gregaria . Chromosoma 63, 287–294

JONES B.L., LOOKHART G.L., MAK A., COOPER D.B. 1982. Sequences of purothionins and their inheritance in diploid, tetraploid and hexaploid wheats. J Hered 73: 143-144.

JONES, G. H. & FRANKLIN, F. C. H. 2006. Meiotic crossing-over: obligation and interference. *Cell,* 126**,** 246-248.

Khademian, H., Giraut, L., Drouaud, J., & Mézard, C. (2013). Characterization of meiotic non-crossover molecules from Arabidopsis thaliana pollen. *Methods in molecular biology (Clifton, N.J.)*, *990*, 177–190. https://doi.org/10.1007/978-1-62703-333-6_18

Kbiri, N., Dluzewska, J., Henderson, I. R., & Ziolkowski, P. A. (2022). Quantifying Meiotic Crossover Recombination in Arabidopsis Lines Expressing Fluorescent Reporters in Seeds Using SeedScoring Pipeline for CellProfiler. *Methods in molecular biology (Clifton, N.J.)*, *2484*, 121–134. https://doi.org/10.1007/978-1-0716-2253-7_10

KEE, N., SIVALINGAM, S., BOONSTRA, R. & WOJTOWICZ, J. 2002. The utility of Ki-67 and BrdU as proliferative markers of adult neurogenesis. *Journal of neuroscience methods,* 115**,** 97-105.

KEENEY, S., GIROUX, C. N. & KLECKNER, N. 1997. Meiosis-specific DNA double-strand breaks are catalyzed by Spo11, a member of a widely conserved protein family. *Cell,* 88**,** 375-84.

KERBY K AND KUSPIRA J. 1987. The phylogeny of the polyploid wheats Tritium aestium (bread wheat) and Triticum turgidum (macaroni wheat). Genome 29: 722-737.

KERBY K AND KUSPIRA J. 1988. Cytological evidence bearing on the origin of the B genome in polyploid wheats. Genome 30: 36-43.

KIHARA H. 1919. Uber cytologische studien bei einigen Getredearten. Mt. I. Spezies-bastard des Weizen und Wizenroggen-bastarde. Bot Mag 33: 17-38.

KIHARA, H. 1924. Cytologische und genetische Studien bei wichtigen Getreidearten mit besonderer Rucksicht auf das Verhalten der Chromosomen und die Sterilitat in den Bastarden. *Mem. Coll. Sci., Kyoto Imp. Univ.,* 1**,** 1-200.

KIHARA, H. 1944. Discovery of the DD-analyser, one of the ancestors of Triticum vulgare. *Agric. Hort.,* 19**,** 13-14.

KIM, H., & CHOI, K. (2022). Fast and Precise: How to Measure Meiotic Crossovers in Arabidopsis. Molecules and cells, 45(5), 273–283. https://doi.org/10.14348/molcells.2022.2054

Kivikoski, M., Rastas, P., Löytynoja, A. and Merilä, J., 2023. Predicting recombination frequency from map distance. *Heredity*, *130*(3), pp.114-121.

KLECKNER, N. 2006. Chiasma formation: chromatin/axis interplay and the role(s) of the synaptonemal complex. *Chromosoma,* 115**,** 175-94.

KLECKNER, N., ZICKLER, D., JONES, G. H., DEKKER, J., PADMORE, R., HENLE, J. & HUTCHINSON, J. 2004. A mechanical basis for chromosome function. *Proceedings of the National Academy of Sciences,* 101**,** 12592-12597.

KLEIN, F., MAHR, P., GALOVA, M., BUONOMO, S. B., MICHAELIS, C., NAIRZ, K. & NASMYTH, K. 1999. A central role for cohesins in sister chromatid cohesion, formation of axial elements, and recombination during yeast meiosis. *Cell,* 98**,** 91-103.

KNIGHT, E., GREER, E., DRAEGER, T., THOLE, V., READER, S., SHAW, P. & MOORE, G. 2010. Inducing chromosome pairing through premature condensation: analysis of wheat interspecific hybrids. *Funct Integr Genomics,* 10**,** 603-8.

KNOLL, A., HIGGINS, J. D., SEELIGER, K., REHA, S. J., DANGEL, N. J., BAUKNECHT, M., SCHRÖPFER, S., FRANKLIN, F. C. & PUCHTA, H. 2012. The Fanconi anemia ortholog FANCM ensures ordered homologous recombination in both somatic and meiotic cells in Arabidopsis. *Plant Cell,* 24**,** 1448-64.

KOSZUL, R. & ZICKLER D. 2012. La Theorie de la Chiasmatypie: Nouvelle interprétation des cinèses de maturation, *Genetics* 191 (2): 319–346

KRASINSKA, L., BESNARD, E., COT, E., DOHET, C., MÉCHALI, M., LEMAITRE, J. M. & FISHER, D. 2008. Cdk1 and Cdk2 activity levels determine the efficiency of replication origin firing in Xenopus. *Embo j,* 27**,** 758-69.

KUBALÁKOVÁ, M., KOVÁROVÁ, P., SUCHÁNKOVÁ, P., CÍHALÍKOVÁ, J., BARTOS, J., LUCRETTI, S., WATANABE, N., KIANIAN, S. F. & DOLEZEL, J. 2005. Chromosome sorting in tetraploid wheat and its potential for genome analysis. *Genetics,* 170**,** 823-9.

Kurzbauer, M. T., Pradillo, M., Kerzendorfer, C., Sims, J., Ladurner, R., Oliver, C., Janisiw, M. P., Mosiolek, M., Schweizer, D., Copenhaver, G. P., & Schlögelhofer, P. 2018. *Arabidopsis thaliana* FANCD2 Promotes Meiotic Crossover Formation. *The Plant cell*, *30*(2), 415–428.

LAM I, KEENEY S. 2015. Nonparadoxical evolutionary stability of the recombination initiation landscape in yeast. Science 350: 932–937

LAMBING, C., OSMAN, K., NUNTASOONTORN, K., WEST, A., HIGGINS, J. D., COPENHAVER, G. P., YANG, J., ARMSTRONG, S. J., MECHTLER, K. & ROITINGER, E. 2015. Arabidopsis PCH2 mediates meiotic chromosome remodeling and maturation of crossovers. *PLoS Genetics,* 11**,** e1005372.

LAMBING, C., TOCK, A. J., TOPP, S. D., CHOI, K., KUO, P. C., ZHAO, X., OSMAN, K., HIGGINS, J. D., FRANKLIN, F. C. H. & HENDERSON, I. R. 2020. Interacting Genomic Landscapes of REC8-Cohesin, Chromatin, and Meiotic Recombination in Arabidopsis[CC-BY]. *The Plant Cell,* 32**,** 1218-1239.

LAMBING C, KUO P, KIM J, OSMAN K, WHITBREAD AL, YANG J, et al. (2022) Differentiated function and localisation of SPO11-1 and PRD3 on the chromosome axis during meiotic DSB formation in Arabidopsis thaliana. PLoS Genet 18(7): e1010298. https://doi.org/10.1371/journal. pgen.1010298

LEE, D. H., KAO, Y. H., KU, J. C., LIN, C. Y., MEELEY, R., JAN, Y. S. & WANG, C. J. 2015. The Axial Element Protein DESYNAPTIC2 Mediates Meiotic Double-Strand Break Formation and Synaptonemal Complex Assembly in Maize. *Plant Cell,* 27**,** 2516-29.

LEVY, A. A. & FELDMAN, M. 2022. Evolution and origin of bread wheat. *Plant Cell,* 34**,** 2549-2567.

LHUISSIER, F. G., OFFENBERG, H. H., WITTICH, P. E., VISCHER, N. O. & HEYTING, C. 2007. The mismatch repair protein MLH1 marks a subset of strongly interfering crossovers in tomato. *The Plant Cell,* 19**,** 862-876.

LI, L.-F., ZHANG, Z.-B., WANG, Z.-H., LI, N., SHA, Y., WANG, X.-F., DING, N., LI, Y., ZHAO, J. & WU, Y. 2022. Genome sequences of five Sitopsis species of Aegilops and the origin of polyploid wheat B subgenome. *Molecular plant,* 15**,** 488-503.

LIBUDA, D. E., UZAWA, S., MEYER, B. J., & VILLENEUVE, A. M. (2013). Meiotic chromosome structures constrain and respond to designation of crossover sites. *Nature*, *502*(7473), 703–706. https://doi.org/10.1038/nature12577

LIU, S., LIU, Y., YANG, X., TONG, C., EDWARDS, D., PARKIN, I. A., ZHAO, M., MA, J., YU, J. & HUANG, S. 2014. The Brassica oleracea genome reveals the asymmetrical evolution of polyploid genomes. *Nature communications,* 5**,** 1-11.

López, E., Pradillo, M., Oliver, C., Romero, C., Cuñado, N. and Santos, J.L., 2012. Looking for natural variation in chiasma frequency in Arabidopsis thaliana. *Journal of experimental botany*, *63*(2), pp.887-894.

LUKASZEWSKI, A. J., KOPECKY, D. & LINC, G. 2012. Inversions of chromosome arms 4AL and 2BS in wheat invert the patterns of chiasma distribution. *Chromosoma,* 121**,** 201-8.

LYNN, A., SOUCEK, R. & BÖRNER, G. V. 2007. ZMM proteins during meiosis: crossover artists at work. *Chromosome Res,* 15**,** 591-605.

MAEDA T. 1930. The meiotic divisions in pollen mother cells of the sweet-pea (Lathyrus odoratus) with special reference to the cytological basis of crossing-over. Mem. Coll. Sci. Kyoto Imp. Univ. 5: 125–137

MAHJOOB, M.M.M.; CHEN, T.-S.; GORAFI, Y.S.A.; YAMASAKI, Y.; KAMAL, N.M.; ABDELRAHMAN, M.; IWATA, H.; MATSUOKA, Y.; TAHIR, I.S.A.; TSUJIMOTO, H. 2021. Traits to Differentiate Lineages and Subspecies of Aegilops tauschii, the D Genome Progenitor Species of Bread Wheat. Diversity 13, 217. https://doi.org/10.3390/d13050217

MAINIERO, S. & PAWLOWSKI, W. P. 2014. Meiotic chromosome structure and function in plants. *Cytogenet Genome Res,* 143**,** 6-17.

MALIK, S. B., RAMESH, M. A., HULSTRAND, A. M. & LOGSDON, J. M., JR. 2007. Protist homologs of the meiotic Spo11 gene and topoisomerase VI reveal an evolutionary history of gene duplication and lineage-specific loss. *Mol Biol Evol,* 24**,** 2827-41.

MANCERA, E., BOURGON, R., BROZZI, A., HUBER, W. & STEINMETZ, L. M. 2008. High-resolution mapping of meiotic crossovers and non-crossovers in yeast. *Nature,* 454**,** 479-85.

MARCUSSEN, T., SANDVE, S. R., HEIER, L., SPANNAGL, M., PFEIFER, M., INTERNATIONAL WHEAT GENOME SEQUENCING CONSORTIUM, JAKOBSEN, K. S., WULFF, B. B., STEUERNAGEL, B. & MAYER, K. F. 2014. Ancient hybridizations among the ancestral genomes of bread wheat. *science,* 345**,** 1250092.

MARTÍN, A. C., ALABDULLAH, A. K. & MOORE, G. 2021. A separation-of-function ZIP4 wheat mutant allows crossover between related chromosomes and is meiotically stable. *Scientific reports,* 11**,** 1-13.

MARTÍN, A. C., BORRILL, P., HIGGINS, J., ALABDULLAH, A., RAMÍREZ-GONZÁLEZ, R. H., SWARBRECK, D., UAUY, C., SHAW, P. & MOORE, G. 2018. Genome-Wide Transcription During Early Wheat Meiosis Is Independent of Synapsis, Ploidy Level, and the Ph1 Locus. *Front Plant Sci,* 9**,** 1791.

MARTÍN, A. C., REY, M.-D., SHAW, P. & MOORE, G. 2017. Dual effect of the wheat Ph1 locus on chromosome synapsis and crossover. *Chromosoma,* 126**,** 669-680.

MARTÍN, A. C., SHAW, P., PHILLIPS, D., READER, S. & MOORE, G. 2014. Licensing MLH1 sites for crossover during meiosis. *Nature communications,* 5**,** 1-5.

MARTINEZ, M., NARANJO, T., CUADRADO, C., & ROMERO, C. 1996. Synaptic behaviour of the tetraploid wheat *Triticum timopheevii*. Theoretical and applied genetics, 93(7), 1139–1144. https://doi.org/10.1007/BF00230137

MARTINEZ, M., CUÑADO, N., CARCELÉN, N. & ROMERO, C. 2001. The Ph1 and Ph2 loci play different roles in the synaptic behaviour of hexaploid wheat Triticum aestivum. *Theoretical and Applied Genetics,* 103**,** 398-405.

MARTÍNEZ, M., NARANJO, T., CUADRADO, C., & ROMERO, C. 2001. The synaptic behaviour of the wild forms of *Triticum turgidum* and *T. timopheevii*. Genome, 44(4), 517–522. https://doi.org/10.1139/g01-031

MARTINEZ-PEREZ, E., SHAW, P., ARAGON-ALCAIDE, L. & MOORE, G. 2003. Chromosomes form into seven groups in hexaploid and tetraploid wheat as a prelude to meiosis. *Plant J,* 36**,** 21-9.

MARTINEZ-PEREZ, E., SHAW, P. J. & MOORE, G. 2000. Polyploidy induces centromere association. *The Journal of cell biology,* 148**,** 233-238.

MARTINI, E., DIAZ, R. L., HUNTER, N. & KEENEY, S. 2006. Crossover homeostasis in yeast meiosis. *Cell,* 126**,** 285-295.

MATSUOKA, Y. 2011. Evolution of polyploid Triticum wheats under cultivation: the role of domestication, natural hybridization and allopolyploid speciation in their diversification. *Plant and cell physiology,* 52**,** 750-764.

MAYER, K. F., MARTIS, M., HEDLEY, P. E., SIMKOVÁ, H., LIU, H., MORRIS, J. A., STEUERNAGEL, B., TAUDIEN, S., ROESSNER, S., GUNDLACH, H., KUBALÁKOVÁ, M., SUCHÁNKOVÁ, P., MURAT, F., FELDER, M., NUSSBAUMER, T., GRANER, A., SALSE, J., ENDO, T., SAKAI, H., TANAKA, T., ITOH, T., SATO, K., PLATZER, M., MATSUMOTO, T., SCHOLZ, U., DOLEZEL, J., WAUGH, R. & STEIN, N. 2011. Unlocking the barley genome by chromosomal and comparative genomics. *Plant Cell,* 23**,** 1249-63.

MAZINA, O. M., MAZIN, A. V., NAKAGAWA, T., KOLODNER, R. D. & KOWALCZYKOWSKI, S. C. 2004. Saccharomyces cerevisiae MER3 helicase stimulates 3′–5′ heteroduplex extension by Rad51: implications for crossover control in meiotic recombination. *Cell,* 117**,** 47-56.

MCFADDEN, E. S. & SEARS, E. R. 1946. The origin of Triticum spelta and its free-threshing hexaploid relatives. *Journal of heredity,* 37**,** 107-116.

MELLO-SAMPAYO, T. 1971. Genetic regulation of meiotic chromosome pairing by chromosome 3D of Triticum aestivum. *Nat New Biol,* 230**,** 22-3.

MERCIER, R., MÉZARD, C., JENCZEWSKI, E., MACAISNE, N. & GRELON, M. 2015. The molecular biology of meiosis in plants. *Annual review of plant biology,* 66**,** 297-327.

MIKI Y., K. YOSHIDA, N. MIZUNO, S. NASUDA, K. SATO, S. TAKUMI. 2019. Origin of wheat B-genome chromosomes inferred from RNA sequencing analysis of leaf transcripts from section Sitopsis species of Aegilops DNA Res., 26 (), pp. 171-182

MIMITOU, E. P. & SYMINGTON, L. S. 2009. DNA end resection: many nucleases make light work. *DNA Repair (Amst),* 8**,** 983-95.

MOENS, P. B., MARCON, E., SHORE, J. S., KOCHAKPOUR, N. & SPYROPOULOS, B. 2007. Initiation and resolution of interhomolog connections: crossover and non-crossover sites along mouse synaptonemal complexes. *J Cell Sci,* 120**,** 1017-27.

MONTGOMERY T. H. 1901. A study of the chromosomes of the germ cells of metazoa. Trans. Am. Phil. Soc. 20: 154–230

MOORE, G. 2014. The control of recombination in wheat by Ph1 and its use in breeding. *Crop Breeding***,** 143-153.

MORGAN, C., FOZARD, J. A., HARTLEY, M., HENDERSON, I. R., BOMBLIES, K. & HOWARD, M. 2021a. Diffusion-mediated HEI10 coarsening can explain meiotic crossover positioning in Arabidopsis. *Nature communications,* 12**,** 1-11.

MORGAN, C., WHITE, M. A., FRANKLIN, F. C. H., ZICKLER, D., KLECKNER, N. & BOMBLIES, K. 2021b. Evolution of crossover interference enables stable autopolyploidy by ensuring pairwise partner connections in Arabidopsis arenosa. *Curr Biol,* 31**,** 4713-4726.e4.

MOSES MJ (1956) Chromosomal structures in crayfish spermatocytes. J Biophys Biochem Cytol 2:215–218

MUKAI, Y., NAKAHARA, Y. & YAMAMOTO, M. 1993. Simultaneous discrimination of the three genomes in hexaploid wheat by multicolor fluorescence in situ hybridization using total genomic and highly repeated DNA probes. *Genome,* 36**,** 489-494.

MULLER, H. J. 1916. The mechanism of crossing-over. *The American Naturalist,* 50**,** 193-221.

NARANJO, T. 2015. Forcing the shift of the crossover site to proximal regions in wheat chromosomes. Theor Appl Genet 128, 1855–1863NARANJO T, VALENZUELA N, PERERA E. 2010. Chiasma frequency is region-specific and chromosome conformation-dependent in a rye chromosome added to wheat. Cytogenet Genome Res 129:133–142

NASMYTH, K. & HAERING, C. H. 2005. The structure and function of SMC and kleisin complexes. *Annual review of biochemistry,* 74**,** 595.

NEALE, M. J. & KEENEY, S. 2006. Clarifying the mechanics of DNA strand exchange in meiotic recombination. *Nature,* 442**,** 153-8.

NEWTON, W. & DARLINGTON, C. 1929. Meiosis in polyploids. *Journal of Genetics,* 21**,** 1-15.

NONOMURA, K.-I., NAKANO, M., FUKUDA, T., EIGUCHI, M., MIYAO, A., HIROCHIKA, H. & KURATA, N. 2004. The novel gene HOMOLOGOUS PAIRING ABERRATION IN RICE MEIOSIS1 of rice encodes a putative coiled-coil protein required for homologous chromosome pairing in meiosis. *The Plant Cell,* 16**,** 1008-1020.

NOVAK, J. E., ROSS-MACDONALD, P. B. & ROEDER, G. S. 2001. The budding yeast Msh4 protein functions in chromosome synapsis and the regulation of crossover distribution. *Genetics,* 158**,** 1013-1025.

OKAMOTO, M. 1957. Asynaptic effect of chromosome V. *Wheat Inf. Serv.,* 5**,** 6.

OSMAN, K., ALGOPISHI, U., HIGGINS, J. D., HENDERSON, I. R., EDWARDS, K. J., FRANKLIN, F. C. H. & SANCHEZ-MORAN, E. 2021. Distal bias of meiotic crossovers in hexaploid bread wheat reflects spatio-temporal asymmetry of the meiotic program. *Frontiers in Plant Science,* 12**,** 631323.

OSMAN, K., HIGGINS, J. D., SANCHEZ-MORAN, E., ARMSTRONG, S. J. & FRANKLIN, F. C. H. 2011. Pathways to meiotic recombination in Arabidopsis thaliana. *New Phytologist,* 190**,** 523-544.

OSMAN, K., SANCHEZ-MORAN, E., HIGGINS, J. D., JONES, G. H. & FRANKLIN, F. C. H. 2006. Chromosome synapsis in Arabidopsis: analysis of the transverse filament protein ZYP1 reveals novel functions for the synaptonemal complex. *Chromosoma,* 115**,** 212-219.

OSMAN, K., SANCHEZ-MORAN, E., MANN, S. C., JONES, G. H. & FRANKLIN, F. C. H. 2009. Replication protein A (AtRPA1a) is required for class I crossover formation but is dispensable for meiotic DNA break repair. *The EMBO journal,* 28**,** 394-404.

OSMAN, K., YANG, J., ROITINGER, E., LAMBING, C., HECKMANN, S., HOWELL, E., CUACOS, M., IMRE, R., DÜRNBERGER, G., MECHTLER, K., ARMSTRONG, S. & FRANKLIN, F. C. H. 2018. Affinity proteomics reveals extensive phosphorylation of the Brassica chromosome axis protein ASY1 and a network of associated proteins at prophase I of meiosis. *Plant J,* 93**,** 17-33.

OSMAN, K., FRANKLIN, F. C. H., & SANCHEZ-MORAN, E. (2022). Cytogenetic Techniques for Analyzing Meiosis in Hexaploid Bread Wheat. Methods in molecular biology (Clifton, N.J.), 2484, 71–84. https://doi.org/10.1007/978-1-0716-2253-7_6

PACHAURI, R. K. & REISINGER, A. 2008. Climate change 2007. Synthesis report. Contribution of Working Groups I, II and III to the fourth assessment report.

PAGE, S. L. & HAWLEY, R. S. 2004. The genetics and molecular biology of the synaptonemal complex. *Annu. Rev. Cell Dev. Biol.,* 20**,** 525-558.

PAN J, SASAKI M, Kniewel R, Murakami H, Blitzblau HG, Tischfield SE, Zhu X, Neale MJ, Jasin M, Socci ND, et al. 2011. A hierarchical combination of factors shapes the genome-wide topography of yeast meiotic recombination initiation. Cell 144: 719–731.

PANIZZA, S., MENDOZA, M. A., BERLINGER, M., HUANG, L., NICOLAS, A., SHIRAHIGE, K. & KLEIN, F. 2011. Spo11-accessory proteins link double-strand break sites to the chromosome axis in early meiotic recombination. *Cell,* 146**,** 372-383.

Parra-Nunez, P., Pradillo, M. and Santos, J.L., 2019. Competition for chiasma formation between identical and homologous (but not identical) chromosomes in synthetic autotetraploids of Arabidopsis thaliana. *Frontiers in Plant Science*, *9*, p.1924.

PEACOCK W. J. 1970. Replication, recombination and chiasmata in Goniaea australasiae (Orthoptara: Acrididae). Genetics 65: 593–617

PEDERSEN, C. & LANGRIDGE, P. 1997. Identification of the entire chromosome complement of bread wheat by two-colour FISH. *Genome,* 40**,** 589-593.

PERRY, J., KLECKNER, N. & BÖRNER, G. V. 2005. Bioinformatic analyses implicate the collaborating meiotic crossover/chiasma proteins Zip2, Zip3, and Spo22/Zip4 in ubiquitin labeling. *Proc Natl Acad Sci U S A,* 102**,** 17594-9.

PREECE, C., LIVARDA, A., CHRISTIN, P. A., WALLACE, M., MARTIN, G., CHARLES, M., JONES, G., REES, M., & OSBORNE, C.P. 2017. How did the domestication of Fertile Crescent grain crops increase their yields?. Functional ecology, 31(2), 387–397. https://doi.org/10.1111/1365-2435.12760

Preuss, D., Rhee, S. Y., & Davis, R. W. (1994). Tetrad analysis possible in Arabidopsis with mutation of the QUARTET (QRT) genes. Science (New York, N.Y.), 264(5164), 1458–1460. https://doi.org/10.1126/science.8197459

PRIETO, P., MOORE, G. & READER, S. 2005. Control of conformation changes associated with homologue recognition during meiosis. *Theoretical and applied genetics,* 111**,** 505-510.

Pyatnitskaya, A., Borde, V. & De Muyt, A. 2019. Crossing and zipping: molecular duties of the ZMM proteins in meiosis. *Chromosoma* **128**, 181–198.

Pyatnitskaya, A., Andreani, J., Guérois, R., De Muyt, A., & Borde, V. (2022). The Zip4 protein directly couples meiotic crossover formation to synaptonemal complex assembly. Genes & development, 36(1-2), 53–69. https://doi.org/10.1101/gad.348973.121

Quarrie, S.A., Steed, A., Calestani, C., Semikhodskii, A., Lebreton, C., Chinoy, C., Steele, N., Pljevljakusić, D., Waterman, E., Weyen, J. and Schondelmaier, J., 2005. A high-density genetic map of hexaploid wheat (Triticum aestivum L.) from the cross Chinese Spring× SQ1 and its use to compare QTLs for grain yield across a range of environments. *Theoretical and Applied Genetics*, *110*, pp.865-880.

Qu, P., Wang, J., Wen, W., Gao, F., Liu, J., Xia, X., Peng, H. and Zhang, L., 2021. Construction of consensus genetic map with applications in gene mapping of wheat (Triticum aestivum L.) using 90K SNP array. *Frontiers in Plant Science*, *12*, p.727077.

REY, M. D., MARTÍN, A. C., HIGGINS, J., SWARBRECK, D., UAUY, C., SHAW, P. & MOORE, G. 2017. Exploiting the ZIP4 homologue within the wheat Ph1 locus has identified two lines exhibiting homoeologous crossover in wheat-wild relative hybrids. *Mol Breed,* 37**,** 95.

REY, M. D., MARTÍN, A. C., SMEDLEY, M., HAYTA, S., HARWOOD, W., SHAW, P. & MOORE, G. 2018. Magnesium Increases Homoeologous Crossover Frequency During Meiosis in ZIP4 (Ph1 Gene) Mutant Wheat-Wild Relative Hybrids. *Front Plant Sci,* 9**,** 509.

RILEY R. 1974. Cytogenetics of chromosome pairing in wheat. Genetics, 78(1), 193–203. https://doi.org/10.1093/genetics/78.1.193

RILEY, R. & CHAPMAN, V. 1958. Genetic control of the cytologically diploid behaviour of hexaploid wheat. *Nature,* 182**,** 713-715.

RODRIGUEZ, S., MAESTRA, B., PERERA, E., DIEZ, M. & NARANJO, T. 2000. Pairing affinities of the B-and G-genome chromosomes of polyploid wheats with those of Aegilops speltoides. *Genome,* 43**,** 814-819.

ROSS, K. J., FRANSZ, P., ARMSTRONG, S. J., VIZIR, I., MULLIGAN, B., FRANKLIN, F. C., & JONES, G. H. 1997. Cytological characterization of four meiotic mutants of Arabidopsis isolated from T-DNA-transformed lines. Chromosome research : an international journal on the molecular, supramolecular and evolutionary aspects of chromosome biology, 5(8), 551–559. https://doi.org/10.1023/a:1018497804129

ROSS-MACDONALD, P. & ROEDER, G. S. 1994. Mutation of a meiosis-specific MutS homolog decreases crossing over but not mismatch correction. *Cell,* 79**,** 1069-1080.

Roy, B., Copenhaver, G. P., & von Arnim, A. G. (2011). Fluorescence-tagged transgenic lines reveal genetic defects in pollen growth--application to the eIF3 complex. PloS one, 6(3), e17640. https://doi.org/10.1371/journal.pone.0017640

SAKAMURA, T. 1918. Kurze Mitteilung ueber die Chromosomenzahlen und die Verwandtschaftsverhältnisse der Triticum-arten. *Shokubutsugaku Zasshi,* 32**,** 150-153.

SALAMINI, F., ÖZKAN, H., BRANDOLINI, A., SCHÄFER-PREGL, R. & MARTIN, W. 2002. Genetics and geography of wild cereal domestication in the near east. *Nature Reviews Genetics,* 3**,** 429-441.

SANCHEZ-MORAN, E., ARMSTRONG, S., SANTOS, J., FRANKLIN, F. & JONES, G. 2002. Variation in chiasma frequency among eight accessions of Arabidopsis thaliana. *Genetics,* 162**,** 1415-1422.

SÁNCHEZ-MORÁN, E., BENAVENTE, E. & ORELLANA, J. 2001. Analysis of karyotypic stability of homoeologous-pairing (ph) mutants in allopolyploid wheats. *Chromosoma,* 110**,** 371-377.

SANCHEZ-MORAN, E., OSMAN, K., HIGGINS, J., PRADILLO, M., CUNADO, N., JONES, G. & FRANKLIN, F. 2008. ASY1 coordinates early events in the plant meiotic recombination pathway. *Cytogenetic and genome research,* 120**,** 302-312.

SANCHEZ MORAN, E., ARMSTRONG, S. J., SANTOS, J. L., FRANKLIN, F. C. & JONES, G. H. 2001. Chiasma formation in Arabidopsis thaliana accession Wassileskija and in two meiotic mutants. *Chromosome Res,* 9**,** 121-8.

SÁNCHEZ-MORÁN, E., JONES, G. H., FRANKLIN, F. C., & SANTOS, J. L. 2004. A puromycin-sensitive aminopeptidase is essential for meiosis in Arabidopsis thaliana. The Plant cell, 16(11), 2895–2909. https://doi.org/10.1105/tpc.104.024992

SANCHEZ-MORAN, E., SANTOS, J. L., JONES, G. H., & FRANKLIN, F. C. (2007). ASY1 mediates AtDMC1-dependent interhomolog recombination during meiosis in Arabidopsis. Genes & development, 21(17), 2220–2233. https://doi.org/10.1101/gad.439007

SAX, K. 1918. The behavior of the chromosomes in fertilization. *Genetics,* 3**,** 309.

SAX, K. 1922. Sterility in wheat hybrids. II. Chromosome behavior in partially sterile hybrids. *Genetics,* 7**,** 513.

SCHOMMER, C., BEVEN, A., LAWRENSON, T., SHAW, P. & SABLOWSKI, R. 2003. AHP2 is required for bivalent formation and for segregation of homologous chromosomes in Arabidopsis meiosis. *The Plant Journal,* 36**,** 1-11.

SCHWARZACHER, T. 2003. DNA, chromosomes, and in situ hybridization. *Genome,* 46**,** 953-962.
SEARS E.R. 1952. Homoeologous chromosomes in Triticum aestivum. Genetics 37:624.
SEARS E.R. 1954. The Aneuploids of common wheat. Research Bulletin Missouri Agricultural Experiment Station 572: 1-58.
SEARS, E. 1958. Intergenomic chromosome relationships in hexaploid wheat. Proc. Int. Congress Genet., 258-259.
SEARS, E. R. 1977. Genetics society of canada award of excellence lecture an induced mutant with homoeologous pairing in common wheat. *Canadian Journal of Genetics and Cytology,* 19**,** 585-593.
SEARS E. R. 1976. Genetic control of chromosome pairing in wheat. Annual review of genetics, 10, 31–51. https://doi.org/10.1146/annurev.ge.10.120176.000335
SEARS, E. R. 1982. A WHEAT MUTATION CONDITIONING AN INTERMEDIATE LEVEL OF HOMOEOLOGOUS CHROMOSOME PAIRING. *Canadian Journal of Genetics and Cytology,* 24**,** 715-719.
SEPSI, A., HIGGINS, J. D., HESLOP-HARRISON, J. S. & SCHWARZACHER, T. 2017. CENH 3 morphogenesis reveals dynamic centromere associations during synaptonemal complex formation and the progression through male meiosis in hexaploid wheat. *The Plant Journal,* 89**,** 235-249.
Serin, E.A., Snoek, L.B., Nijveen, H., Willems, L.A., Jiménez-Gómez, J.M., Hilhorst, H.W. and Ligterink, W., 2017. Construction of a high-density genetic map from RNA-Seq data for an Arabidopsis bay-0× Shahdara RIL population. *Frontiers in genetics*, *8*, p.201.
SERRA, H., SVAČINA, R., BAUMANN, U., WHITFORD, R., SUTTON, T., BARTOŠ, J. & SOURDILLE, P. 2021. Ph2 encodes the mismatch repair protein MSH7-3D that inhibits wheat homoeologous recombination. *Nature communications,* 12**,** 1-10.
SHEN, Y., TANG, D., WANG, K., WANG, M., HUANG, J., LUO, W., LUO, Q., HONG, L., LI, M. & CHENG, Z. 2012. ZIP4 in homologous chromosome synapsis and crossover formation in rice meiosis. *J Cell Sci,* 125**,** 2581-91.
SHEWRY, P. R. & HEY, S. J. 2015. The contribution of wheat to human diet and health. *Food and energy security,* 4**,** 178-202.
Singer, T., Fan, Y., Chang, H.S., Zhu, T., Hazen, S.P. and Briggs, S.P., 2006. A high-resolution map of Arabidopsis recombinant inbred lines by whole-genome exon array hybridization. *PLoS Genetics*, *2*(9), p.e144.
SOARES, N. R., MOLLINARI, M., OLIVEIRA, G. K., PEREIRA, G. S. & VIEIRA, M. L. C. 2021. Meiosis in polyploids and implications for genetic mapping: a review. *Genes,* 12**,** 1517.
SOUSTELLE, C., VEDEL, M., KOLODNER, R. & NICOLAS, A. 2002. Replication protein A is required for meiotic recombination in Saccharomyces cerevisiae. *Genetics,* 161**,** 535-47.
STAHL, F. W., FOSS, H. M., YOUNG, L. S., BORTS, R. H., ABDULLAH, M. F. & COPENHAVER, G. P. 2004. Does crossover interference count in Saccharomyces cerevisiae? *Genetics,* 168**,** 35-48.
STURTEVANT, A. H. 1915. The behavior of the chromosomes as studied through linkage. *Zeitschrift für induktive Abstammungs-und Vererbungslehre,* 13**,** 234-287.
SU, D., CHEN, L., SUN, J., ZHANG, L., GAO, R., LI, Q., HAN, Y. & LI, Z. 2020. Comparative chromosomal localization of 45S and 5S rDNA sites in 76 purple-fleshed sweet potato cultivars. *Plants,* 9**,** 865.
SUGIMOTO-SHIRASU, K., STACEY, N. J., CORSAR, J., ROBERTS, K. & MCCANN, M. C. 2002. DNA topoisomerase VI is essential for endoreduplication in Arabidopsis. *Curr Biol,* 12**,** 1782-6.
SUNG, P., KREJCI, L., VAN KOMEN, S. & SEHORN, M. G. 2003. Rad51 recombinase and recombination mediators. *Journal of Biological Chemistry,* 278**,** 42729-42732.
SUTTON W. S. 1902. On the morphology of the chromosome group in Brachystola magna. Biol. Bull. 4: 24–39
SUTTON W. S. 1903. The chromosomes in heredity. Bio. Bull. 4: 231–251
SUTTON, T., WHITFORD, R., BAUMANN, U., DONG, C., ABLE, J. A. & LANGRIDGE, P. 2003. The Ph2 pairing homoeologous locus of wheat (Triticum aestivum): identification of candidate meiotic genes using a comparative genetics approach. *Plant J,* 36**,** 443-56.
STEBBINS G.L. 1971. Chromosomal evolution in higher plants. Arnold D (De). Publ. Ltd. London VIII: 216.

STERN C., 1931. Cytological-genetic studies as evidence for Morgan's theory of factor exchanges (Zytologisch-genetische Untersuchungen als Beweis für die Morgansche Theorie des Faktorenaustausches). Biol. Zentralbl. 51: 547–587 (in German)

STRASBURGER E., 1888. Nuclear and cell division in the plant kingdom, in addition to an annex on fertilization. Histological contributions (Uber Kern-undZelltheilung in Planzenreiche, nebst einem Anhang über Befruchtung. Histologische Beiträge), p. 258, Vol. I Gustav Fischer, Jena, Germany (in German)

STURTEVANT A. H. 1913. The linear arrangement of six sex-linked factors in Drosophila, as shown by their mode of association. J. Exp. Zool. 14: 43–59

SVAČINA, R., SOURDILLE, P., KOPECKÝ, D. & BARTOŠ, J. 2020. Chromosome pairing in polyploid grasses. *Frontiers in Plant Science,* 11**,** 1056.

SYBENGA, J. 1975. The quantitative analysis of chromosome pairing and chiasma formation based on the relative frequencies of MI configurations. *Chromosoma,* 50**,** 211-222.

SYBENGA, J. 2012. *Meiotic configurations: a source of information for estimating genetic parameters*, Springer Science & Business Media.

SYM, M., & ROEDER, G. S. (1994). Crossover interference is abolished in the absence of a synaptonemal complex protein. Cell, 79(2), 283–292. https://doi.org/10.1016/0092-8674(94)90197-x

SYM, M., ENGEBRECHT, J. A. & ROEDER, G. S. 1993. ZIP1 is a synaptonemal complex protein required for meiotic chromosome synapsis. *Cell,* 72**,** 365-78.

SZOSTAK, J. & ORR-WEAVER, T. Rothstein Rothstein. R. and Stahl, FW (1983). *The double-strand break repair model for recombination. Cell,* 33**,** 25-35.

TANG, Z., YANG, Z. & FU, S. 2014. Oligonucleotides replacing the roles of repetitive sequences pAs1, pSc119. 2, pTa-535, pTa71, CCS1, and pAWRC. 1 for FISH analysis. *Journal of Applied Genetics,* 55**,** 313-318.

TAYLOR J. H. 1965. Distribution of tritium-labeled DNA among chromosomes during meiosis I spermatogenesis in the grasshopper. J. Cell Biol. 25: 57–67

THE INTERNATIONAL WHEAT GENOME SEQUENCING CONSORTIUM (IWGSC), APPELS, R., EVERSOLE, K., STEIN, N., FEUILLET, C., KELLER, B., ROGERS, J., POZNIAK, C. J., CHOULET, F. & DISTELFELD, A. 2018. Shifting the limits in wheat research and breeding using a fully annotated reference genome. *Science,* 361**,** eaar7191.

THE INTERNATIONAL WHEAT GENOME SEQUENCING CONSORTIUM (IWGSC), MAYER, K. F., ROGERS, J., DOLEŽEL, J., POZNIAK, C., EVERSOLE, K., FEUILLET, C., GILL, B., FRIEBE, B. & LUKASZEWSKI, A. J. 2014. A chromosome-based draft sequence of the hexaploid bread wheat (Triticum aestivum) genome. *Science,* 345**,** 1251788.

THOMPSON EA, ROEDER GS (1989) Expression and DNA sequence of RED1, a gene required for meiosis I chromosome segregation in yeast. Molecular & General Genetics 218: 293–301.

TOCK, A. J., HOLLAND, D. M., JIANG, W., OSMAN, K., SANCHEZ-MORAN, E., HIGGINS, J. D., EDWARDS, K. J., UAUY, C., FRANKLIN, F. C. H. & HENDERSON, I. R. 2021. Crossover-active regions of the wheat genome are distinguished by DMC1, the chromosome axis, H3K27me3, and signatures of adaptation. *Genome research,* 31**,** 1614-1628.

TSUBOUCHI, T., ZHAO, H. & ROEDER, G. S. 2006. The meiosis-specific zip4 protein regulates crossover distribution by promoting synaptonemal complex formation together with zip2. *Dev Cell,* 10**,** 809-19.

VIERA, A., RUFAS, J. S., MARTÍNEZ, I., BARBERO, J. L., ORTEGA, S. & SUJA, J. A. 2009. CDK2 is required for proper homologous pairing, recombination and sex-body formation during male mouse meiosis. *J Cell Sci,* 122**,** 2149-59.

Van Bueren, E.L., Jones, S.S., Tamm, L., Murphy, K.M., Myers, J.R., Leifert, C. and Messmer, M.M., 2011. The need to breed crop varieties suitable for organic farming, using wheat, tomato and broccoli as examples: A review. *NJAS-Wageningen Journal of Life Sciences*, *58*(3-4), pp.193-205.

van Tol, N., Rolloos, M., van Loon, P., & van der Zaal, B. J. (2018). MeioSeed: a CellProfiler-based program to count fluorescent seeds for crossover frequency analysis in *Arabidopsis thaliana*. *Plant methods*, *14*, 32. https://doi.org/10.1186/s13007-018-0298-3

VRIELYNCK, N., CHAMBON, A., VEZON, D., PEREIRA, L., CHELYSHEVA, L., DE MUYT, A., MÉZARD, C., MAYER, C. & GRELON, M. 2016. A DNA topoisomerase VI-like complex initiates meiotic recombination. *Science,* 351**,** 939-43.

VRIELYNCK, N., SCHNEIDER, K., RODRIGUEZ, M., SIMS, J., CHAMBON, A., HUREL, A., DE MUYT, A., RONCERET, A., KRSICKA, O., MÉZARD, C., SCHLÖGELHOFER, P. & GRELON, M. 2021. Conservation and divergence of meiotic DNA double strand break forming mechanisms in Arabidopsis thaliana. *Nucleic Acids Res,* 49**,** 9821-9835.

WALL, A., RILEY, R. & CHAPMAN, V. 1971. Wheat mutants permitting homoeologous meiotic chromosome pairing. *Genetics Research,* 18**,** 311-328.

Wang, M., Wang, K., Tang, D., Wei, C., Li, M., Shen, Y., Chi, Z., Gu, M., & Cheng, Z. (2010). The central element protein ZEP1 of the synaptonemal complex regulates the number of crossovers during meiosis in rice. The Plant cell, 22(2), 417–430. https://doi.org/10.1105/tpc.109.070789

WANG, K., WANG, M., TANG, D., SHEN, Y., QIN, B., LI, M. & CHENG, Z. 2011. PAIR3, an axis-associated protein, is essential for the recruitment of recombination elements onto meiotic chromosomes in rice. *Mol Biol Cell,* 22**,** 12-9.

WANG, T. F., KLECKNER, N. & HUNTER, N. 1999. Functional specificity of MutL homologs in yeast: evidence for three Mlh1-based heterocomplexes with distinct roles during meiosis in recombination and mismatch correction. *Proc Natl Acad Sci U S A,* 96**,** 13914-9.

WARD, J. O., REINHOLDT, L. G., MOTLEY, W. W., NISWANDER, L. M., DEACON, D. C., GRIFFIN, L. B., LANGLAIS, K. K., BACKUS, V. L., SCHIMENTI, K. J. & O'BRIEN, M. J. 2007. Mutation in mouse hei10, an e3 ubiquitin ligase, disrupts meiotic crossing over. *PLoS genetics,* 3**,** e139.

WEISMANN A, 1885. The continuity of the germ-plasm as the foundation of a theory of heredity (Die Kontinuität des Keimplasmas: eine Theorie der Vererbung) pp. 161–248 Essays upon Heredity and Kindred Biological Problems. Clarendon Press, Oxford (in German)

WEST, A. M., ROSENBERG, S. C., UR, S. N., LEHMER, M. K., YE, Q., HAGEMANN, G., CABALLERO, I., USÓN, I., MACQUEEN, A. J., HERZOG, F. & CORBETT, K. D. 2019. A conserved filamentous assembly underlies the structure of the meiotic chromosome axis. *Elife,* 8.

WHITE, C. I. 2008. News from Arabidopsis on the Meiotic Roles of Blap75/Rmi1 and Top3α. *PLoS Genetics,* 4**,** e1000306.

WIJERATNE, A. J., CHEN, C., ZHANG, W., TIMOFEJEVA, L. & MA, H. 2006. The Arabidopsis thaliana PARTING DANCERS gene encoding a novel protein is required for normal meiotic homologous recombination. *Mol Biol Cell,* 17**,** 1331-43.

WILSON, E. & MORGAN, T. H. 1920. Chiasmatype and crossing over. *The American Naturalist,* 54**,** 193-219.

WOLTERING, D., BAUMGARTNER, B., BAGCHI, S., LARKIN, B., LOIDL, J., DE LOS SANTOS, T. & HOLLINGSWORTH, N. M. 2000. Meiotic segregation, synapsis, and recombination checkpoint functions require physical interaction between the chromosomal proteins Red1p and Hop1p. *Molecular and cellular biology,* 20**,** 6646-6658.

WU TC, LICHTEN M. 1994. Meiosis-induced double-strand break sites determined by yeast chromatin structure. Science 263: 515–518

YANG, C., HU, B., PORTHEINE, S. M., CHUENBAN, P., & SCHNITTGER, A. (2020). State changes of the HORMA protein ASY1 are mediated by an interplay between its closure motif and PCH2. Nucleic acids research, 48(20), 11521–11535. https://doi.org/10.1093/nar/gkaa527

YANG, C., SOFRONI, K., HAMAMURA, Y., HU, B., ELBASI, H. T., BALBONI, M., CHU, L., STANG, D., HEESE, M., & SCHNITTGER, A. (2022). ZYP1-mediated recruitment of PCH2 to the synaptonemal complex remodels the chromosome axis leading to crossover restriction. Nucleic acids research, 50(22), 12924–12937. https://doi.org/10.1093/nar/gkac1160

YANT, L., HOLLISTER, J. D., WRIGHT, K. M., ARNOLD, B. J., HIGGINS, J. D., FRANKLIN, F. C. H. & BOMBLIES, K. 2013. Meiotic adaptation to genome duplication in Arabidopsis arenosa. *Curr Biol,* 23**,** 2151-6.

YU, H. G. & KOSHLAND, D. E. 2003. Meiotic condensin is required for proper chromosome compaction, SC assembly, and resolution of recombination-dependent chromosome linkages. *J Cell Biol,* 163**,** 937-47.

YUAN WY, LI XW, CHANG YX, WEN RY, CHEN GX, et al. (2009) Mutation of the rice gene PAIR3 results in lack of bivalent formation in meiosis. Plant Journal 59: 303–315.

ZAKHARYEVICH, K., MA, Y., TANG, S., HWANG, P. Y., BOITEUX, S. & HUNTER, N. 2010. Temporally and biochemically distinct activities of Exo1 during meiosis: double-strand break resection and resolution of double Holliday junctions. *Mol Cell,* 40**,** 1001-15.

ZALEVSKY, J., MACQUEEN, A. J., DUFFY, J. B., KEMPHUES, K. J. & VILLENEUVE, A. M. 1999. Crossing over during Caenorhabditis elegans meiosis requires a conserved MutS-based pathway that is partially dispensable in budding yeast. *Genetics,* 153**,** 1271-1283.

ZANDERS, S., & ALANI, E. (2009). The pch2Delta mutation in baker's yeast alters meiotic crossover levels and confers a defect in crossover interference. PLoS genetics, 5(7), e1000571. https://doi.org/10.1371/journal.pgen.1000571

ZHANG, H., BIAN, Y., GOU, X., ZHU, B., XU, C., QI, B., LI, N., RUSTGI, S., ZHOU, H. & HAN, F. 2013. Persistent whole-chromosome aneuploidy is generally associated with nascent allohexaploid wheat. *Proceedings of the National Academy of Sciences,* 110**,** 3447-3452.

ZHANG, L., LIANG, Z., HUTCHINSON, J. & KLECKNER, N. 2014. Crossover patterning by the beam-film model: analysis and implications. *PLoS genetics,* 10**,** e1004042.

ZICKLER, D. & KLECKNER, N. 1998. The leptotene-zygotene transition of meiosis. *Annu Rev Genet,* 32**,** 619-97.

ZICKLER, D. & KLECKNER, N. 1999. Meiotic chromosomes: integrating structure and function. *Annual review of genetics,* 33**,** 603.

ZICKLER, D. & KLECKNER, N. 2015. Recombination, Pairing, and Synapsis of Homologs during Meiosis. *Cold Spring Harb Perspect Biol,* 7.

ZICKLER, D. & KLECKNER, N. A few of our favorite things: Pairing, the bouquet, crossover interference and evolution of meiosis. Seminars in cell & developmental biology, 2016. Elsevier, 135-148.Ziolkowski, P.A., Underwood, C.J., Lambing, C., Martinez-Garcia, M., Lawrence, E.J., Ziolkowska, L. et al (2017) Natural variation and dosage of the HEI10 meiotic E3 ligase control Arabidopsis crossover recombination. Genes Dev. 31, 306–317 https://doi.org/10.1101/gad.295501.116

Appendix:

Material	Genome	Mean Chiasma Frequency per cell	Mean Chiasma Frequency per bivalent
T. monococcum	AA	15.46±0.16	2.209±0.02
Ae. speltoides	BB	15.92±0.16	2.274±0.02
Ae. tauschii	DD	15.38±0.16	2.197±0.02
Kr	AABB	28.4±0.31	2.029±0.02
Cap	AABB	32.54±0.29	2.324±0.02
Lnd	AABB	31.62±0.26	2.259±0.02
CS	AABBDD	46.36±0.39	2.208±0.02
Cad	AABBDD	44.2±0.25	2.105±0.01
Pg	AABBDD	44.8±0.35	2.133±0.02
Fld	AABBDD	45.46±0.41	2.165±0.02

Table 0.1: Mean chiasma frequency per cell and per bivalent in pollen mother cells (± Standard Error) (row data for figure 4.5 and 4.6).

Material	P-value
CS *vs* Cad	1.47542E-05
CS *vs* Pa	0.004243598
CS *vs* Fld	0.120734789

Cad *vs* Pa	0.179255059
Cad *vs* Fld	0.012198219
Par *vs* Fld	0.233437293

Table 0.2: P-value of the comparison of the mean chiasma frequency in hexaploid wheats (row data for figure 4.5).

Material	P-value
Kr *vs* Cap	8.37961E-16
Kr *vs* Lnd	5.68853E-12
Cap *vs* Lnd	0.022915107

Table 0.3: P-value of the comparison of the mean chiasma frequency in tetraploid wheats (row data for figure 4.5).

Material	P-value
AA *vs* BB	0.053829
AA *vs* DD	0.733219
BB *vs* DD	0.026864

Table 0.4: P-value of the comparison of the mean chiasma frequency in diploid wheat (row data for figure 4.5).

Material	P-value
CS *vs* Cad	0.0008
CS *vs* Pa	0.0035
CS *vs* Kr	<0.0001
CS *vs* Cap	<0.0002
Cad *vs* Fld	0.04
Cad *vs* Kr	0.004
Cad *vs* Cap	<0.0001
Cad *vs* Lan	<0.0001

Cad *vs* AA	0.007
Cad *vs* BB	<0.0002
Cad *vs* DD	0.005
Par *vs* Kr	0.0002
Par *vs* Cap	<0.0001
Par *vs* Lan	0.0002
Par *vs* AA	0.014
Par *vs* BB	0.0004
Par *vs* DD	0.016
Fld *vs* Kr	0.0007
Fld *vs* Cap	<0.0001
Fld *vs* Lan	0.005
Fld *vs* BB	0.004
Kr *vs* Cap	<0.0001
Kr *vs* Lan	<0.0001
Kr *vs* AA	<0.0001
Kr *vs* BB	<0.0001
Kr *vs* DD	<0.0001
Cap *vs* Lan	0.02
Cap *vs* AA	0.0006
Cap *vs* DD	0.0006
Lan *vs* DD	0.04
BB *vs* DD	0.016

Table 0.5: P-value of the comparison of the mean chiasma frequency per bivalents in all wheats (row data for figure 4.6).

Material	Genome	Mean Chiasma Frequency per ring bivalents
T. monococcum	AA	2.109±0.0352

Ae. speltoides	BB	2.217±0.0324
Ae. tauschii	DD	2.137±0.0378
Kr	AABB	1.830±0.0345
Cap	AABB	2.250±0.0295
Lnd	AABB	2.156±0.0264
CS	AABBDD	2.102±0.0246
Cad	AABBDD	2.010±0.0185
Pg	AABBDD	2±0.0308
Fld	AABBDD	1.944±0.0336

Table 0.6: Mean chiasma frequency per ring bivalents in all wheats (row data for figure 4.7).

Material	Genome	Mean Chiasma Frequency per rod bivalents
T. monococcum	AA	0.1000±0.0174
Ae. speltoides	BB	0.0571±0.0152
Ae. tauschii	DD	0.06±0.0163
Kr	AABB	0.1986±0.0169
Cap	AABB	0.0743±0.0155
Lnd	AABB	0.1029±0.0129
CS	AABBDD	0.1057±0.009
Cad	AABBDD	0.0952±0.0135
Pg	AABBDD	0.1333±0.0157
Fld	AABBDD	0.221±0.0178

Table 0.7: Mean chiasma frequency per rod bivalents in all wheats (row data for figure 4.8).

Material	P-value

CS *vs* Fld	<0.0001
CS *vs* Kr	<0.0003
Cad *vs* Fld	<0.0001
Cad *vs* Kr	0.0003
Pa *vs* Fld	0.017
Fld *vs* Cap	<0.0001
Fld *vs* Lan	<0.0001
Fld *vs* AA	0.0002
Fld *vs* BB	<0.0001
Fld *vs* DD	<0.0001
Kr *vs* Cap	<0.0001
Kr *vs* Lan	<0.001
Kr *vs* AA	<0.004
Kr *vs* BB	<0.0001
Kr *vs* DD	<0.0001

Table 0.8: P-value of the comparison of the mean chiasma frequency of rod bivalents in all wheats (row data for figure 4.9).

Material	P-value
CS *vs* Fld	0.012
CS *vs* Kr	<0.0001
CS *vs* Cap	0.0097
Cad *vs* Kr	0.0008
Cad *vs* Cap	<0.0001
Cad *vs* Lan	0.0008
Cad *vs* BB	<0.0001
Par *vs* Kr	0.0175
Par *vs* Cap	<0.0001

Par *vs* Lan	0.01
Par *vs* BB	0.0002
Fld *vs* Cap	<0.0001
Fld *vs* Lan	0.0001
Fld *vs* AA	0.044
Fld *vs* BB	<0.0001
Fld *vs* DD	0.0105
Kr *vs* Cap	<0.0001
Kr *vs* Lan	<0.0001
Kr *vs* AA	<0.0001
Kr *vs* BB	<0.0001
Kr *vs* DD	<0.0001
Cap *vs* Lan	0.555
Cap *vs* AA	0.113
Cap *vs* BB	>0.999
Cap *vs* DD	0.580
Lan *vs* AA	>0.999
Lan *vs* BB	0.997
Lan *vs* DD	>0.999
AA *vs* BB	0.655

Table 0.9: P-value of the comparison of the mean chiasma frequency of ring bivalents in all wheats (row data for figure 4.10).

Material	Genome	Mean Chiasma Frequency per distal (d) localization
T. monococcum	AA	1.366±0.0349
Ae. speltoides	BB	1.446±0.0253
Ae. tauschii	DD	1.311±0.035
Kr	AABB	1.2±0.027
Cap	AABB	1.384±0.0196

Lnd	AABB	1.366±0.0200
CS	AABBDD	1.260±0.0266
Cad	AABBDD	1.451±0.0153
Pg	AABBDD	1.305±0.0260
Fld	AABBDD	1.112±0.0217

Table 0.10: Mean chiasma frequency of distal chiasmata in all wheats (row data for figure 4.11).

Material	P-value
CS *vs* Cad	<0.0001
CS *vs* Fld	0.001
CS *vs* Cap	0.013
CS *vs* BB	<0.0001
Cad *vs* Pa	0.0003
Cad *vs* Fld	<0.0001
Cad *vs* Kr	<0.0001
Cad *vs* Lan	0.044
Cad *vs* DD	0.021
Pa *vs* Fld	<0.0001
Par *vs* BB	0.008
Fld *vs* Cap	<0.0001
Fld *vs* Lan	<0.0001
Fld *vs* AA	<0.0001
Fld *vs* BB	<0.0001
Fld *vs* DD	0.0003
Kr *vs* Cap	<0.0001
Kr *vs* Lan	0.0002
Kr *vs* AA	0.013
Kr *vs* BB	<0.0001

Table 0.11: P-value of the comparison of the mean chiasma frequency of distal chiasmata. Welch's ANOVA (N=50) (row data for figure 4.12).

Material	Genome	Mean Chiasma Frequency per interstitial 1 (i^1) localization
T. monococcum	AA	0.2714±0.0235
Ae. speltoides	BB	0.2829±0.0222
Ae. tauschii	DD	0.3657±0.0356
Kr	AABB	0.3229±0.205
Cap	AABB	0.2314±0.012
Lnd	AABB	0.21±0.011
CS	AABBDD	0.319±0.0165
Cad	AABBDD	0.2114±0.009
Pg	AABBDD	0.2495±0.015
Fld	AABBDD	0.3381±0.0158

Table 0.12: Mean chiasma frequency of (i^1) in all wheats (row data for figure 4.13).

Material	P-value
CS *vs* Cad	<0.0001
CS *vs* Fld	>0.999
CS *vs* Cap	0.0018
CS *vs* Lnd	<0.0001
Cad *vs* Fld	<0.0001
Cad *vs* Kr	0.0002
Cad *vs* DD	0.004

Pa *vs* Fld	0.004
Fld *vs* Cap	<0.0001
Fld *vs* Lan	<0.0001
Kr *vs* Cap	0.01
Kr *vs* Lan	0.0004
Cap *vs* DD	0.02
Lan *vs* DD	0.004

Table 0.13: P-value of the comparison of the interstitial (i^1) chiasmata in all wheats (row data for figure 4.14).

Material	Genome	Mean Chiasma Frequency per interstitial 2 (i^2) localization
T. monococcum	AA	0.2800±0.0219
Ae. speltoides	BB	0.2257±0.0241
Ae. tauschii	DD	0.2686±0.0269
Kr	AABB	0.2587±0.017
Cap	AABB	0.3314±0.0172
Lnd	AABB	0.3486±0.0168
CS	AABBDD	0.3267±0.0156
Cad	AABBDD	0.2629±0.0158
Pg	AABBDD	0.3352±0.1731
Fld	AABBDD	0.3743±0.0165

Table 0.14: Mean chiasma frequency of interstitial (i^2) chiasmata in all wheats (row data for figure 4.15).

Material	P-value
CS *vs* BB	0.02
Cad *vs* Fld	0.0002

Cad *vs* Lan	0.015
Par *vs* BB	0.017
Fld *vs* Kr	0.014
Fld *vs* AA	0.039
Fld *vs* BB	<0.0001
Fld *vs* DD	0.053
Cap *vs* BB	0.026
Lan *vs* BB	0.003

Table 0.15: P-value of the comparison of the interstitial (i^2) chiasmata in all wheats (row data for figure 4.16).

Material	Genome	Mean Chiasma Frequency per interstitial 3 (i^3) localization
T. monococcum	AA	0.1943±0.0145
Ae. speltoides	BB	0.1886±0.0149
Ae. tauschii	DD	0.1314±0.0134
Kr	AABB	0.1571±0.0119
Cap	AABB	0.2114±0.0132
Lnd	AABB	0.2100±0.0136
CS	AABBDD	0.2067±0.014
Cad	AABBDD	0.0914±0.006
Pg	AABBDD	0.1352±0.007
Fld	AABBDD	0.2371±0.011

Table 0.16: Mean chiasma frequency of interstitial (i^3) chiasmata in all wheats (row data for figure 4.17).

Material	P-value
CS *vs* Cad	<0.0001
CS *vs* Pa	0.001

CS *vs* DD	0.01
Cad *vs* Pa	0.001
Cad *vs* Fld	<0.0001
Cad *vs* Kr	0.0003
Cad *vs* Cap	<0.0001
Cad *vs* Lan	<0.0001
Cad *vs* AA	<0.0001
Cad *vs* BB	<0.0001
Pa *vs* Fld	<0.0001
Par *vs* Cap	0.0002
Par *vs* Lan	0.0003
Par *vs* AA	0.025
Par *vs* BB	0.09
Fld *vs* Kr	0.0001
Fld *vs* DD	<0.0001
Cap *vs* DD	0.002
Lan *vs* DD	0.003
AA *vs* DD	0.085

Table 0.17: P-value of the comparison of the interstitial (i^3) chiasmata in all wheats (row data for figure 4.18).

Material	Genome	Mean Chiasma Frequency per proximal (p) localization
T. monococcum	AA	0.097±0.016
Ae. speltoides	BB	0.1314±0.0177
Ae. tauschii	DD	0.1200±0.0143
Kr	AABB	0.0628±0.008
Cap	AABB	0.1657±0.012
Lnd	AABB	0.1243±0.011

CS	AABBDD	0.0952±0.007
Cad	AABBDD	0.077±0.007
Pg	AABBDD	0.108±0.007
Fld	AABBDD	0.102±0.009

Table 0.18: Mean chiasma frequency of (p) chiasmata in all wheats (row data for figure 4.19).

Material	P-value
CS *vs* Cap	0.0003
Cad *vs* Cap	<0.0001
Cad *vs* Lan	0.02
Par *vs* Kr	0.009
Par *vs* Cap	0.009
Fld *vs* Cap	0.005
Kr *vs* Cap	<0.0001
Kr *vs* Lan	0.001
Kr *vs* BB	0.03
Kr *vs* DD	0.04
Cap *vs* AA	0.04

Table 0.19: P-value of the comparison of (p) chiasmata in all wheats (row data for figure 4.20).

Material	Genome	Mean Chiasma Frequency per bivalents
T. monococcum	AA	2.320±0.0923

Kr	AABB	2.320±0.1086
Cap	AABB	2.140±0.094
Lnd	AABB	2.18±0.088
CS	AABBDD	1.94±0.1046
Cad	AABBDD	1.960±0.1068
Pg	AABBDD	1.840±0.119
Fld	AABBDD	1.940±0.101

Table 0.20: Mean chiasma frequency of chromosome 5A in all wheat (row data for figure 4.23).

Material	Genome	Mean Chiasma Frequency per rod bivalents
T. monococcum	AA	0.34±0.097
Kr	AABB	0.52±0.125
Cap	AABB	0.24±0.078
Lnd	AABB	0.24±0.078
CS	AABBDD	0.74±0.113
Cad	AABBDD	0.42±0.086
Pg	AABBDD	0.56±0.086
Fld	AABBDD	0.86±0.121

Table 0.21: Mean chiasma frequency of rod bivalents in chromosome 5A (row data for figure 4.25).

Material	Genome	Mean Chiasma Frequency per ring bivalents
T. monococcum	AA	1.98±0.162
Kr	AABB	1.8±0.185
Cap	AABB	1.86±0.153
Lnd	AABB	1.94±0.144
CS	AABBDD	1.2±0.185

Cad	AABBDD	1.54±0.174
Pg	AABBDD	1.28±0.189
Fld	AABBDD	1.08±0.182

Table 0.22: Mean chiasma frequency of ring bivalents in chromosome 5A (row data for figure 4.27).

Material	Genome	Mean Chiasma Frequency per cell/bivalent
Ae. speltoides	BB	2.42±0.081
Kr	AABB	2.02±0.092
Cap	AABB	2.14±0.057
Lnd	AABB	1.92±0.084
CS	AABBDD	1.98±0.072
Cad	AABBDD	1.86±0.08
Pg	AABBDD	2.06±0.092
Fld	AABBDD	2±0.098

Table 0.23: Mean chiasma frequency of chromosome 1B (row data for figure 4.33).

Material	Genome	Mean Chiasma Frequency per rod bivalents
Ae. speltoides	BB	0.16±0.072
Kr	AABB	0.24±0.067
Cap	AABB	0.02±0.02
Lnd	AABB	0.26±0.068
CS	AABBDD	0.18±0.0618
Cad	AABBDD	0.28±0.07
Pg	AABBDD	0.22±0.065
Fld	AABBDD	0.36±0.0845

Table 0.24: Mean chiasma frequency of rod bivalents in chromosome 1B (row data for figure 4.35).

Material	Genome	Mean Chiasma Frequency per ring bivalents
Ae. speltoides	BB	2.26±0.127
Kr	AABB	1.78±0.146
Cap	AABB	2.12±0.0678
Lnd	AABB	1.66±0.142
CS	AABBDD	1.8±0.121
Cad	AABBDD	1.58±0.140
Pg	AABBDD	1.84±0.144
Fld	AABBDD	1.64±0.165

Table 0.25: Mean chiasma frequency of ring bivalents in chromosome 1B (row data for figure 4.37).

Material	Genome	Mean Chiasma Frequency per distal (d) localization
Ae. speltoides	BB	0.84±0.104
Kr	AABB	1.12±0.102
Cap	AABB	1.16±0.091
Lnd	AABB	1.08±0.098
CS	AABBDD	1.26±0.089
Cad	AABBDD	1.16±0.082
Pg	AABBDD	1.18±0.093
Fld	AABBDD	1.02±0.096

Table 0.26: Mean chiasma frequency of (d) chiasmata in chromosome 1B (row data for figure 4.39).

Material	Genome	Mean Chiasma Frequency per interstitial 2 (i^2) localization
Ae. speltoides	BB	0.44±0.081
Kr	AABB	0.12±0.046

Cap	AABB	0.26±0.062
Lnd	AABB	0.16±0.053
CS	AABBDD	0.22±0.059
Cad	AABBDD	0.24±0.061
Pg	AABBDD	0.26±0.068
Fld	AABBDD	0.2±0.057

Table 0.27: Mean chiasma frequency of (i^2) chiasmata in chromosome 1B (row data for figure 4.41).

Material	Genome	Mean Chiasma Frequency per interstitial 3 (i^3) localization
Ae. speltoides	BB	0.38±0.069
Kr	AABB	0.1±0.042
Cap	AABB	0.02±0.02
Lnd	AABB	0.04±0.027
CS	AABBDD	0.06±0.033
Cad	AABBDD	0.06±0.033
Pg	AABBDD	0.16±0.052
Fld	AABBDD	0.24±0.61

Table 0.28: Mean chiasma frequency of (i^3) chiasmata in chromosome 1B (row data for figure 4.43).

Material	Genome	Mean Chiasma Frequency per cell/bivalent
Ae. speltoides	BB	1.92±0.039
Kr	AABB	1.82±0.102
Cap	AABB	2.38±0.089
Lnd	AABB	2.12±0.113
CS	AABBDD	2.46±0.091
Cad	AABBDD	2.28±0.103

Pg	AABBDD	2.240±0.112
Fld	AABBDD	1.94±0.116

Table 0.29: Mean chiasma frequency of chromosome 5B (row data for figure 4.45).

Material	Genome	Mean Chiasma Frequency per rod bivalent
Ae. speltoides	BB	0.08±0.038
Kr	AABB	0.4±0.075
Cap	AABB	0.16±0.05
Lnd	AABB	0.38±0.085
CS	AABBDD	0.48±0.115
Cad	AABBDD	0.32±0.087
Pg	AABBDD	0.38±0.089
Fld	AABBDD	0.92±0.114

Table 0.30: Mean chiasma frequency of per rod bivalents in chromosome 5B (row data for figure 4.47).

Material	Genome	Mean Chiasma Frequency per ring bivalent
Ae. speltoides	BB	1.84±0.077
Kr	AABB	1.42±0.167
Cap	AABB	2.22±0.135
Lnd	AABB	1.74±0.18
CS	AABBDD	1.98±0.184
Cad	AABBDD	1.96±0.169
Pg	AABBDD	1.86±0.183
Fld	AABBDD	1.02±0.196

Table 0.31: Mean chiasma frequency of per ring bivalents in chromosome 5B (row data for figure 4.49).

Material	Genome	Mean Chiasma Frequency per distal (d) localization
Ae. speltoides	BB	1.56±0.076
Kr	AABB	0.84±0.1
Cap	AABB	1.32±0.092
Lnd	AABB	1.08±0.117
CS	AABBDD	1.46±0.091
Cad	AABBDD	1.06±0.092
Pg	AABBDD	1.1±0.118
Fld	AABBDD	0.84±0.1

Table 0.32: Mean chiasma frequency of (d) chiasmata in chromosome 5B (row data for figure 4.51).

Material	Genome	Mean Chiasma Frequency per interstitial 2 (i^2) localization
Ae. speltoides	BB	0
Kr	AABB	0.36±0.068
Cap	AABB	0.4±0.069
Lnd	AABB	0.42±0.07
CS	AABBDD	0.16±0.052
Cad	AABBDD	0.28±0.064
Pg	AABBDD	0.32±0.066
Fld	AABBDD	0.34±0.067

Table 0.33: Mean chiasma frequency of (i^2) chiasmata in chromosome 5B (row data for figure 4.53).

Material	Genome	Mean Chiasma Frequency per interstitial 3 (i^3) localization
Ae. speltoides	BB	0
Kr	AABB	0.14±0.049
Cap	AABB	0.24±0.061
Lnd	AABB	0.24±0.061
CS	AABBDD	0.58±0.07
Cad	AABBDD	0.32±0.066
Pg	AABBDD	0.4±0.069
Fld	AABBDD	0.34±0.067

Table 0.34: Mean chiasma frequency of (i^3) chiasmata in chromosome 5B (row data for figure 4.55).

Material	Genome	Mean Chiasma Frequency per cell/bivalents
Ae. tauschii	DD	1.82±0.054
CS	AABBDD	1.92±0.08
Cad	AABBDD	2.12±0.083
Pg	AABBDD	2.04±0.063
Fld	AABBDD	2.34±0.1

Table 0.35: Mean chiasma frequency of chromosome 1D (row data for figure 4.57).

Material	Genome	Mean Chiasma Frequency per rod bivalent
Ae. tauschii	DD	0.18±0.0548
CS	AABBDD	0.24±0.067
Cad	AABBDD	0.2±0.069
Pg	AABBDD	0.16±0.066

Fld	AABBDD	0.22±0.071

Table 0.36: Mean chiasma frequency of rod bivalents in chromosome 1D (row data for figure 4.59).

Material	Genome	Mean Chiasma Frequency per ring bivalent
Ae. tauschii	DD	1.64±0.11
CS	AABBDD	1.68±0.135
Cad	AABBDD	1.92±0.133
Pg	AABBDD	1.88±0.11
Fld	AABBDD	2.12±0.155

Table 0.37: Mean chiasma frequency of ring bivalents in chromosome 1D (row data for figure 4.61).

Material	Genome	Mean Chiasma Frequency per proximal (p) localization
Ae. tauschii	DD	0
CS	AABBDD	0.08±0.038
Cad	AABBDD	0.18±0.055
Pg	AABBDD	0.12±0.05
Fld	AABBDD	0.34±0.07

Table 0.38: Mean chiasma frequency of p chiasmata in chromosome 1D (row data for figure 4.65).

Material	Genome	Mean Chiasma Frequency per cell/bivalent
Ae. tauschii	DD	2.14±0.09
CS	AABBDD	2.56±0.095
Cad	AABBDD	2.4±0.098

Pg	AABBDD	2.42±0.99
Fld	AABBDD	2.44±0.115

Table 0.39: Mean chiasma frequency of chromosome 5D (row data for figure 4.67).

Material	Genome	Mean Chiasma Frequency per rod bivalent
Ae. tauschii	DD	0.18±0.062
CS	AABBDD	0.26±0.085
Cad	AABBDD	0.2±0.069
Pg	AABBDD	0.28±0.085
Fld	AABBDD	0.4±0.098

Table 0.40: Mean chiasma frequency per rod bivalents in chromosome 5D (row data for figure 4.69).

Material	Genome	Mean Chiasma Frequency per ring bivalent
Ae. tauschii	DD	1.96±0.132
CS	AABBDD	2.3±0.162
Cad	AABBDD	2.2±0.151
Pg	AABBDD	2.14±0.164
Fld	AABBDD	2.04±0.191

Table 0.41: Mean chiasma frequency per ring bivalents in chromosome 5D (row data for figure 4.71).

FISH chromosomes	CS (mean)	CS *ph1b* (mean	P-value

5A	1.94±0.104	1.28±0.07	0.0001
1B	1.98±0.07	1.6±0.09	0.0001
5B	2.46±0.09	1.3±0.08	<0.0001
6B	2.2±0.12	1.6±0.08	0.0001
1D	1.92±0.08	1.78±0.08	0.03
5D	2.54±0.09	1.8±0.09	<0.0001

Table 0.42: Mean chiasma frequency of FISH chromosomes in CS WT and *CS ph1b* (row data for figure 5.9).

FISH chromosomes	Cap (mean)	Cap *ph1c* (mean	P-value
5A	2.14±0.09	1.74±0.09	0.001
1B	2.14±0.05	1.72±0.08	0.002
5B	2.38±0.08	1.56±0.12	<0.0001
6B	2.02±0.05	1.6±0.08	0.03

Table 0.43: Mean chiasma frequency of FISH chromosomes in Cappelli WT and *ph1c* (row data for figure 4.16).

FISH chromosomes	Langdon (mean)	Langdon 5D (5B) (mean)	P-value
5A	2.18±0.08	1.36±0.12	0.0001
1B	1.92±0.08	1.46±0.11	0.001
5B	2.1±0.11	1.56±0.12	0.001
6B	2.06±0.06	1.6±0.09	0.001

Table 0.44: Mean chiasma frequency of FISH chromosomes in Langdon WT and Langdon 5D (5B) (row data for figure 4.23).